

DRAFT

**PROBABILISTIC RISK ASSESSMENT
FOR THE UTAH MULTI-HAZARDS PROJECT**

Martin W. McCann, Jr.

Jack R. Benjamin and Associates, Inc.
444 Castro Street, Suite 501
Mountain View, CA 94041

ABSTRACT

As part of a pilot study, the State of Utah, Division of Comprehensive Emergency Management, and the Federal Emergency Management Agency (FEMA) undertook a pilot project to develop a multi-hazards emergency management program. Among the tasks performed was the development of a probabilistic risk assessment methodology to evaluate the consequences of the multiple hazards that may impact the state, notably along the populated reaches of the Wasatch Front. A probabilistic approach offers a comprehensive summary of the likely consequences in the event a major disaster should occur. It identifies the possible scenarios that may take place, and estimates the likelihood of their occurrence. For purposes of emergency management planning and public policy decision making, it is important to have a clear understanding of the consequences, in terms of both their possible magnitude and likelihood. With this input, the decision maker can make informed, logical plans to mitigate and respond to the impact of a major disaster. This work represented the initial step to develop a comprehensive risk assessment procedure that will become an integral part of an active multi-hazards emergency management program.

In the first part of the project, guidelines were provided for conducting a probabilistic assessment of the consequences to the following primary natural hazards in Utah: earthquakes, floods, dam failures, and landslides. The framework of the probabilistic model included the following elements: hazard evaluation, exposure assessment, vulnerability or damage assessment, and risk quantification. In a hazard evaluation, in addition to identifying the possible hazards that exist, a probabilistic assessment is also made of the possible serial occurrences of multiple hazards such as earthquakes and a seismically-induced dam failure. In assessing the consequences to each hazard occurrence, the random factors that influence the estimation of casualties, such as season of the year, time of day, effectiveness of warning systems, etc. were also incorporated in the analysis. In the final quantification of risk, probabilistic input on each hazard and their consequences were expressed in probabilistic terms. The emergency manager would be provided with input on the possible magnitude of casualties (e.g., deaths, injuries, homeless) and the likelihood that such losses would be incurred. Similarly, the availability of emergency services following a disaster would be expressed in the same manner. For example, it is possible to estimate the likelihood that a given number of hospitals will be operational after an earthquake.

The multi-hazards risk assessment is intended to provide the emergency planner with a clear picture of the possible hazard/consequence scenarios that can occur. Rather than conservatively selecting the worst situation as a design basis event, the decision maker is provided with an evaluation of the consequences in terms that express the extent of losses and their likelihood.

INTRODUCTION

The State of Utah faces the unique challenge of addressing the problem of multi-hazards emergency management. Unlike many other areas in the U.S. that face potential catastrophic loss due to single or multiple hazard occurrences, Utah finds itself in a situation where 90 percent of the state's population lies at the foot of the Wasatch Mountains, which is the focus of the major hazards that could occur in the state. The Wasatch Fault, which is a portion of the Intermountain Seismic Belt, is a highly active source of seismicity in the region, capable of producing intense ground shaking and surface faulting due to events as high as magnitude 7.5. The occurrence of earthquakes along the Wasatch Front, in addition to posing a direct threat, could initiate other hazardous events as well, including dam failure and landslides in the canyons above populated areas.

In response to the clear and present danger of the multi-hazards that threaten the major economic, social, and political centers of Utah, the state has embarked on a comprehensive emergency management program. This effort, entitled, "The Utah Multi-Hazards Project," is a pilot program funded by the Federal Emergency Management Agency. It is designed to establish a methodology to identify the hydrologic and geologic hazards in Utah, to assess the consequences of their occurrence, and to establish the groundwork of a methodology to aid local officials in emergency planning and mitigation of the risks to local communities.

Within a comprehensive emergency management plan there are a number of interrelated elements that ultimately lead to the development of measures to mitigate the consequences anticipated from a major disaster. Figure 1 displays schematically the general format of a comprehensive emergency management program. As illustrated in the figure, the

results of a risk assessment provide input to the development of emergency operation plans to meet the needs immediately after a major disaster and to formulate long- and short-term mitigation efforts.

In order to provide this information to emergency management planners and public policy makers, a probabilistic risk assessment approach is used. Risk assessment procedures are used extensively in engineering practice and have become an attractive tool for decision makers who must make important public policy decisions involving highly uncertain events, such as extreme floods, earthquakes, landslides, etc. In a probabilistic risk assessment, information is presented in terms of the magnitude of the potential disaster and its likelihood of occurrence.

To assess the intensity of major natural hazards and the consequences of these events is highly uncertain. As an example, it is easy to recognize that when a major earthquake occurs there is uncertainty in the prediction of the spatial intensity of ground shaking, in the extent of damage to buildings and other structures, in estimates of how many casualties there will be, or which emergency services will be available. The same can be said for other disasters as well. Where multi-hazard events can occur essentially simultaneously, such as a seismically-induced dam failure, the consequences of serial hazard occurrences become harder to plan for without an indication of their likelihood.

Within the scope of the Utah Multi-Hazards Project, guidelines to perform a probabilistic risk assessment procedure were developed to evaluate the many hydrologic and geologic hazards that threaten the populated areas of the state. In this paper, an overview of the approach taken is presented with particular emphasis given to seismic risk assessments.

METHODOLOGY FOR MULTI-HAZARDS RISK ASSESSMENT

Overview

An important element in the development of an emergency management program is to establish in the planning stages a clear, comprehensive view of the demands that will be placed on local and national emergency services immediately following a major disaster. In the pre-disaster planning stages, it is necessary to know the likelihood and degree of damage to structures and loss of life and injuries that can be expected. Information reported in this manner provides the emergency planner with a composite, two-dimensional view of the potential consequences. By reporting the degree to which emergency services will be available immediately after a major disaster in the same way, a direct comparison and assessment can be made of their adequacy.

An assessment of the consequences of a major disaster is a task that must deal with a variety of uncertainties. For example, there is uncertainty associated with the random occurrence of a disaster such as the chance it will occur in any given year, the location, the time of day, and season of the year. Given its occurrence, there is uncertainty in the assessment of the consequences, including the damage to buildings, availability of emergency services, assessment of life loss, and the response of the public to warnings. Currently, a standard procedure does not exist that systematically incorporates these and other uncertain factors in a consequence evaluation.

The purpose of the work for the State of Utah was to present guidelines to evaluate the consequences to the multi-hazards experienced in Utah in a probabilistic format. Although methods to evaluate the risk due to major natural disasters and to plan mitigation measures are not well established, the basic steps in the process are generally recognized to consist of:

- Hazard evaluation
- Exposure assessment (the population and property at risk)
- Vulnerability assessment
- Risk quantification
- Establishment of a program of risk mitigation, including emergency operation plans
- Updating emergency operation plans in light of the changing environment (i.e., physical, political, social, economic)

In this work we were concerned with the first four steps that compose the assessment of risk.

A hazard evaluation involves the identification of the natural or man-made conditions that represent a source of danger. A hazard may be caused by some external initiating event, such as the intense ground shaking produced by an earthquake, or it may occur as a random, isolated event such as the flood produced by a failure of a dam due to foundation instability.

Exposure refers to the property (i.e., buildings, homes, agricultural farmland, factories, etc.), and lives which are exposed to the potential hazards. In other words, that which is at risk.

Vulnerability refers to the expected degree of damage experienced by the elements exposed to the hazard. A relationship describing the expected damage to one-story residences exposed to flood waters is an example of a vulnerability assessment.

When the uncertainty in the hazard and consequence assessments are considered, it is possible to imagine that a variety of scenarios could occur at random. A simple example can illustrate this. Consider that two levels of earthquake ground motion intensity are postulated, each with a probability of occurring. Also, consider that a dam could fail or not fail when exposed to each level of earthquake. Depending on the level of the earthquake, the probability of dam failure would be different. In this case, four possible scenarios might occur. For each level of earthquake intensity, there could be failure or no failure of the dam. The likelihood of each scenario would be the product of the individual event probabilities (i.e., probability of dam failure given the earthquake intensity times the probability of the earthquake).

In the final risk quantification the likelihood of all possible hazard/consequence scenarios is assessed. The formal quantification of the impact of a major disaster involves a logical combination of the random events that result in adverse consequences. The steps in the procedure are described subsequently.

Initiating/Emergency Planning Events

In order to assess emergency management needs in the event of a major disaster, it is important to quantify the risk on a per event basis. In this way, emergency service capabilities can be directly measured against the demands posed by each disaster. For this reason, individual events are generally defined to serve as the basis for consequence evaluation and the design of emergency operation plans.

In the multi-hazards project work the following initiating hazard events were considered:

- Earthquake
- Flood
- Dam Failure
- Landslide

It is a fairly common practice to develop emergency management plans and mitigation programs on the basis of worst case hazard scenarios. As an example, the consequences to the probable maximum flood might be assessed and used as the basis to make emergency operation plans. The concept of considering worst case hazard scenarios as the basis for emergency management planning is not necessarily realistic. One reason is that, as well as not accounting for the uncertainty with respect to event location, there is no concept of the likelihood of occurrence. Also, from an economic perspective it may not be cost effective, or politically feasible to design emergency operation plans for Armageddon. Furthermore, in the development of a comprehensive multi-hazards emergency management plan, the likelihood of occurrence for different worst case events may be very different. For example, the maximum credible earthquake may have a return period of 250 years, while the average waiting time for the probable maximum flood may be 100,000 years. Clearly an inconsistency exists in terms of the level of risk being considered in each case. However, the use of worst case scenarios in the course of an analysis can be informative since it helps to establish an upper bound on the anticipated losses and required emergency services.

Two planning events were selected as the basis to evaluate losses, prepare emergency operation plans, and develop mitigation programs. A planning event is the primary hazard that initiates one or more of the potential hazards that a community may be exposed to, and is used as the basis to design emergency management systems. It is also referred to as the initiating event which may trigger one or a series of additional hazards. The two planning events considered herein were the events that have an annual probability of 0.01 or a 100-year return period and the worst case or maximum credible event.

To perform the risk assessment, the planning event is conservatively located where its occurrence will result in the most severe consequences. The degree of conservatism will depend on the likelihood that an event of the same size could occur elsewhere, without adverse impact on the study area.

Hazards and Hazard Sequences

Given the occurrence of an initiating event, single or multiple hazards may occur in various parts of a region. The occurrence of one or more hazards may be dependent, not only on the fact that the initiating event has occurred (e.g., 100-year flood), but on other hazards as well. In other words, there may be a probabilistic dependence between the occurrence of one or more hazards. The situation of a seismically induced dam failure is an example of the dependence between two hazards, ground shaking and flooding due to a dam break.

Given the occurrence of an initiating event (e.g., 100-year flood, dam break, etc.), an assessment is made to evaluate the likelihood of each hazard that can occur, either individually or in series with other hazards. In order to establish an eventual probabilistic characterization of the multiple hazards and hazard sequences that could occur, a systematic procedure is required. The general steps and examples for the State of Utah are listed below.

- Identify the potential initiating events that could occur in the region.
- Determine the hazards generated by each initiating event, including primary, secondary, etc. throughout the study area.
- Establish the interrelationship between hazard types to determine the dependencies that may exist, in order to develop an event tree of the multiple hazard sequences that could occur.

- Select a model or statistical approach to define the likelihood of each hazard intensity level.
- According to the combination of events depicted in the event tree, evaluate the likelihood of each hazard sequence throughout the region.

Table 1 lists the initiating multi-hazards in Utah addressed in this work. Note that the hazards listed are natural geologic or hydro-logic hazards only, with the exception of dam failures. No direct consideration is given to technological hazards such as fires, chemical spills, or radiation release.

The event or logic tree approach to multi-hazard assessment is effective since it can be used to illustrate graphically the potential hazard scenarios that could occur. Figure 2 is an example of the seismic hazard event sequences that could occur. Each branch of the event tree represents a possible scenario that could occur within a study area or could be experienced at a given site. The probability that a given sequence would occur is simply the product of the probabilities along the branch. Since each event is typically defined by a number of discrete values, the actual number of branches (scenarios) is far more than shown in the figure.

Exposure

For a prescribed study area, an inventory is required to identify the type, number and location of each element at risk (e.g., property, population). The development of an accurate and complete inventory of the elements at risk is an important phase of the risk assessment. In order that pertinent information be collected, the inventory system should be developed in consultation with the risk analyst and the appropriate experts to ensure completeness. Generally, the step of

establishing the inventory system would be performed once, with the exception of possible modifications when applied to a new region or when additional hazards are considered.

Vulnerability Assessment

The vulnerability assessment task involves the development or use of available methods to assess the likelihood and degree of damage to structures and systems exposed to the variety of hazards considered in the multi-hazards analysis. Included in this phase of the analysis is the estimation of casualties.

Structure and Component Fragility

Each hazard type imposes on the structures and systems in the vicinity where it occurs some form of external load. Depending on the severity of the applied loads and the capacity of the element being challenged, some degree of damage may be experienced. There are, however, a number of uncertainties involved in assessing the damage to structures. For example, an assessment of the damage to a building exposed to the strong shaking of an earthquake is uncertain because of unknown design and construction irregularities, variability in the strength of construction materials, uncertainty in predicting the actual response of a structure to the violent shaking induced by an earthquake, among other reasons. Although it is difficult to predict the precise level of strong shaking at which damage or failure would occur, it is possible to define a range over which it is likely to take place. Within this range, the assessment of the likelihood of failure or damage increases from a probability of zero (e.g., no chance of failure) to a probability of one (e.g., certain failure). The relationship which describes the probability of failure at various hazard levels is known as a fragility curve. A fragility curve can be defined for structures exposed to ground shaking, flooding, landslide, or any other hazard. A graphic illustration of a fragility curve is given in Figure 3.

For the purpose of emergency management planning, fragility curves can be used in conjunction with estimates of the severity of each hazard to predict the probability that a structure will fail or the degree of damage that it is likely to sustain.

Commonly, fragility curves assume that a structure, component or system is in one of two possible states--either completely failed or not failed. In many cases, this distinction is appropriate. However, in some cases damage may occur in varying degrees from no damage to collapse or complete failure. For each hazard and structure type considered, the number and definition of each damage state must be established. An important step in this consideration is to define the damage level at which a loss of function occurs. It is of critical importance in emergency planning to quantify the availability of services, shelter, and transportation routes when a disaster occurs. In many cases, nonavailability may occur at a damage level considerably less than complete collapse, and therefore loss of function is more likely to occur than collapse.

For use in risk assessment studies designed to provide input to emergency management planning, it is neither practical nor necessary to develop fragility curves on a structure-by-structure basis. That is, it is not appropriate to develop a fragility curve for every single-family residence exposed to earthquake ground shaking. Rather, it is adequate to have a generic curve for each type of single-family residence. This limits the number of fragility curves required to the number of structure types in the study area. In cases where there are only a few critical structures to be considered in the analysis, structure-specific fragility curves can be developed.

Assessment of Casualties and Homeless

An evaluation of the number of casualties due to a major disaster depends on a number of factors including the type of hazard, time of year, time of day, whether a warning system exists, and the population.

distribution with respect to hazards that may result in loss of life (e.g., earthquakes, floods), and the type of structures that house people. Other factors include the fraction of those that would be killed or injured given a particular hazard. Some of the considerations listed above involve the inherent randomness of when a disaster is likely to occur, while others are the result of uncertainties in predicting the outcome of events. In this phase of the risk assessment, the major sources of uncertainty in estimating the potential casualties are considered. Table 2 summarizes the random variables that should be taken into account in the estimation of the number of casualties in the event of a major disaster.

To quantify the likelihood and number of casualties, the following general approach is outlined. Figure 4 presents an example using an event tree to display the various random events that influence the estimate of casualties, while at the same time addressing how likely it is that each scenario, or combination of random factors, is to occur. Note that from each hazard type, the number of factors included in the analysis and the method of estimating the number of casualties will differ.

To evaluate the number of people left homeless after a major disaster also depends on a number of factors. Among them are the time of year, type of hazard, type of construction of single-family residences, apartment buildings, etc., and availability of utilities (e.g., gas, electricity) following the disaster. The assessment of the numbers of homeless can be performed in much the same way as the analysis for the number of casualties. The use of data from past disasters is also a useful way to calibrate a model.

Risk Quantification

In this phase of the risk analysis, the individual components of the analysis are combined, to probabilistically quantify the consequences to each initiating event. A generic list of the type of results that can be assessed is given along with a brief discussion of the format for quantifying them.

In order to effectively plan for a major disaster, answers to a number of questions are required. Among them are:

- How many casualties will there be? How likely is it?
- How many people will require shelter?
- What will the availability of medical services be (e.g., hospitals, beds, doctors, nurses, etc.)?
- What modes of transportation will be available?
- Will public services such as police and fire be operational?
- Will lifeline systems such as water and electricity be available? Where?

From questions such as these, a list of the information required for emergency planning can be established. However, as expressed previously, there are a number of uncertainties involved in estimating the consequences of a major disaster. Therefore, it is generally not possible to provide a single answer to these questions. Instead, the range of hazard/consequence scenarios is considered to estimate the distribution on the possible consequences. Table 3 summarizes the type of results provided by the risk analysis.

Table 1
Multi-Hazards Considered in this Work

Initiating Event	Hazard Order*		
	First	Second	Third
Earthquakes	Ground Shaking	Liquefaction Dam Failure** Landslide	Flooding Dam Failure, Flooding Reservoir Waves Natural Dam Formed
	Fault Offset	Dam Failure	Flooding
Floods	Flooding (depth and velocity of water)	Dam Failure Erosion	Flooding
Landslide/ Debris Flow	Massive Earth Movement Natural Dam Formed	Reservoir Waves Dam Failure	Dam Failure Flooding
Dam Failure	Flooding		

*Fourth and higher order hazards are not shown.

**Dam failure could be caused by liquefaction, which would in turn be the result of strong ground shaking.

Table 2

Random Variables in the Estimation of Casualties

Variable	Sources of Uncertainty
Time of year	Transient versus permanent population
Time of day	Population distribution during work or commuter hours versus the time in residence
Estimation of the fraction killed	Uncertainty due to the inexactness of methods/information to predict the number of people killed in a major disaster
Estimation of the fraction injured	Uncertainty due to the inexactness of methods/information to predict the number of people injured in a major disaster
Warning and warning systems	In the case of some hazards such as floods and dam failures, some warning to evacuate may be available; if a warning system exists, there is uncertainty as to its effectiveness

Table 3

Partial List of Information and Format of Results
Provided by a Risk Analysis

Factor	Result
<u>Casualties</u> - Deaths - Injuries - Homeless	Probability distribution on the number in each category
<u>Medical Services</u> - Hospitals - Medical Staff	Probability that any or all hospitals will be functioning Probability that an adequate staff will be available
<u>Transportation</u> - Highways - Railroads - Airports - Ports	Probability that critical transportation routes will be available
<u>Shelters</u>	Probability distribution on the number of people that shelter could be provided for

SUMMARY

Guidelines for conducting a probabilistic risk assessment for application in multi-hazards emergency management planning were presented. The results of a probabilistic analysis offer the emergency planner a two-dimensional view of the potential impact of a major disaster, providing a measure of the magnitude of the consequences of individual scenarios and their likelihood of occurrence. In a similar manner, the degree and likelihood that emergency services will be available in the period immediately following the disaster are assessed. With this type of input, an emergency manager is in a position of knowing what the likely, as well as incredible or worst case consequences are, thus avoiding overly conservative assessments of the need for emergency services. Given the formal, systematic approach of a probabilistic procedure, the relative contribution of any aspect of the risk analysis can be determined and the level of improvement of proposed mitigation measure easily assessed.

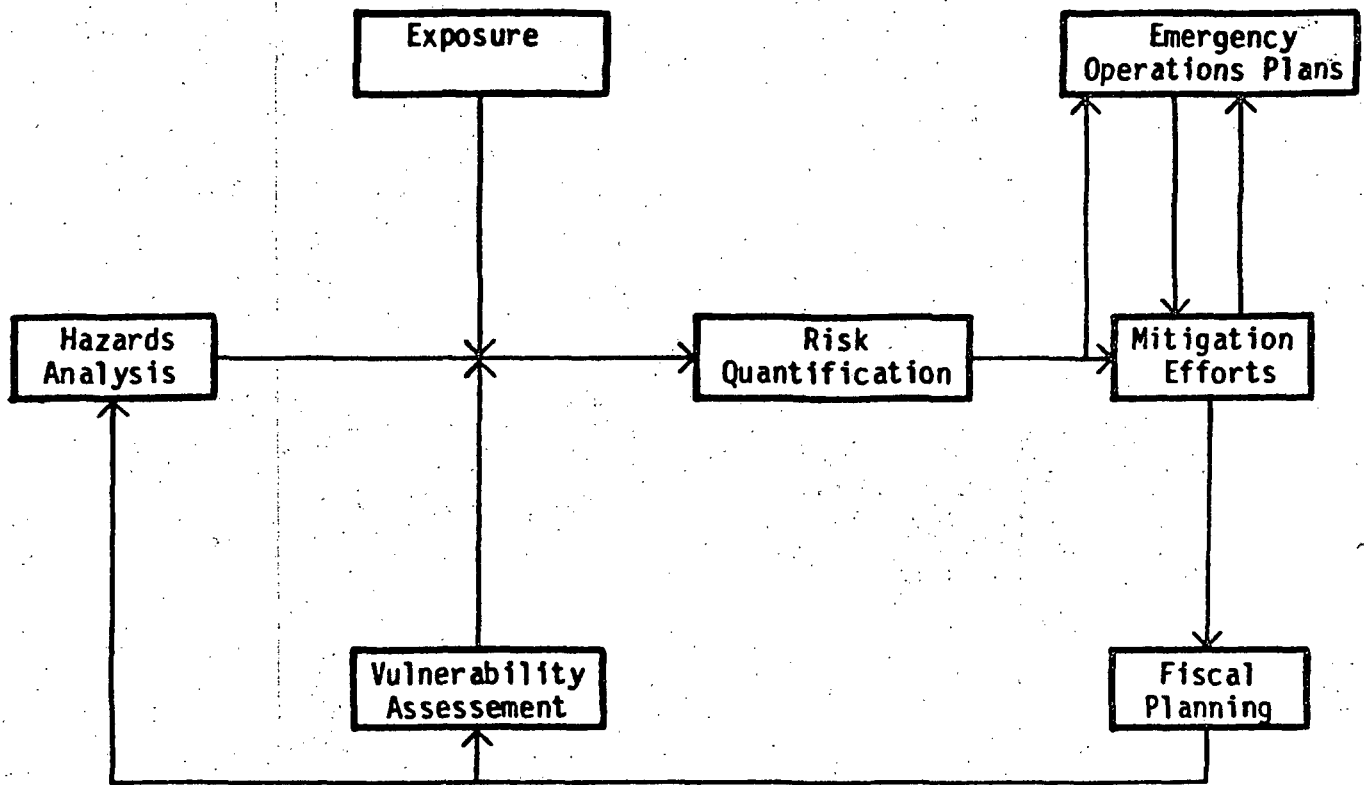


Figure 1 Schematic illustration of the basic elements of a comprehensive emergency management program.

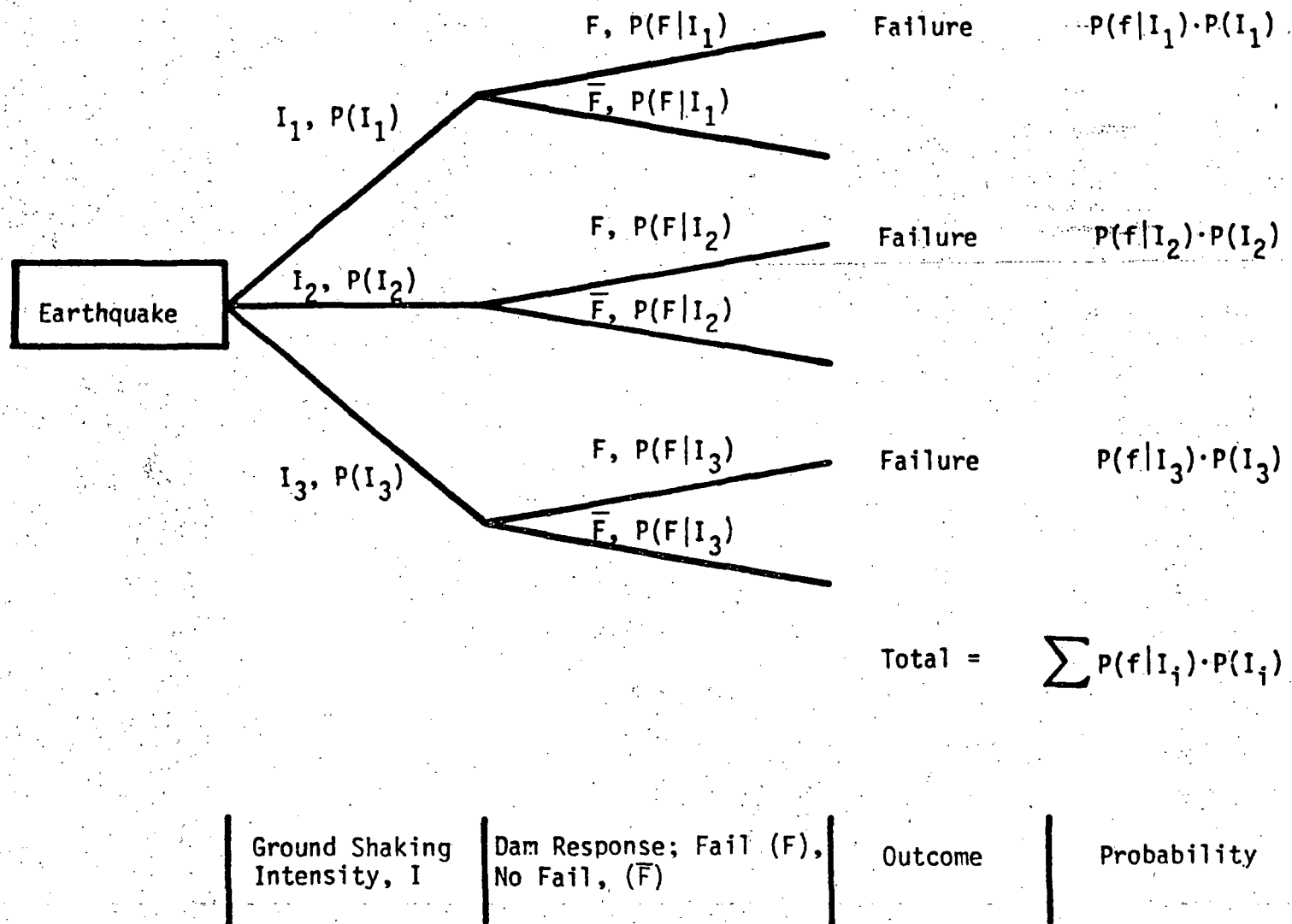


Figure 2 An example illustration of an event tree approach to evaluate the probability of an event sequence.

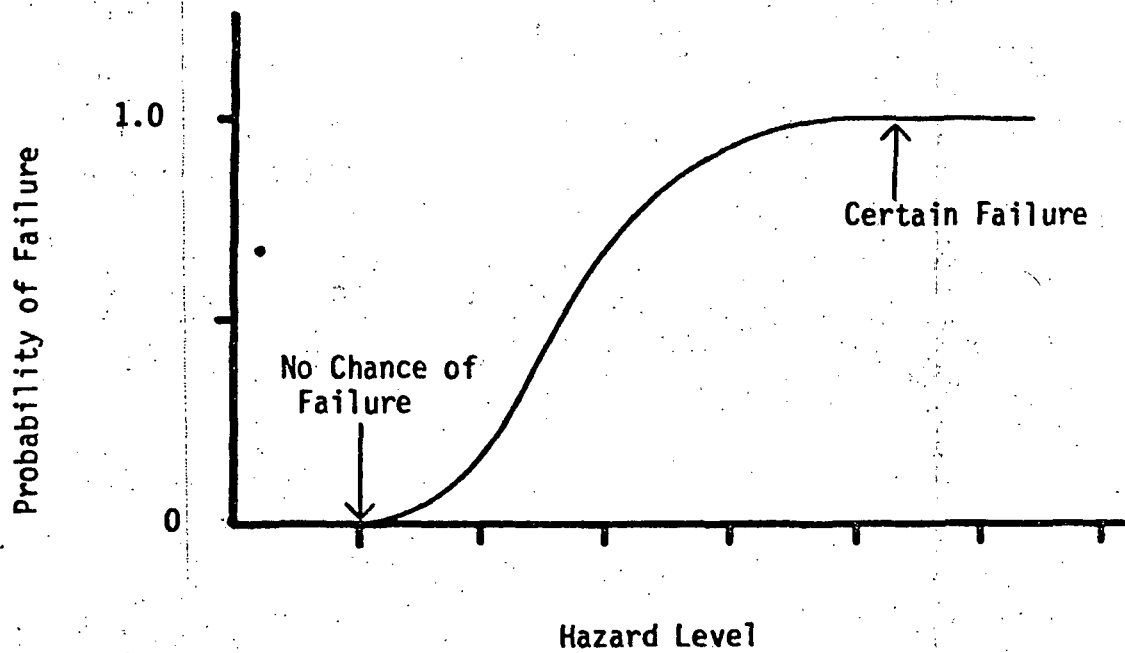


Figure 3 An example of a fragility curve that is defined for each structure and system type exposed to a given hazard.

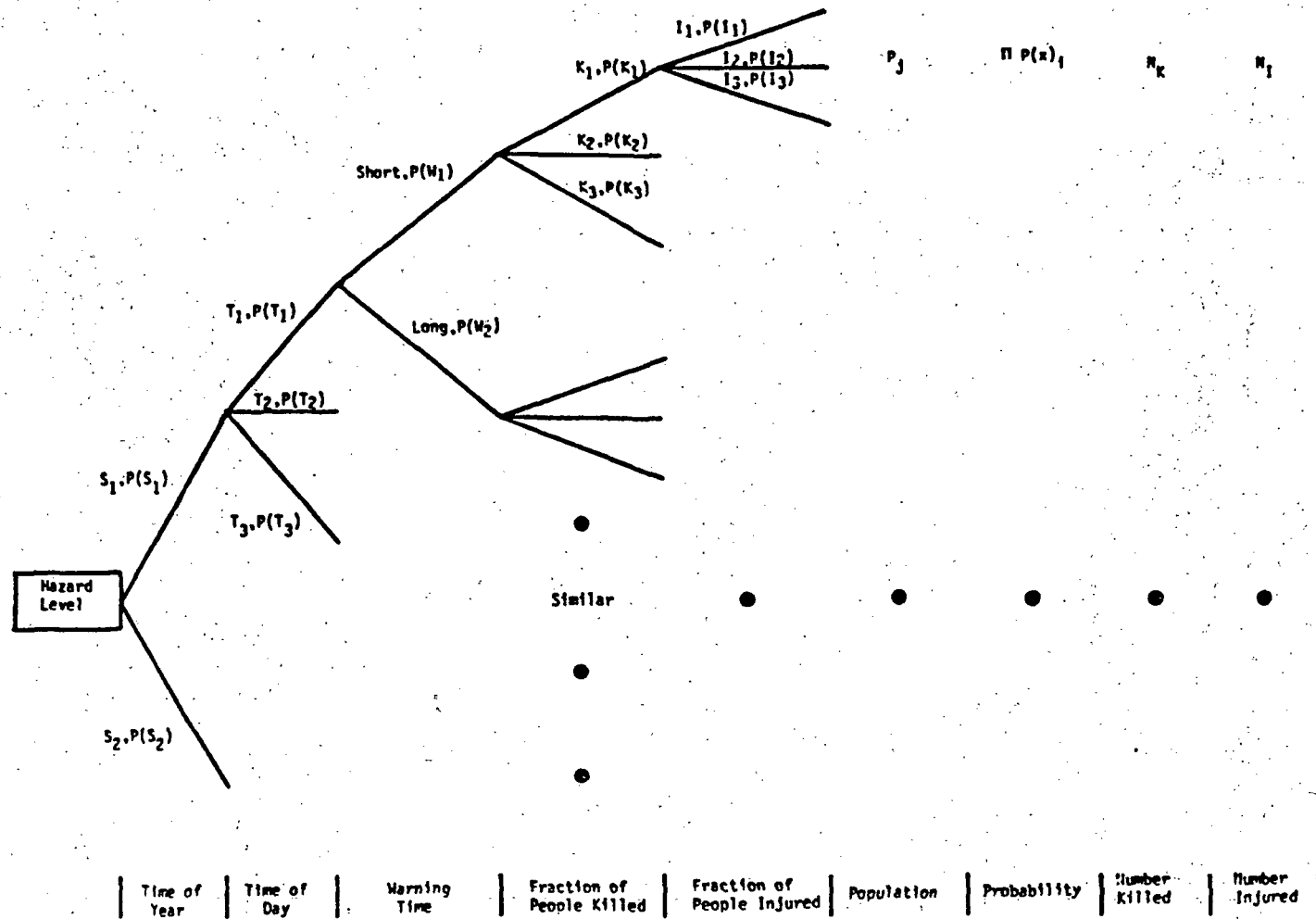


Figure 4 An example of the procedure to estimate the probability distribution on the number of deaths in the event of a major disaster.

**WORKSHOP ON
"EVALUATION OF REGIONAL AND URBAN EARTHQUAKE
HAZARDS AND RISK IN UTAH"**

**Salt Lake City, Utah
August 14-16, 1984**

**Sponsored by
U.S. Geological Survey
Federal Emergency Management Agency
National Bureau of Standards
Utah Geological and Mineral Survey
Utah Division of Comprehensive Emergency Management
University of Utah**

**Special Technical Sessions organized by
Walter Arabasz, University of Utah
Robert Buckman, U.S. Geological Survey
Lawrence Reaveley, Reaveley Engineers & Associates, Inc.**

The papers contained in this notebook are preliminary and have not been edited or reviewed for conformity with U.S. Geological Survey standards and stratigraphic nomenclature. They are provided to supplement the oral presentations. A proceedings containing the final papers will be published within approximately 4 months after the date of the workshop.

TABLE OF CONTENTS

SPECIAL TECHNICAL SESSIONS

TUESDAY AND WEDNESDAY EVENINGS, AUGUST 14-15, 1984

Paper Number

1. *Earthquake Behavior in the Wasatch Front Area: Association with Geologic Structure, Space-Time Occurrence, and Stress State, by Walter Arabasz*
2. *Investigation of Historical Seismicity in the Salt Lake City Portion of the Wasatch Front Region of Utah, Using Documentary Sources, by Sherry Oaks*
3. *Contemporary Vertical Tectonics Along the Wasatch Fault Zone Measured By Repeated Geodetic Leveling, by Spencer Wood*
4. *Constraints on the In-Situ Stress Field Along the Wasatch Front, by Mary Lou Zoback*
5. *Preliminary Investigation of Quaternary Geology Along the Southern Part of the Wasatch Fault Zone, Central Utah, by Michael Machette*
6. *Earthquake Recurrences Estimated by Calibrating Quantitative Geologic Rate Estimates, by David Perkins and Paul Thenhaus*
7. *A Plan for Evaluating Hypothesized Segmentation of the Wasatch Fault, by Russell Wheeler*
8. *Near Surface Faulting Associated with Holocene Fault Scarps, Wasatch Fault Zone Utah: A Preliminary Report, by Anthony Crone and Samuel Harding*
9. *An Effort to Determine Poisson's Ratio In-Situ for Near Surface Layers, by Don Steeples, Richard Miller, and Kenneth King*
10. *Investigations of an M_L 4.3 Earthquake in the Western Salt Lake Valley Using Digital Seismic Data, by James Pechmann and Bergthora Thorbjarnardottir*
11. *Near Source Characteristics of Strong Ground Motion for Moderate to Large Earthquakes—An Update and Suggested Application to the Wasatch Fault Zone of North/Central Utah, by Kenneth Campbell*
12. *Analysis of the Earthquake Ground Shaking Hazard for the Salt Lake City-Ogden-Provo Region, by Maurice Power, David Schwartz, Robert Youngs, and F. H. Swan*
13. *Probabilistic Risk Assessment for the Utah Multi-Hazard Project, by Martin McCann*

by Carl A. von Hake,

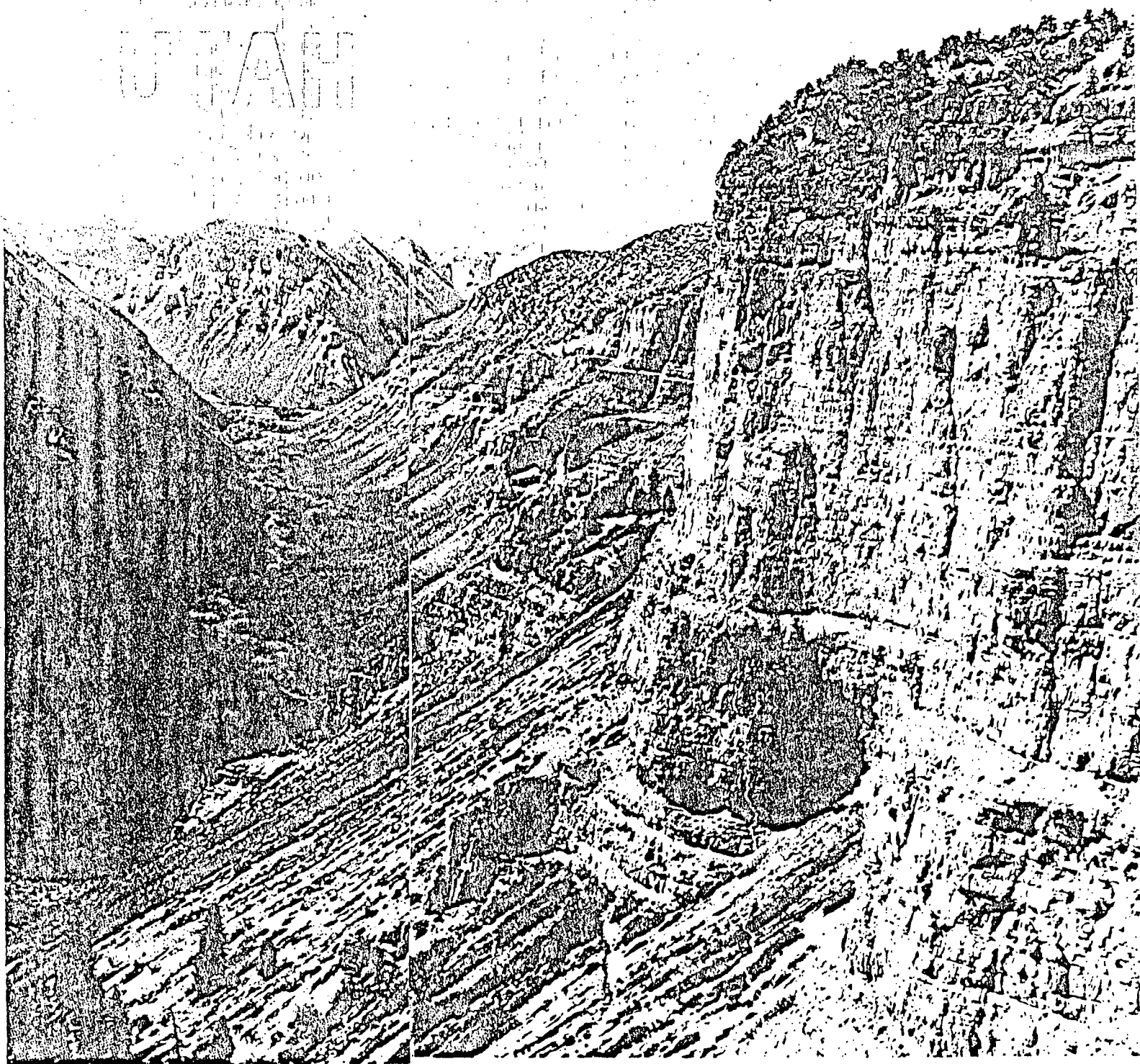
National Oceanic and Atmospheric
Administration,
Boulder, Colo.

The earthquakes of Utah are part of an active belt of seismicity that extends northward from the Gulf of California through western Arizona, central Utah, southeastern Idaho, western Wyoming, western Montana, and into western British Columbia. Seventy-four shocks of intensity V or greater (Modified Mercalli Scale) are listed in *Earthquake History of the United States* (Pub. 41-1, 1973, revised ed., U.S. Government Printing Office.) A detailed catalog of Utah earthquakes from 1850 through June 1965 (in the *Bulletin of the Seismological Society of America*, 1967, vol. 57, pp. 689-718) listed 609 events, of which at least 38 were damaging. About 200 of these were instrumental epicenters determined from the University of Utah Seismograph Network.

Major fault zones along which many Utah earthquakes have occurred are the East Cache, Hansel Valley, Hurricane, Sevier, Thousand Lakes, Tushar (Elsinore), and Wasatch fault zones. Previous articles in the *Earthquake Information Bulletin* ("Seismicity and Earthquake Hazards of the Wasatch Front, Utah" by Robert B. Smith, vol. 6, no. 4, July-August 1974, and "Earthquake Hazards in Sensitive Clays Along the Wasatch Front, Utah," vol. 8, no. 4, July-August 1976) have discussed earthquake hazards in the Wasatch fault zone.

The following summary includes earthquakes centered in Utah with maximum intensity VII or greater. Information on the many additional damaging shocks is contained in the references cited in the first paragraph.

Three distinct shocks rocked the Ogden area on July 18, 1894. Walls cracked (VI-VII) and dishes were shaken from tables. Many people were frightened during the violent motion. Another shock of similar intensity occurred on August 1, 1900, near Santaquin. An adobe house was split in two (VI-VII), and people were thrown from their beds. A chimney was damaged, dishes were broken, and



some plastic at Goshen. There were additional reports that the deep shafts of a mine were shifted so that the cage could not be operated.

On November 13, 1901, a strong earthquake caused extensive damage from Parowan to Richfield. Brick buildings and many chimneys were damaged; some rockslides were reported near Beaver. Earth cracks with the ejection of water and sand were reported (VIII); in addition, some creeks increased their flow. The total felt area covered about 129 500 square kilometers. Intensity VI effects were observed over a 26 000-km² area. Aftershocks continued for several weeks, the strongest of which was on November 14. Considerable damage resulted at Pine Valley, St. George, and Santa Clara from an earthquake on November 17, 1902. Chimneys were destroyed (VII) at Pine Valley and Santa Clara; additional damage occurred at Pinto and Toquerville. Reports were also received of a felt earthquake at Salt Lake City, 400 kilometers away; this may have been a distinct shock at about the same time.

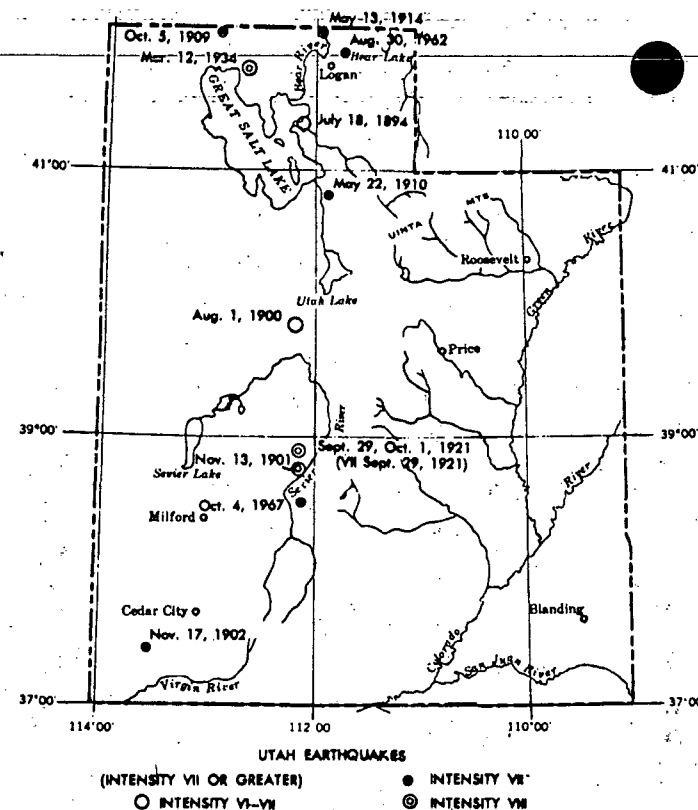
A series of 30 to 60 earthquakes were reported in the vicinity of Garland and Tremonton between October and December 1909. Some of the shocks were strong enough to throw down chimneys (VII). Two tremors about 35 minutes apart were reported felt over a wide area of northwestern Utah on October 5, 1909. These reports probably are related to one event in the series. A May 22, 1910, earthquake damaged many chimneys (VII) at Salt Lake City and several old buildings. Two aftershocks of less intensity were felt.

The area around Ogden was strongly shaken on May 13, 1914. This disturbance was probably caused by a slip along the Wasatch fault; the 1910 tremor was also related to this fault. Windows were broken and chimneys thrown down (VII) at Ogden; near panic was reported at Central Junior High School. Dishes rattled and furniture moved at Farmington. The shock was felt from Collinston on the north to Riverton, south of Salt Lake City, an area covering about 20 700 km².

After several weeks of preliminary tremors, two strong earthquakes about 12 hours apart shook Elsinore, Monroe, and Richfield on September 29, 1921. The first shock, at 7:12

AM, lasted 7 to 10 s and threw down scores of chimneys (VIII), tore plaster from ceilings, and fractured walls at Elsinore. In addition, gables of houses were thrown out and the foundation of a new school sank 1 foot, leaving gaps between the walls and the roof. Total damage was estimated at \$100 000. Another shock of intensity VII occurred at 7:30 PM on the same day. On October 1, there was yet another strong tremor causing further damage at Elsinore. A number of brick and stone buildings were rendered uninhabitable by the 8:32 AM earthquake (VIII). The Monroe City Hall, built of rock, was severely damaged. Large rock falls were caused on both sides of the Sevier Valley. Warm springs were discolored for hours with iron oxides. Aftershocks continued until December 20, the most important being those on October 27, which were felt sharply at Richfield, and on November 1.

On March 12, 1934, at 8:06 AM, an earthquake of intensity VIII originating near Kosmo, on the north shore of Great Salt Lake, affected an area of about 440 000 km², including much of northern Utah and parts of Idaho, Montana, Nevada, and Wyoming. This tremor, which measured magnitude 6.6, could have caused great damage in a densely populated area. Because of the sparse settlement in the region there was very little damage—mostly demolished chimneys and cracked walls in poorly constructed buildings. Two deaths, however, were attributable to the shock. The outstanding feature of the earthquake, related to the Hansel Valley fault, was the emission of large quantities of water from fissures and craterlets. Considerable faulting occurred in the epicentral region. Precise leveling revealed that areas sank to depths up to 390 mm. The onset of the shock was abrupt. There were no foreshocks, but the usual aftershocks continued for 2 days; only one, at 11:20 AM on the same day, was outstanding (magnitude 6.0). There was moderate damage over a broad area, including Salt Lake City, where plaster fell. All chimneys fell in Kosmo and Monument; fissures, holes, cracks, and springs appeared in connection with a belt of fractures at least 8 km long. The second shock was slightly less severe than the main tremor. Intensities for the aftershock are very unrelia-



ble because many observers tried to describe both earthquakes in a single report. Another strong aftershock (magnitude 5.5) affected an area of about 45 000 km² in northern Utah and southern Idaho on May 6. It was reported to be strongest in Salt Lake City and Preston, Idaho, where the intensity reached VI.

Damages estimated at \$1 million resulted from an August 30, 1962, shock in the East Valley fault zone. The magnitude 5.7 earthquake caused significant damage at Franklin, Lewiston, Logan, Preston, and Richmond. Cache County was designated a disaster region by the Small Business Administration. The greatest damage occurred at Richmond (VII) where at least nine houses were declared unsafe for occupancy, one church was damaged beyond repair, numerous houses lost walls, and 75 percent of the older brick chimneys fell. At Logan, principal building damage was cracked and twisted walls. Brick and timber fell through a church roof. At Lewiston, one brick wall fell and many chimneys were damaged. A sugar refinery near Lewiston sustained major damage when large pieces of cement coping fell, penetrating lower-level roofs. Four schools in Cache

County were seriously damaged. The shock was felt over an area of approximately 168 000 km². Minor aftershocks, with slight additional damage, were reported through September 9.

On October 4, 1967, a magnitude 5.2 earthquake caused damage in the Marysvale area. Ceilings and walls cracked in numerous houses in Marysvale (VII). About 1 mile north of Marysvale, well water was badly muddied for 24 h. At Koosharem, chimneys and plaster cracked. Chimneys were partially knocked down at Joseph. Rockslides were reported in the Joseph, Junction City, and Sevier areas. The tremor was felt over 38 800 km² of southern Utah and a few places in northern Arizona. Several aftershocks were felt.

Slight damage was reported at a number of northern Utah towns from a March 28, 1975, earthquake centered near the Idaho-Utah border. Ridgedale (VIII) and Malad City (VII), Idaho, sustained the most damage from this magnitude 6.1 shock. All of northern Utah felt the tremor; the 160 000-km² felt area also included parts of Idaho, Nevada, Wyoming, and a few places in northwestern Colorado.

EXTENSIONAL AND COMPRESSIONAL PALEOSTRESSES AND THEIR RELATIONSHIP TO
PALEOSEISMICITY AND SEISMICITY, CENTRAL SEVIER VALLEY, UTAH

by

R. Ernest Anderson and Theodore P. Barnhard
U.S. Geological Survey
Denver, Colorado 80225

INTRODUCTION

Background: The historic seismic flux along most of the Wasatch fault zone is lower than in many of the adjacent parts of the intermountain seismic belt (Arabasz and others, 1979). It is generally not possible to correlate the sparse diffuse seismicity along the zone with the Wasatch fault (Smith, 1978; Wechsler, 1979; Arabasz and Smith, 1981) thus severely limiting the opportunity to understand the behavior of the fault. In contrast, the seismic flux is relatively high along the south-southwesterly projection of the Wasatch fault zone in the central Sevier Valley region (fig. 1). There the historic earthquake record since 1850 includes nine earthquakes of estimated magnitude 5.0 or greater and the seismicity pattern for the period July 1962-June 1978 shows concentrated activity (Arabasz and others, 1979). Because the seismic flux of the central Sevier Valley region is high relative to that of the Wasatch fault, it has attracted seismicity studies by staff and students from the University of Utah in the hope of improving understanding of earthquakes and earthquake processes in the eastern Great Basin (W. J. Arabasz, oral commun., 1981). In particular, systematic microseismicity studies were conducted intermittently in the region from 1979 through 1982 (McKee and Arabasz, 1982; McKee, 1982; Julander and Arabasz, 1982; Julander, 1983). In the vicinity of the southern termination of the Wasatch fault south of Nephi, Utah, McKee and Arabasz (1982) obtained focal mechanisms by iteratively inverting SV/P amplitude ratios. The mechanisms indicate a

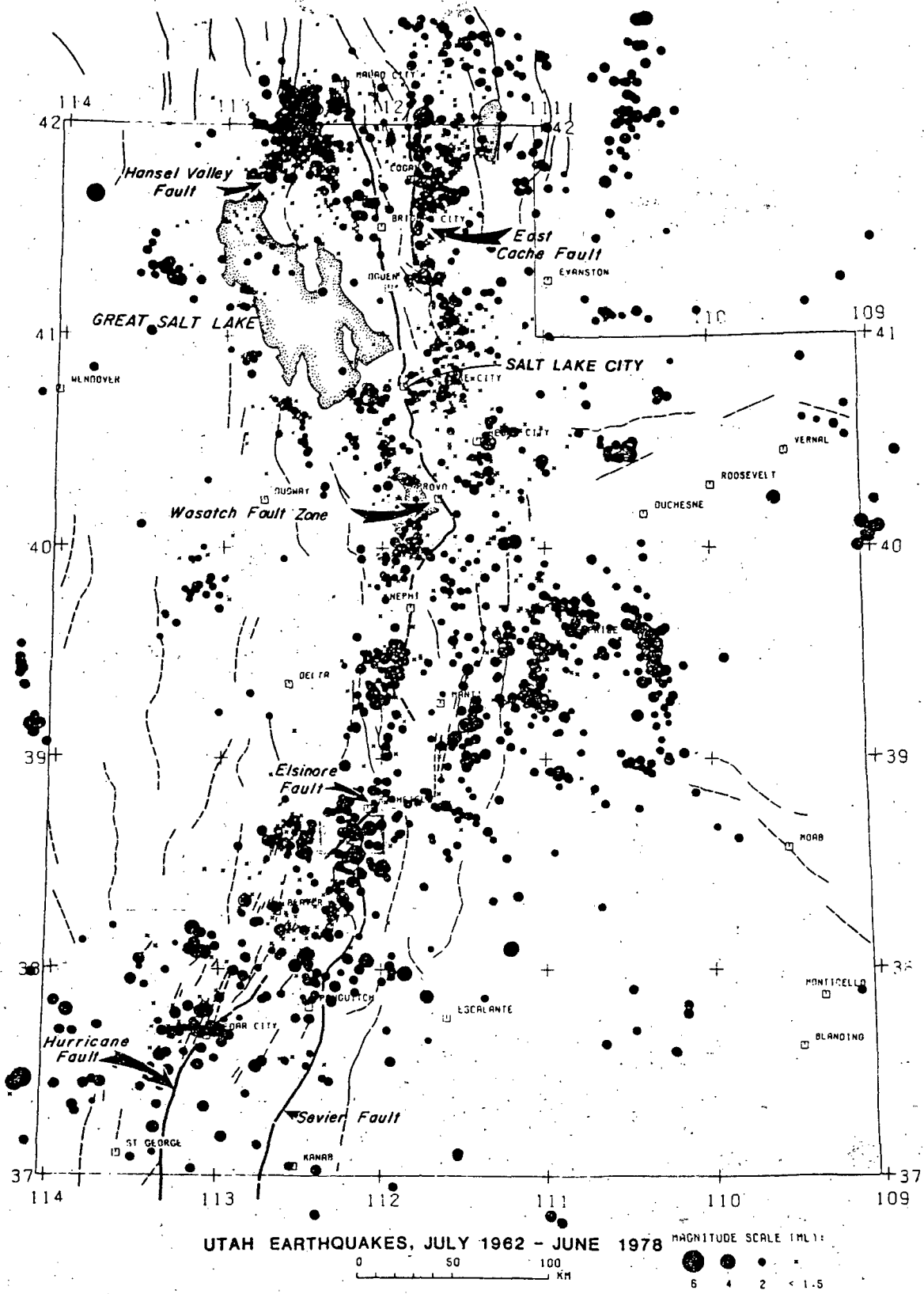


Figure 1.—Location of study area (shaded) and distribution of earthquake epicenters in Utah for the period July 1962–June 1978 (from Arabasz and others, 1979).

mixture of strike slip and normal slip on steep- to moderate-dipping planes. Fault plane solutions from the central Sevier Valley region show that current seismicity in part of the region is dominated by strike-slip (SS) events and includes some oblique-slip (OS) events to depths of 10 km. Epicentral distributions show that some of this seismicity is localized on or near major mapped faults or at places where such faults are intersected by transverse faults. Late Cenozoic SS faults had not been reported for the central Sevier Valley region so no inferences could be made relating the SS seismicity to such faulting (Julander, 1983). Although the microseismicity results do not shed much light on the expected behavior of the Wasatch fault, the occurrence of SS dominated seismicity in a region where conventional wisdom would predict normal faulting seemed worthy of geologic investigation.

Purpose: In June 1983, a systematic search for geologic evidence for SS faulting was begun. The search was successful and it is now clear that the geologic record contains abundant evidence of late Cenozoic SS faulting in the region. The purpose of this report is to present the preliminary findings.

Geologic context: The portion of the central Sevier Valley region from which fault-slip data were collected includes parts of the Pavant Range, Tushar Mountains, Antelope Range, and Sevier Plateau, all of which flank the Sevier River Valley (fig. 2). The study area lies within a zone that is transitional physiographically, structurally, and geophysically from the Basin and Range on the west to the Colorado Plateau on the east (Keller and others, 1975; Smith, 1978; Rowley and others, 1979). It is located on the northern flank of the enormous Marysvale volcanic field, which developed between about 27 and 16 m.y. ago. The faults studied cut rocks of the volcanic field as well as overlying rhyolitic ash-flow tuffs and sedimentary rocks. Fault displacements range from a few centimeters to a few kilometers. Three major

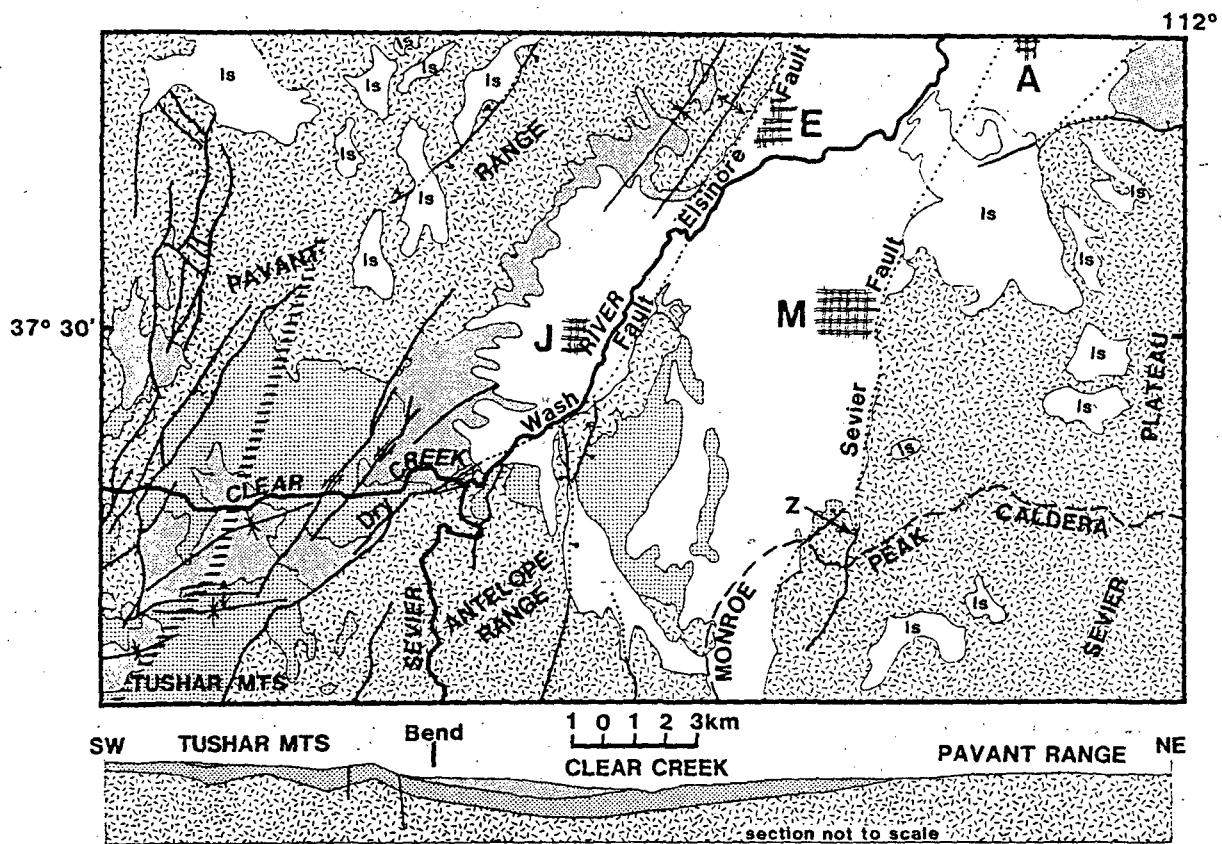


Figure 2.—Geologic map and cross sectional sketch of the central Sevier Valley area, Utah, showing the Joe Lott tuff (stippled) and underlying volcanic rocks (hachured) and overlying basin-fill sedimentary rocks (shaded). Landslide masses are labeled ls and areas of Quaternary alluvium are unpatterned. Faults and folds are shown with standard symbols. Map is generalized from Cunningham and others (1983) and Callaghan and Parker (1962). Line of hachures marks approximate line of cross section. E, Elsinore; M, Monroe; J, Joseph; A, Annabella; Z, exposure of splay of Sevier fault referred to in text.

north- to northeast-trending faults (fig. 2) were previously named and interpreted as normal faults--the Sevier, Dry Wash, and Elsinore (Callaghan and Parker, 1961, 1962; Cunningham and others, 1983). Except for the southern part of the Dry Wash fault, these faults tend to be buried by range-flanking alluvium and their slip characteristics can only be evaluated indirectly by searching for clues on small- and intermediate-scale faults in the adjacent bedrock. The three northeast-trending faults located northwest of and parallel to the Dry Wash fault (fig. 2) were mapped by Callaghan and Parker (1961) and apparently have large displacements. Several previously mapped faults of moderate displacement are also shown on figure 2, but it should be emphasized that most of the slip data on which this report is based come from small unmapped faults with displacements ranging to as much as a few meters.

Methods: In this report faults referred to as small-displacement faults have known or estimated offsets from a few centimeters to a few meters, those referred to as large-displacement faults have known or inferred displacements greater than 30 m, and the remainder are referred to as intermediate-displacement faults. Field procedure for this study consists simply of measuring the orientation of fault surfaces and movement-related striae on those surfaces and determining the slip sense for motions parallel to those striae. The data are classified according to the displacement amount and the certainty with which the sense of slip was determined. Data analysis consists of a preliminary separation into faulting mode with faults whose rake angles exceed 45° separated into a dip-slip mode and those less than 45° into a SS mode. Oblique-slip faults are relatively uncommon so computations can be performed without treating them separately. Paleostress computations utilizing methods similar to those described by Angelier (1979) are performed on data representing each mode; first with all measurements weighted equally

and second with a weighting bias given to measurements according to the greater amount of fault displacement. None of the computations reveal significant shifts in the positions of stress axes due to weighting, indicating that the large and small faults behaved similarly during the deformation responsible for the striations. In the absence of evidence to the contrary, the striae are assumed to represent the youngest deformation on a fault. The lack of evidence that fault size influences paleostress orientations provides justification for estimating regional paleostress from fault populations that are dominated by small faults.

Data processing problems have not been fully resolved so the stress-axis orientations are reported without detailed information on their quality. They should be considered as tentative.

RESULTS

For the purpose of discussing the computational results and their relationship to mapped structures the fault-slip data are grouped into four subareas (fig. 2): (1) the west margin of the Sevier Plateau where it trends east-northeast in the Annabella area, (2) the west margin of the Sevier Plateau where it trends northerly south of Monroe, (3) the northernmost Antelope Range, and (4) the Clear Creek area which includes the Dry Wash fault and the area to the northwest of it.

Data distributions for fault strike, dip, and rake as well as for the proportion of SS to DS motion are illustrated for the four subareas in figures 3 through 6. The distributions show that in each subarea there is a mixture of SS and DS motions (figs. 5 and 6) on faults that tend to dip steeply (fig. 4). Faults in the Clear Creek subarea have conspicuously homogeneous steep dips and bimodal rakes as an excellent example of the mixture of faulting modes (figs. 4, 5,). Not only are SS faults in that subarea more numerous

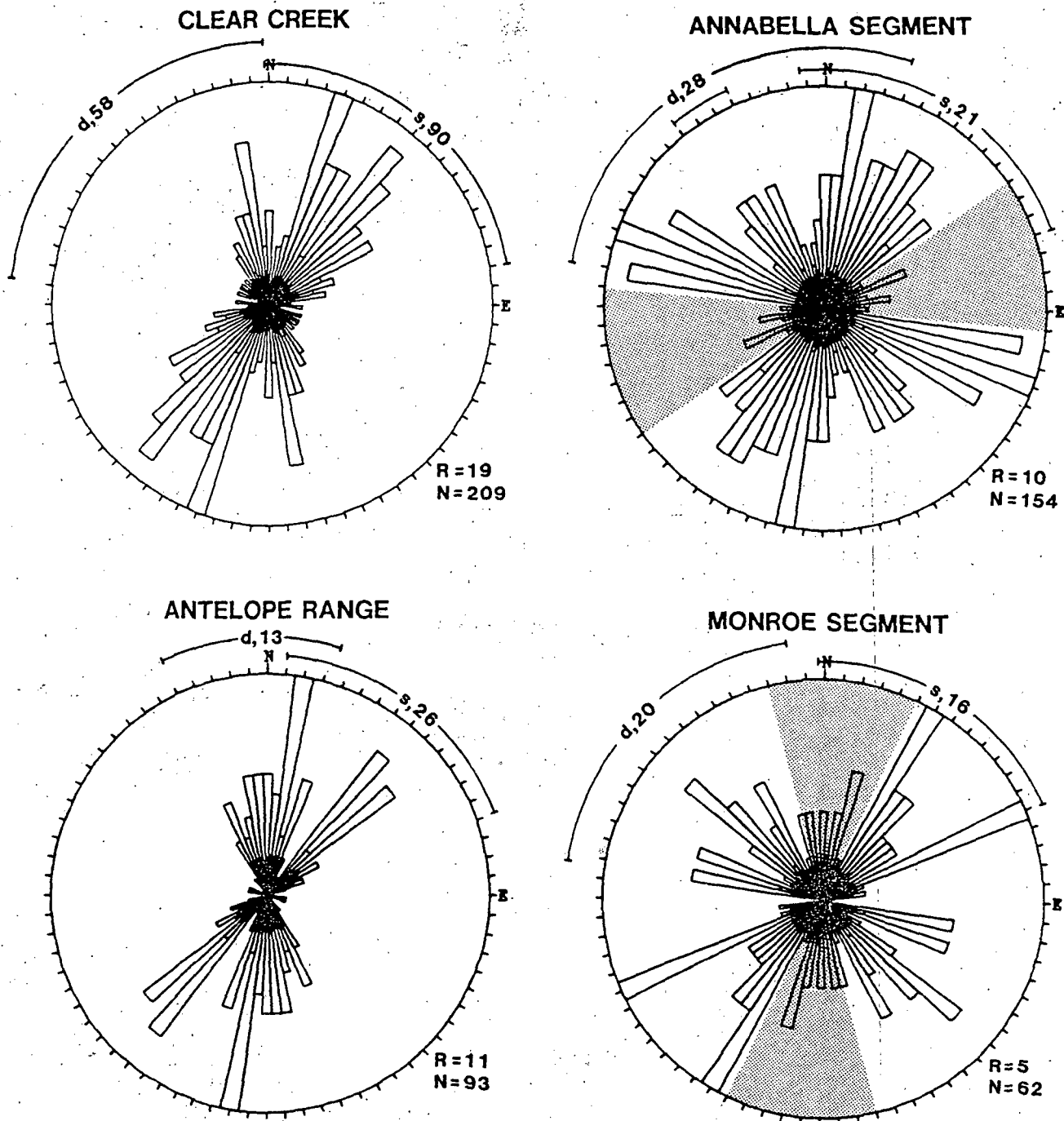


Figure 3.—Azimuthal distribution of strikes of all faults from four separate subareas. N = sample size; R = radius value of plot; d and s and the bars and numbers adjacent to them give the strike range and sample sizes of dextral and sinistral faults, respectively, using 45° as the cut-off limit for rake angles. For the Clear Creek and Monroe subareas there is no overlap in the range of strikes for dextral and sinistral faults. For the Annabella segment subarea there is some overlap and three sinistral faults have strikes well into the range for dextral faults (indicated by short bar). For the Antelope Range subarea the bars only indicate the range of strikes of most sinistral and dextral faults because 26 percent of the dextral faults fall beyond the dextral bar and 17 percent of the sinistral faults fall beyond the sinistral bar. Shaded areas show trend of margin of Sevier Plateau along the Annabella and Monroe segments (plus and minus 20°).

DIP

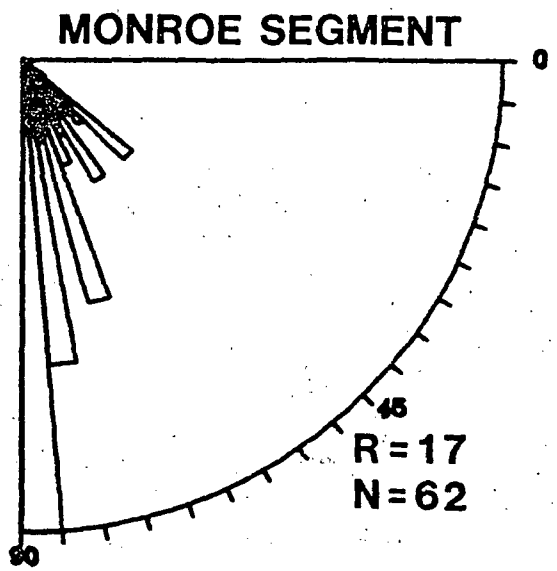
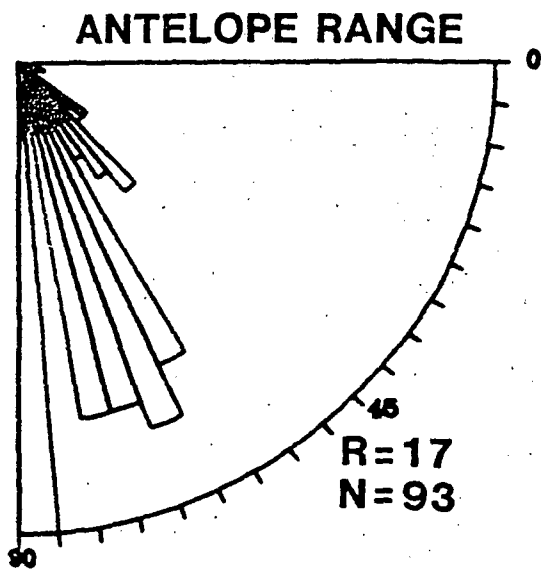
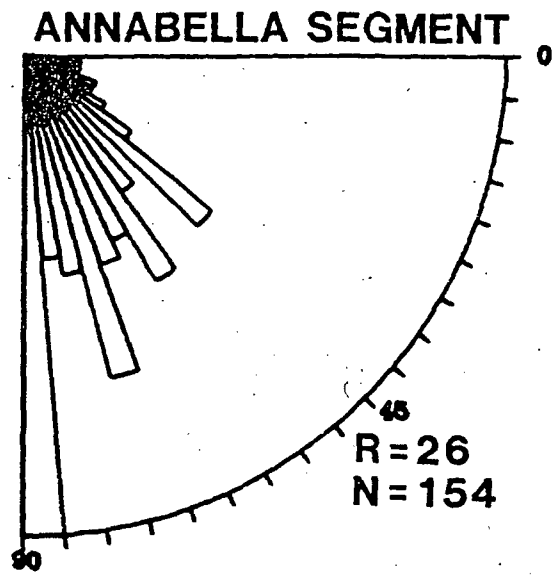
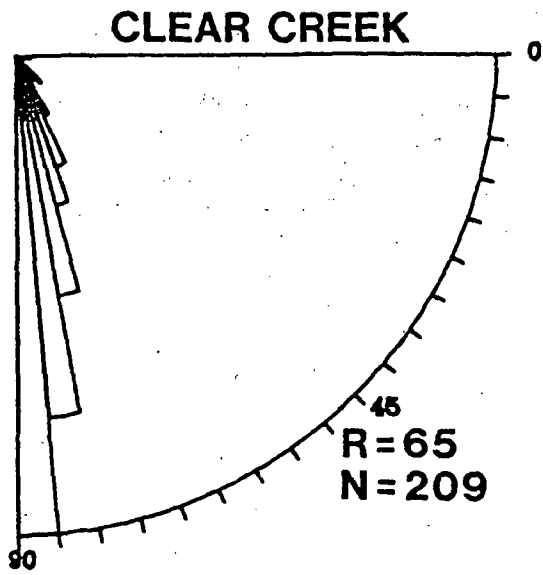


Figure 4.—Distributions of dip angles for all faults from four separate subareas.
N = sample size; R = radius value of plot.

RAKE

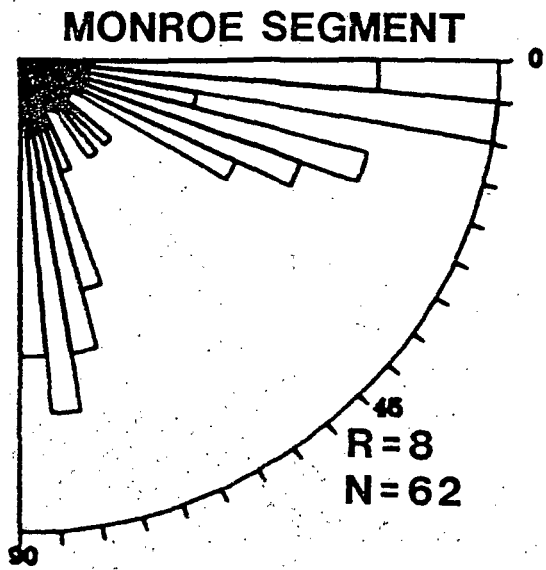
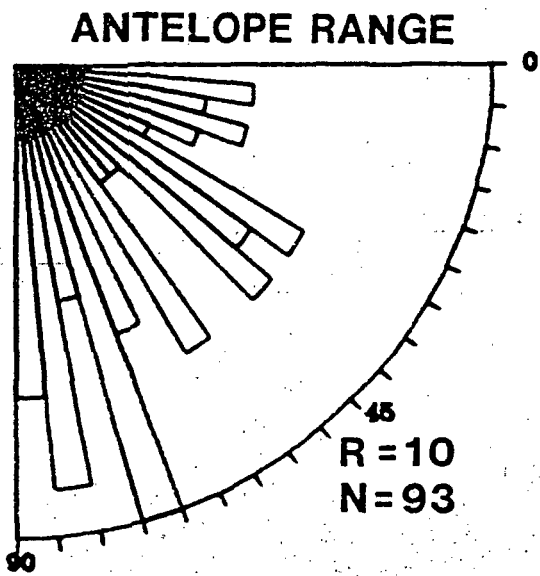
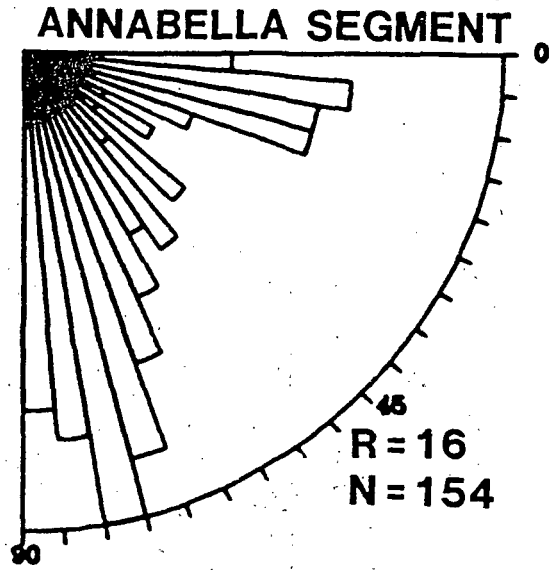
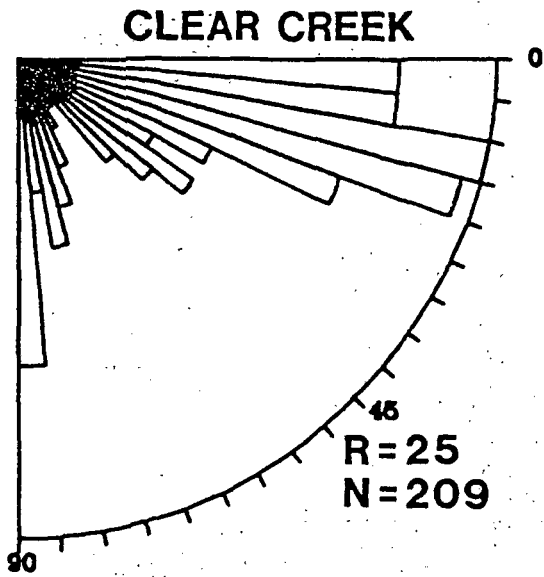


Figure 5.—Distribution of rake angles for all faults from four separate subareas.
N = sample size; R = radius value of plot.

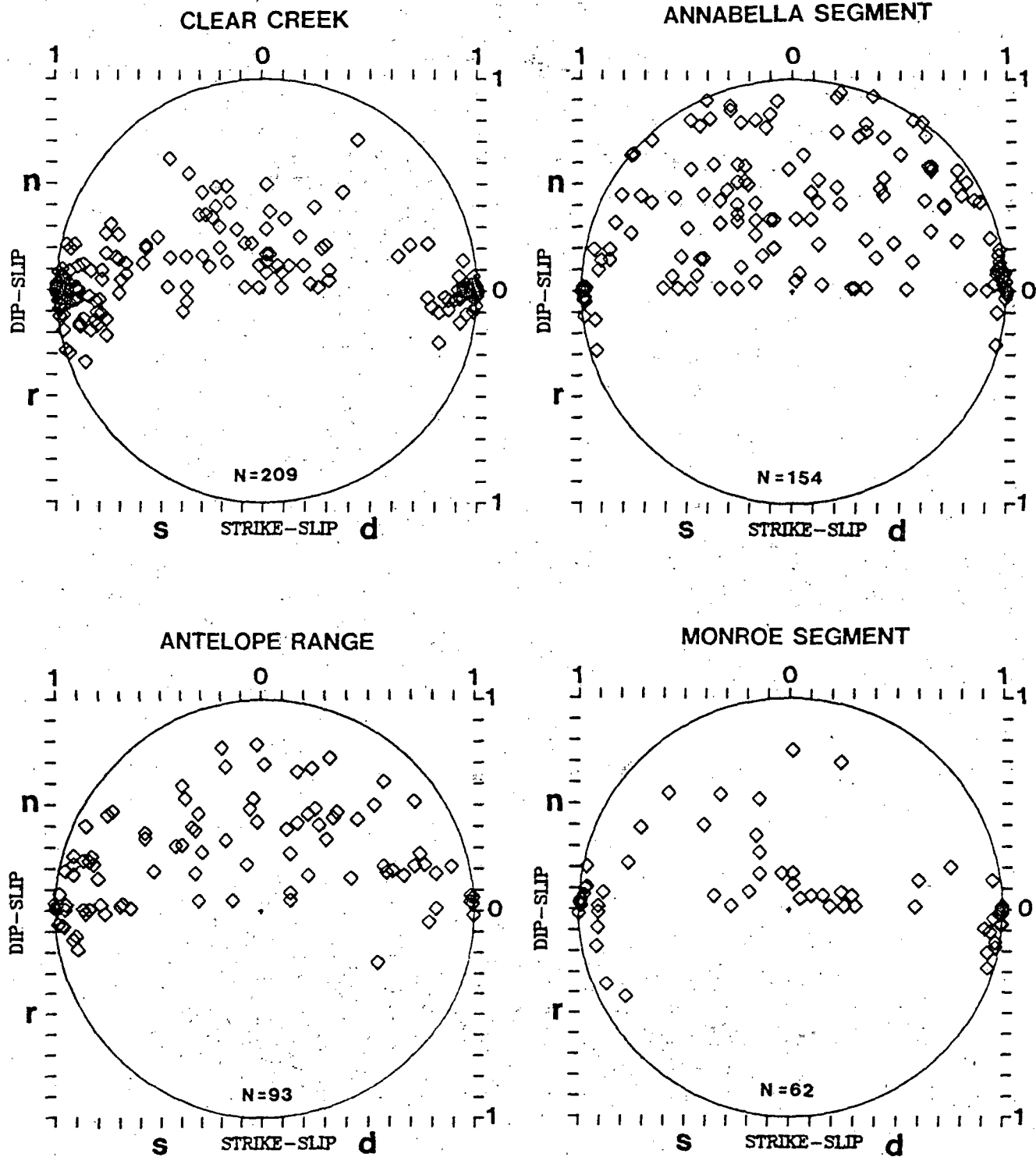


Figure 6.—Plot of SS versus DS components of fault motions for all faults in four separate subareas. Each symbol corresponds to an individual striated fault. Abscissae: ratio of strike separation to net separation (s, sinistral; d, dextral). Ordinates: ratio of horizontal component of dip separation to net separation (n, normal; r, reverse). N = sample size.

than DS faults (fig. 6) they also have larger displacements. Faults that have moderate dips and oblique slip are very sparse in the Clear Creek and Monroe areas and are more numerous in the Annabella and northernmost Antelope Range subareas (figs. 4 and 5). Distributions of fault strikes (fig. 3) show a north-northeast maximum in the azimuthal range 010 to 030 for each subarea, and in each there is a submaximum or node 20° - 35° clockwise from the north-northeast maximum. There is a diversity of structural settings represented by the four subareas, so these similarities in fault-strike distributions are unexpected.

Sevier Plateau, Annabella Segment

The location of the trace of the Sevier fault north of Monroe (referred to herein as the Annabella segment) is conjectural. The plateau-margin escarpment bends sharply eastward as it is traced to the north and it is uncertain whether the Sevier fault follows that bend and assumes an east-northeast strike or, as indicated by Callaghan and Parker (1961), strikes N. 35° E. beneath a thick mantle of landslide and alluvial debris to reemerge at the west base of bedrock hills northeast of Annabella. Regardless of the location of the main fault trace, the east-northeast trend of the plateau margin is fault controlled, as shown by Rowley and others (1981). It provides a sharp contrast with the Monroe segment which trends northerly. Volcanic rocks in the upthrown block are mildly faulted with stratal dips that average only about 5° . Bedrock north of the main escarpment dips northward as much as 35° and is downthrown or downbent more than 400 m (Rowley and others, 1981).

Strikes of 154 small-displacement faults along the Annabella segment are very diverse (fig. 3), and 61 have rakes less than 45° and 93 have rakes greater than 45° . The fault-slip data clearly represent a heterogeneous mixture of DS, OS, and SS motions (fig. 5). Because the rake distribution is

bimodal it is reasonable to separate the data into DS and SS subsets before performing computations. The strike histogram (fig. 3) shows that few faults parallel the fault-controlled plateau margin along the Annabella segment.

Paleostress axes computed from the DS subset are of good quality because the subset is large enough to perform the computations using a large sample of faults (N=61) with dips between 20° and 80° and rakes greater than 60° . East-west extension is indicated (fig. 7). The SS subset yields paleostress orientations that suggest north-south compression. Because σ_3 for the two faulting modes has a somewhat similar east-west azimuth and there is no indication from the data distributions of the SS and DS subsets (not illustrated here) that DS faulting uses different systems of faults than SS faulting, both faulting modes are assumed to belong to the same tectonic regime.

Sevier Plateau, Monroe Segment

A northerly trending segment of the Sevier fault is well defined, though almost completely buried, south of Monroe where it apparently controls the N. 5° E. trend of the plateau margin for about 6 km. It is referred to herein as the Monroe segment. The fault was seen at only one locality (Z, fig. 2) where its attitude is N. 7° E., 70° W., and it cuts conspicuously intact Oligocene andesite. It is marked by a 1- to 2-m-wide rib of massive secondary silica that has been prospected locally. Striations on and within the silica have a gentle rake to the north. Though neither the sense nor amount of displacement is known, the striations suggest that this segment of the Sevier fault may at times have experienced predominantly SS motion.

Strike distributions of 56 small- and 6 intermediate-displacement faults that cut weakly tilted volcanic rocks in the footwall (eastern) block of the Monroe segment show no tendency to parallel the plateau margin (fig. 3). Of

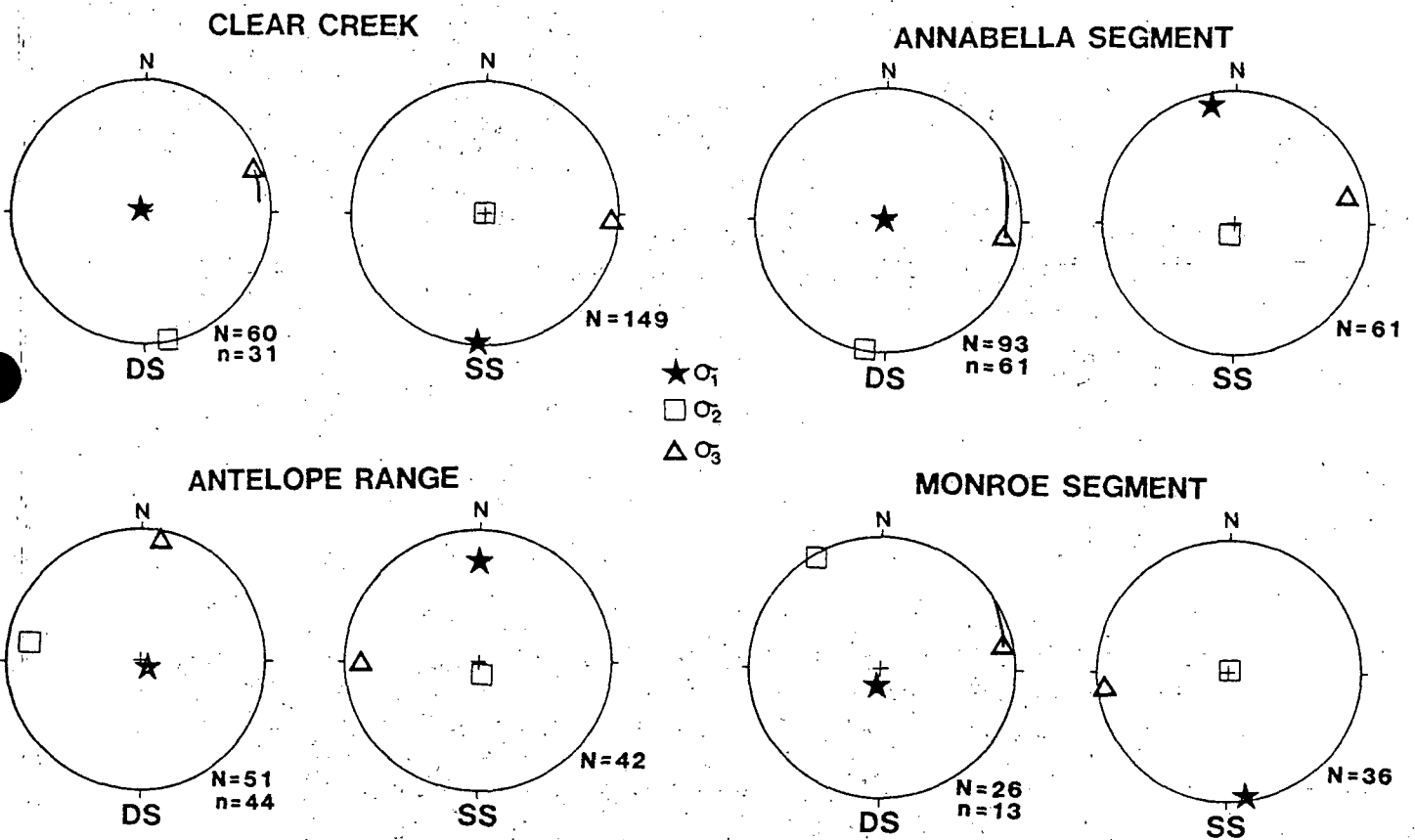


Figure 7.—Paleostress axes computed from SS and DS subsets from the four subareas. All axes are computed from data samples that are not weighted for fault size because weighting does not produce significant changes in axial orientations. All DS axes are computed from samples that have been "cleaned" by eliminating faults with rakes less than 60° or dips greater than 80° and less than 20° . The tie lines extending from the σ_3 axes show the shift produced by "cleaning." The axis for the Antelope Range shows no significant shift and is anomalous when compared with σ_3 axes from the other three subareas. N = sample size before "cleaning"; n = sample size after cleaning.

14 faults whose strikes fall within 20° of the plateau margin, only 3 dip toward the valley and show normal displacement. If the Monroe segment of the Sevier fault is a major range-front normal fault it is clearly not reflected as such in the small to intermediate faults of its footwall block. Of the 62 faults, 36 have rakes less than 45° and 26 have rakes greater than 45° . Their strikes show northwest and northeast maxima. The data suggest heterogeneous slip on faults that bear no obvious relationship to the buried plateau-margin fault.

Stress-axis orientations computed from the small sample of faults are very similar to those computed for the Annabella segment (fig. 7). The similarity, together with the lack of any obvious relationship to the plateau-margin faults in either area, suggests either that the small faults along the Annabella-Monroe segments predate plateau uplift and were not reactivated during uplift or that they represent a complicated uplift-related paleostress history that includes important components of north-south compression. The latter possibility is favored.

Northernmost Antelope Range

The part of the Antelope Range adjacent to the Dry Wash fault consists of a fault-repeated sequence of Oligocene and Miocene flows and tuffs with east to northeast dips ranging from 5° to 45° (Cunningham and others, 1983). Mapped faults strike mostly northwest and northeast, and strikes of those studied are bimodally distributed with northerly and northeasterly maxima (fig. 3). Fault-slip data from the subarea were not combined with data from northwest of the Dry Wash fault because the northernmost Antelope Range consists of a more orderly arrangement of fault-tilted blocks than most other areas in the region and therefore seemed to provide an opportunity to compare computed paleostress with an established structural pattern.

Paleoslip was measured on 83 faults mostly within 2 km southeast of the trace of the Dry Wash fault. Displacement on 74 of them are known or estimated to be less than a meter. Displacement on the remaining nine range from a few meters to more than 100 m. Fault strikes show less scatter than for areas along the margin of the Sevier Plateau (fig. 3). Many of the same faults were activated during SS and DS faulting modes as shown by polyphase striae. Striae with two or more separate orientations were observed on 11 faults and on each the older one has the lowest rake. Many of the youngest striae indicate oblique slip—a feature that is probably responsible for the less conspicuous bimodal distribution of rake angles than is seen for the other subareas (fig. 5). Although data are sparse, the consistency in relative age of striae is not seen in other areas studied. Because it exists in the Antelope Range the low-rake measurements from polyphase surfaces are included in the SS subset and the moderate- to high-rake measurements in the DS subset. The SS subset contains measurements from 42 faults and the DS from 51 faults.

Paleostress axes computed from unweighted subsets are shown in figure 7. The SS subset yields axes suggesting north-south compression and east-west extension similar to the SS subsets from the margin of the Sevier Plateau. The DS subset yields a typically steep σ_1 , but, surprisingly, it indicates a north-northeast orientation for σ_3 . Such an orientation is inconsistent with the mapped pattern of faulting and tilting from which an approximately east-west σ_3 might be predicted. The 010 azimuth computed for σ_3 is not significantly altered by weighting (as noted above), nor is it significantly altered if axes are computed from a population that contains only faults that dip between 20° and 80° and have rakes greater than 60° . Also, an early computation from part of the data gathered during an early field trip (N=31)

shows a similar azimuth for σ_3 . These additional computations increase confidence in the validity of the σ_3 azimuth.

Because DS striations are consistently younger than SS ones, a possible explanation for the discrepancy between expected and computed σ_3 for DS motions may be that they are younger than and unrelated to block faulting and tilting. According to such an explanation faults that formed during an early episode of block tilting responding to east-west extension would have been reactivated as SS faults and their striations obliterated in a subsequent stress regime characterized by north-south compression. The compressional event would, in turn, have been superseded by a young mild episode of approximately north-south extension and OS and DS faulting. Alternatively the block tilting could have coincided with the compressional event as an inhomogeneous response to complex permutations of σ_1 and σ_2 (Angelier and others, in press). In either alternative, the 010 orientation of σ_3 is anomalous.

Clear Creek

The Clear Creek area straddles the boundary between the Pavant Range to the north and the Tushar Mountains to the south (fig. 2). It includes data from the Dry Wash fault as well as several other mapped northeast-trending faults.

Callaghan and Parker (1962) considered the southern Pavant Range to be a broad south-plunging anticline as defined by late Tertiary strata. It is separated from the structurally elevated volcanic edifice of the Tushar Mountains to the south by a broad open east-trending synclinal sag with a structural relief of almost 2 km (fig. 2). This sag, named the Clear Creek downwarp by Callaghan and Parker (1962) is the dominant structure in the Clear Creek area. It involves strata as young as the Pliocene Sevier River

formation and, according to Rowley and others (1979) defines part of a 150-km-long east-trending structural lineament that has existed for the last 27 m.y. Several upright open east-trending map-scale folds that also involve Pliocene strata are mapped by Callaghan and Parker (1962) on the south flank of the Clear Creek downwarp (fig. 2). These folds have structural relief of about 200 m.

The Clear Creek downwarp and the folds on its southern flank terminate eastward against the Dry Wash fault. The Dry Wash is a major sinistral-slip fault as indicated by common subhorizontal striations and corrugations and the geometry and stratigraphic position of rock slabs that are distributed along it. Net displacement on the Dry Wash could be as much as 8 km on the basis of structural and stratigraphic terminations (Cunningham and others, 1983) and stratigraphic contrasts across it (T. A. Steven, oral commun., 1983). Directly northwest of the Dry Wash fault two additional northeast-trending map-scale faults display abundant evidence of sinistral slip and have net slip of as much as 1 km. These faults also offset strata that were previously folded, although some of their displacement is probably accommodated by the east-trending folds that are located near their southwestern terminations (fig. 2). The folds are cut by many small-displacement steep SS faults. Detailed study of 81 of these faults in axial and opposed-limb positions show that they comprise northeast-trending sinistral (33) and northwest-trending dextral (48) sets that (1) offset one another, (2) have broad ranges in strike with no overlap, and (3) contain striations whose rake angles are independent of position on the fold (fig. 8). These relationships indicate that the sinistral and dextral sets are conjugate. Mohr-Coulomb theory (Anderson, 1951) would predict that they formed under conditions of north-south compression. Their relationship to folding suggests that they formed late in

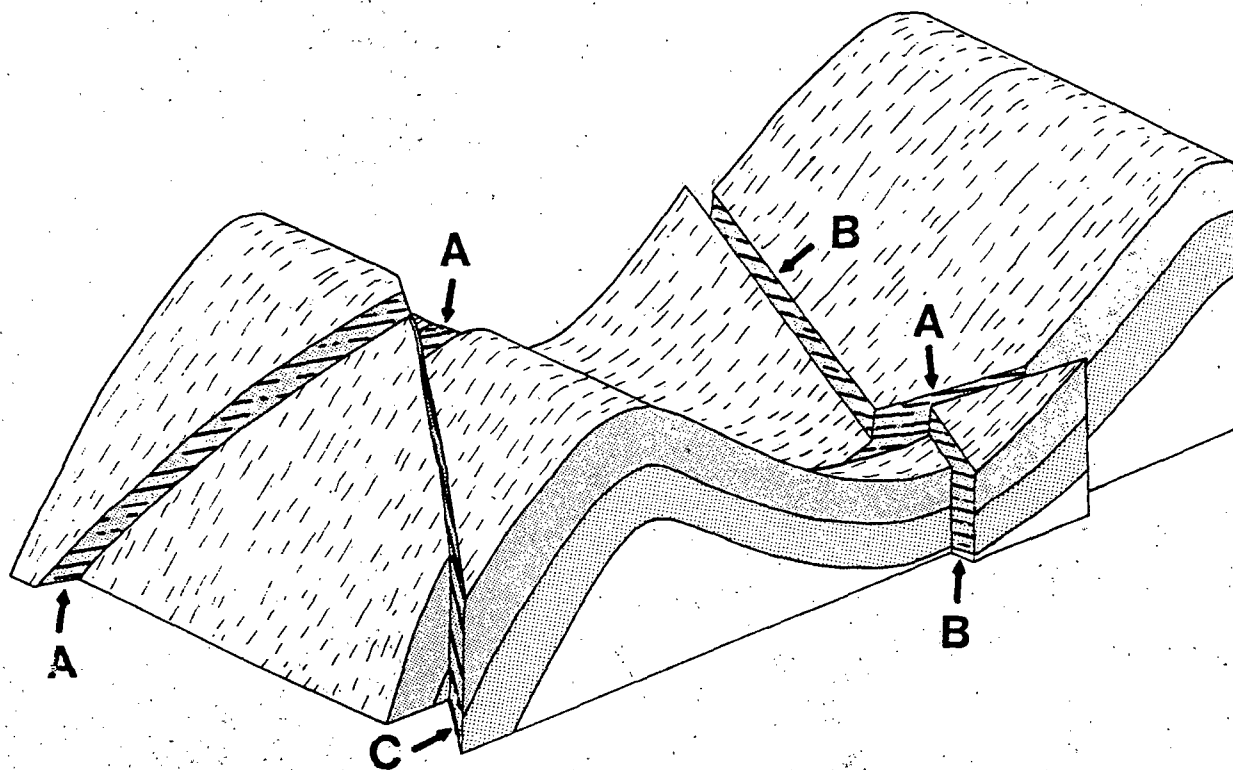


Figure 8.—Schematic block-diagram showing a fold cut by a sinistral fault (A) and two dextral faults (B, C). Heavy lines symbolize striae on fault surfaces. Fault C offsets fault A and fault A offsets fault B as indication of conjugate behavior. Also, rake of striae is independent of position in fold.

the folding history or perhaps after folding, a suggestion that is consistent with the map-scale relationships of sinistral faults to folds noted above.

Dextral faults with small displacements are sparse in the rocks adjoining the Dry Wash fault on the northwest. Though displacements on these faults are very much less than on the adjacent sinistral faults, the two sets are mutually offsetting and their strikes fall into the same range as for the small faults that cut the folds. These small dextral faults were probably active in the same north-south compressional stress field as the large faults, the folds, and the small faults that cut the folds. On this basis all SS data (149 faults) from the Clear Creek area are combined into a single set from which paleostress axes are computed (fig. 7). The axes indicate a north-south maximum compressive stress consistent with that indicated by Mohr-Coulomb mechanics and with orientations computed from SS subsamples from the other three subareas.

Dip-slip striations were measured on 60 faults in the Clear Creek area. Five of these faults show evidence of polydirectional slip. Of those, the dip slip is younger than the strike slip on three and older on two. Thus, no evidence is provided for a temporal separation of SS and DS faulting. Only 31 of the 60 faults have dips between 80° and 20° and rakes greater than 60° . A limited stress tensor computed from those 31 measurements shows σ_3 at azimuth 75° which is within 20° of σ_3 computed from the SS faults (94°). The mapped structures together with the fault-slip data suggest an inhomogeneous late Cenozoic stress history characterized by a permutation of σ_1 and σ_2 in a stress field with σ_3 oriented east-northeast to east-west and dominated by north-south compression.

Other Areas

Fault-slip data from four other areas in or near the central Sevier Valley region provide qualitative indications that the compressional paleostress shown by geologic mapping and fault-slip studies in the four subareas described above is not anomalous. The areas are (1) the southeast margin of the Pavant Range along the Elsinore fault (fig. 2), (2) roadcuts along Interstate 70, 10 km west of the area covered by figure 2 at the latitude of Clear Creek, (3) roadcuts along Interstate 15, 20 km west of the area covered by figure 2 at the latitude of Monroe, and (4) bedrock east of Beaver, Utah, 40 km southwest of the Clear Creek area.

In the vicinity of Elsinore, the structure of the margin of the Pavant Range is dominated by northeast-trending open folds (fig. 2). Strata in the southeasternmost fold limb dip about 50° toward Sevier Valley giving the range-front structure the form of a monocline rather than a fault. The monoclinical form continues 5 km beyond the area covered by figure 2 to the vicinity of Richfield. It has a complex appearance because it involves rocks that were faulted and tilted by earlier deformation and has important down-to-axis faulting associated with it.

Of 59 small- and intermediate-displacement faults observed along the range front between Elsinore and Richfield, only 13 strike within 25° of the N. 35° E. trend of the range front, and, of those, only 3 dip southeast--the dip direction that one would expect if the faults are part of a range-front fault system. Of the three, one shows a sinistral-strike slip, one has polydirectional striae indicating early normal and late sinistral displacements, and one shows normal slip. Thus, only 1 of 59 faults has an orientation and slip sense similar to what would be expected for a range-front normal fault system. As with the Monroe and Annabella segments of the Sevier

fault, if the Elsinore fault exists as a range-bounding normal fault it is clearly not reflected as such in the small- to intermediate-displacement faults in its footwall block. Faults that strike northeast dip mostly northwest, and their DS component is down toward the range--a displacement aspect that is common in monoclinial flexures along range fronts. Many faults strike north to northwest and have striae with a bewildering variety of rake angles and polyphase slip. On the basis of the geometry of their intersection with bedding, the dip slip on many of these faults could be related to an early episode of northeast-southwest extension. Though the fault-slip data are too few and heterogeneous to use as a basis for paleostress computations, much of the OS and SS motion on these faults could be related to reactivation of early normal faults in a compressional stress field analogous to the one that controlled late Cenozoic structural development in the Clear Creek area. Neither their formation nor their possible reactivation is likely to be directly related to a range-front normal fault system. If a range-front fault exists in the Elsinore-Richfield area, it is buried beneath the Quaternary alluvium that flanks the range and is probably a continuation of the sinistral-slip Dry Wash fault. The northeast-trending open folds that dominate the structure of this area are considered analagous to those whose axes parallel the trace of late Cenozoic SS faults in the Mercury quadrangle, Nevada Test Site, Nevada (Barnes and others, 1982).

Between the Pavant Range and Tushar Mountains along Interstate 70 several roadcuts provide good exposures of faulted Oligocene and Miocene volcanic and sedimentary rocks in a west-northwest to east-southeast cross-strike distance of about 1.5 km. The rocks dip east to southeast 15° - 25° and are cut by numerous steep northeast-trending faults. The area is one in which the stratal repeat patterns and physiography are suggestive of a simple pattern of

normal faulting (Cunningham and others, 1983), but the striae tell a much different story. Slip orientations and senses were measured on 20 faults ranging in displacement from about 20 cm to more than 100 m (fig. 9). Eight of the 20 faults have measured or estimated displacements of 10 m or more, and the sense of slip was determined with certainty on 14 of them. The large-displacement faults have gouge zones ranging in width to 50 cm. The gouge has a strong internal shear fabric whose geometry and orientation are consistent with the orientation and sense of displacement measured on the planar walls of the shear zone suggesting an unusually high degree of uniformity of fault motion. One fault strikes north and is dextral. The remaining 19 strike northeast and 17 are certainly or probably sinistral and two are normal (fig. 9). These excellent exposures show that fault deformation in the area is dominated by northeast-trending sinistral faults and that no significant difference exists between the slip on large- and small-displacement faults.

Strongly fractured Oligocene volcanic rocks are exposed in roadcuts along the northbound and southbound lanes of Interstate 15 about 6 km north of the junction with Interstate 70 (fig. 9). The exposures are located a few kilometers west of the boundary between the Basin and Range and faulted transition zone. The strata strike west-northwest and dip gently south-southwest whereas the average strike of faults in the area is 015° (Cunningham and others, 1983). Because the faults strike approximately perpendicular to the strike of the beds, the beds cannot be assumed to be tilted by fault displacements. Displacement amounts on individual faults are not known but are assumed, on the basis of fracture appearances, to range from a few centimeters to a few meters. Unpublished geologic mapping in the area shows at least 200 m of apparent sinistral offset between the exposures along the northbound and southbound lanes. The orientation and sense of slip were

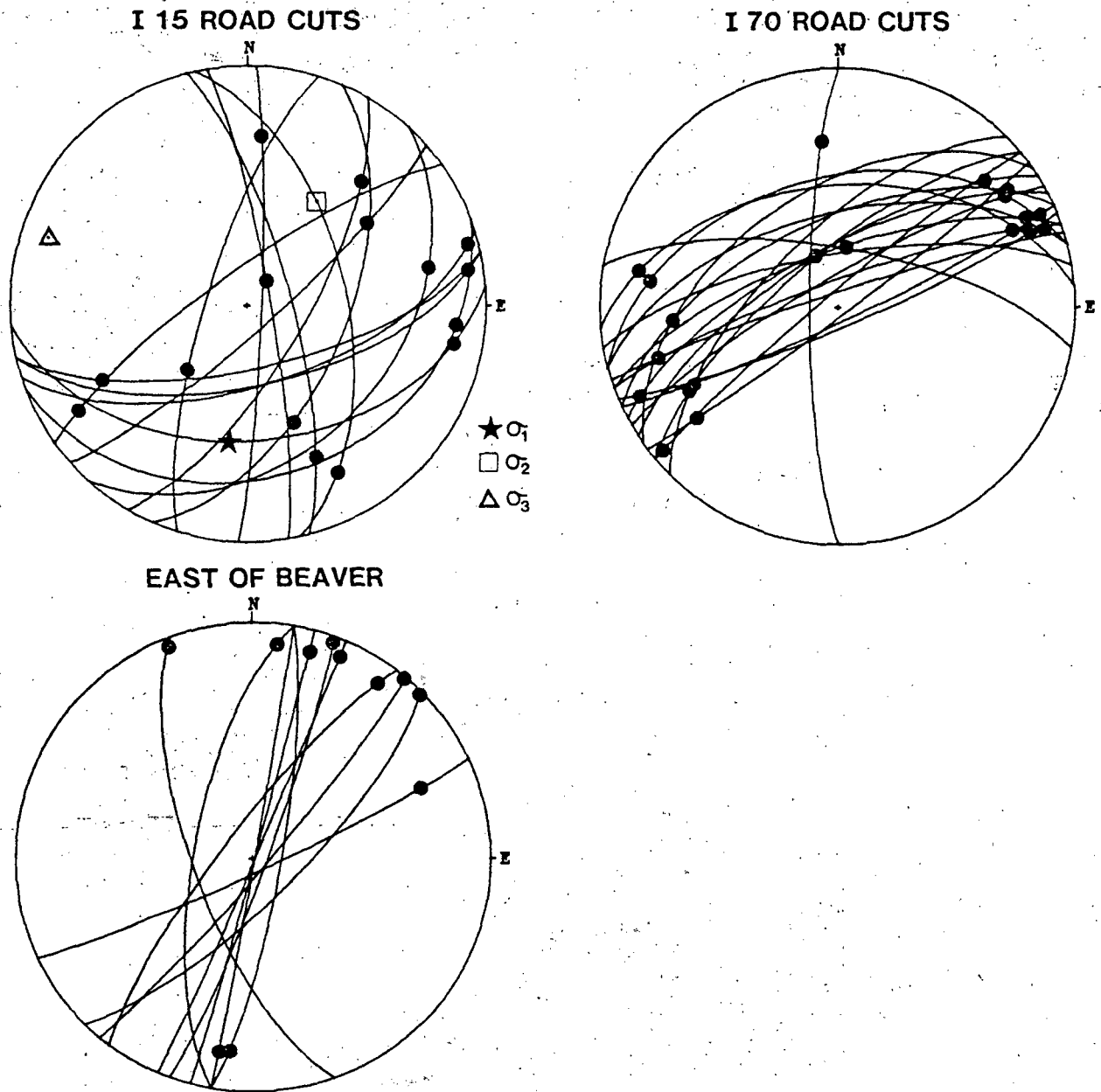


Figure 9.—Lower-hemisphere stereographic plots of faults as great-circle arcs and striae in those faults as dots. Faults at I-70 roadcuts are sinistral except for a north-trending dextral and two DS faults. The faults at the I-15 roadcuts that strike between 015° and 085° are all sinistral. The others are dextral except for the normal fault with a steep rake. The slip sense was not determined for the faults east of Beaver. The computed stress axes for the faults from the I-15 roadcuts are poorly constrained because of the small sample size and predominance of sinistral slip.

measured on six faults in the eastern cut and nine in the western cut. These faults, which range in strike from 345° through 0° to 085° and in dip from 28° to 85° , are probably representative of the range of principal fault orientation in the vicinity of the cuts. Two contrasting slip orientations were measured on 4 of the 15 faults and on each the sense of both motions is similar (all are predominantly sinistral). Of the 15 faults 3 northerly trending ones are predominantly dextral, 7 northeasterly trending ones are predominantly sinistral, and the remainder show a predominance of dip slip (fig. 9). Paleostress axes computed from the 15 faults (using the youngest motions on faults with two orientations) are shown in figure 9. They are poorly constrained because of the small size of the data set.

The fault boundary between the Basin and Range province and the faulted transition to the Colorado Plateau is located about 4 km east of Beaver, Utah. Striations on 10 small- and 1 intermediate-displacement faults that strike north to northeast and cut gently tilted and weakly faulted late Cenozoic bedrock along the Beaver River east of the province-bounding fault indicate predominantly SS motions (fig. 9). The 10 small faults are located in an area of less than 5 km^2 within 2 km east of the province-bounding fault that separates Beaver Valley from the Tushar Mountains. They appear to represent the only fault deformation to which the rocks have been subjected. Late Quaternary fault scarps are abundant in the basin-fill sediments of Beaver Valley (Machette and others, 1981). Conventional wisdom would predict normal DS displacements on those faults as well as on the province-bounding fault. However, the area is located along the southwesterly projection of major faults in the Clear Creek area that are now known to be SS faults. The occurrence of SS faults in bedrock may not be as anomalous as it seems at first.

In summary, not only do striated faults in the four subareas described in this report provide a strong record of SS faulting, but similar faulting is seen in four well-exposed areas in and near the central Sevier Valley area. Together the data show that late Cenozoic SS faulting is common in the region. This is consistent with earlier observations of widespread Neogene SS faulting in southwestern Utah (Anderson, 1980). The data from Interstate 15 roadcuts and the area east of Beaver show that Cenozoic bedrock directly east and west of the Basin and Range province boundary was involved in SS faulting.

AGE OF FAULTING

Rowley and others (1979) conclude that the major faulting in the Clear Creek area took place after 7 m.y. ago and Rowley and others (1981) conclude that the main uplift of the Sevier Plateau (about 1.5 km) took place in less than 2.5 m.y. between 7.6 and 4.8 m.y. ago. Anderson and Bucknam (1979) noted fault scarps of probable late Pleistocene age along the Sevier fault near Annabella and along the Elsinore fault near Elsinore. Callaghan and Parker (1961) noted that Quaternary river terraces northeast of Joseph appear to be tilted eastward by displacement on the Dry Wash fault. Thus, displacements on the major faults in central Sevier Valley probably extend from latest Miocene through Pleistocene. At the I-15 roadcuts the northeast-trending faults from which SS data were gathered are located along the strike projection of northeast-trending faults that cut basaltic lavas of Quaternary age directly south-southwest of the roadcuts (Steven and others, 1979). The simplest interpretation of available data from that area is that the measured striations include a record of Quaternary displacements and that the faults that cut Quaternary basalts are not simple normal faults.

CONCLUSIONS

Listed below are 12 conclusions that can be drawn regarding the late Cenozoic structure of the central Sevier Valley region.

1. The Dry Wash fault and two other northeast-trending, map-scale faults to the northwest of it have major cumulative sinistral displacement that may approach 10 km. They are genetically and mechanically related to abundant small-displacement faults in the Clear Creek area, and, together, they form conjugate sinistral and dextral systems with large dispersion of strikes. On the basis of Mohr-Coulomb mechanics all these faults formed in a late Cenozoic compressional stress field with σ_1 oriented approximately north-south.
2. East-trending folds with amplitudes of 200 m and wavelengths of 1 km formed in the same compressional stress field as the faults of conclusion 1. The fault-fold patterns combine to show that the Pliocene and Pleistocene(?) structural fabric of the Clear Creek area formed predominantly under conditions of horizontal compression and it represents tectonically significant sinistral shear and north-south shortening.
3. Strike-slip faulting is the major and youngest mode of faulting at widespread localities in southwestern Utah showing that the late Cenozoic structural style of central Sevier Valley is not anomalous.
4. Small- and intermediate-displacement faults in bedrock adjacent to Sevier Valley along the Elsinore fault and along the Monroe and Annabella segments of the Sevier fault do not reflect the trend or slip sense of range-front normal faults that have been inferred by previous workers to lie buried beneath range-bounding Quaternary alluvium in those areas.

5. Because the Dry Wash fault is a major SS fault that projects northeast toward the Elsinore fault, and because there is little evidence in the bedrock adjacent to the trace of the buried Elsinore fault that it is a normal fault, the Elsinore fault is probably continuous with the sinistral Dry Wash fault. Sinistral slip on two minor faults near Elsinore support this conclusion. Also, the open folds that parallel the Elsinore fault are probably genetically related to it. This latter suggestion is based on an analogy with similar open folds related to late Cenozoic SS faults in the southern Nevada Test Site.
6. The northerly trending segment of the Sevier fault south of Monroe has probably experienced SS motion.
7. On the basis of observations leading to conclusions 4, 5, and 6, vertical structural differentiation between Sevier Valley and its flanking mountains (Pavant Range and Sevier Plateau) was probably accomplished by a combination of monoclinial flexing and, on the average, OS faulting.
8. Slip data from more than 550 faults (mostly of small displacement but including some of intermediate and large displacement) from the central Sevier Valley area represent a heterogeneous mixture of DS, OS, and SS motions as the youngest slip events on those faults. Rake distributions tend to be strongly bimodal and show that OS faults are relatively uncommon. Such bimodal mixtures of predominantly SS and DS faults are found elsewhere in the Basin and Range. Together with strike and dip distributions, they show that deformation is dominated by two different faulting modes that do not utilize separate and distinct systems of faults in a given mass of rock.
9. Paleostress orientations computed from subsamples of faults with rakes less than 45° are remarkably similar for the four subareas in the central

Sevier Valley area. The orientations suggest subhorizontal north-south maximum compressive stress as part of the late Cenozoic structural history of central Sevier Valley. For the Clear Creek subarea the orientations agree well with paleostress deduced qualitatively from fault-fold patterns. The four subareas have sharply contrasting local structural settings so the occurrence of and consistency in computed and deduced compressional paleostress is unexpected and surprising. The consistency suggests that the orientations have regional significance.

10. Because weighting according to fault size does not significantly influence paleostress orientations, the assumption is made that displacements on the abundant small faults are representative of displacements on the large faults. Because the small structures involve the same rocks as the large ones they are interpreted to be of the same latest Miocene through Pleistocene age as the large faults. Pressure-axis orientations inferred from seismicity studies (Julander, 1983) apparently reflect the superposition of horizontal compression (north-south to northeast-southwest) upon east-west extension (Julander and Arabasz, 1982). The OS and SS faulting modes indicated by focal mechanism solutions derived from microseismicity studies and regional earthquake monitoring in the area are generally consistent with extensional and compressional paleostress states computed from hundreds of faults in the central Sevier Valley region suggesting a temporal continuity between seismicity and paleoseismicity. Deformational models developed to explain the seismicity must be consistent with the youngest part of the geologic record and they must accommodate folding as well as

SS and DS faulting. Also, they should be representative of the full size range of faults and folds--including approximately 2 km of vertical structural relief on the Clear Creek downwarp.

11. The DS and SS faulting modes for three of the four subareas yield separate paleostress axes that suggest permutations of σ_1 and σ_2 consistent with the model of combined lateral and vertical contraction associated with east-west extension deduced from the seismicity data. These relationships suggest that SS and DS faulting belong to the same tectonic regime and that the permutations do not represent major reorganizations of regional stress. For the Clear Creek subarea and the margin of the Pavant Range between Elsinore and Richfield this suggestion is supported by the complex patterns of polyphase slip on numerous faults.
12. Some SS faults in the central Sevier Valley area are as large and as young as the largest and youngest known or inferred normal faults and must therefore be considered to represent a similar level of earthquake hazard. This conclusion is supported by the apparent stress-state correspondence between seismicity and paleoseismicity.

REFERENCES

- Anderson, E. M., 1951, The dynamics of faulting (2d ed.; 1st ed., 1942):
Edinburgh, Oliver and Boyd, 206 p.
- Anderson, R. E., 1980, Factors that complicate determination of the
neotectonic stress field in southwestern Utah: Geological Society of
America Abstracts with Programs, v. 12, no. 6, p. 265-266.
- Anderson, R. E., and Bucknam, R. C., 1979, Map of fault scarps on
unconsolidated sediments, Richfield 1° by 2° quadrangle, Utah: U.S.
Geological Survey Open-File Report 79-1236, 17 p., 1 pl.

Angelier, J., 1979, Determination of the mean principal stress for a given fault population: *Tectonophysics*, v. 56, p. T17-T26.

Angelier, J., Colletta, B., and Anderson, R. E., 1985, Neogene paleostress changes in the Basin and Range--a case study at Hoover Dam, Nevada-Arizona: *Geological Society of America Bulletin*, [in press].

Arabasz, W. J., and Smith, R. B., 1981, Earthquake prediction in the intermountain seismic belt--An intraplate extensional regime, in Simpson, D. W., and Richards, P. G., eds., *Earthquake prediction--An international review*: American Geophysical Union, Maurice Ewing Series, v. 4, p. 238-258.

Arabasz, W. J., Smith, R. B., and Richins, W. D., eds., 1979, *Earthquake studies in Utah, 1850-1978*: Salt Lake City, Utah, University of Utah Seismograph Stations, Special Publication, 552 p.

Barnes, Harley, Ekren, E. B., Rodgers, C. L., and Hedlund, D. C., 1982, *Geologic and tectonic maps of the Mercury quadrangle, Nye and Clark Counties, Nevada*: U.S. Geological Survey Miscellaneous Investigations Map I-1197, scale 1:24,000.

Callaghan, Eugene, and Parker, R. L., 1961, *Geology of the Monroe quadrangle, Utah*: U.S. Geological Survey Geologic Quadrangle Map GQ-155, scale 1:62,500.

_____ 1962, *Geology of the Sevier quadrangle, Utah*: U.S. Geological Survey Geologic Quadrangle Map GQ-156, scale 1:62,500.

Cunningham, C. G., Steven, T. A., Rowley, P. D., Glassgold, L. B., and Anderson, J. J., 1983, *Geologic map of the Tushar Mountains and adjoining areas, Marysvale volcanic field, Utah*: U.S. Geological Survey Miscellaneous Investigations Map I-1430-A, scale 1:50,000.

- Hulen, J. B., and Sandberg, M., 1981, Exploration case history of the Monroe KGRA, Sevier County, Utah: U.S. Department of Energy Technical Report DOE/ID/12079-11, ESL149, 82 p.
- Julander, D. R., 1983, Seismicity and correlation with fine structures in the Sevier Valley area of the Basin and Range-Colorado Plateau transition, south-central Utah: Salt Lake City, Utah, University of Utah M.S. thesis, 142 p.
- Julander, D. R., and Arabasz, W. J., 1982, Seismicity and correlation with fine structure in the Sevier Valley area of the Basin and Range-Colorado Plateau transition, south-central Utah: EOS (American Geophysical Union Transactions), v. 63, no. 45, p. 1024.
- Keller, G. R., Smith, R. B., and Braile, L. R., 1975, Crustal structure along the Great Basin-Colorado Plateau transition from seismic refraction profiling: Journal of Geophysical Research, v. 80, p. 1093-1098.
- Machette, M. N., Steven, T. A., Cunningham, C. G., and Anderson, J. J., 1981, Geologic map of the Beaver 15-minute quadrangle, Beaver County, Utah: U.S. Geological Survey Open-File Report 81-951, 11 p., 1 pl.
- McKee, M. E., 1982, Microearthquake studies across the Basin and Range-Colorado Plateau transition zone in central Utah: Salt Lake City, Utah, University of Utah M.S. thesis, 118 p.
- McKee, M. E., and Arabasz, W. J., 1982, Microearthquake studies across the Basin and Range-Colorado Plateau transition in central Utah, in Nielson, D. L., ed., Overthrust belt of Utah: Utah Geological Association Publication 10, p. 137-149.

- Richins, W. D., Arabasz, W. J., Hathaway, G. M., Oehmich, P. J., Sells, L. L., and Zandt, G., 1981, Earthquake data for the Utah region July 1, 1978 to December 31, 1980: Salt Lake City, Utah, University of Utah Seismograph Stations, Special Publication, 127 p.
- Rowley, P. D., Steven, T. A., Anderson, J. J., and Cunningham, C. G., 1979, Cenozoic stratigraphic and structural framework of southwestern Utah: U.S. Geological Survey Professional Paper 1149, 22 p.
- Rowley, P. D., Steven, T. A., and Kaplan, A. M., 1981, Geologic map of the Monroe NE quadrangle, Sevier County, Utah: U.S. Geological Survey Miscellaneous Field Studies Map MF-1330, scale 1:24,000.
- Smith, R. B., 1978, Seismicity, crustal structure, and intraplate tectonics of the Western Cordillera: Geological Society of America Memoir 152, p. 111-144.
- Steven, T. A., Rowley, P. D., Hintze, L. F., Best, M. G., Nelson, M. G., and Cunningham, C. G., compilers, 1978, Preliminary geologic map of the Richfield 1° by 2° quadrangle, Utah: U.S. Geological Survey Open-File Report 78-602, scale 1:250,000.
- Wechsler, D. J., 1979, An evaluation of hypocenter location techniques with applications to southern Utah--regional earthquake distributions and seismicity of geothermal areas: Salt Lake City, Utah, University of Utah M.S. thesis, 225 p.

INVESTIGATION OF HISTORICAL SEISMICITY IN THE SALT LAKE CITY PORTION
OF THE WASATCH FRONT REGION OF UTAH USING DOCUMENTARY SOURCES

by

Sherry D. Oaks

U.S. Geological Survey
Box 25046, MS 966
Denver Federal Center
Denver, Colorado 80225

ABSTRACT

Extensive investigation of the historical documentary record is being undertaken by this study as a part of determining the frequency of occurrence and the extent of physical effects of earthquakes in the Salt Lake City portion of the Wasatch Front area of Utah. Although the investigation is preliminary at this time, it is evident that (1) untapped primary sources are available for investigation, (2) many of those sources have a high degree of historic reliability, (3) some of the sources have a significant homogeneity, (4) the spatial distribution of the sources improves previous location bias, and (5) the numerous types of sources available for Salt Lake City in particular are sufficient to provide an accurate picture of historic seismicity in that area. The three phases of this study include information garnered from intensive checking of original documentary sources from 1850 to the present to uncover as much data as possible on the following:

Phase I--dates and times of events felt in the area

Phase II--felt area, intensity, epicentral region and effects
of those earthquakes including damage reports

Phase III--societal response to earthquakes through time

While the investigation will include those events that affected the study region (fig. 1), it will focus on the effects of earthquakes in Salt Lake City. However, any data located during the course of the study that will aid

in a more complete record of the historic seismicity for the State of Utah as a whole will be made available.

Phase I--Identifying the dates and times of events

Pre-instrumental Utah earthquakes have been listed in catalogs (Holden 1898, McAdie 1907, Townley and Allen 1939, Williams and Tapper 1953, Coffman and von Hake 1973, U.S. Geological Survey, 1976, Arabasz and others, 1979, Askew and Algermissen 1983) and in bulletins and journals (for example, United States Earthquakes or the Bulletin of the Seismological Society of America). The published catalogs listed above were checked and the data on earthquakes were traced to the original sources. The original sources used in those compilations were not always primary sources but sometimes secondary ones. Errors, omissions, and duplications in such compendia are often perpetuated from one list to another through time because of that practice. The use of primary sources eliminates those compilation errors (Oaks 1981, Ambraseys 1983). Therefore, earthquake accounts in published works were traced to the primary sources to determine which ones had been used. Additional primary documentary sources (some types have been used in published lists and some have never been used, for example, army medical records) were checked to solve the problems which included uncertainties surrounding the date or time. Those primary sources were subjected to strict tests of reliability (S. D. Oaks 1981, unpub. rept., 1984). In addition some sources, such as meteorological station reports, were selected not only in terms of reliability but because they exhibited a desirable spatial distribution. For example, traditionally newspapers have been relied upon to provide a great deal of information for earthquake catalogs. Although they are a reasonably good source of data, they

are spatially biased to the population centers that produced them. Many of the meteorological stations were located in other, often rural, areas. Investigations of historic seismicity using documentary sources in areas of the Basin and Range province, which lie outside the present study area, have shown that as many as 50 percent more historic earthquakes have occurred in some of those nonurban places than are listed in catalogs.

The data that have been located and tested (along with additional sources to be investigated in 1985) will serve as a basis for an updated catalog of Utah earthquakes. The updated catalog will contain events $I_0 \geq III$ (M.M.) in an effort to present a more detailed list of historic seismicity for the study area. Again, the focus will be on earthquake effects in Salt Lake City, the Wasatch Front, and the State of Utah, respectively.

Phase II--Identifying the felt area, intensity, epicentral region, and damaging effects of earthquakes

The existing catalogs were also checked for poorly documented events (those where felt area, intensity, epicentral region, or all of the above were questionable or unknown). Again, primary sources were checked to ascertain the most reliable data available. As in phase I, documentary sources for phase II were not only located, but subjected to reliability tests.

More information to help define the effects of Utah earthquakes is being gathered. Intensity maps will be prepared for events for which sufficient data are located. While some intensity data have been collected, additional data points need to be located before phase II can be completed. This task will be accomplished over the course of the next year, again, with special attention to the effects of earthquakes in the study area, but with

consideration for the region. The information collected for this phase will be aimed at defining the effects of earthquakes on the metropolitan areas of the study region, specifically Salt Lake City. Damage to various building types and different sites will be detailed whenever possible.

Primary documentary sources (mostly weather records) have been located and some have been searched for earthquake information for the following places during the periods listed.

Utah	
Alta-----	1889-1891
Bearer-----	1889-1892
Bingham-----	1889-1892
Brock-----	1888-1889
Camp Scott (on Blacks Fork of Green River)-----	1857-1858
Castlegate-----	1891-1892
Cedar City-----	1899-1900
Cisco-----	1891-1892
Coalville-----	1869-1872
	1873
	1874-1882
	1883
Corinne-----	1871-1874
Deseret-----	1891-1892
Fillmore-----	1892
Fort Crittenden (formerly Camp Floyd; Cedar Valley)-----	1858-1861
Fort Douglas-----	1889-1892
Fort Duchesne-----	1889-1893

Utah--Continued

Fort Thornburgh (at junction of Duchesne and Greene Rivers)-----	1881-1884
Frisco-----	1885-1887
Grafton (Kane County)-----	1865-1866
Greenriver-----	1891-1892
Grouse Creek-----	1890-1892
Harrisburg Washington County)-----	1867-1872
Heberville (Washington County)-----	1861
Kanab-----	1872-1879
Lake Park (Davis County)---	1888-1892
Levan-----	1889-1892
Loa-----	1892
Logan-----	1883-1892
Losee (Garfield County)---	1889-1892
Manti-----	1892
Modena-----	1900-1907
Moab-----	1889-1892
Mount Carmel-----	1874-1892
Mount Pleasant-----	1889-1891
Nephi-----	1883-1892
Ogden-----	1889-1892
Park City-----	1889-1892
Parowan-----	1890-1892
Price-----	1888
Provo-----	1889-1892
Randolph-----	1892
Richfield-----	1889-1892
Rockville-----	1866

Utah--Continued

St. George-----	1862
	1863
	1864
	1865-1866
	1869
	1870
	1880
	1889-1892
Salt Lake City-----	1854
	1857
	1858
	1859
	1861
	1863
	1864-1868
	1869-1871
	1872-1873
	1882
	1874-1907
Scotfield-----	1891-1892
Snowville-----	1889
	1890-1892
Soldier Summit-----	1891
	1892
Spring Lake (Utah County)---	1875
Stockton-----	1889-1892
Taylor's Ranch (Emery County)-----	1889-1891
Teasdale-----	1891
Thistle-----	1892
Tonaquint (Washington County)-----	1861
	1862

Utah--Continued

Uintah (Weber County)-----	1890-1891
Vineland (Washington County)-----	1864
Wanship-----	1866
	1867
	1869
Young's Springs-----	1883-1884

Phase III--Societal response to earthquakes $I_0 \geq V$ (M.M.) in Salt Lake City

The third part of the study will seek to assess the societal response to earthquakes in the Wasatch Front area with particular attention to Salt Lake City. Societal response is a subject area where historical documentary research can make a unique contribution in telling us how society has adapted in the past to the earthquake hazard.

To accomplish this phase primary documentary sources including not only traditionally used newspapers, but also institutional and personal papers such as church records and diaries, are slated for investigation. While the sources have been identified and some have been checked, this part of the study will be the last phase to be completed because the basic investigation of Utah earthquakes needs to be completed first (phase I and II). Once the accuracy of that chronology is determined and the physical effects in Salt Lake City are ascertained, the societal response to those earthquakes will be explained. Actions of individuals, groups, and institutions will be detailed as the historic record permits. A historical survey of how the earthquake hazard has been perceived in Salt Lake City and how the actual earthquake events have affected that perception through time will be investigated.

REFERENCES

- Ambraseys, N. N., 1983, Notes on historical seismicity: Seismological Society of America, v. 73, no. 6, p. 1917-1920.
- Arabasz, W. J., Smith, R. B., and Richins, W. D., 1979, Earthquake studies in Utah, 1850-1978: Salt Lake City, University of Utah Seismograph Stations Department of Geology and Geophysics, 552 p.
- Askew, Bonny, and Algermissen, S. T., 1983, An earthquake catalog for the Basin and Range province, 1803-1977: U.S. Geological Survey Open-File Report 83-86, 41 p.
- Coffman, J. L., and von Hake, C. A., eds., 1973, Earthquake history of the United States: Washington, U.S. Department of Commerce, National Oceanic and Atmospheric Administration Environmental Data Service, 208 p.
- Holden, E. S., 1898, A catalogue of earthquakes on the Pacific Coast 1769 to 1897: Smithsonian Miscellaneous Collections, v. 37, no. 1087, 253 p.
- McAdie, A. G., 1907, Catalogue of earthquakes on the Pacific Coast 1897-1906: Smithsonian Miscellaneous Collections, v. 49, no. 1721, 64 p.
- Oaks, S. D., 1981, Historical data for the 1882 earthquake in the Rocky Mountain region, in Geologic and seismologic investigations for Rocky Flats Plant: Dames and Moore, Denver, Colorado, appendix H, p. 1-207.
- Townley, S. D., and Allen, M. W., 1939, Descriptive catalog of earthquakes of the Pacific Coast of the United States 1769 to 1928: Seismological Society of America Bulletin, v. 29, no. 1, p. 1-297.
- U.S. Geological Survey, 1976, A study of earthquake losses in the Salt Lake City, Utah, area: U.S. Geological Survey Open-File Report 76-89, 357 p.
- Williams, J. S., and Tapper, M. L., 1953, Earthquake history of Utah 1850-1949: Seismological Society of America, v. 43, no. 3, p. 191-218.

Figure 1 for Oaks, Sherry D. abstract "Investigation of Historical Seismicity in the Salt Lake City Portion of the Wasatch Front Region of Utah Using Documentary Sources"

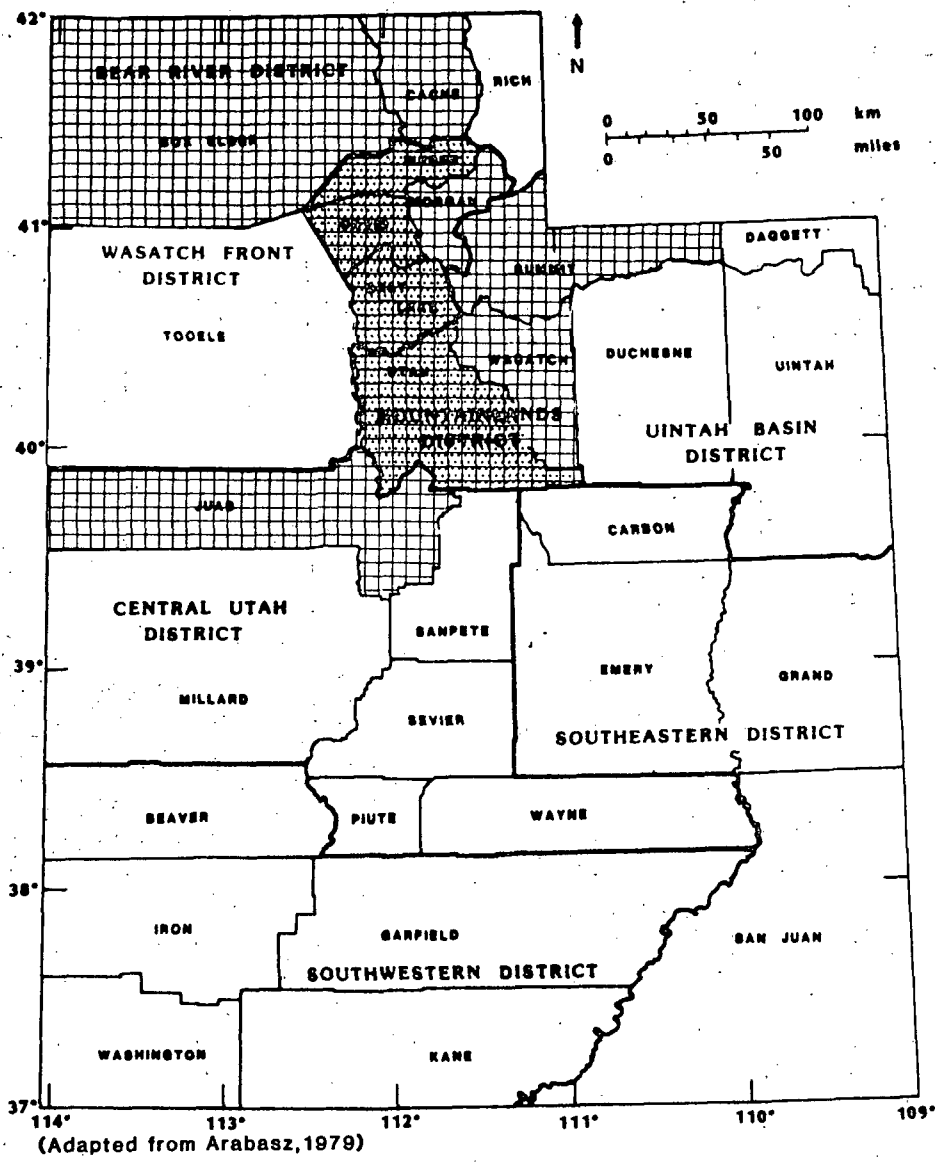
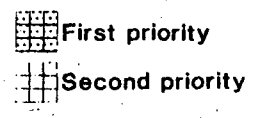


Figure 1 : Counties in study area



CONTEMPORARY VERTICAL TECTONICS ALONG THE WASATCH FAULT ZONE
MEASURED BY REPEATED GEODETIC LEVELING

by

Spencer H. Wood

Branch of Engineering Geology and Tectonics

U.S. Geological Survey

Mailing address: Department of Geology and Geophysics

Boise State University, Boise, Idaho 83702

(208)385-3629 or 385-1631

INTRODUCTION

Apparent ground-surface tilt and vertical movement can be derived from a comparison of repeated geodetic leveling of permanent benchmark monuments. Elevations have been surveyed by precise geodetic leveling along many main roads and railroads in Utah. The present study has concentrated on repeated surveys across the Wasatch Fault in Weber Canyon near South Ogden (Figure. 1) because an apparent ground-surface tilt with a 12-cm vertical component is associated with the fault and developed since a 1958 survey (Wood and Bucknam, 1983). This vertical movement has considerable significance with regard to contemporary pre-seismic strain accumulation in the fault zone, and implications with regard to the frequency and nature of earthquake occurrence and tectonic deformation. This line and the route from Ogden, Utah to Rock Springs, Wyoming was relevelled by the National Geodetic Survey (NGS), June - October, 1983, using newly developed procedures designed to eliminate the past difficulties with slope-dependent, systematic, cumulative errors in height determination and in vertical crustal-movement studies. The 12-cm vertical movement is based largely upon baseline elevations from leveling in 1958. The 1958 precise geodetic leveling observations have been coded and recalculated using the NGS computer program, REDUC 4, to estimate and apply a refraction correction (Figure 2).

Detailed data on the spatial and temporal nature of vertical tectonic deformation of a region of would be extremely useful for earthquake-hazard

evaluation and for long-term forecasting and possibly short-term prediction of earthquake occurrence. Repeated geodetic leveling is still the best available method for obtaining quantitative profiles of ground-surface tilt and elevation change. New procedures of the NGS have largely resolved problems of slope-dependent systematic errors and can resolve 1 mm / km of vertical movement or 1 microradian of tilt. Limitation on obtaining regional coverage of this kind of data is the current cost of \$350 / km for single-run, precise geodetic leveling a line of benchmarks. Other systems for obtaining elevation differences of tectonic interest over continental distances are under development (Panel on Crustal Movements, NRC, 1981), but none are routinely used in Utah.

Recovery of older baseline elevation data from past geodetic leveling surveys in the United States is a long-term project of the NGS (Holdahl, 1983). Controversy over vertical-crustal movement measurements by leveling over the past 6 years has now focused largely on the error caused by vertical temperature gradients near the ground that cause bending of the line of sight between the telescopic level instrument and the rod. This refraction error has been found to be considerable, particularly along gently-sloping railroad routes where long-sight lines are possible. Error increases as the square of the the sight-length, and prior to 1964, the NGS permitted 70-m sight lengths rather than the 50 meter limitation currently used. This correction was neglected until about 1977. Current field procedures and data reduction of the NGS are designed to correct for refraction and other accumulating systematic errors discussed by Balazs and Young (1982). A method has been developed by Holdahl (1982, 1983) to recalculate older data and incorporate an estimate of the vertical temperature gradient from single temperature measurements and knowledge of typical seasonal meteorological conditions in the United States. Coding and recalculating the repeated surveys for Utah is a considerable task and is not a

high priority for the limited staff of the NGS. Therefore we are reviewing the old observed elevations and will request only the most critical lines. We are also coding some of the USGS precise leveling for recalculation.

Lake levels of Great Salt Lake and Utah Lake are referenced to shoreline benchmarks from time to time on this project as a means of obtaining an independent set of data on vertical tectonic movement. A site on Farmington Bay within 3 km of the Wasatch Fault (Fig. 1) is being installed with an electronic, digitally-recording water-level monitoring and data transmission system. The time record of water levels will be continuously differenced with data from another site on the same body of water 15 or more km further west. The pair of sites will act as a long-baseline tiltmeter to monitor movement of the earth's surface near the fault with respect to points to the west.

LEVELING DATA ANALYZED ALONG THE WASATCH FRONT

The 1958 elevations have been recalculated using the REDUC 4 program of the National Geodetic Survey. The 1983 elevations were obtained by procedures recently developed to minimize the systematic errors. To illustrate the nature of the accumulated refraction error when it is not considered, this accumulated correction is profiled along the level line discussed in this paper (Fig. 3 and 4). The correction for the 1958 data is based upon an estimation procedure discussed above, whereas the correction for the 1983 data is based upon actual measurement of the temperature gradient at every instrument set-up along the line. The correction applied to the 1958 data accumulates along the line to 17

mm, and appears as a small tilt in a releveling comparison. In all cases, the refraction correction is added to the elevation difference between two points, for refraction of the sight line has the effect of shortening the surveyed elevation difference. The correction applied to the 1983 data is only 5 mm along the same line. It is much smaller because the sight lines are shorter. When refraction corrections are applied, a tilt amounting to $17\text{mm} - 5\text{mm} = 12\text{mm}$ over the length of the line would be appear as an apparent elevation change due entirely to different conditions of sight-line refraction experienced by the two surveys. In this case, this erroneous small tilt is in the same sense as the hill slope because the earlier survey obtained erroneously lower elevation differences when leveling uphill, whereas the more recent survey obtained somewhat greater elevation difference over the same route.

The 1974 and 1979 elevations surveyed by the U.S. Geological Survey (USGS) over the eastern part of the Weber Canyon line have not been corrected for refraction or for possible rod-calibration error, but it is felt that the data is useful and accurate at originally calculated for the following reasons. These surveys used rods calibrated at three points, and had maximum permissible sight lengths of 50 m, and otherwise adhered to procedures used by the National Geodetic Survey for precise geodetic leveling. The levels did not contain the magnetic component that has recently been discovered as a source of error in the Zeiss NI-1 type of level. Furthermore, the 1974 and 1979 elevations agree rather closely, and show only a small amount of elevation change when compared (Fig. 2). In fact the elevations agree within 10 mm, except for two marks that are apparently unstable near the western end and have moved upward about 15 mm with respect to other benchmarks along the line in the time interval 1979.4 to 1983.8. Consideration in the previous paragraph of the refraction error actually experienced in surveying along the same line, shows that this type of error is

small and should not accumulate to more than about 15 mm. It does accumulate most rapidly between benchmarks 41-FMK and N-134, and the small tilt of the 1979 and 1983 elevation comparison between benchmarks 41-FMK and 34-A could be attributed to refraction error. That tilt indicated by the 1979 USGS data is of interest because it is our most recent measurement and it also occurs within in the Wasatch Fault zone. Unfortunately the USGS line was not extended far enough to the west to define the configuration of the tilt. We must rely on the the 1983 to 1958 comparison for a measure of the nature of tilting across the fault zone.

The 1983 to 1958 comparison shows an apparent elevation change of about 120 mm across the Wasatch Fault zone. Unfortunately the configuration of that tilt is not known between benchmarks A-92 and J-134, where most of the tilt was developed, because the intervening 1958 benchmarks were destroyed by new construction and road realignment. Nevertheless, the tilt amounts to 100 mm over 10 km, or 10 microradians, which is an order of magnitude greater than any expected random or systematic cumulative error. The tilt is also exactly the the configuration expected along a straining normal fault, with the greatest tilt developed in the hanging wall of the fault, and a lesser amount developed in the footwall side of the fault (Fig. 4 and 5).

POSSIBLE CAUSES OF GROUND-SURFACE TILT OTHER THAN TECTONIC STRAIN ACCUMULATION

Other causes of deformation of the earth's surface are (1) continued isostatic rebound of the area of the earth's crust loaded by Pleistocene Lake Bonneville and more recently, subsidence of the crust on account of

the load imposed the 3-meter rise in the level of Great Salt Lake from 1982 to present; (2) natural dewatering and compaction of the lacustrine sediments in the Salt Lake Basin in response to the present load of overlying sediments; and (3) artificially induced subsidence in areas of groundwater withdrawal from confined aquifers, particularly in the Weber Delta area.

Deformation of Pleistocene Lake Bonneville shorelines by isostatic rebound is documented by Crittenden (1963,1967). The main area of rebound is a broad area centered on the Lakeside Mountains along the southwest shore of the Great Salt Lake (Fig.7) where the total rebound has been 67 m in response to a 290 m lowering of the lake since its high stand about 16,000 yrs ago. Total crustal tilt from isostatic rebound may be 400 to 800 microradians (down-to-the-east). Crittenden estimated that there may be 20 m of rebound yet to go and that the current rate of uplift of the central area should be about 1 mm/yr. The current rate of crustal tilt along the Wasatch front should be about 0.1 microradians per year, down to the east. A level line being run this year (1984) from Brigham City west to the Nevada border should detect rebound when compared to corrected earlier surveys.

The current 3-meter rise in lake level since 1982 should ultimately produce only 0.6 m of subsidence in the central rebound area of which only about 3 per cent (20 mm) might be immediate elastic response (roughly calculated using Crittenden's methods). Viscous response of the mantle is very slow, such that after 10 years, only 0.3 per cent or 2 mm should have subsided. It is therefore unlikely that the current rise in lake level can account for much of the observed tilt in Weber Canyon. It is significant, however, that the magnitude of Holocene tilt from isostatic

rebound is of the same order as that typically observed as coseismic deformation from large, normal-fault, earthquakes (100 to 500 microradians) and that the tilt is developed over a length of at least 80 km. Isostatic rebound during the late Pleistocene was very likely a factor in the strain accumulation on the Wasatch Fault and consequently in the earthquake recurrence intervals during the Pleistocene.

Natural compaction of the sedimentary fill in the Salt Lake Basin would probably cause tilt down to the west in proportion to the thickness of clayey sediments upon bedrock. I have not studied the deep section in the Weber Delta area and I am not in a position to estimate compaction as a possible cause of the observed tilt in Weber Canyon, although the data to do so is forthcoming in an article containing seismic reflection profiles of the area soon to be published in the Journal of Geophysical Research (R.B. Smith, oral communication, 1984). Older drill hole data is reported in Feth and others (1966). The fact that tilt is also occurring in the canyon directly underlain by Paleozoic and Precambrian bedrock would seem to discount sediment compaction as a possible cause. The rate at which tilt is occurring is also large with respect to the rate at which sediment is known to compact in other basins.

Groundwater is withdrawn from deep wells in the Weber Delta area (Feth and others, 1966). A very preliminary map of approximate water level declines in the confined system, over the period 1953 to 1982, was furnished by T. Arno (U.S. Geological Survey) and is shown in Fig. 3. The control on water level declines is limited to the few wells shown. Water level declines greater than 12 m (40 feet) are indicated in the area west of Hill Air Force Base. It is possible that subsidence on the order of 30 cm (1 ft) could have occurred in the area of greatest aquifer pressure

decline, particularly if the aquifers contained a substantial cumulative thickness of thin clayey aquitard layers and lenses (Poland, 1969). In many areas of the western United States underlain by unconsolidated lacustrine deposits, subsidence has initiated after 15 to 20 m (45 - 60 ft) of water pressure decline. Further water pressure declines have been known to produce up to 1 foot of land surface subsidence for 20 feet (6 m) of pressure decline (Poland and others, 1975). In the area in which tilt is occurring, the water level declines appear to have been less than 30 feet, and unlikely to produce detectable subsidence. Also, artificially induced subsidence would not affect the area of bedrock in the Wasatch range which is also tilting down to the west.

DISCUSSION

This paper has presented the evidence for relatively large rates of tectonic strain and uplift across the Wasatch Fault. I feel we have exhausted most of the possible objections to this data by recalculating the 1958 data, and releveling the line in 1983. The case rests largely on the validity of the 1958 elevations. The 1983, 1979, and 1974 elevations agree so closely that one cannot argue away their validity.

The 1958 to 1983 comparison indicates an average rate of uplift of 4 mm / yr over the past 25 years. This rate is about four times greater than the rate determined by trenching and dating offset sediments at the Kaysville site, about 15 km to the south. At this site along the Wasatch Fault, Schwartz and others (1983) determined a late Holocene vertical slip rate of 1.3 (+0.5, -0.2) mm/yr. Farther south, at the Hobble Creek site, Schwartz and others (1983) report a Holocene slip rate of 1.0 ± 0.1 mm /

yr. The rate determined in the present study is considerably larger than determined by geologic studies, and supports the idea that strain rates along the fault may differ laterally and episodically. Along this segment of the Wasatch Fault between Salt Lake City and Ogden two events have occurred within the last 1580 150 years as determined at the Kaysville site (Swan and others, 1980; Schwartz and others, 1983) . The interval between these events was 500 to 1000 years. Net tectonic displacement for individual faulting events range from 1.7 to 3.7 m. No surface faulting events have occurred on the Wasatch front in the past 136 years, and the last event on the Salt Lake City - Ogden segment occurred within the last 500 years. If uplift is occurring at an average rate of 4 mm / yr as indicated in this study, the net tectonic displacement per event of 1.7 to 3.7 m, would indicate recurrence intervals of 425 to 850 years. Another indication of the total amount of strain accumulation before an earthquake may be taken empirically from measured coseismic deformation from earthquakes with normal faulting in the western U.S. (Fig. 5). Maximum coseismic tilt in the hanging- wall block ranges from 100 microradians in the Borah Peak earthquake measurement to 500 microradians in the Hebgen Lake earthquake measurement. The geodetic leveling data in Weber Canyon shows that 10 microradians of tilt accumulated in 25 years, or an average tilt rate of 0.25 microradians per year. Dividing this rate into the measured coseismic tilts at other localities suggests recurrence rates on the order of 400 to 2000 years which is similar to the recurrence rates obtained from slip rates of past events.

PLANS FOR FURTHER RESEARCH

This project is currently limited to evaluating and reporting on available geodetic leveling data and a modest program of releveling of about 15 additional km each year that is not a part of the NGS program, but which takes advantage of that agencies larger releveling program to re-establish the North American Vertical Control Datum, and is done by their crews. In 1983 a line of bench marks was extended west of the NGS route in order to better define deformation in the Wasatch Fault near Ogden. In 1984, the 1974 USGS Parley's Canyon line (Fig. 1) will be partly releveled. A "long-baseline tiltmeter" will also be set up using lake levels of the Great Salt Lake, and about 1 year of data should be available for the 1986 report for the Wasatch Front project.

The National Geodetic Survey is currently releveling parts of northern Utah as a part of its program to re-establish a North America Vertical Control Datum. It is important to encourage the NGS to design and route the new work so that we can monitor vertical crustal movement in Utah and other areas of earthquake hazard concern. If correctly designed, these long level lines are useful in detecting regional warping and also in detecting zones of strain that may not have obvious topographic or geologic expression.

The Wasatch Front offers an ideal situation for a greatly expanded geodetic program to study crustal deformation processes in an extensional tectonic terrane. The fact that a major earthquake may be forecasted for the segment south of Brigham City, localizes the area for instrumentation for detecting precursory events that may lead to a short-term prediction, in which geodetic methods to monitor crustal movements will play an important part. Perhaps more importantly, geodetic level profiles offer a means of exploring for other areas of strain accumulation that are not so

clearly manifested in topographic or geologic expression as is the Wasatch fault. For instance, in Figure 7, the tilt that involves 4 closely spaced benchmarks just west of benchmark S-134, and the reversal in tilt direction 15 km west of the Utah/Wyoming line may be zones of elastic strain accumulation and not rigid block movement. If significant elastic strain accumulation is detected, such areas are worthy of further earthquake hazard investigations. Seismically active areas are known for surprises. It should not surprise anyone familiar with California earthquake history if a major earthquake occurs on some lesser known fault in the northern Utah area, and not on the Wasatch Fault.

REFERENCES CITED

- Arabasz, W.J., and Smith, R. B., 1981, Earthquake prediction in the Intermountain seismic belt -- an intraplate extensional regime. in Earthquake Prediction, and International Review. American Geophysical Union Maurice Ewing Series v. 4. edited by D.W. Simpson and P.G. Richards.
- Balazs, E.I., and Young, G.M., 1982, Corrections applied by the National Geodetic Survey to precise leveling observations: NOAA Technical Memorandum NOS NGS 34, National Geodetic Information Center, Rockville, MD 20852, 12 p.
- Crittenden, M.D., Jr., 1963, Effective viscosity of the Earth derived from isostatic loading of Pleistocene Lake Bonneville: Journal of Geophysical Research, v. 68, p.5517-5530.
- _____, 1967, Viscosity and finite strength of the mantle as determined from water and ice loads: Geophysical Journal of the Royal Astronomical Society, v. 14, 261-279.
- Feth, J.H., Barkes, D.A., Moore, L.G., Brown, R.J., and Veirs, C.E., 1966, Lake

- Bonneville--geology and hydrology of the Weber Delta District, including Ogden, Utah. U. S. Geological Survey Professional Paper 518, 76 p.
- Holdahl, S.R., 1982, Recomputation of vertical crustal motions near Palmdale, California, 1959 - 1975: Journal of Geophysical Research, v.87, p. 9374-9388.
- Holdahl, S.R., 1983, The correction for refraction and its impact on the North America Vertical Datum: Surveying and Mapping, v. 43, p. 123-140.
- Meyers, W.B. and Hamilton, W., 1964, Deformation accompanying the Hebgen Lake earthquake of August 17, 1959: U. S. Geological Survey Professional Paper 435, p 55 - 98.
- Panel on Crustal Movement Measurement, U.S. National Research Council, 1981, Geodetic Monitoring of Tectonic Deformation -- Toward a Strategy: National Academy Press, Washington, D.C., 109 p.
- Poland, J.F., 1969, Status of present knowledge and needs for additional research on compaction of aquifer systems. p. 11-21 in Land Subsidence, Proceedings of the Tokyo Symposium, September, 1969, UNESCO, Paris.
- Poland, J.F., Lofgren, B.E., Ireland, R.L., and Pugh, R.G., 1975, Land subsidence in the San Joaquin Valley as of 1972. U. S. Geological Survey Professional Paper 437-H, 18 p.
- Reil, O.E., 1957, Damage to Nevada highways: Bulletin of the Seismological Society of America, v. 47, 349-362.
- Savage, J.C., and Hastie, L.M., 1969, A dislocation model for the Fairview Peak Nevada, earthquake: Bulletin of the Seismological Society of America, v.59, 1937-1948.
- Schwartz, D.P., Hanson, K.L., and Swan, F.H., III, 1983, Paleoseismic investigations along the Wasatch fault zone, an update: in Geologic excursions in neotectonics and engineering geology in Utah: Utah Geological and Mineral

Survey Special Studies no. 62, p. 45-49.

Snay, R.A., Smith, R.B., Soler, T., 1984, Horizontal strain across the Wasatch Fault near Salt Lake City, Utah. Journal of Geophysical Research, v. 89, p. 1113 - 1112.

Swan, F.H. III, Schwartz, D.P. , and Cluff, L.S., 1980, Recurrence of moderate-to-large magnitude earthquakes produced by surface faulting on the Wasatch Fault Zone, Utah: Bulletin of the Seismological Society of America, v. 70, p. 1421-1462.

Wood, S.H., and Bucknam, R.C., 1983, Vertical movement on the Wasatch fault zone: Northern Utah: Earthquake Notes, v.54, no. 1, p. 102.

FIGURE CAPTIONS

Fig. 1. Network of level lines and lake-level sites for monitoring vertical tectonic movement along the Wasatch Front in the Salt Lake City - Ogden area. (Not shown on this map are the route of the 1903, 1953, and 1967 geodetic leveling surveys of the NGS that run north-south and just west of the fault. These surveys are being re-evaluated for validity of observed elevations)

Fig. 2. Profiles of apparent elevation change across the Wasatch fault in Weber Canyon near Ogden (bottom of page). In all profiles, elevations determined in previous years are subtracted from the 1983 elevations and the changes are arbitrarily referenced to bench mark S-134 near Mountain Green, Utah. Above the elevation change profile is a profile of elevation through Weber Canyon along the 1983 leveling route. Profile west of G-134 does not correspond to leveling route. At top of page is a profile of the refraction corrections applied to the 1983 observations, and the estimated refraction corrections applied to the 1958 data. The difference between these two curves has been applied to the 1983- 1958 profile at the bottom of the page, and the effect has been to remove a very slight amount of down to the west tilt. The apparent elevation change at the bottom of the page is interpreted to be a down-to-west tectonic tilt.

Fig. 3. Map showing benchmark location in the Ogden area. Contours show the water-level declines in confined aquifers in the Weber delta area from 1952 to 1983 (preliminary and unpublished data from Ted Arno, 1982).

Figure 4. Conceptual model of the zone of strain accumulation and the anticipated coseismic tectonic deformation from a large earthquake on the Wasatch Fault zone, based upon data in Figure 5. Depiction of the Wasatch fault as a listric normal fault is suggested in articles published by Arabazs and Smith (1979) and Snay and Smith (1984).

Figure 5. Profiles of coseismic vertical deformation experienced in three large earthquakes involving normal faulting in the western United States. Hebgen Lake profile is constructed from data on Plate xx in Meyers and Hamilton (1964). Fairview Peak profile is from Reil (1959) and Savage and Hastie (1969). Borah Peak profile is unpublished and preliminary data furnished by Ross Stein, U.S. Geological Survey (1984).

Figure 6. Map showing deformation of the Pleistocene Lake Bonneville shoreline (from Crittenden, 1963).

Figure 7. Profile of apparent elevation change with respect to benchmark S-134 near Mountain Green, Utah. The 1958 recalculated elevations are subtracted from the elevations determined by the 1983 releveling of the line from Ogden to Rock Springs, Wyoming. Only the segment to Evanston, Wyoming is shown.

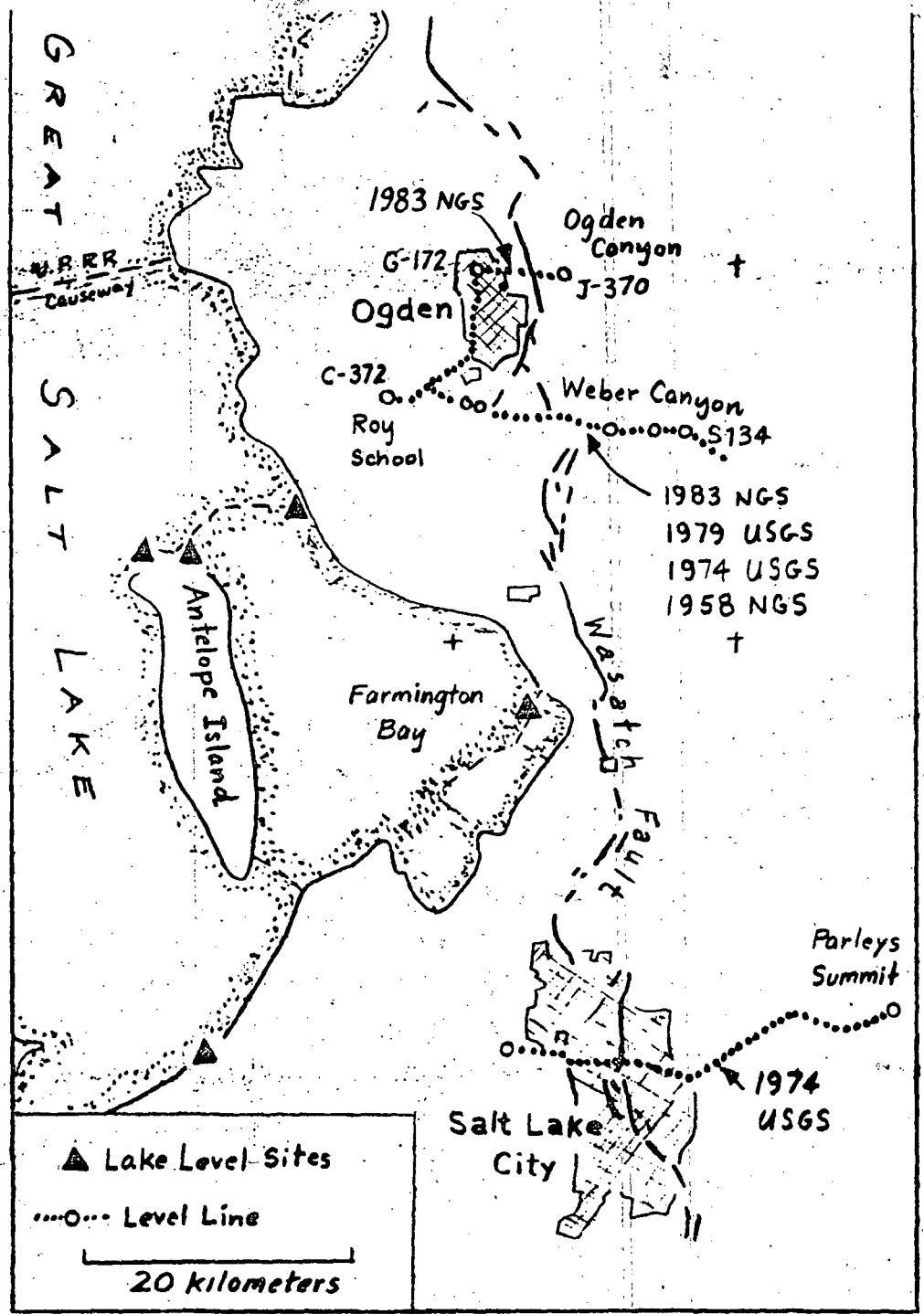


Fig 1.

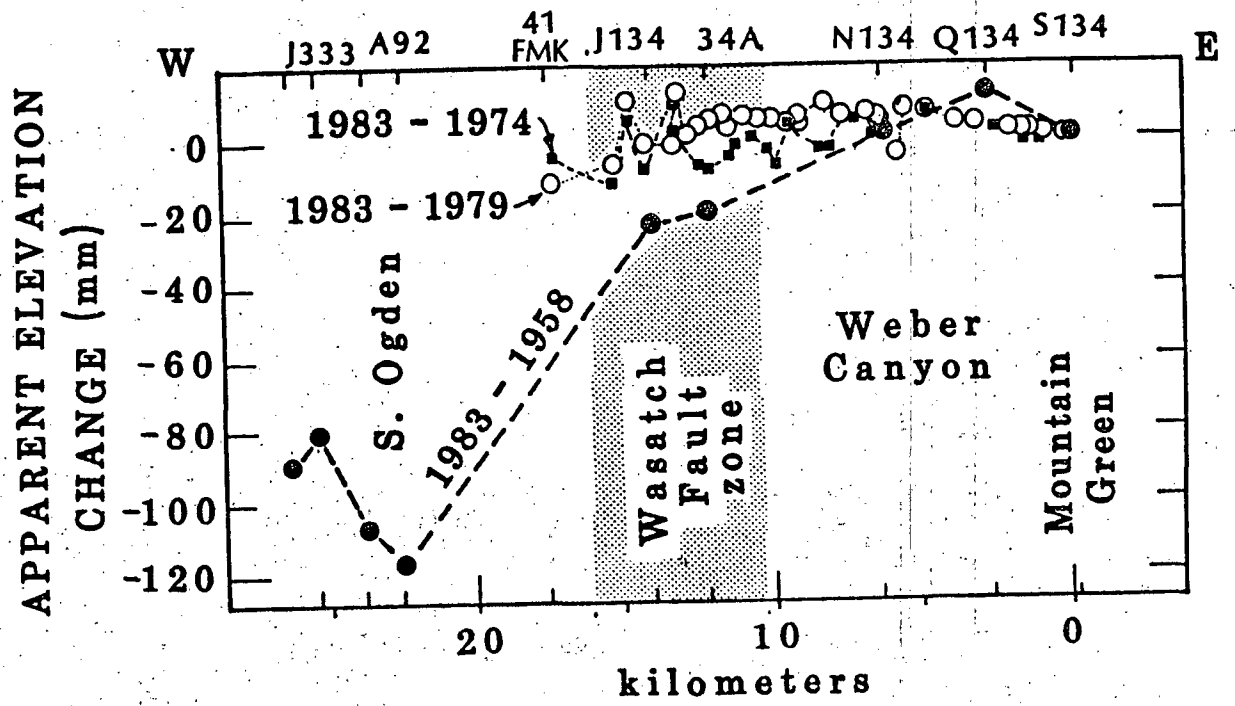
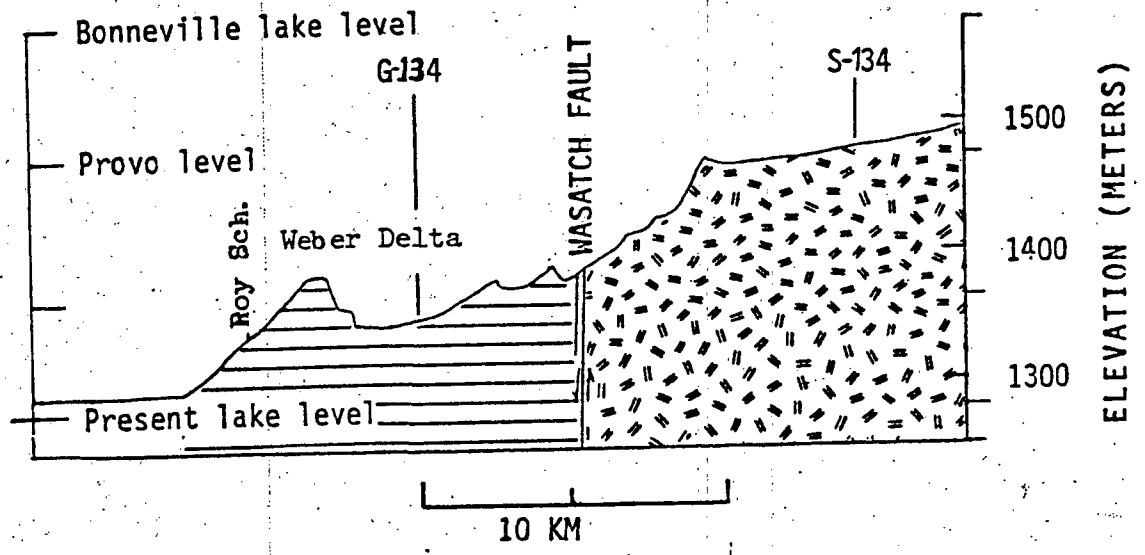
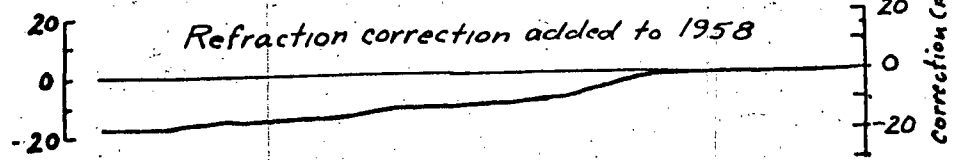
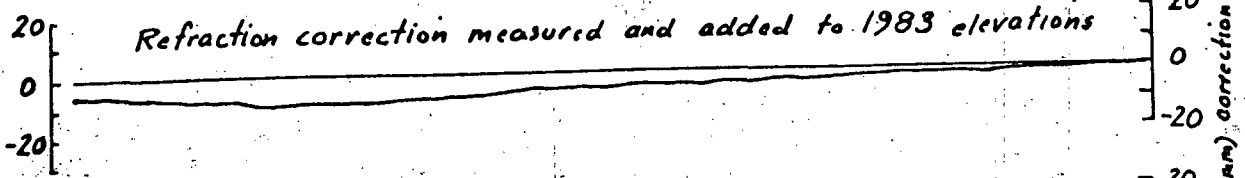


Fig.

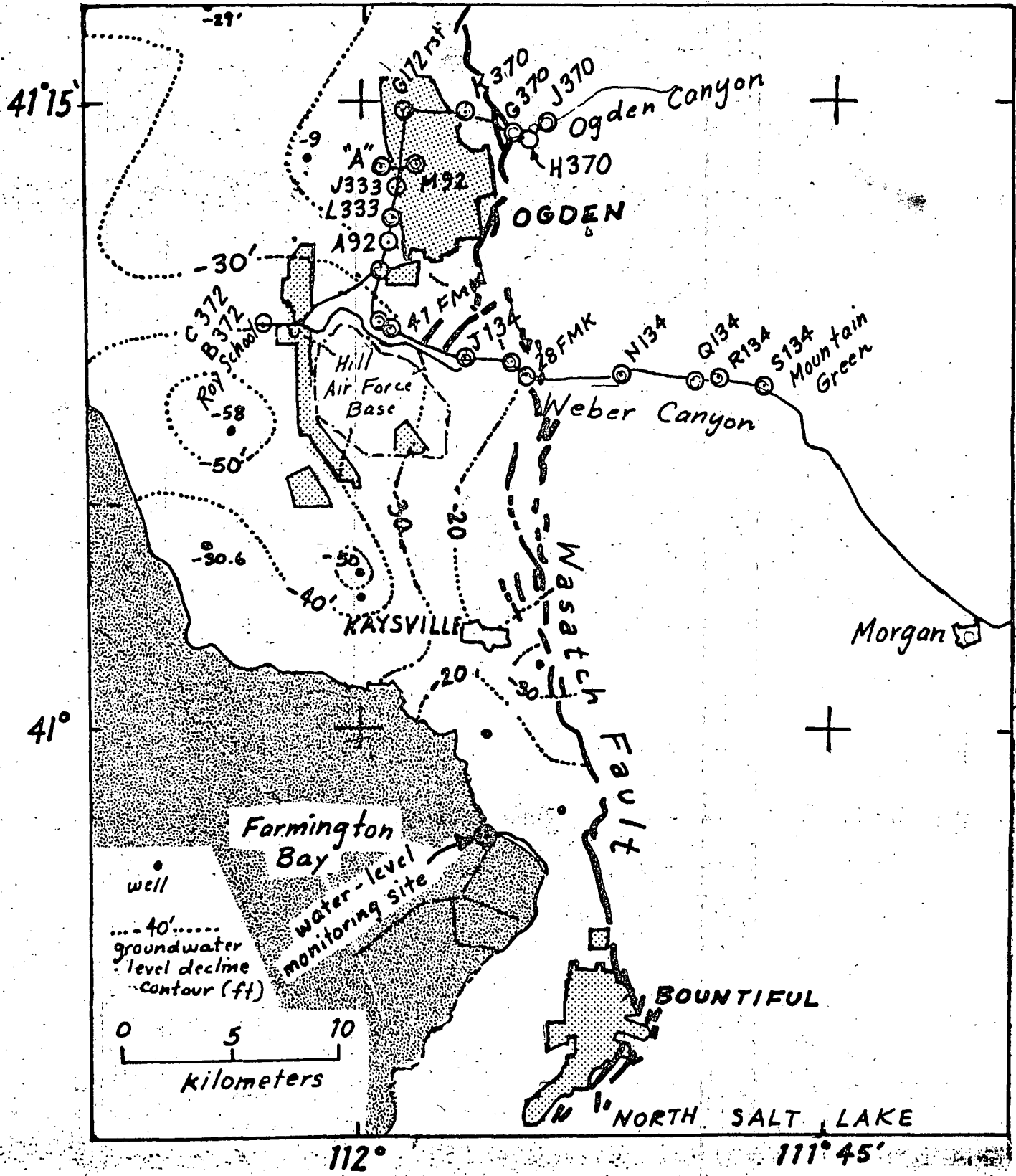
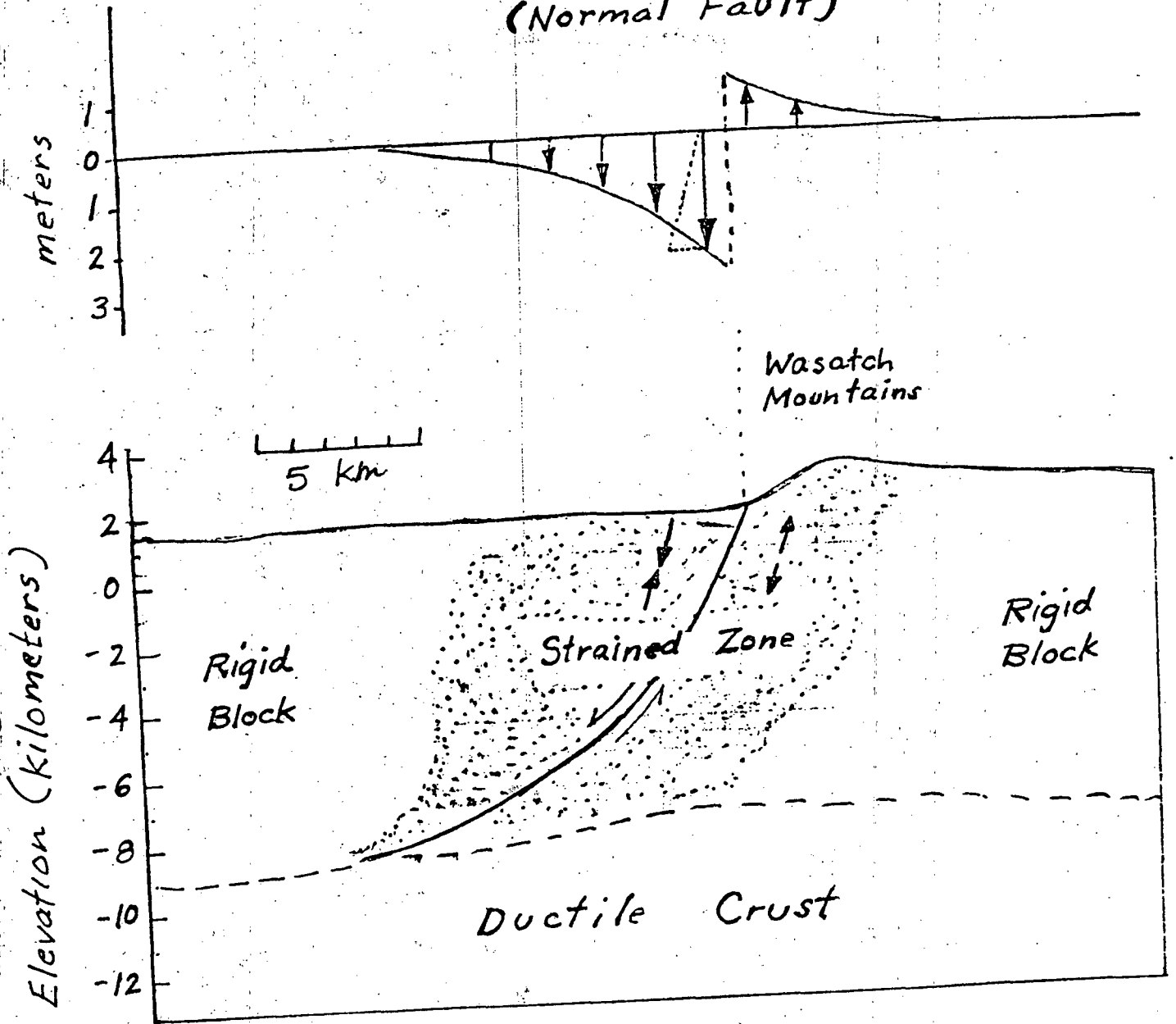


Fig. 3

COSEISMIC VERTICAL DEFORMATION (Normal Fault)



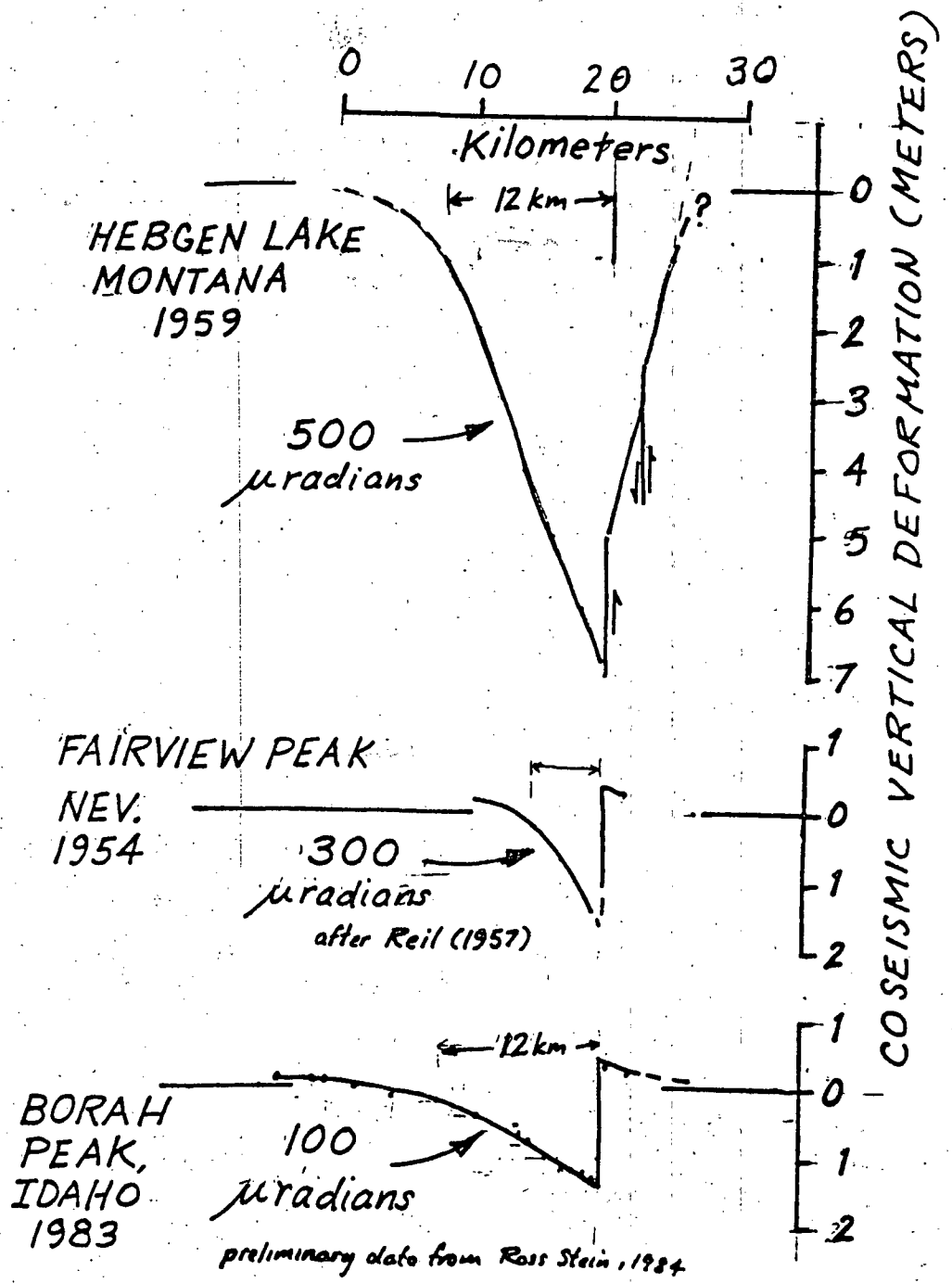
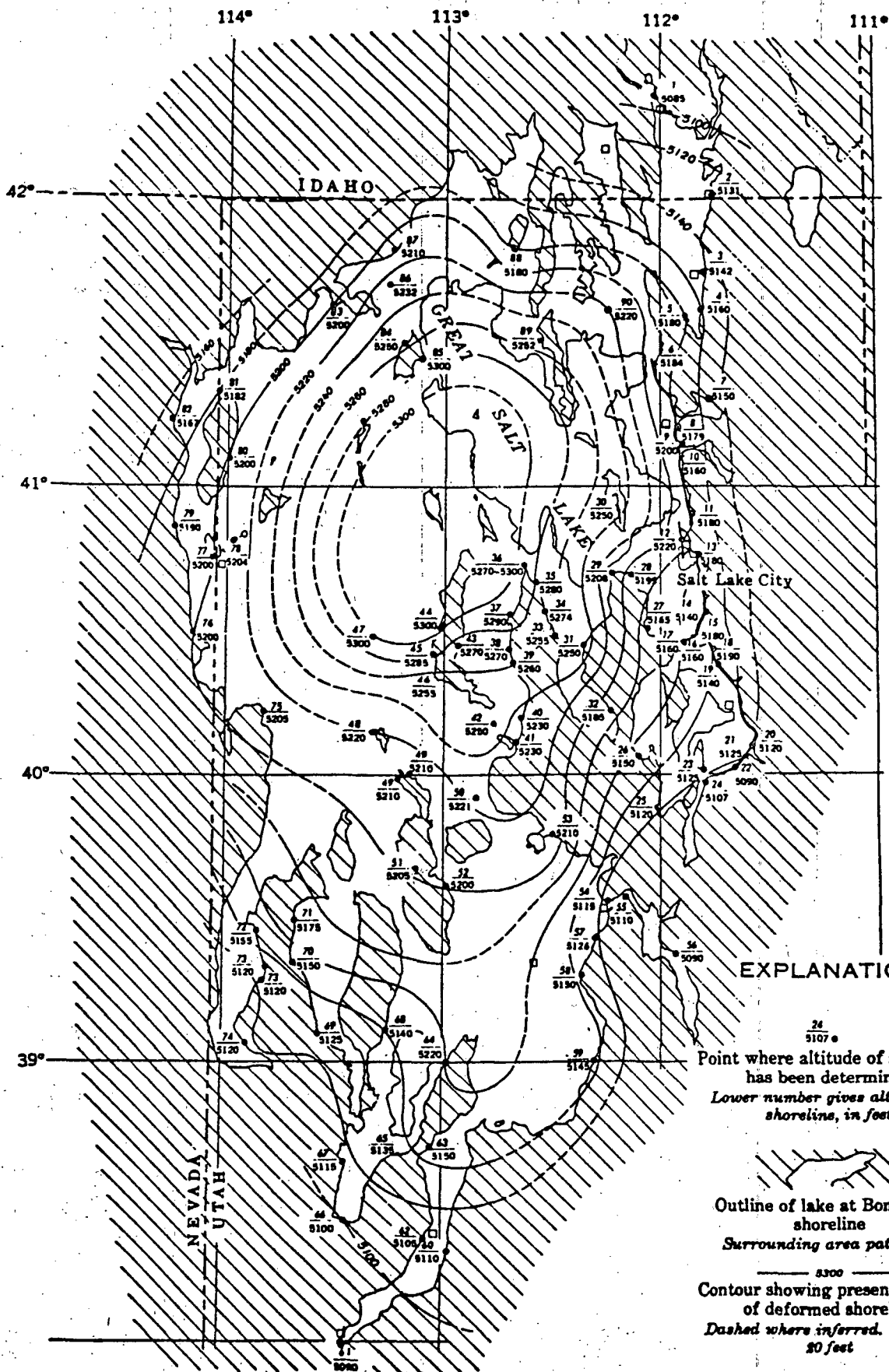
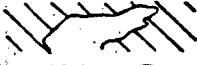



Fig. 5



EXPLANATION

$\frac{24}{5107}$
 Point where altitude of shoreline
 has been determined
*Lower number gives altitude of
 shoreline, in feet*


 Outline of lake at Bonneville
 shoreline
Surrounding area patterned

 5300
 Contour showing present altitude
 of deformed shoreline
*Dashed where inferred. Interval
 80 feet*


 Wasatch fault

0 50 MILES

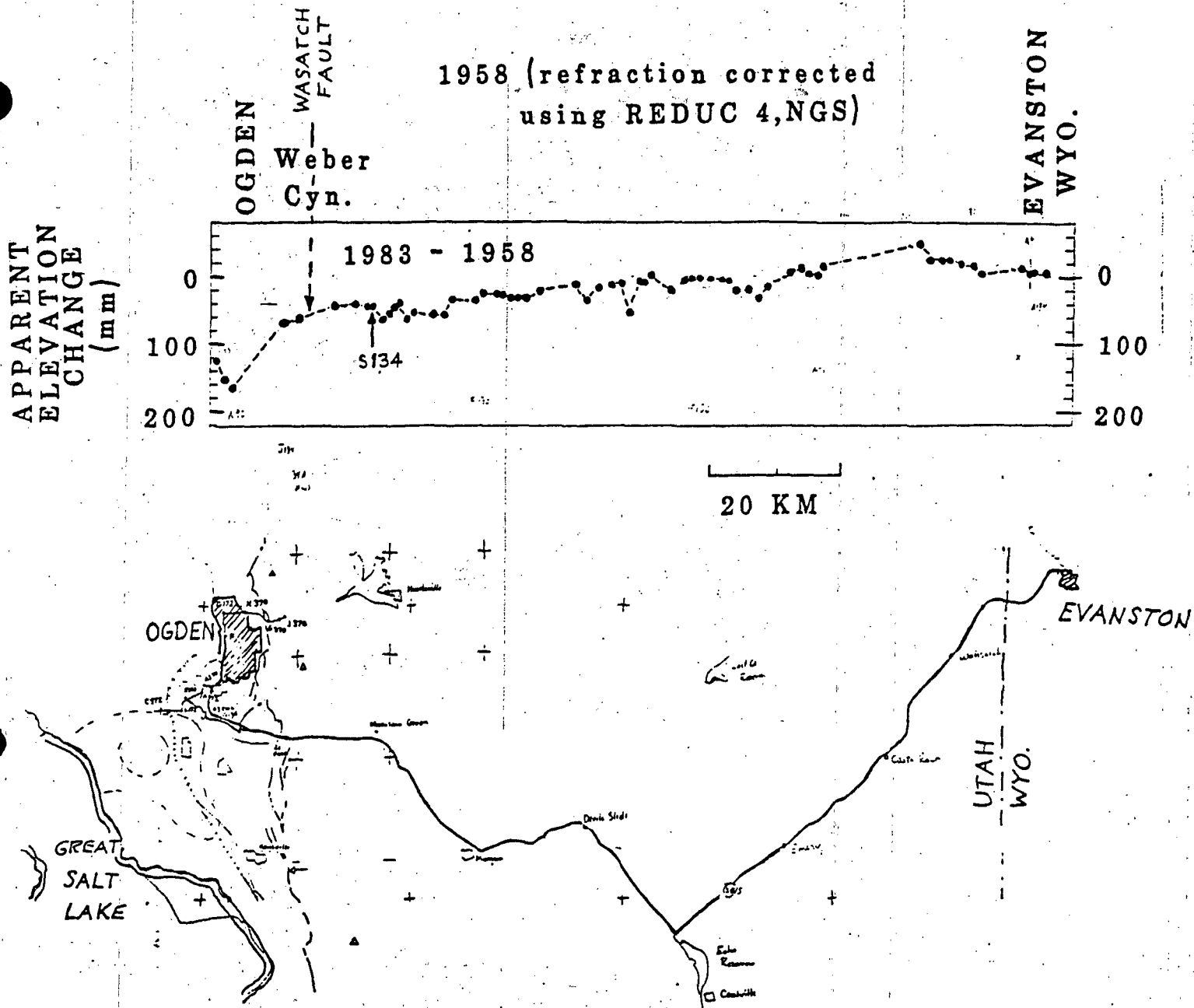


Figure 7. Profile of apparent elevation change with respect to bench mark S-34 near Mountain Green. The 1958 recalculated elevations are subtracted from the elevations determined by the 1983 NGS releveing. The line was releveled from Ogden, Utah to Green River, Wyoming, but only the segment to Evanston, Wyo. is shown.

Constraints on the In-Situ Stress Field Along the Wasatch Front

by

Mary Lou Zoback
U.S. Geological Survey, MS 977
345 Middlefield Road
Menlo Park, CA 94025

INTRODUCTION

The in situ stress field is directly responsible for both seismic and aseismic deformation. The sense and style of brittle deformation on a given fault plane depends upon the orientation of the principal stress field and a linear quantity, θ , that depends on the relative magnitudes of the principal stresses. Knowledge of this θ value and of the principal stress orientations can be combined with frictional faulting constraints to assess both the style (direction of slip) and the likelihood of slip on any pre-existing fault plane.

Available stress data along the Wasatch front including earthquake focal mechanisms, Holocene slickenside studies, and hydraulic fracturing tests have been integrated with analysis of stress-induced well bore elongation ("breakouts") in five deep wells in the vicinity of the southern Wasatch fault. These data provide a consistent description of the in-situ stress field which should allow for a better understanding of both seismicity and geodetic strain data as well as providing a foundation for assessing seismic risk associated with pre-existing faults.

DESCRIPTION OF THE IN-SITU STRESS FIELD

As mentioned above, only the orientation of the principal stress field and a value (θ) expressing the relative magnitudes of these

stresses are needed to predict the direction of slip on any given fault plane. The ϕ value was first described by Bott (1959) and is defined in the following manner:

$$\phi = \frac{S_2 - S_3}{S_1 - S_3} \quad (1)$$

where S_1 = maximum principal stress, S_2 = intermediate principal stress, and S_3 = minimum principal stress (all stresses are compressive). Thus, ϕ may range from 0 ($S_2 = S_3$) to 1 ($S_1 = S_3$). Angelier (1979) presented a simple graphical method for predicting the possible range in slip direction for any arbitrary fault plane for fixed stress axes (see Figure 1). However, unless additional information is known about the absolute magnitudes of the stresses, it is impossible to tell what are likely slip directions, i.e., in which part of this range the maximum resolved shear stress exceeds the shear strength of the fault.

Laboratory and theoretical studies of slip on pre-existing fault planes suggest a linear frictional sliding law of the following form:

$$\tau = \mu(S_N - P) + S_0 \quad (2)$$

where τ = maximum resolved shear stress, μ is the coefficient of friction (generally between 0.6-0.85 for most rocks), S_N is the normal stress across the fault plane, P is pore pressure, and S_0 is the frictional cohesive strength of the fault due to some sort of healing mechanism (often zero, generally less than 500 bars). To determine the values of S_N and τ , information on the absolute magnitudes of the principal stresses must be known.

The generally N-S trending active normal faulting in the northern Basin and Range province suggests a stress regime of the following form:

- S₁ = vertical and equal to the weight of the lithostat (S_v)
- S₂ = horizontal and approximately N-S
- S₃ = horizontal and approximately E-W

For a complete understanding of the stress field in a particular region within the Basin and Range province we need to know the actual orientation of the stresses, the ϕ value, and information on the absolute magnitudes of the stresses. There now exists a sufficient amount of geophysical and geologic data for the Wasatch front region to constrain all of these parameters.

ORIENTATION OF THE PRINCIPAL STRESSES

Wellbore elongation (breakouts), analyses of Holocene slickensides, earthquake focal mechanisms, and the orientation of hydraulic fractures all yield data on principal stress orientation. Both earthquake focal mechanisms and slickenside studies along the Wasatch front region suggest an approximate E-W orientation for S₃ (Zoback, 1983). The fault slip data described in that report have been reanalyzed (using the iterative fault slip analysis method of Angelier, 1984) with an additional measurement along the Wasatch near Deweyville, Utah. The best fitting stress tensor (Table 1) lies approximately in horizontal and vertical planes with a S₃ orientation of N75°E (the deviation of the stress tensor from true horizontal and vertical planes is probably largely due to the small number and limited orientations of the fault planes

sampled). The focal mechanisms discussed in Zoback (1983) have also been reanalyzed; in that paper the focal mechanisms were treated as individual faults by selection of a likely nodal plane as the fault plane. Angelier (1984) suggests that the best method for analyzing a group of focal mechanisms is to include both nodal planes and their possible slip directions, an inversion of this data set yields a reliable estimate of the stress orientation but not the ϕ value. Applying this type of analysis to the Wasatch front focal mechanisms yields a S_3 orientation of $N91^\circ E$ (Table 1). The results of both these analyses are not surprising in view of the fact that both data sets reflect normal fault deformation on predominately N-S trending fault planes.

Directions of wellbore elongations ("breakouts") have been analyzed for five deep wells in the vicinity of the southern Wasatch fault (see Figure 2 for locations). Other studies using data from commercially available four arm caliper logs have indicated that the average azimuth of these borehole elongations is very consistent within a given well or oil field (Cox, 1970; Babcock, 1978; Schafer, 1980; Brown and others, 1980). Bell and Gough (1979) and numerous other workers (Springer and Thorpe, 1981; Gough and Bell, 1981, 1982; Plumb, 1982; Healy and others, 1982; Hickman and others, 1982; Blumling and others, 1983; Cox, 1983; and Zoback and others, 1984) have suggested that the consistent azimuth of the long dimension of the hole is parallel to the azimuth of the minimum horizontal stress (S_3 in a normal faulting case).

High resolution four-arm dipmeter logs were provided by Doug Sprinkel of Placid Oil for five deep exploration wells drilled in the vicinity of

the southern Wasatch fault. Total depths for the five wells varied from 3996 to 5569 meters (see caption for Figure 2 for details). Major portions of all five wells were extensively washed out (symmetric enlargement of the well bore observed in two perpendicular directions); however, well-defined breakout zones (using the criteria of Bell and Gough, 1979 and Cox, 1983) were observed in each well. Azimuths of well-defined breakout zones were determined for each hole and are shown on rose diagrams in Figure 3.

The breakout azimuths varied considerably from well to well and within a single well. Breakouts were found primarily in the northeast and northwest quadrant. A composite of reliable breakouts for all five wells is also shown in Figure 3. The azimuths span the compass, however there is a slight tendency for them to lie within the northeast quadrant (N 0°E to N80°E). Interestingly, the number of breakouts with an approximately E-W orientation (the expected S_3 azimuth) is not significantly greater than in many other directions. The results to date suggest that there is no strongly preferred orientation of the minimum horizontal stress in the region sampled. As discussed in more detail below, these data may indicate that both the minimum and maximum horizontal principal stresses (assumed to be S_3 and S_2 respectively) are approximately equal in magnitude.

Hydraulic fractures (the strike of which indicates the orientation of the maximum horizontal principal stress, S_2 in a normal faulting regime) have been investigated in 5 wells in the Wasatch front region (Figure 2). Three of the wells lie east of the Wasatch fault, two in the

Raft River geothermal field (Keys, 1980) and the other in the Roosevelt Hot Springs field (Keys, 1979). In all three of these geothermal wells the observed hydraulic fractures were inadvertently induced probably as result of overpressure during drilling (Keys, 1979, 1980). Such drilling-induced hydraulic fractures are not uncommon in normal faulting stress regimes (e.g. Nevada Test Site, Stock and others, 1983) and are indicative of the low magnitude of the minimum horizontal stress (which in normal faulting regimes corresponds to the minimum principal stress, S_3).

In Raft River Well 4 a hydraulic fracture was logged using a borehole televiewer from a depth of 1428 m to 1485 m with an average azimuth of $N72^\circ E$, implying an S_3 azimuth of 162° (Table I, Figure 4a). In Raft River Well 5 (located approximately 500 m from Well 4) a hydraulic fracture was logged from a depth of 1391 m to 1434 m with an average azimuth of $N29^\circ E$ (Table I, Figure 4a). In the Roosevelt Hot Springs well the drilling induced hydraulic fracture had an average azimuth of $N35^\circ E$ (Table I, Figure 4a).

Hydraulic fracturing tests were conducted in two wells southeast of Provo, Utah, approximately 20 km east of the Wasatch fault, in an area of young although not substantial normal faulting. The two wells, DH-103 and DH-101, were located within 500 m of one another. The wells were drilled by the U.S. Bureau of Reclamation in 1980-1981 as part of a feasibility study for the Fifth Water Powerplant site. Using a borehole televiewer, Zoback (1981) logged five new hydraulic fractures in DH-103 induced by testing at depths between 574 and 603 m with azimuths of

174°, 159°, 156°, 154°, and 148° (Figure 4a). In addition, numerous drilling induced hydraulic fractures were logged. These fractures had a mean strike of about N80°E (Figure 4b).

In DH-101, located only 500 m away, hydraulic fracturing tests were made at 9 depth intervals between 458 and 570 m, Haimson (1981). Hydraulic fracture orientations were obtained from 8 of these tests using both impression packers and a borehole televiewer log. The mean direction of the fractures was $105^\circ \pm 15^\circ$ although one fracture had a strike of N20°E (Figure 4a).

Thus, the orientations of all hydraulic fractures done in the Wasatch front region (Figure 4a) differ significantly. The hydraulic fractures created by testing in the two Fifth Water wells show a mean difference of about 60°. In addition, the drilling-induced hydraulic fractures in DH-103 (Figure 4b) represent a direction somewhat intermediate between the two test-induced fracture orientations. The three hydraulic fractures from wells east of the Wasatch front also show inconsistent directions. These data, when considered with the borehole elongation analysis (see Table 1), seem to support the hypothesis that both horizontal principal stresses are approximately equal in magnitude implying that there is no strongly preferred orientation for the least principal stress, S_3 .

Relative Magnitudes of the Principal Stresses, σ

Information on the relative magnitudes of stresses comes from both deformation and hydraulic fracturing data. Since the value of the

maximum horizontal stress (S_2 in a normal faulting regime) is poorly determined in hydraulic fracturing tests (Zoback and Healy, 1984), the ϕ values determined by this method can be considered to be only approximate values.

The low ϕ value determined by Angelier's fault slip inversion technique for the Holocene slickenside data along the Wasatch fault zone is not surprising since the observed slickensides had very steep rakes ($56^\circ - 87^\circ$, with 8 of the 9 angles greater than 73° , Zoback, 1983). (The rake is the angle in the fault plane between horizontal and the slickensides, a 90° angle is pure down-dip slip.) As illustrated in

Figure 1, in a normal faulting regime with a low ϕ value ($\phi \approx 0$) the expected slip direction is always down-dip, regardless of the strike of the fault. This is because of the very low shear stresses (difference between stresses) in the horizontal plane. Thus, the tendency toward predominately down-dip slip on the observed fault planes whose strikes varied 85° (between $N45^\circ W$ and $N40^\circ E$) is, as the analysis concluded, indicative of a very low ϕ value, approximately equal to zero.

In fact, the earthquake focal mechanism data show a similar pattern. All Wasatch front mechanisms are predominantly normal dip-slip events showing only small components of strike slip motion. Computed rakes on all possible nodal planes ranged from 53° to 90° , with one low value of 25° .

The wide range in azimuth of the hydraulic fractures (Figure 4a), as discussed above, is also consistent with a nearly radial horizontal

stress field, i.e. a stress field in which the horizontal stresses are equal in all directions. The lack of well-defined, preferred borehole elongation direction (Figure 3) also supports this view. Thus, all the data considered together suggest a θ value of approximately zero. The strong preference for active deformation to occur on generally N-S striking planes probably reflects the strong influence of pre-existing zones of weakness.

Absolute Magnitudes of the Principal Stresses

Zoback and Healy (1984) have recently reviewed in-situ stress measurements made at depths in areas of active faulting. The data indicate that the magnitude of principal stress differences in the shallow crust are controlled by the frictional strength of the active faults, where the frictional strength is consistent with laboratory-derived coefficients of friction between 0.6 and 1.0. The general frictional sliding law (equation 2) reduces to the following relationship between principal stresses (S_1 and S_3) pore pressure (P) and the coefficient of friction (μ) for optimally-oriented fault-planes (planes in which S_2 , the intermediate stress, is in the plane of the fault):

$$\frac{S_1 - P}{S_3 - P} = [(\mu^2 + 1)^{1/2} + \mu]^2 \quad (3)$$

In a normal faulting regime, $S_1 = S_v$ (weight of the overburden), S_3 = minimum horizontal stress (which is obtained directly by hydraulic fracturing tests).

In each of four examples of stress measurements in areas of normal faulting (including the Fifth Water, Utah and Nevada Test Site) Zoback and Healy (1984) show that the magnitude of S_3 has approximately the value (given by equation(3) with $\mu = 0.6 - 1.0$) at which normal faulting would be expected to occur on optimally-oriented planes. Figure 5 shows plots of the minimum horizontal stress values (S_3) as a function of depth together with the range in values for frictional strength at which normal faulting is expected for the pore pressure shown. Also shown in Figure 5 is measurement of the minimum horizontal stress determined from an "acid-breakdown hydrofrac" at 5070 m depth in the Chevron USA #1 Chriss Canyon well, located less than 10 km east of the southern Wasatch fault (Arabasz, 1984--see Figure 2 for location). As noted by Arabasz the measured value of S_3 is also consistent with the range predicted by frictional strength values, hydrostatic pore pressure, and a reasonable estimate of S_v .

The available data on stress magnitudes thus indicates that stress differences (the difference between S_1 and S_3) are quite large in areas of active normal faulting in general and in the Wasatch front region in particular. The stress differences appear limited by critical values predicted from frictional strength of pre-existing optimally-oriented faults.

Concluding Remarks

Available data on the in-situ stress field in the Wasatch front region indicate high stress stress differences between the maximum

principal stress, S_1 , (assumed vertical) and the minimum horizontal stress. The data also indicate that both horizontal stresses are approximately equal in magnitude ($\theta \approx 0$) and that there is no strongly preferred orientation for the minimum horizontal stress, S_3 , other than that dictated by the generally N-S normal faults which are currently active.

The implications of this conclusion, if correct, are far-reaching. Since faulting is driven by the difference between the maximum and minimum principal stress ($S_1 - S_3$) and if $\theta \approx 0$ then normal faults of a wide variety of azimuths may be potentially active. In addition, following a major stress release event (large earthquake) it is possible that the previous intermediate stress value, S_2 , might become the new minimum stress; i.e., even the small stress drops of earthquakes (typically 30-100 bars) may be enough to cause an exchange in the relative magnitude of the two horizontal stresses. Temporal variations of the horizontal stress field (magnitude and/or orientation) thus may be strongly influenced by where we are in the earthquake cycle itself. In addition, the near equality of the horizontal stresses may also help understand the complicated recent geodetic strain data along the Wasatch which yield two nearly orthogonal directions of extensional strain (Prescott and others, 1979; Snay and others, 1984).

TABLE 1

Orientation of Principal Stress

Type of data	S ₁		S ₂		S ₃		φ
	Az	Dip	Az	Dip	Az	Dip	
Angelier analysis of Holocene slickenside data	268°	75°	164°	4°	73°	15°	0.06
Analysis of Wasatch front focal mechanisms	255°	76°	0°	4°	91°	13°	intermediate
Well bore elongation	no preferred orientation of horizontal principal stresses						assumed 0
Raft River well #4 drilling induced fracture	Vertical?		72°	0°	162°	0°	no information
Raft River well #5 drilling induced fracture	Vertical?		29°	0°	119°	0°	no information
Roosevelt Hot Springs well drilling induced fracture	Vertical?		35°	0°	125°	0°	no information
Fifth Water DH103 hydraulic fracture (tests)	Vertical?		163°	0°	73°	0°	0.09-0.50 mag- nitude of S ₂ poorly con- strained
Fifth Water DH163 drilling induced fractures	Vertical?		80°	0°	170°	0°	no information
Fifth Water DH101 hydraulic fracture (tests)	Vertical?		15°	0°	105°	0°	0.29-0.50

Figure Captions

Figure 1. Angular variation of maximum shear stress (slip direction) with θ , when stress axes S_1 , S_2 , S_3 are fixed: n = fault normal; τ_0 = projection of S_1 on the fault; τ_1 = projection of S_3 on the fault. When θ goes from 0 to 1, the orientation of the maximum shear stress goes from τ_0 to τ_1 . Shown are the range in possible slip directions for two faults in a normal faulting regime where S_3 is oriented east-west.

Figure 2. Location map for wells discussed in text. Wells which were analysed for borehole elongation: a - Henley #1 (TD=3996m), b - Paxton #1 (TD=4520m), c - Monroe #13-7 (TD=4795m), d - WXC USA #1-2 (TD=5569m), e - WXC State #2 (TD=4236m). Wells in which hydraulic fractures were reported: f - Raft River Well 4 and Well 5; g - Roosevelt Hot Springs well; h - Fifth Water DH 101 and DH 103; i - Chevron USA #1 Chriss Canyon.

Figure 3. Rose diagrams of borehole elongation azimuths in the analyzed wells.

Figure 4. a) Rose diagram of all hydraulic fracture orientations reported from wells in the Wasatch front region. b) Rose diagram of drilling induced hydraulic fractures in Fifth Water DH-103 (M. D. Zoback, written communication, 1984).

Figure 5. Minimum principal stress values measured in three wells in the Wasatch front region. Also shown is the estimated magnitude of the vertical principal stress, the pore pressure, and the expected range for S_3 for active normal faulting based on equation 3.

- Angelier, J., 1979, Determination of the mean principal stresses for a given fault population: *Tectonophysics*, v. 56, p. T17-26.
- Angelier, J., 1984, Tectonic analysis of fault slip data sets: *Journal of Geophysical Research*, v. 89, p. (in press).
- Arabasz, W. J., 1984, Swarm seismicity and deep hydraulic fracturing within 10 kilometers of the southern Wasatch fault: *Earthquake Notes*, v. 55, p.1.
- Babcock, E. A., 1978, Measurement of subsurface fractures from dipmeter logs: *Association of Petroleum Geologists Bulletin*, v. 62, p. 1111-1126.
- Bell, J. S., and Gough, D. I., 1979, Northeast-southwest compressive stress in Alberta: evidence from oil wells: *Earth and Planetary Science Letters*, v. 45, p. 472-479.
- Blumling, P., Fuchs, K., and Schneider, T., 1983, Orientation of the stress field from breakouts in a crystalline well in a seismic active area: *Physics of the Earth and Planetary Interiors*, in press.
- Bott, M. H. P., 1959, The mechanisms of oblique slip faulting: *Geological Magazine*, v. 96, p. 109-117.
- Brown, R. O., Forgotson, J. M., and Forgotson, Jr., J. M., 1980, Predicting the orientation of hydraulically created fractures in the Cotton Valley Formation of east Texas: *Society Petroleum Engineering paper SPE 9269*, 55th Annual Meeting, Dallas, Texas.

Cox, J. W., 1970, The high resolution dipmeter reveals dip-related borehole and formation characteristics: 11th Annual Logging Symposium, Society of Professional Well Log Analysts, Los Angeles, California.

---, 1983, Long axis orientation in elongated boreholes and its correlation with rock stress data: Society of Professional Well Log Analysts, Twenty-Fourth Annual Logging Symposium, Calgary.

Gough, D. I., and Bell, J. S., 1981, Stress orientations from oil well fractures in Alberta and Texas: Canadian Journal of Earth Science, v. 18, p. 638-645.

-----, 1982, Stress orientations from borehole wall fractures with examples from Colorado, east Texas, and northern Canada: Canadian Journal of Earth Sciences, v. 19, p. 1958-1970.

Haimson, B. C., 1981, Hydrofracturing studies drillhole DH-101, fifth water underground power plant site, Diamond Fork Power System - Bonneville Unit, Central Unit Project: Report to the Bureau of Reclamation.

Hickman, S. H., Healy, J. H., Zoback, M. D., Svitek, J. F., and Bretcher, J. E., 1982, In-situ stress, borehole elongation, and natural fracture distribution at depth: EOS (American Geophysical Union Transactions), v. 63, p. 1118.

Keys, W. S., 1979, Borehole geophysics in igneous and metamorphic rocks: Proceedings of the Society of Professional Well Log Analysts, 20th Annual Logging Symposium, Tulsa, Oklahoma, p. 001-0026.

----, 1980, The application of the acoustic televiewer to the characterization of hydraulic fractures in geothermal wells: Proceedings of the First Geothermal Reservoir Well Stimulation Symposium, San Francisco, California, February 7, 1980, p. A1-A11.

Plumb, R. A., 1982, Breakouts in the geothermal well, Auburn, N.Y.: EOS (American Geophysical Union Transactions), v. 63, p. 1118.

Prescott, W. H., Savage, J. C., and Hiroshita, 1979, Strain accumulation rates in the western United States between 1970 and 1978: Journal of Geophysical Research, v. 84, p. 5423-5435.

Schafer, J. N., 1980, A practical method of well evaluation and acreage development for the naturally fractured Austin Chalk formation in The Log Analyst, p. 10-23.

Snay, R. A., Smith, R. B., and Solder, T., 1984, Horizontal strain across the Wasatch front near Salt Lake City, Utah: Journal of Geophysical Research, v. 89, p. 1113-1122.

Springer, J. E., and Thorpe, R. K., 1981, Borehole elongation versus in-situ stress orientation: Paper UCRL - 87018 presented at International Conference on In-Situ Testing of Rock and Soil Masses, Santa Barbara, California, Jan. 4-8, 1982.

Stock, J., Healy, J., and Svitek, J., 1983, The orientation of the current stress field on Yucca Mountain, Nevada, as determined from televiewer logs, EOS (American Geophysical Union Transactions); v. 64, p. 319.

Zoback, M. D., 1981, Hydraulic fracturing stress measurements and fracture studies in hole DH-103 Fifth Water Power Plant Site, Central Utah Project: Report to U.S. Bureau of Reclamation.

Zoback, M. D., and Healy, J. H., 1984, Friction, faulting and in-situ stress: *Annales Geophysicae*, in press.

Zoback, M. D., Moos, D., Mastin, L., and Anderson, R. N., 1984, Wellbore breakouts and in-situ stress: *Journal of Geophysical Research*, in press.

Zoback, M. L., 1983, Structure and Cenozoic tectonism along the Wasatch fault zone, Utah in *Geological Society of America Memoir 157*, p. 3-27.

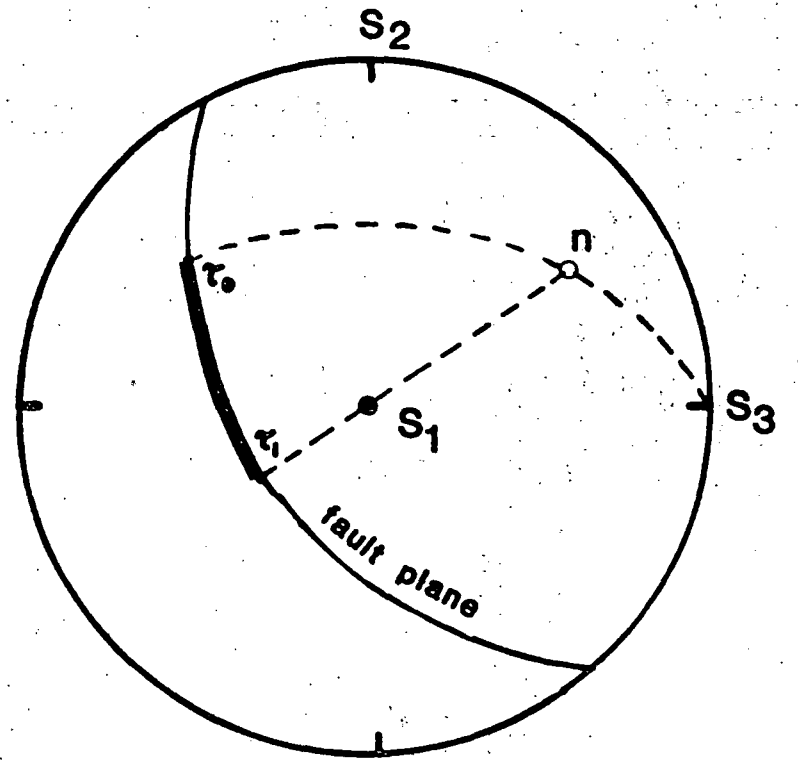
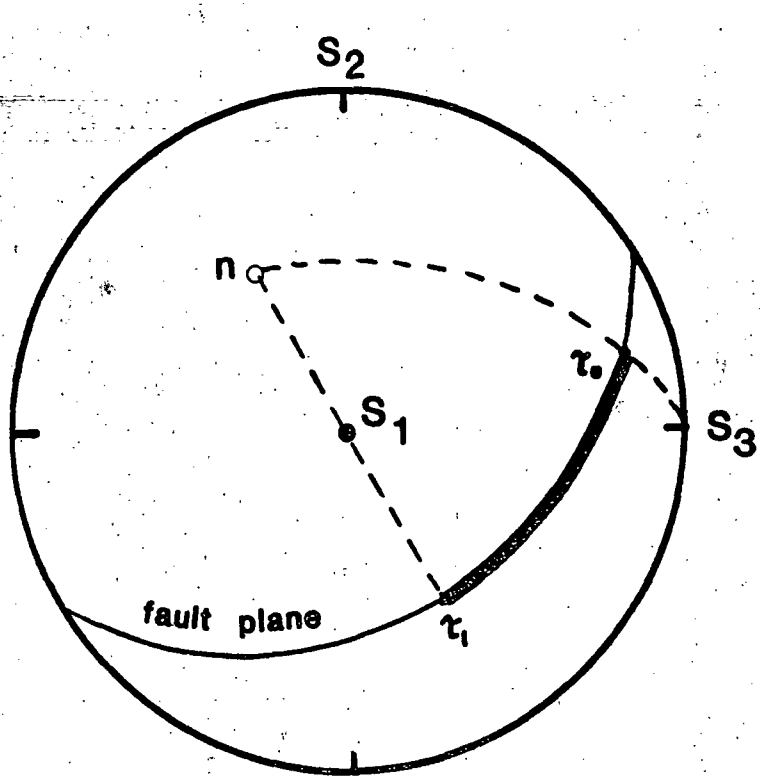
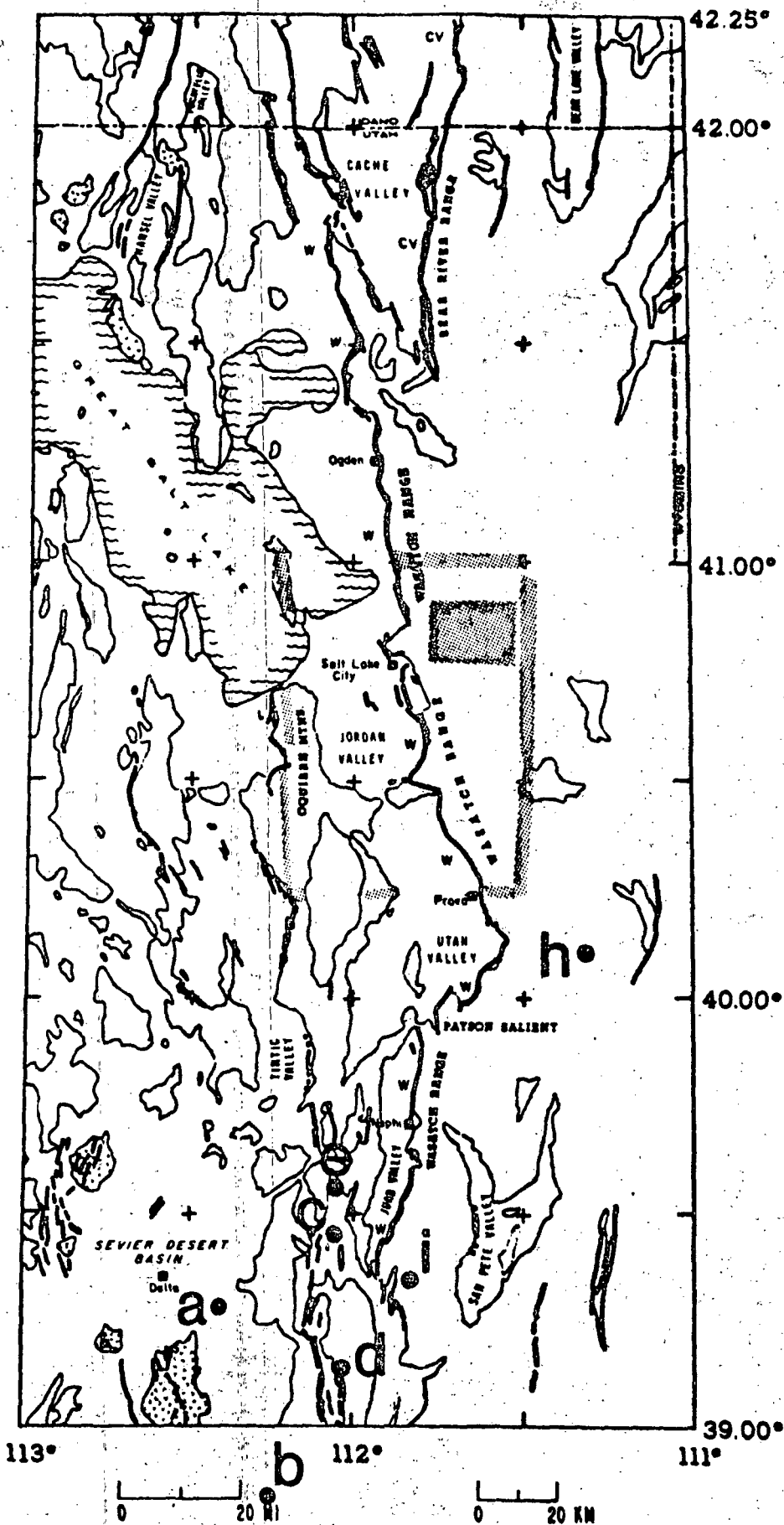







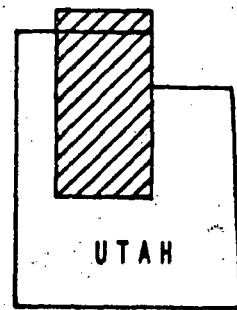
Fig. 1



EXPLANATION

-  Quaternary and Pliocene volcanic rocks
-  Late Cenozoic basin fill
-  Bedrock (Early Tertiary to Precambrian)
-  Contact
-  Fault (normal) dotted where inferred

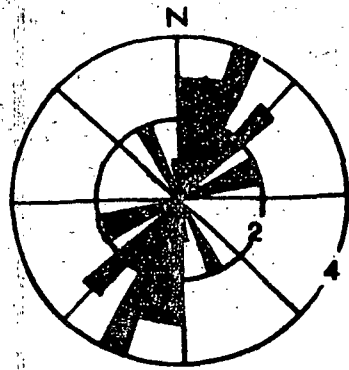
base map from Hintze (1960)
Geologic Map of Utah



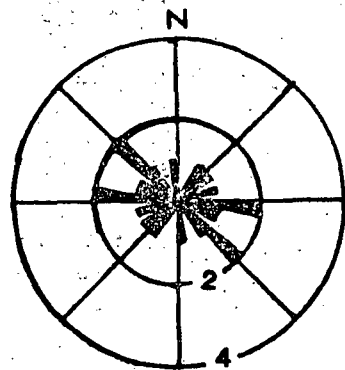
AREA OF STUDY

.g

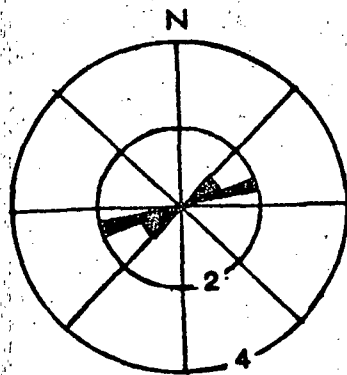
Fig 2



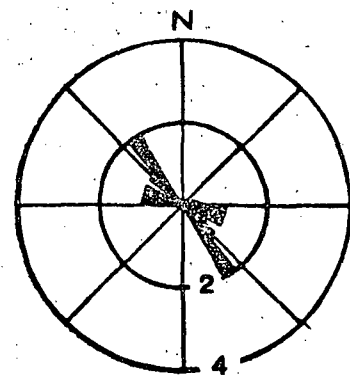
Henley #1
22 meas.



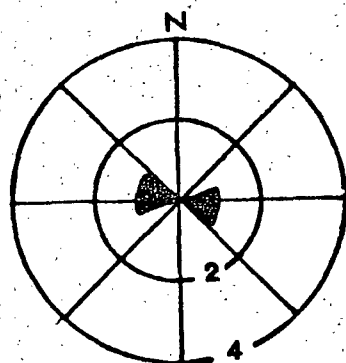
Paxton #1
11 meas.



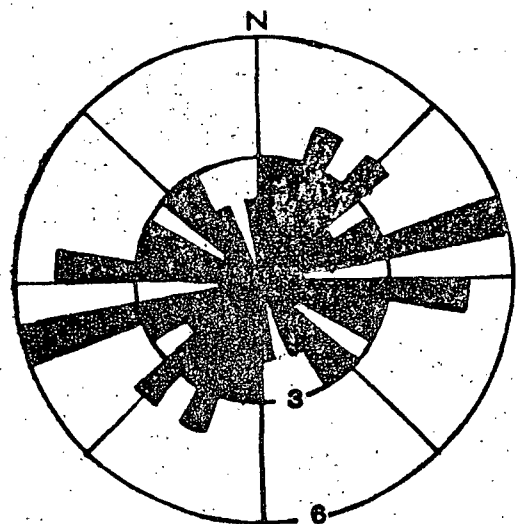
Monroe #13-7
5 meas.



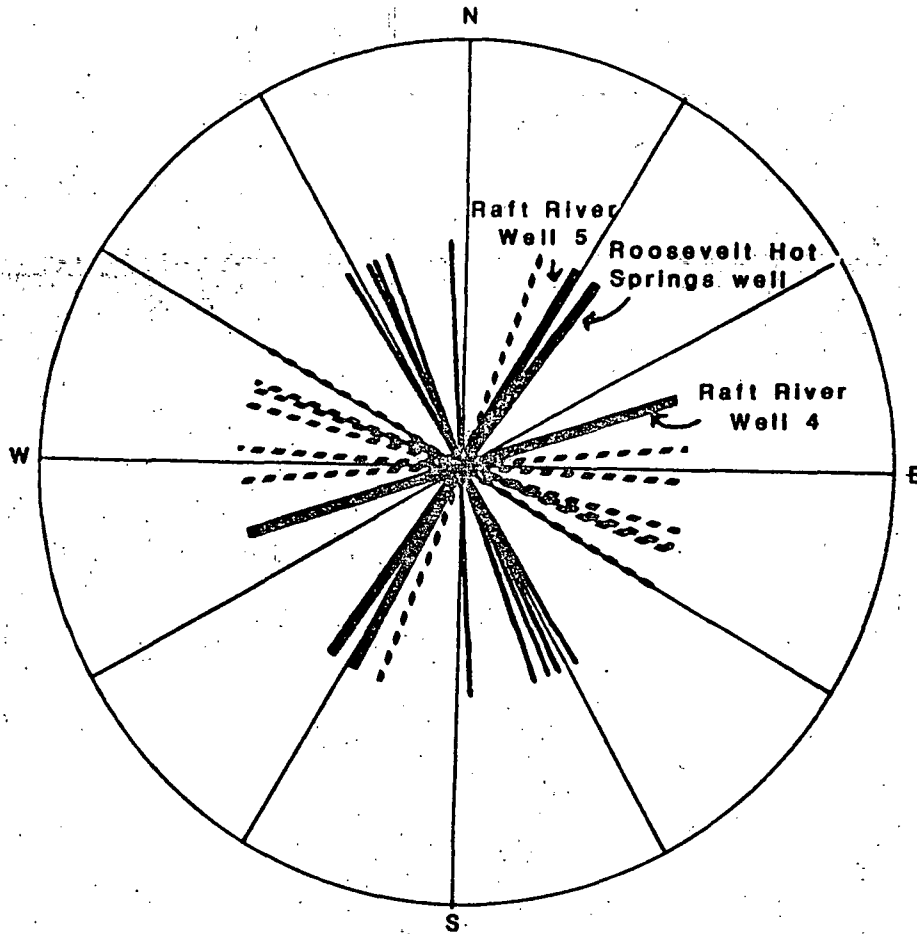
WXC USA #1-2
6 meas.



WXC State #2
5 meas.



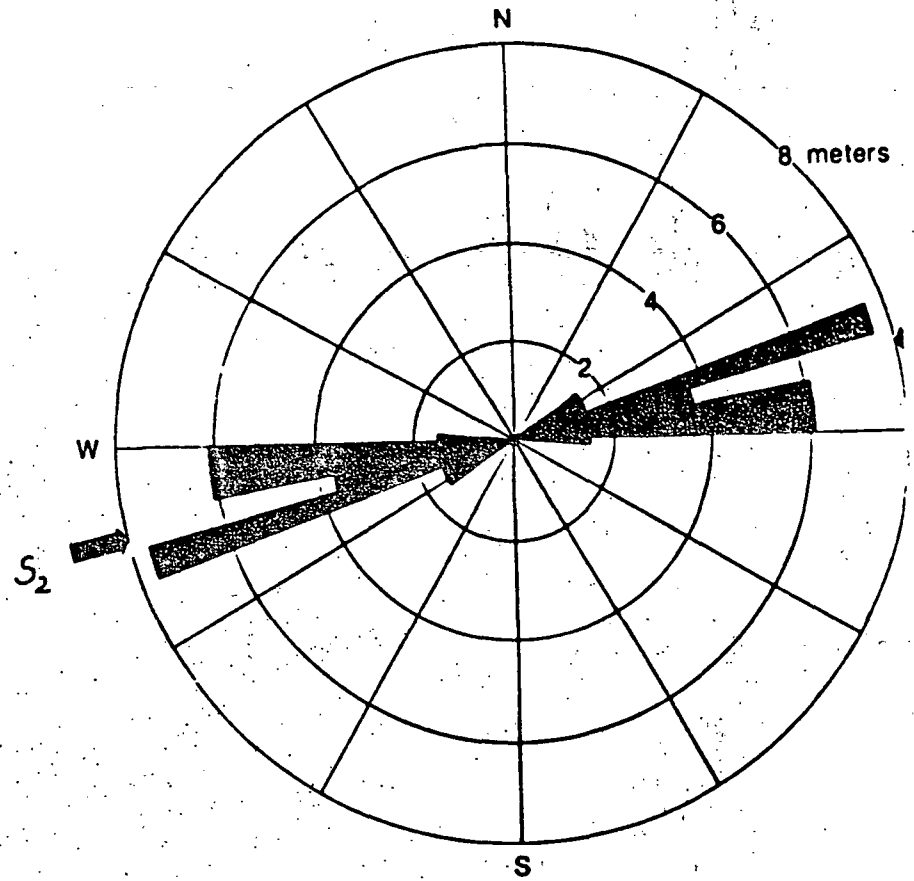
Composite
49 meas.



A) HYDRAULIC FRACTURE ORIENTATIONS
WASATCH FRONT REGION

----- Fifth Water DH101

———— Fifth Water DH103



B) 5TH WATER UTAH DH 103
DRILLING INDUCED FRACTURES

Fig. 4

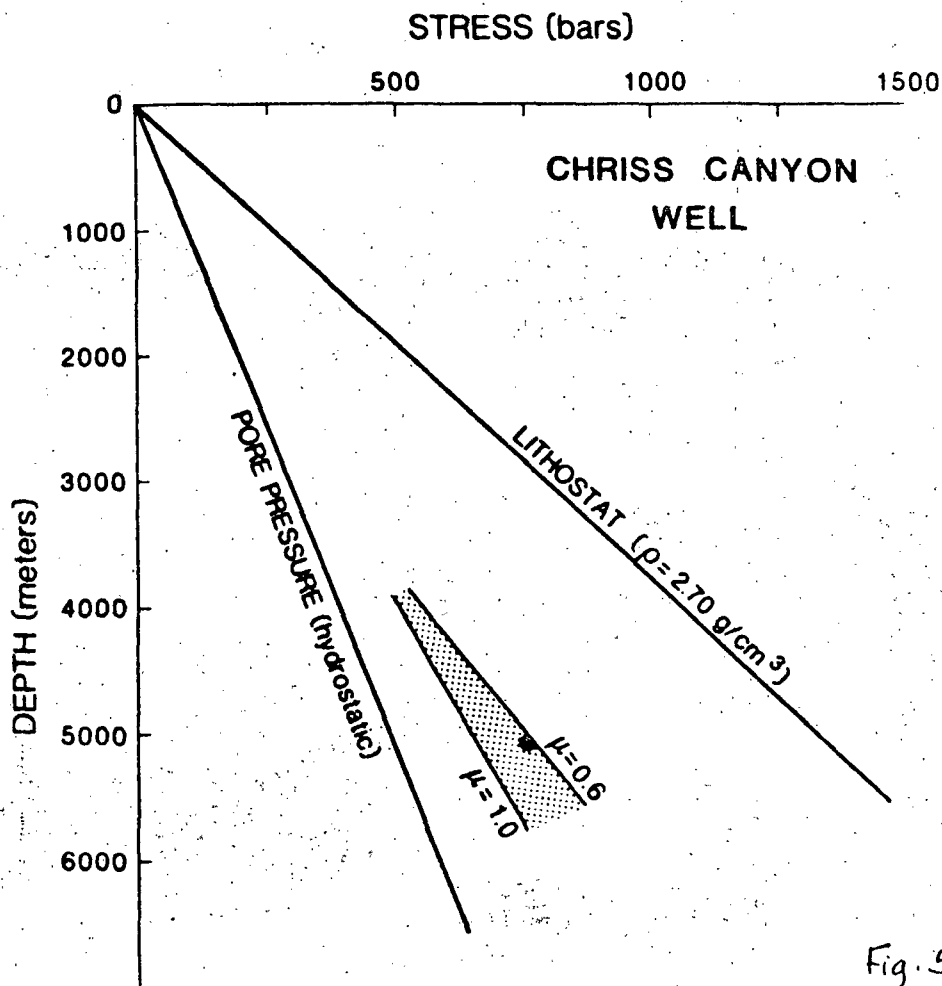
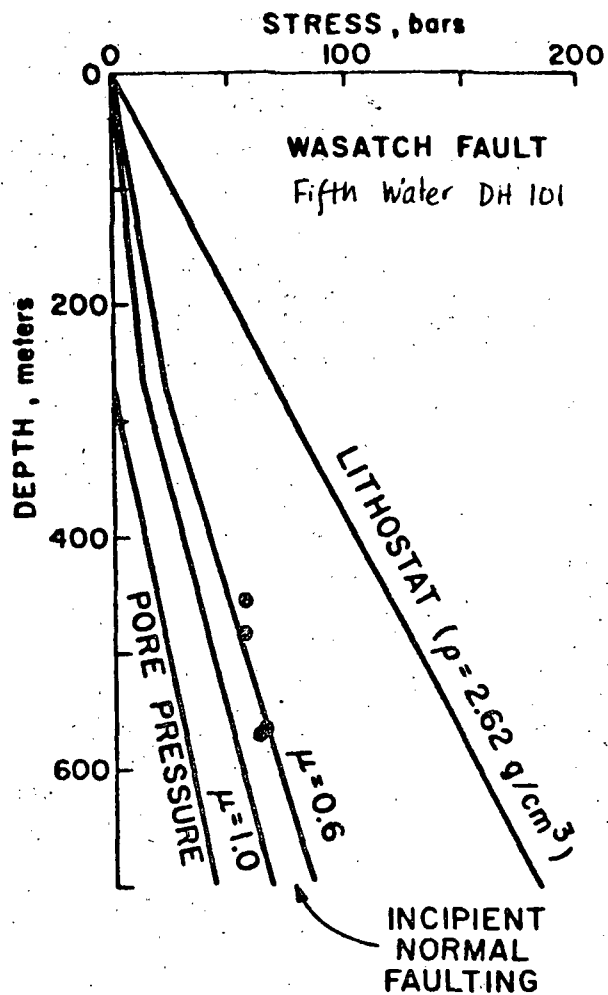
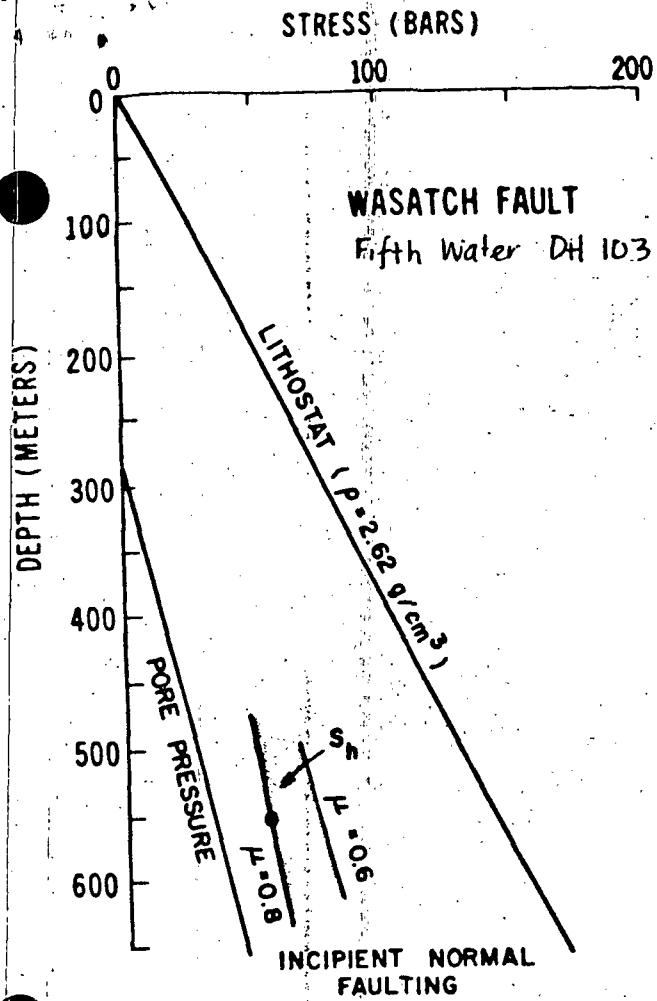


Fig. 5

Preliminary investigations of Quaternary geology along the southern part
of the Wasatch fault zone, central Utah

Michael N. Machette
U.S. Geological Survey
MS 913, Federal Center
Denver, Colorado 80225

Introduction

The Levan and Nephi segments are the southernmost of six fault segments of the Wasatch fault zone proposed by Schwartz and Coppersmith (1984). Young fault scarps of the Levan segment extend 38 km, from 2 km northeast of Fayette to 5 km northeast of Levan. Scarps of the Nephi segment extend 33 km, from the north edge of Nephi to about 1 km northeast of Spring Lake, a small community about 5 km south of Payson. The young surface ruptures of these two segments are separated by a 16-km-long gap where young scarps are not present.

Trench investigations by Schwartz and others (1983; also in Schwartz and Coppersmith, 1984) at North Creek near the center of the Nephi segment reveal three distinct episodes of surface rupture, each having 2.0-2.6 m offset, and an estimated average recurrence interval of 1,700-2,600 yrs. The most recent movement, however, occurred within the past 1,100 yrs and perhaps in the past 300-500 yrs. The Nephi segment probably has the the youngest surface rupturing and scarps of the whole Wasatch fault zone (see discussion of Schwartz and Coppersmith, 1984). To the north, in the Salt Lake and Utah Valleys, pre-Lake Bonneville age deposits can rarely be related to the Wasatch fault zone (W. E. Scott, pers. commun., 1984), and where observed, the

deposits typically are exposed only on one side of the fault zone. Lake Bonneville could have only occupied the Juab Valley for a few thousands of years (Scott and others, 1983) and nowhere do lake deposits straddle the Nephi segment. Thus, pre-Bonneville age deposits, particularly those that form alluvial fans, are better preserved in the Juab Valley than at most other localities to the north.

This study has benefitted from the high runoff of the last two years, which has freshened up many stream exposures. For example, the fault is now well exposed in Quaternary deposits along Willow Creek and Mona Creek on the Nephi segment and along Deep Creek on the Levan segment. The new exposures greatly increase the possibility of finding material to date faulting events and to better define the chronology of stratigraphic units exposed along the fault.

Geologic investigations

Studies were conducted in order to better understand the paleoseismicity of the Nephi and Levan segments as well as the relationship between young faulting events and 1) bedrock structure, and 2) mass-movement processes (landsliding, emplacement of debris flows, and colluviation). Studies include detailed surface mapping at scales of 1:12,000 and 1:24,000 of a several-km-wide zone along the fault, systematic measurement of about 100 topographic profiles of fault scarps, detailed stratigraphy of selected exposures of Quaternary deposits, description and sampling of surficial deposits and soils for characterization and age determinations, and compilation of bedrock geology of selected areas. The influence of major contrasts in bedrock structure and lithology along the range front on the location, geometry, and magnitude of surface faulting is being investigated.

Scarp morphology data will be used to investigate the relation between maximum scarp-slope angle (θ) and scarp height (H_s , single-event scarps; H_m , multiple-event scarps; Machette and McGimsey, 1983). The data will be compared to the scarp morphology data of Bucknam and Anderson (1979) from central Utah to analyze recency of faulting, and used to construct a general surface rupture envelope for young surface faulting events. Comparison with the rupture envelope of the 1983 M_s 7.3 Borah Peak earthquake (Crone and Machette, 1984) may help model ground breakage based on "characteristic" amounts of offset that might occur along individual segments of the Wasatch fault zone.

Results of current research

1) The steepness and height of the Nephi fault scarps formed in unconsolidated deposits indicate late Holocene movement at least from Mendelhall Creek on the north to Nephi on the south. The data analyzed so far show that single-event scarps less than 2.5 m in height (H_s , fig. 1A) generally have maximum slope angles less than 32° , whereas larger scarps have maximum slope angles that are at or exceed the angle of repose of unconsolidated surficial deposits. Along the Nephi segment the small scarps and the youngest element of larger compound fault scarps are old enough to have had their free faces removed, whereas free faces are commonly seen on historic fault scarps in the Basin and Range. The Nephi H_s data plot slightly above (younger than) that of the Fish Springs fault (fig. 1B; Bucknam and Anderson, 1979), which I estimate to be of late(?) Holocene age. However, the height-angle relation for composite, multiple-event scarps (H_m , fig. 1A) plot slightly below the Fish Springs fault (Bucknam and Anderson, 1979). The relation between H_s and θ for

the scarps suggest very young movement along the main strand of the Nephi segment: the support Schwartz and others (1983) minimum age limit age of 1,100 C^{14} yrs B.P. for the most recent surface rupture at the North Creek site, but do not necessarily support their estimate of only 300-500 years for the age of the most recent rupture.

About 40 profiles have been measured along the Levan segment, but this data has not yet analyzed, and only three profiles been measured from the Santaquin Valley end of the Nephi segment. These profiles and additional ones along the Provo segment will be analyzed in the coming year.

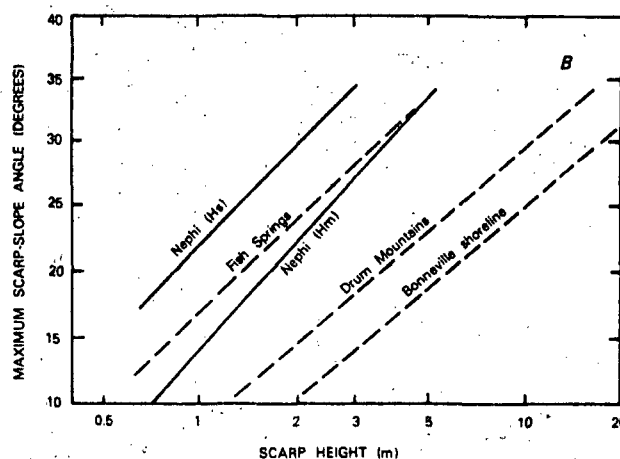
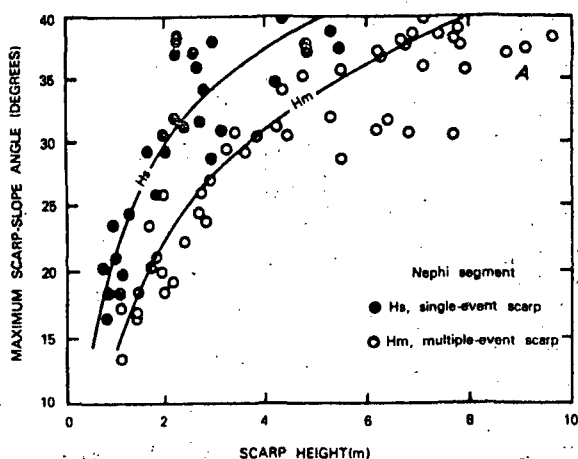


FIGURE 1A. Morphometric data for single-event and multiple-event fault scarps along the Nephi segment of the Wasatch fault zone. Curved lines labelled Hs and Hm are the lines of best fit for respective data sets. Gray stippled area indicates common angles of repose of unconsolidated surficial materials (32° - 36°).

FIGURE 1B. Lines of best fit for data from the Nephi fault scarps (Hs and Hm) and data from other fault scarps in central Utah (modified from Bucknam and Anderson, 1979).

2) Although the Nephi and Levan segments are separated by a 16-km-long gap in Holocene and latest Pleistocene surface faulting, strong geomorphic and geologic evidence indicates earlier Quaternary faulting in the gap. Levan Ridge is a large composite Quaternary alluvial-fan system that separates the northern and southern parts of Juab Valley. The gradient of the alluvial fan steepens across the projection of a major north-south fault that separates the adjacent bedrock hills from the east side of the Juab valley. This steepened gradient may be an old, degraded multiple-event fault scarp. If correct, it implies that a fault connection between the Levan and Nephi segments has been inactive for tens(?) of thousands of years.

3) Deep incision along the south side of Willow Creek during the spring flooding of 1983 exposed the fault and associated colluvial wedges. Two surface faulting events are apparent in the exposure, and evidence of perhaps third event may be present below the level of exposure. Three profiles of the fault scarp on the Willow Creek terrace fan have an average height of 6.6 m, a maximum scarp-slope angle of 37° , and a minimum surface offset of 5.2-6.0 m (the base is buried by post-fault alluvium). The young surface faulting relations at Willow Creek are very similar to those at the North Creek site of Schwartz and others (1983). The scarp there has a height of 7.2 m, a maximum slope angle of $38-40^{\circ}$, and apparently was produced by three separate surface faulting events. R. C. Bucknam collected charcoal from the faulted alluvium at North Creek and Schwartz and others (1983) obtained a date of 4580 C^{14} yrs B.P. on the charcoal. This date converts to calendar dates of 5129-5494 yrs B.P. (Schwartz and Coppersmith, 1984). R. R. Shroba (pers. commun., 1984) and my studies of soils developed on the faulted deposits at North Creek and at

Willow Creek suggest a mid(?) Holocene age based on an A, weak Bs, stage I Cca soil horizon profile. The soils and the dated alluvium suggest that some of the fans at the mouths of major canyons along the Nephi segment that are offset by repeated surface faulting events were deposited during the Altithermal portion of the Holocene, about 4,000-6,000 yrs ago. An additional constraint on the age of the faulted deposits may be forthcoming from wood collected about 100 m east of the fault scarp. A tree stump in alluvium of Willow Creek was buried in growth position and rooted in the third oldest of 12 units exposed along the south wall of the creek. The stump appears to have been broken off during deposition of unit 5, a massive light gray-brown pebbly debris-flow deposit. A C^{14} age from the wood will date material about 2 meters below the surface of the faulted fan terrace and thus provide a maximum age for the 5.2-6.0 m of offset at Willow Creek.

4) Three buried A horizons having disseminated charcoal were collected from scarp colluvium in the Birch Creek gravel pit and may provide additional constraints on the age of fault-related young deposits on the Nephi segment. C^{14} ages from these horizon should help estimate rates of deposition of scarp colluvium adjacent to the fault and may indicate the length of time separating individual surface faulting events. The dates should also give a maximum age of the overlying fan alluvium of Little Birch Creek (the small drainage on the south side of the Birch Creek gravel pit).

5) Perhaps the most interesting preliminary result of these studies is the estimation of a pre-Lake Bonneville slip rate for the Nephi segment. Faulted fan deposits of pre-Bonneville age are preserved at the mouth of Gardner Creek, a moderate-size stream valley that drains the southwest end of the Wasatch Range, about 3 km northeast of Nephi. Recurrent late Pleistocene and

Holocene faulting along the Nephi segment has left a series of three alluvial-fan complexes plastered against the sides of Gardner Creek canyon.

These deposits are informally referred to as young (Qfy), middle (Qfm), and old (Qfo) alluvial-fan deposits. Qfy is probably mid-Holocene in age, based on the degree of soil development and correlation with mid-Holocene alluvial fan deposits at Willow Creek and North Creek. The downdropped portion of these alluvial fans is probably overlain by thick, westward-thinning wedges of younger (middle and late Pleistocene) alluvium. Holocene alluvium, most of which may have been deposited during the warm, dry Altithermal (about 4,000-6,000 yrs ago), forms a thin surface mantle on the downdropped fault block.

The mid(?)-Holocene deposits are offset about 3.9 m (scarp heights are about 4.2 m) at Gardner Creek. Using an average age estimate of 5,000 yrs for the faulted deposits, the average slip rate is about 0.8 m/ka, or 60 percent of the rate at North Creek (1.3 m/ka). The difference in these two rates may reflect the proximity of Gardner Creek to the southern termination of the Nephi segment where displacement amounts could be expected to diminish toward the segment boundary. North Creek and Willow Creek, by contrast, lie near the center of the segment where displacement amounts could be the largest.

The remnants of middle and old fan alluvium (Qfm and Qfo) that are preserved on the upthrown fault block may have been deposited in response to major climatically induced changes in sediment supply and stream flow such has been recognized to the south in the Beaver basin. Uranium-trend age determinations from soils and quantitative analyses of soil-carbonate content (Machette, 1984) suggest that the major constructional alluvial landforms (piedmont slopes, terraces, and alluvial fans) in the Beaver basin are related to changes in climatic episodes, from glacial to interglacial conditions.

By analogy in north-central Utah, the middle and old fan deposits probably correlate with the interglacials that followed the two major pre-Pinedale glaciations. The younger of the two interglacials probably is about 130,000 yrs old and the older is probably about 250,000 yrs old.

A 1984 excavation in the surface of Qfo at Gardner Creek revealed a well developed soil that is characterized by a one-meter-thick K horizon. Thin laminae (weak stage IV morphology) are discontinuously formed in the upper 10 cm of the K horizon; downward, the morphology grades from strong stage III to weak stage III. Overlying the K horizon is a 10 cm thick Btca horizon, and a thin A horizon (a large unseen part of the B horizon probably has been engulfed by the K horizon). Even though the soil is formed in limestone-rich alluvium, the development and thickness of the K horizon represent a substantial accumulation of pedogenic carbonate, the majority of which probably is supplied by airborne dust (Machette, 1985). It probably represents several hundreds of thousand of years of soil-carbonate accumulation, which is consistent with the assumed 250,000 year age for the deposit on which it is formed. This soil appears better developed than the type Promintory Soil of Morrison (1965) that is formed in gravel bars of Little Valley age (see Scott, 1982, for discussion of stratigraphy, ages, and soils). Scott (1982, p. 3) considers the deposits of the Little Valley lake cycle to be $150,000 \pm 25,000$ yrs old, generally correlative with tills of the Bull Lake glaciation of the Rocky Mountains that probably ended about 140,000 yrs ago (Pierce and others, 1976).

Adjacent to the mouth of Gardner Creek, scarps formed in Qfo are 25-26 m high, have slope angles of 38° - 40° , and are buried by an unknown thickness of young fan alluvium at their bases. In the interfluvium between the Gardner Creek and Red Canyon (the next major drainage to the south), the scarps show

the least amount of burial and reach a maximum height of about 32 m. There is evidence that the surface offset is actually more than 32 m. The steepest portion (θ) of the scarp in Qfo is in the lower 1/3 of the slope. Typically, θ is found in a mid-slope position (this general relation has been confirmed by numerous trench exposures along the Wasatch fault zone and in other trenches across faults in the Basin and Range). The steepened portion is interpreted here as the position of most recent surface rupturing. Thus, one could argue that an unseen, lower portion of the large fault scarp is buried on the downthrown fault block. Using this line of evidence, a geometric reconstruction of the fault scarp in old fan deposits could permit as much as 50 m of surface offset. Backtilt and grabens further complicate the reconstruction, but both reduce the amount of surface offset in relation to the height of the main scarp (see discussion of these factors in Swan and others, 1980). For determining a pre-Bonneville slip rate at Gardner Creek, I favor an intermediate offset value of 40 m (-8 m, + 10 m). On the basis of this intermediate value and an assumed age of 250,000 yrs for Qfo, the cumulative late Quaternary slip rate at Gardner Creek is 0.16 m/ka (the range in values is 0.13-0.20 m/ka).

Speculations about the mechanism and timing of apparent changes in slip rate

There is good evidence that the post-Bonneville (past 15,000 yrs) slip rate is at least five times faster than the pre-Bonneville (more than 25,000 yrs) slip rate along the Nephi segment. Although not presented here, there is evidence for a similar contrast in slip rates on the Provo and Salt Lake City segments of the Wasatch fault zone. I propose that the anomalously high slip rates during the past 15,000 yrs (latest Pleistocene and Holocene) along the Wasatch fault zone are related to empoundment of Lake Bonneville.

The high slip rates may reflect perturbation of ambient shear stresses on the Wasatch fault zone by increased hydrostatic head and resultant subsurface pore pressure, as well as by loading and unloading of the crust during the lakes' rapid expansion and contraction in the late Pleistocene.

The Holocene slip rates at the Hobble Creek and North Creek sites are high (table 1; 0.08-1.0 and 1.3 m/ka, respectively), yet are apparently slower than those recorded by offset of the Provo- and Bonneville-age surfaces (estimates range from less than 1.7 to as much as 3.9 m/ka; Swan and others, 1980; Schwartz and Coppersmith, 1984). Thus, there also may be a trend of progressively declining slip rates in the Holocene, from a peak in Bonneville time (15,000-25,000 yrs ago).

Table 1. Cumulative slip rates (m/ka) on the southern Wasatch Fault zone

Time interval	Hobble Creek	North Creek	Gardner Creek
Mid Holocene	1.0 ¹	1.3 ²	0.78
Post-Bonneville (17,000 yrs B.P.)	3.9 ¹	n.d.	n.d.
Pre-Bonneville (250,000 yrs B.P.)	n.d.	0.21 ³	0.16
Cenozoic	0.4 for the central Wasatch Fault zone ⁴		

1 Data from Swan and others, 1980.

2 Data from Schwartz and others, 1983.

3 Calculated from ratio of pre-Bonneville to mid Holocene slip rates at Gardner Creek times mid Holocene slip rate at North Creek.

4 Data from Naesar and others, 1983.

Slip rates for pre-Bonneville deposits are considerably slower (0.1-0.2 m/ka) as evidenced by relatively small amounts of offset in the Gardner Creek fans, and in Little Valley age (Bull Lake) tills at Dry Creek and at Little Cottonwood Canyon (W. E. Scott, pers. commun., 1984). If the mid-Holocene slip rates at Gardner Creek are extrapolated to the older fans, about 200 m of offset should have occurred in the past 250,000 yrs, compared to the estimated 32-50 m of offset that can be shown. Thus, there is evidence of a 4-5 fold increase in cumulative offset rates through the latest part of the Quaternary.

The characteristic earthquake model of Schwartz and Coppersmith (1984) infers repeated, rupture events that produce about 2 m of vertical offset on discrete segments of the Wasatch fault zone. If this model is accepted, a pre-Bonneville slip rate of 0.2 m/ka requires a interval of about 10,000 yrs between events. This recurrence interval is in sharp contrast to the 2,000-1,000 yr intervals variously calculated for individual segments of the fault zone during post-Bonneville time, and to Schwartz and Coppersmith's (1984) preferred 444 yr interval for the whole of the Wasatch fault zone.

The long-term (Cenozoic) slip rate for central part of the Wasatch fault zone is about 0.4 m/ka (Naesar and others, 1983) based on fission-track ages. This rate falls between the post- and pre-Bonneville rates as one might expect, especially if it records cyclic, long- and short-period fluctuations in slip rate. For example, a combination of 20,000-yr-long intervals of 2 m/ka average slip rate and 100,000-yr-long intervals of 0.2 m/ka average slip rate yield a cumulative slip rate of 0.5 m/ka.

Perhaps the cause of the changes in slip rate is a hydro-tectonic mechanism. A large lake would produce hydrostatic head and increased pore pressure, and could have a triggering mechanism related to isostatic loading and unloading during lake expansion and contraction. The combination of these factors could cause an increased slip rate (and hence more earthquakes) by focusing regional stresses on a primed structure (the Wasatch fault zone). Without a large lake, the pore pressure is decreased to the ambient level, the hydrostatic load is removed, and the shear stress is redistributed over the eastern Basin and Range Province in a more orderly manner. The presence of a large lake, or a series of repeated large lakes, during the Quaternary may have focused earthquakes on the Wasatch fault zone.

Further research

Mapping and stratigraphic studies of the Quaternary geology along the Wasatch Fault zone will continue northward into the Utah Lake Valley from Payson on the south to Alpine on the north. This stretch of the fault zone is essentially the 55-km-long Provo segment proposed by Schwartz and Coppersmith (1984). Data from the Hobble Creek site suggest that the Provo segment has a relatively fast post-Provo (<13,500 yrs B.P.) rate of offset (0.85-1.0 m/ka) and has been most recently active about 1,000 yrs ago (Swan and others, 1980). Six to seven rupture events have been suggested for displacement of the Provo-age surface, which equates to an average recurrence interval of 1,700-2,600 yrs. A specific effort will be made toward better defining the amount of offset in Provo, Bonneville, and pre-Bonneville age deposits, although the latter are not well exposed in the Utah Valley.

References

- Bucknam, R. C., and Anderson, R. E., 1979, Estimation of fault-scarp ages from a scarp-height-slope-angle-relationship: *Geology*, v. 7, no. 1, p. 11-14.
- Cluff, L. S., Brogan, G. E., and Glass, C. E., 1973, Wasatch fault, southern portion--Earthquake fault investigation and evaluation (a guide to land use planning for Utah Geological and Mineralogical Survey): Woodward-Lundgren and Associates, Oakland, California, 79 p., 23 plates (sheets).
- Crone, A. J., and Machette, M. N., 1984, Surface faulting accompanying the Borah Peak earthquake, central Idaho: *Geology*, in press.
- Machette, M. N., 1984, Late Cenozoic geology of the Beaver basin, southwestern Utah: *Brigham Young University Studies in Geology*, in press.
- Machette, M. N., 1985, Calcic soils of the American Southwest, in Weide, D. L., and Faber, M. L., eds., *Soils and Quaternary geomorphology of the American Southwest*: Geological Society of America Special Paper, in press.
- Machette, M. N., and McGimsey, R. G., 1983, Map showing Quaternary and Pliocene faults in the Socorro and western part of the Fort Sumner 1° x 2° quadrangles, central New Mexico: U.S. Geological Survey Miscellaneous Field Studies Map MF-1465-A with pamphlet, scale 1:250,000.
- Morrison, R. B., 1965, New evidence of Lake Bonneville stratigraphy and history from southern Promontory Point, Utah: U.S. Geological Survey Professional Paper 525-C, p. C110-C119.
- Naesar, C. W., Bryant, Bruce, Crittenden, M. D., Jr., and Sorensen, M. L., 1983, Fission-track ages of apatite in the Wasatch Mountains, Utah--an uplift study, in Miller, D. M., Todd, V. R., and Howard, K. A., eds., *Tectonic and stratigraphic studies in the eastern Basin and Range*: Geological Society of America Memoir 157, p. 29-36.

Pierce, K. L., Obradovich, J. D., and Friedman, Irving, 1976, Obsidian hydration dating and correlation of Bull Lake and Pinedale glaciation near West Yellowstone, Montana: Geological Society of America Bulletin, v. 87, no. 5, p. 703-710.

Schwartz, D. P., and Coopersmith, K. J., 1984, Fault behavior and characteristics earthquakes--examples from the Wasatch and San Andreas fault zones: Journal of Geophysical Research, in press.

Schwartz, D. P., Hanson, K. L., and Swan, F. H., III, 1983, Paleoseismic investigations along the Wasatch Fault zone--An update, in Crone, A. J., ed., Paleoseismicity along the Wasatch Front and adjacent areas, Central Utah: Geological Society of America Rocky Mountain and Cordilleran Sections Meeting, Guidebook, Part 2, Utah Geological and Mineral Survey Special Studies 62, p. 45-49.

Scott, W. E., 1982, Guidebook for the 1982 Friends of the Pleistocene, Rocky Mountain Cell, Field trip to Little Valley and Jordan Valley, Utah: U.S. Geological Survey Open-File Report 82-845, 58 p.

Scott, W. E., McCoy, W. D., Shroba, R. R., and Rubin, Meyer, 1983, Reinterpretation of the exposed record of the two last lake cycles of Lake Bonneville, Western United States: Quaternary Research, v. 20, no. 3, p. 261-285.

Swan, F. H., III, Schwartz, D. P., and Cluff, L. S., 1980, Recurrence of moderate to large magnitude earthquakes produced by surface faulting on the Wasatch fault zone, Utah: Bulletin of the Seismological Society of America, v. 70, no. 5, p. 1431-1462.

EARTHQUAKE RECURRENCES ESTIMATED BY
CALIBRATING QUALITATIVE GEOLOGICAL RATE ESTIMATES

by

David M. Perkins

and

Paul C. Thenhaus

Branch of Engineering Geology and Tectonics

U.S. Geological Survey

Golden, Colorado

Introduction

Large scale mapping of regional probabilistic ground motion hazard encourages fine discriminations in source zonation. This will result in smaller source zones. However, as the source zones become progressively smaller, the number of historic earthquakes contained in the zones decreases. Statistically-derived rates of earthquake activity for individual zones, therefore, become increasingly less reliable. We need alternatives to the usual statistical methods which depend entirely on historical seismicity.

During a series of workshops held to define regional source zones for part of the conterminous United States (Thenhaus, 1983), we asked the workshop participants for estimates of maximum magnitude and earthquake rates for each proposed zone. Quantified estimates based on fault scarp studies provided a basis for these estimates throughout the Great Basin. However, in much of the Rocky Mountain region, lack of systematic investigation of young faults precluded quantitative geologic estimates of the recurrence of large earthquakes. Estimates in this region, therefore, were qualitative and

sampled the participants' intuition as to the relative earthquake hazard among zones. These qualitative recurrence estimates were not actually used in the production of the 1982 national hazard map. Instead, an analysis of the historical seismicity was used to estimate zone recurrence rates. However, when the 1983 Borah Peak (Idaho) earthquake occurred in a source zone for which a very low recurrence rate was estimated from the historical seismicity, we decided to look again at the qualitative geological estimates made at the workshops that dealt with the northern and southern Rocky Mountains. Could these qualitative estimates have been used to get a better estimate of the recurrence rate for the vicinity of the Borah Peak earthquake as well as for other source zones in the Rockies?

Figures 1a and 1b show the Rocky Mountain source zones suggested by the attendees of the two workshops. Table 1 shows the qualitative estimates of seismicity and a rough quantitative estimate of relative rate. The question we asked ourselves was whether the qualitative estimates could be calibrated to provide numerical recurrence estimates which could be used in estimates of probabilistic ground-motion hazard.

Calibrations

We compared the rates obtained in the source-zone analysis for the national hazard map (Algermissen and others, 1982) with the qualitative geological estimates. The rates used were normalized to the rate per unit area of the estimated recurrence of magnitude 4.0 to 4.6 earthquakes (intensity V). Table II shows the zone numbers in the northern Rockies from figure 1, the letter indicating geological recurrence estimates for those zones, and the corresponding rate per unit area of the zones from Algermissen

and others (1982). The zones for the national map were somewhat modified from those suggested in the source zone meetings, as have their serial numbers, so a fourth column in the table gives the serial number of the corresponding zone from figure 3 of Algermissen and others (1982, p. 17). In Table II, a rough calibration method groups the geological estimates into four categories and averages the historical recurrence estimates for the four categories.

This method does not give rates for intermediate geological estimates which the workshops participants indicated by using + or - values or by intermediate specifications (e.g., A-B or C-D), because there is not enough rate information available to group at these values. A natural next step, then, is to assign numbers to these distinctions. Figure 2 shows a plot of the natural log of the area-normalized zone rates vs one possible numeration of the qualitative estimates. The numeration was purely arbitrary. It places A, B, C, and D at 9, 6, 3, and 0, respectively, and provides unit differences between A- and B+ and between A and A-, etc. The log of the rates was taken because a plot of the unlogged rates appeared to be exponential. The figure also shows a line indicating the results of a linear least squares regression of the log rates on the numerated qualitative estimates. The regression line gives values for the intermediate qualitative estimates and also provides values for the groups located at a single qualitative estimator. (In a later section we show hazard estimates derived for four source zones, using these estimated normalized rates from the regression line.)

It must be emphasized that the numeration of the qualitative estimates is arbitrary. We could have assigned to A- and B+ the same number. We might even have assigned numbers having a ratio relation. Furthermore, there is no necessary reason for imposing a regression line--we could have just connected cluster centroids. What is interesting in this calibration is that the

predicted rates are values which bear a reasonable relative relation to the quantitative relative estimates made by the workshop participants. The regression rate values for A, B, C, and D are, respectively, 19.4, 6.7, 2.3, and .57. If we normalize so that the value for B is 10.0, the respective values are 29, 10, 3.5, and .85, compared with 40, 10, 3 and 1 for the geologists' estimates of quantitative relative rate.

Application to Borah Peak Vicinity

An indicator of the reasonableness of even the crude, first calibration by grouped averages (Table I) can be obtained by comparing several estimates of the recurrence of an event the size of the 1983 Borah Peak, Idaho earthquake. The earthquake occurred in zone 22. The seismic rate for this zone, from Algermissen and others (1982), yields a recurrence rate for magnitude 7 to 7.6 earthquakes of about one chance in 5000 per year within the approximately 200 km by 100 km area in the vicinity of the earthquake. The zone containing the Borah peak earthquake was rated in category B by the geologists. For all zones rated B in the northern Rockies, the average historical seismicity rate per unit area is about five times the rate for the zone containing the Borah Peak earthquake. Simply increasing the zone rate estimate by the factor of five, we obtain a recurrence rate of about one chance in a thousand in the 200 km by 100 km area.

Further perspective on these two estimates is provided by Ruppel (1964) and by M. H. Hait and W. E. Scott (1978, written communication). Ruppel investigated the faults in a 50-mile by 150-mile area in which the Borah Peak earthquake later occurred, and concluded that "the major displacements probably were completed by late Pleistocene time . . . nevertheless, some

movement is more recent" Hait and Scott reported evidence of Holocene displacements. The fault near the Borah Peak epicenter "has experienced recurrent activity over a period of 10,000 to 100,000 years, the last major event being of Holocene age." Depending on how one interprets these geological estimates, one can calculate recurrences according to the number of such faults in the 20,000 km² area of interest.

Under an assumption that one fault has a recurrence interval of 30,000 years (a rough geometric mean of Hait and Scott's ten and hundred thousand), it would take six such faults in the area to yield a recurrence of 5000 years, about that of the estimate derived from historical seismicity. It would take 30 such faults to yield a recurrence interval of 1000 years for the area. It seems unlikely that there are as many as 30 faults with Holocene displacements in the vicinity of Borah Peak. This would be a higher rate of Holocene faulting than that estimated by Bucknam and others (1980) for one of the more densely faulted areas of western Utah.

Suppose, however, that one fault has a recurrence interval of 5000 years. Then it would require only one such fault to produce the historical recurrence interval and five such faults could produce the recurrence interval derived by calibrated geological estimates. Numbers of this order seem more reasonable. The lack of many historical intensity V earthquakes would argue for an areal recurrence interval at the longer end of the 1000- to 5000-year recurrence estimate. A recurrence interval of 5000 years for the 100x200km area is identical to the recurrence estimate of Bucknam and others for magnitude 7 to 7.6 earthquakes in the previously mentioned area in western Utah, characterized by numerous pre-Holocene faults. The area-normalized rate (1×10^{-5} per 1000 km²) for this recurrence interval is also consistent with the area-normalized rate (5×10^{-6} to 5×10^{-5}) of faulting ($M > 7$) estimated by Wallace

(1978) for zones of Holocene faulting in Utah, western Nevada, and eastern California, exclusive of the rupture zones of historic earthquakes. Thus, the recurrence estimate obtained by averaging the historic rates for B-rated zones in the northern Rocky Mountains is consistent with recurrences estimated for other regions of Basin and Range faulting.

Recurrences at Four Points in Rockies

We used the regression calibration values for the geological recurrence estimates to adjust the areal rates for zones 19, 22, 31, and 38 (Figure 1). The ratio of the regression rate to the rate used in the national hazard map, was used to increase the seismicity in those zones. Figure 3 shows the old vs new ground motion recurrences for four sites, each central to their respective zones for four zones in which the calibration produces increased rates. For a given return period there is an increase in ground motion ranging from a factor of only about 10-25 percent (zone 31) to as much as 150 to 250 percent (zone 38). Zone 38, the northern Rio Grande Rift in Colorado, had particularly concerned geologists as one for which the geomorphology suggested much greater hazard than the historic seismicity would indicate.

Examination of figure 2 shows that just as using the regression estimates increases recurrence rates at some zones where the historical seismicity rate is relatively low, using these estimates will decrease recurrence rates for some zones that have relatively high historical seismicity. We might be somewhat more reluctant to decrease high seismic rates than increase low ones, if we felt that a high seismic rate could be a precursor to larger events. In any case, a general use of the regression estimates for all zones would narrow the range of recurrence rates and hence lower the contrast in ground motion hazard among the zones.

Critique and recommendations

First it should be noted that there are other ways to calibrate qualitative recurrence estimates. Exact numeration is not needed if we just connect cluster centroids and (perhaps) smooth the connections. On the other hand, the numeration could have been one which preserved the 40:10:3:1 quantitative relative rates suggested by the geologists. And as far as the treatment of ordinates is concerned, we could have taken the log of the historical rate estimates one more time before regressing. Clearly, the more one messes around in these ways, the more subjective judgment is brought to bear, and the less consistent may be the results from different analysts' interpretations. However, it is also possible that the calibration process is relatively robust. Different calibration methods may produce rates whose differences are not very significant in their effect on probabilistic ground motion.

A more important subjective judgment to quantify is an estimate of the relative weight to assign to the geologic and seismicity evidence available for each zone. In a regression calibration, individual points might bear greater weight the more one believed the value of the historical seismic evidence in certain zones. However, in assigning a rate to a zone, use of only the regression estimate would force all zone B's, say, to have the same rate, unless some further technique were used to balance the regression estimate against the historic estimate, on a zone-by-zone basis.

The use of calibration techniques of the sort discussed here still depends upon having sufficient seismicity among a number of zones to perform the calibration. We have presented an application which uses the seismicity

of much of the Rocky Mountains. Clearly, in attempting a similar analysis for smaller source zones for a smaller portion of the Rockies, we would be presented with considerably less seismicity and hence more scatter in the rates estimated from historical data.

Recommendations

1. It would be useful to attempt the other techniques suggested above, in order to assess the robustness of the calibration in the northern Rockies.
2. To test the reliability of our calibration, we should see how the rate values for the southern Rockies are predicted by this calibration.
3. We should attempt to find a rationale for weighting the application of historical rates not only in regression calibration but also in assigning rates to individual zones.
4. We should look for an opportunity to apply such an analysis to other regions and sets of smaller source zones. In the one case, there may be a poorer geological basis for rate estimation. In the other case, the historical seismicity is more sparse. These applications will test the limits of application of the technique.

References

- Algermissen, S. T., Perkins, D. M., Thenhaus, P. C., Hanson, S. L., and Bender, B. L., 1982, Probabilistic Estimates of Maximum Acceleration and Velocity in Rock in the Contiguous United States, U.S. Geological Survey Open-File Report 82-1033, 99 pages.
- Bucknam, R. C., Algermissen, S. T., and Anderson, R. E., 1980, Patterns of Late Quaternary Faulting in Western Utah and an Application in Earthquake Hazard Evaluation, in Proceedings of Conference X: Earthquake Hazards Along the Wasatch (and) Sierra-Nevada Frontal Fault Zones, 29 July 1979-1 August 1979, U.S. Geological Survey Open-File Report 80-801, pages 299-314.
- Ruppel, Edward T., 1964, Strike-Slip Faulting and Broken Basin-Ranges in East-Central Idaho and Adjacent Montana, in Geological Survey Research, 1964, U.S. Geological Survey Professional Paper 501-c, pages c14-c18.
- Thenhaus, Paul C., (editor), 1983, Summary of Workshops Concerning Regional Seismic Source Zones of Parts of the Conterminous United States Convened by the U.S. Geological Survey 1979-1980, Golden, Colorado, U.S. Geological Survey Circular 898, 36 pages.
- Wallace, Robert E., 1978, Patterns of Faulting and Seismic Gaps in the Great Basin Province, in Proceedings of Conference VI: Methodology for Identifying Seismic Gaps and Soon-to-Break Gaps, 25-27 May 1978, pages 857-868.

TABLE I

Qualitative Estimates of Recurrence...
 Letters A through D indicate decreasing rate of recurrence.
 For southern Rocky Mountain Zones A:B:C:D is roughly 40:10:3:1.

<u>Zone No.</u> <u>from Figure 1</u>	<u>Relative</u> <u>recurrence rate</u>
15	C
16	B
17	C
18	D
19	B
20	A
21	B
22	B
23	A
24	C
25	C-D
26	C
27	C
<hr/>	
29	B
30	D
31	A
32	A+
33	C
34	A-
35	C-D
36	C
37	C
38	A-B
<hr/>	
38	A
39	D
42	C
43	B
44	A
46	C
47	C
49	A
50	A
51	D
52	B
53	D
54	D

TABLE II

Correspondence between qualitative estimates of source zone recurrences and area normalized rates of recurrence for related source zones from analysis of historical seismicity.

Thenhaus (1983)		Algermissen and others (1982)	
Zone No. from Fig. 1	Relative Rate	Area-normalized Rate	Corresponding Zone Numbers
32	A+	36	40
20	A	25	55,57
23	A	55	56
31	A	14	38 (part)
34	A-	14	38 (part)
38	A-B	4	43
	A-Group Average	25	
16	B	13	64
19	B	3	61
21	B	19	59
22	B	2	58
29	B	7	38,51,52,52
	B-Group Average	9	
15	C	2	63
17	C	2	65
24	C	2	58 (part)
26	C	2	45 (part)
27	C	2	45 (part)
33	C	2	45 (part)
36	C	2	45 (part)
37	C	2	45 (part)
	C-Group Average	2.2	
25	C-D	0.7	54
35	C-D	2	45,50
18	D	0.9	16,44,45
30	D	1.8	49,66
	D-Group Average	1.4	

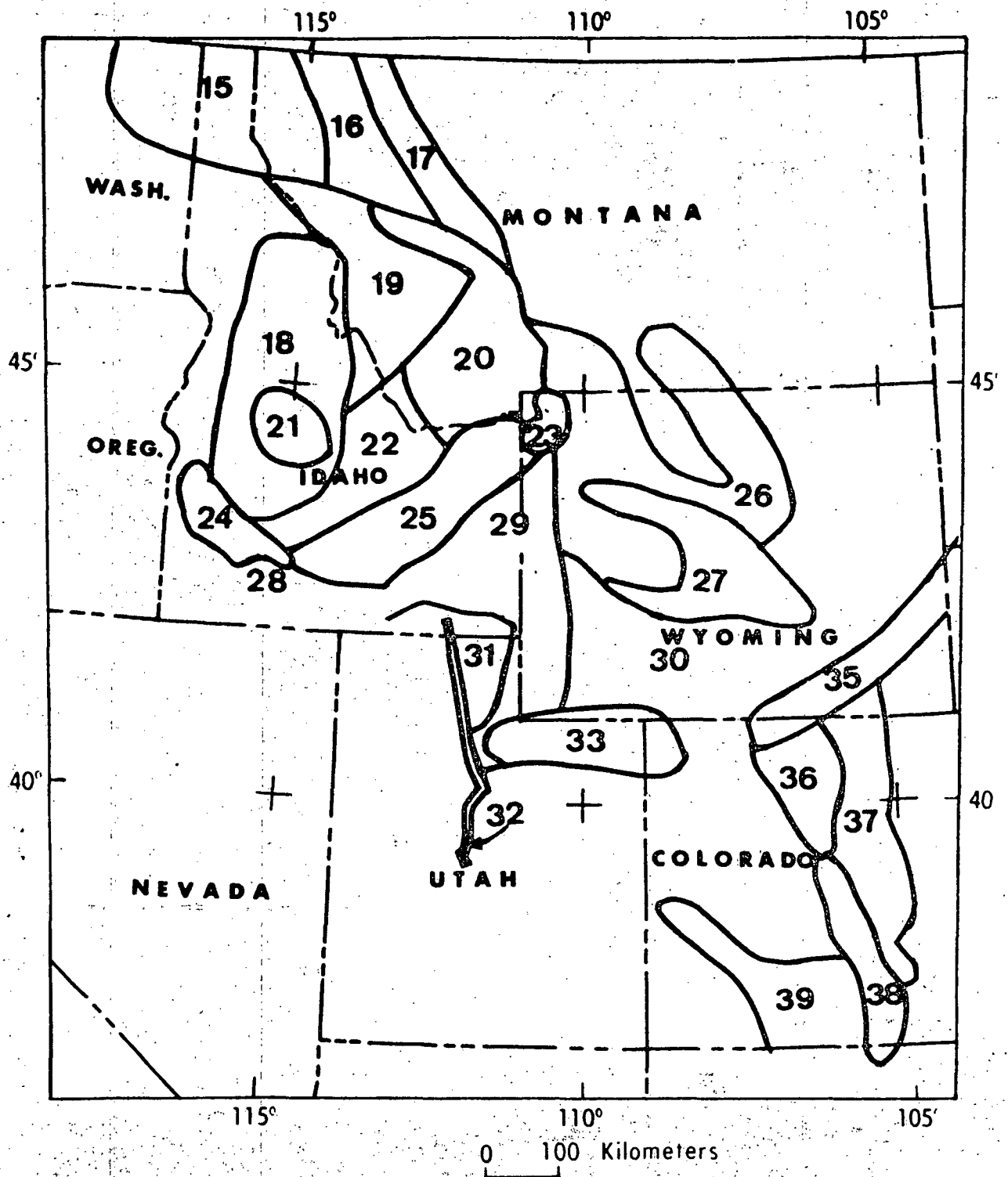


Figure 1a. Seismic source zones for the northern Rockies, from Thenhaus, 1983.

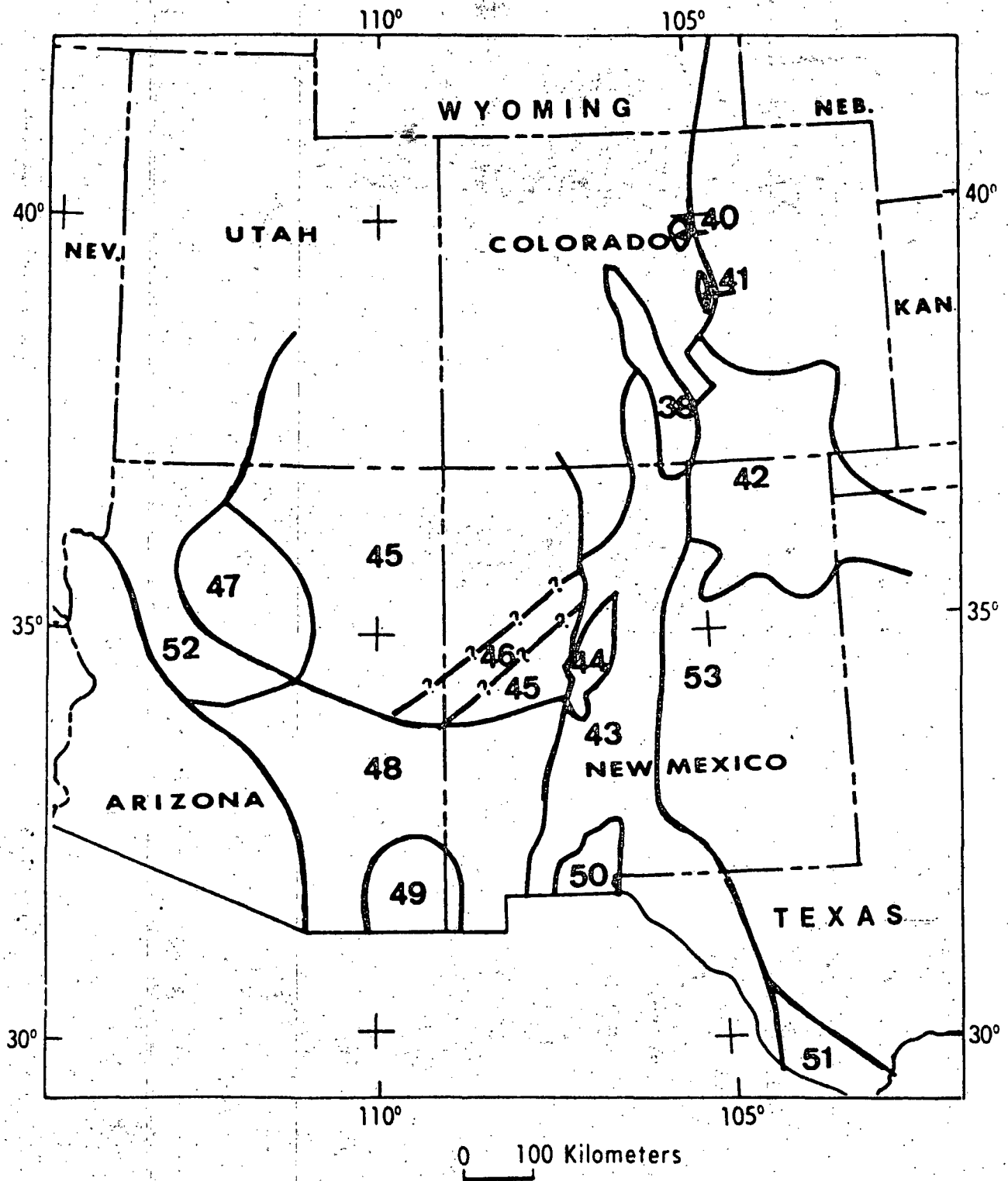


Figure 1b. Seismic source zones for the southern Rockies, from Thenhaus, 1983.

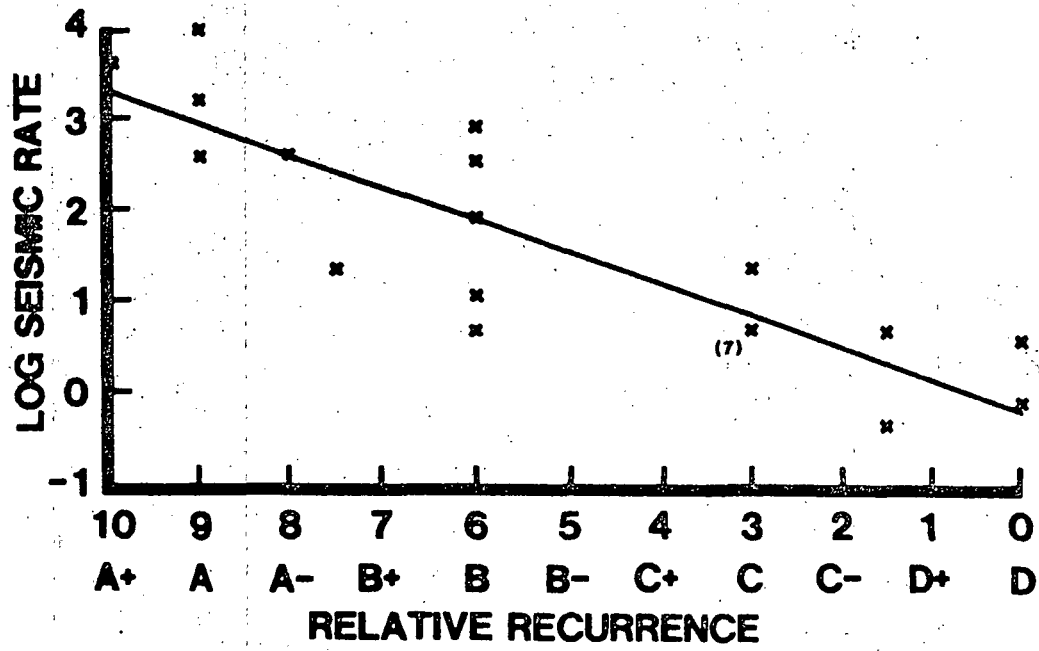
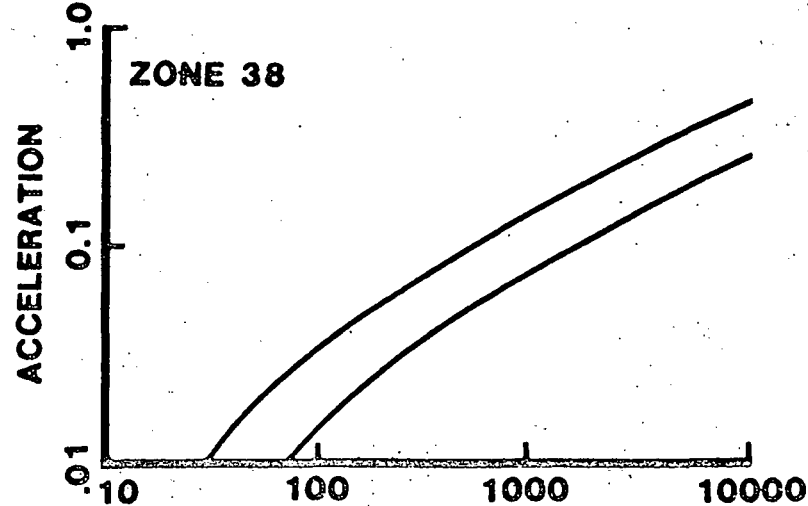
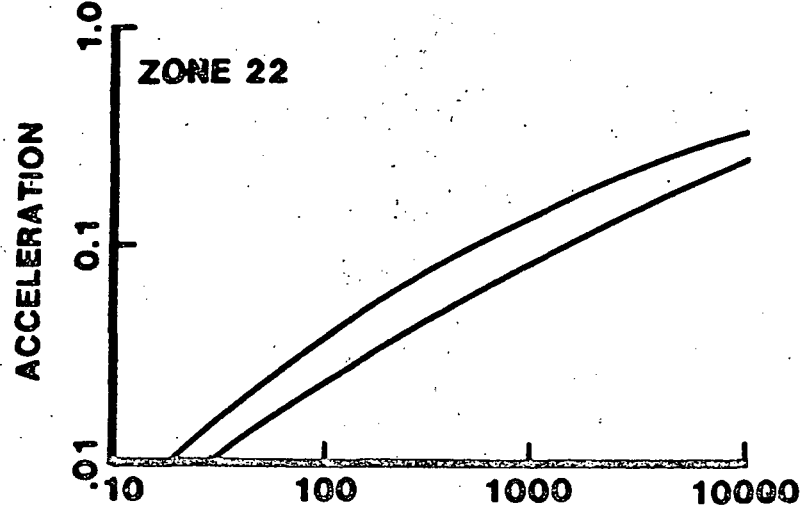
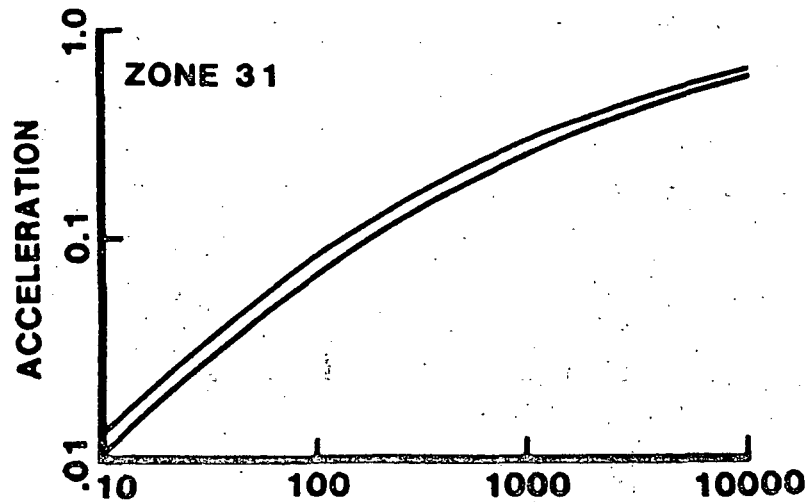
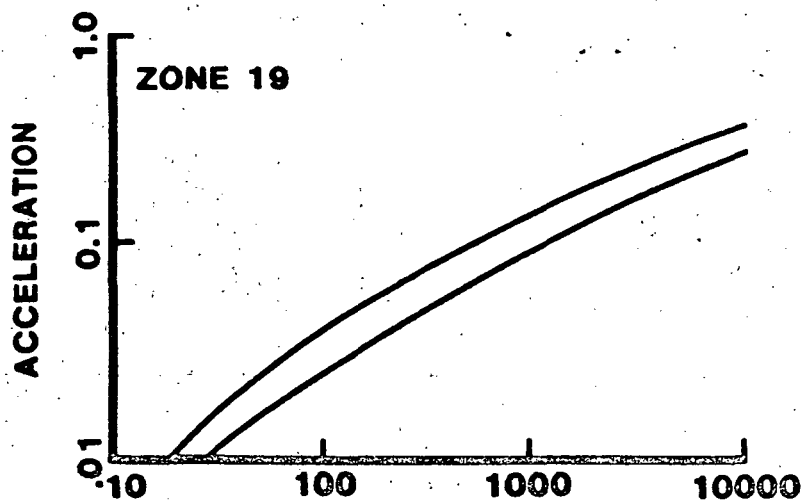


Figure 2. Calibration of qualitative geological rate estimates using regression. Ordinate: natural logarithm of area-normalized rates of source zones of national hazard map (Algermissen and others, 1982). Abscissa: arbitrary numeration of letter-value rate estimates.



YEARS

YEARS

Figure 3: Acceleration vs. return Period estimates for 4 sites central to their respective zones. Curve with lower ground motion value is for seismic rates of national hazard map (Algermissen and others, 1982). Curve with higher value is for recurrence from regression calibration.

A PLAN FOR EVALUATING
HYPOTHESIZED SEGMENTATION OF THE WASATCH FAULT

by

Russell L. Wheeler
U.S. Geological Survey
Denver, Colorado 80225

ABSTRACT

Swan and others (1980) and Schwartz and Coppersmith (1984) hypothesized that seismogenic structure along the Wasatch fault zone is segmented, and that segments tend to rupture completely and independently in earthquakes of characteristic sizes. If true, that would affect hazard evaluation along the Wasatch Front urban corridor. This report proposes ways to evaluate the hypothesis of segmentation. The most direct evaluation would come from more trenching of the Wasatch fault, but probability calculations suggest that that could require several times as many sites as have been trenched thus far. Methods of tectonic geomorphology may also be used to evaluate segmentation. So may statistical evaluation of spatial associations of structural and geophysical anomalies with proposed segment boundaries, and specialized ~~structural studies of proposed boundaries.~~

INTRODUCTION

Schwartz and Coppersmith (1984) hypothesized two things that, if true, would have much impact on evaluation of seismic hazard for the Wasatch Front urban corridor. First, they proposed that the Wasatch fault comprises six segments that are mostly or wholly independent of each other structurally and seismogenically. Second, they proposed that seismic release of energy in a given segment occurs mostly as earthquakes of a size that is characteristic of

that segment. These characteristic earthquakes tend to rupture the whole segment but tend not to rupture across segment boundaries into adjacent segments.

Neither hypothesis implies the other, but if the fault is not segmented then earthquakes of various sizes may be regarded as occurring more or less randomly along the fault. The fault as a whole and any portion of it would be likely to exhibit the standard behavior that is characterized by a constant slope (b value) on a recurrence plot. Of the two hypotheses, segmentation is the more fundamental for understanding behavior of the Wasatch fault. This report outlines a plan for evaluating the segmentation hypothesis.

IMPORTANCE

If segments rupture individually and independently, and usually in earthquakes of a characteristic size, there would be several consequences. First, there would be more large earthquakes than expected from a linear extrapolation of a recurrence relationship that is derived from historical and instrumental earthquakes (Schwartz and Coppersmith, 1984). Such a departure from constant slope of a recurrence plot could reconcile the discrepancy between low observed frequencies of small earthquakes and geologic observations of abundant fault scarps. The scarp observations indicate a frequency of large earthquakes along the Wasatch Front that is about 10 to 30 times that inferred from extrapolation of observed small earthquakes (Schwartz and Coppersmith, 1984, their fig. 13).

Second, Schwartz and Coppersmith (1984, their table 2) suggested that scarp forming events in the past 8,000 years have been concentrated in the four central and most heavily populated segments. Indeed, compared to frequencies expected if scarp forming events were distributed uniformly along the Wasatch fault zone, their data imply that segmentation could nearly double

the frequency of large events in the Salt Lake City and Nephi segments. That increase in frequency would be in addition to the tenfold to thirtyfold increase inferred from scarp abundances.

Third, production of probabilistic maps of seismic hazard uses estimates of three parameters: the magnitude of the largest expected earthquake, the recurrence interval of earthquakes of that size, and the geographic zone over which those two values are expected to apply (Algermissen and others, 1982; Thenhaus, 1983). Segmentation of the Wasatch fault would change estimates of all three parameters, and thus would alter the calculated hazard. If the characteristic earthquake hypothesis is also true, it might not further affect the zones, but would greatly change estimates of maximum magnitudes and recurrence intervals in each zone.

Thus the segmentation hypothesis, particularly with addition of the characteristic earthquake hypothesis, poses questions whose answers will greatly affect hazard evaluation along the Wasatch Front, and particularly in the population centers of the central portions of the front.

STRATEGY

Design of an investigation of segmentation is governed by consideration of pertinent time scales, and of the significance of spatial associations. The portion of the future about which hazard evaluation attempts to draw conclusions is the next decades, centuries, and millennia. Periods extending successively further into the future are of interest for emergency planning, for design of critical structures, and for storage of radioactive or toxic wastes. For example, the probabilistic hazard maps of Algermissen and others (1982) are calculated for the next 10, 50, and 250 years. Thus geological and other data are pertinent to the evaluation of segmentation for hazard purposes only to the degree that those data apply to the coming decades to millennia.

The Wasatch Front lies in an extensional tectonic regime. So does northeastern China (Molnar and Tapponier, 1975, 1977; Zhang and others, 1984). For northeastern China, McGuire (1979) and McGuire and Barnhard (1981) found that seismicity of a 50-year period is best characterized by that of the preceding 50 years. However seismicity of a 200-year period is poorly characterized by that of the preceding 200 years, because Chinese seismicity exhibits an apparent cycle with a period of about 300 years. Implications of those findings for the Wasatch Front, for which Schwartz and Coppersmith (1984) estimated a recurrence interval for scarp forming events of about 444 years, are that useful geologic records will most probably be those that formed during, or can be shown to bear on, the Holocene and late Pleistocene, a length of time over which any such cyclicity is likely to be averaged out.

To identify segment boundaries and to demonstrate their existence and control on Holocene and late Pleistocene evolution of the Wasatch fault zone, Schwartz and Coppersmith (1984) sought spatial coincidences of proposed segment boundaries with anomalies in several types of geological and geophysical data along the front. For instance, they examined breaks and shape changes in the mapped trace of the Wasatch fault, differences in ages of the most recent scarp-forming events, saddles in the Bouguer gravity field over the valleys that border the front on the west, changes in crestal elevation of the Wasatch Range, and changes in morphology of young fault scarps. No one kind of data clearly reveals or convincingly documents segments or their boundaries. However, the argument is that (1) spatial coincidence of anomalies of several kinds is good enough that it cannot be attributed to chance, but must reflect some common underlying cause of the various kinds of anomalies, and (2) each type of anomaly occurs in data of a sort that is likely to reflect structures that are probably responsible for

Holocene seismicity, so that the inferred common cause of the anomalies may also affect that seismicity.

This is a fundamentally statistical argument, so the subjective perception of spatial coincidence, and its evaluation as being better than would be expected from chance, can be tested objectively. That is fortunate, because there are few enough anomalies of few enough kinds that another observer might form the opinion that the coincidence is a result of chance, and that there is no underlying common cause. Such a disagreement between two subjective perceptions is usually difficult to settle without either a properly designed statistical test, or more data. The first alternative is usually quicker and cheaper.

Thus the strategy will be to seek answers to two questions. First, do segments exist along the Wasatch Front, or are they artifacts of perception and a small sample, indistinguishable from patterns arising from chance? Second, if segments exist, have they affected uplift and seismicity along the Wasatch fault both in the Holocene and far enough back in time that they can be expected to continue those effects for the next decades, centuries, and millennia?

INVESTIGATIONS

Several lines of investigation are proposed below. Limits on personnel and funding make it unlikely that all can be pursued to completion by the end of fiscal year 1986. However, all are described here in the hope that other workers may wish to follow one or more of them. A following section gives preliminary results from some of the investigations.

Paleoseismicity and Tectonic Geomorphology

The most direct way to evaluate the hypotheses of segmentation and of characteristic earthquakes together would be to examine the record of Holocene

and late Pleistocene faulting and uplift, as expressed in landforms and in alluvial and colluvial stratigraphy. For example, the most direct evidence for segmentation of the Wasatch fault comes from the trenches described by Swan and others (1980) and Schwartz and Coppersmith (1984), and comprises differences, from segment to segment, in the ages of and intervals between scarp-forming events. However, there is only one trench site per segment, with as many as three trenches per site, so the present trench data cannot determine whether the differences between segments exceed the variability within segments. More trench sites would solve that problem but would be expensive and would require careful preparation. Because of that high cost, decisions about the need for additional trenching of the Wasatch fault and identification of optimal locations for additional trenches might best await results of continuing mapping of late Cenozoic deposits along the Wasatch Front (for example, see M. N. Machette, this volume).

Currey (1982) measured elevations of Bonneville, Provo, and other shorelines throughout the Lake Bonneville basin of Utah, Idaho, and Nevada. Elevations near the Wasatch Front are few, but D. R. Currey (oral and written commun., 1984) estimates that many more could be obtained on both hanging and footwalls of the Wasatch fault. Then perhaps one could determine whether, say, footwall elevations of the Bonneville shoreline differ significantly from one segment to another, or whether pairs of elevations that span the fault demonstrate differing amounts of post-Bonneville dip slip in adjacent segments.

Mayer and Wentworth (1983) demonstrated that statistical analysis of stream-gradient indices can detect the existence and sense of recent dip slip across an inferred fault. Similar analysis, controlled for the effects of lithology of the bedrock and other factors, may be able to detect differences

in uplift rates between segments, and compare such differences to variability within segments (L. Mayer, 1983, and written communs., 1983).

Other numerical or descriptive characterizations of landforms that record uplift may also be able to detect differences between proposed segments that exceed variability within segments. These include elevations of ridge crests atop faceted spurs (Hamblin, 1976; Hamblin and Best, 1980), steepness of the range front (Hamblin and Best, 1980), and determinations of which wall of the Wasatch fault remained stationary while the other wall moved up or down relative to it (Hamblin, 1984).

Spatial Associations

It should be straightforward to design and perform a statistical evaluation of the suggested spatial association of geological and geophysical anomalies with the inferred segment boundaries. The goal would be to determine whether the proposed segment boundaries occur at the same places along the Wasatch Front as do anomalies in structural and geophysical data of types that are available along most or all of the front. For each kind of data used, it must be shown that the kinds of anomalies selected are those that would reflect structures that could localize segment boundaries. Examples include gravity and magnetic data, geometry of thrust sheets along the front, and large features that trend across the front such as the Little Cottonwood stock and the edges of the Uinta aulacogen.

If the proposed segment boundaries as a group are significantly associated with structures that predate the Wasatch fault, then those older structures can be interpreted as having caused segmentation of the fault (Zoback, 1983). If the association is not significant, then either the proposed segment boundaries do not exist, or they exist but represent distortions in the late Quaternary evolution of the Wasatch fault that are

randomly distributed along the front, or the boundaries exist and are long-lasting features of the fault but have not been localized by older structures. Any of those three interpretations would cast doubt on the segmentation hypothesis, the hypothesis of characteristic earthquakes, or both.

Bedrock Structure

Whether or not the proposed boundaries as a group can be shown to be significantly associated with older structures, and interpreted as caused by them, specialized geologic mapping and structural studies of small, selected areas may be able to demonstrate segmentation, control by older structures, or both for a single segment boundary.

Structure maps.--Thrust sheets of the Sevier orogeny reached the Wasatch Front from the west in Cretaceous time (Armstrong, 1968). There, the complex of thrust sheets is interpreted from well, seismic reflection, and stratigraphic data to be 5 to 10 km thick (Standlee, 1982; Smith and Bruhn, 1984). The Wasatch fault cuts that complex. Abrupt, along-strike changes in the geometry of the thrust sheets could have caused interruptions, bends, or en echelon steps in the Wasatch fault zone. If that happened, the result would be segmentation of the fault.

Figure 1 illustrates a way in which the shape and internal structure of a thrust sheet could cause segmentation of a zone of normal faults that cuts it. Figure 1a shows the footwall of an east directed thrust sheet. On the flats the sheet rides on bedding-plane faults. At the longitudinal ramps the thrust fault cuts up section as a reverse fault. Common in thrust complexes are transverse ramps (buried tear faults), where the ramp locally has a different strike and experiences oblique or strike slip. Atop the longitudinal ramps, units that are cut by the ramps are duplicated

structurally. This duplication and related processes form hanging-wall anticlines (fig. 1b). Because little or no duplication occurs above the transverse ramp, and because the longitudinal ramps do not align, the anticlines plunge past each other (fig. 1c).

If instead the two longitudinal ramps of figure 1a represent two thrust faults that lose displacement past each others' tips (fig. 1d), then no transverse ramp need form. The result is a transfer zone (Jones, 1971), in which slip is transferred en echelon from one fault to another, so that all east-west sections through figure 1d experience the same net shortening. Transfer zones and transverse ramps can occur together, and complexities abound in natural examples (Boyer and Elliott, 1982; Harris, 1970).

The portion of the thrust sheet above transverse ramps and transfer zones is structurally disrupted. Where several transverse ramps or transfer zones occur in rough alignment across strike, and are not yet exposed by erosion, their expression in the overlying thrust sheet is a CSD (cross-strike structural discontinuity) (Wheeler, 1980; Wheeler and others, 1979). The rocks exposed in CSD's of the Appalachians differ in various ways from rocks of the same units that are exposed along strike, outside the CSD's (Wheeler and others, 1979). The various structural, geophysical, geomorphic, stratigraphic, hydrologic, and metallogenic anomalies that can be distributed along a CSD allow its recognition, and can be interpreted in terms of underlying, concealed transfer zones and transverse ramps. Some CSD's can be inferred to have formed above causative basement faults, but generally that inference cannot be tested because the rocks that contain the CSD have usually been thrust away from whatever portion of the basement they might originally have overlain (Wheeler, in press).

If a thrust complex, complete with transverse ramps, transfer zones, and perhaps overlying CSD's, such as the Sevier thrust complex (Smith and Bruhn, 1984), is extended in a direction roughly similar to the older direction of thrust transport, normal faults that nucleate between CSD's will propagate along strike and encounter a CSD. If the propagating normal fault stops, bends, splits, changes to strike slip, or is replaced en echelon by another, it is most likely to do so in the weakened, disrupted rock of a CSD, other things being equal. Thus CSD's may partly decouple portions of the extending mass from each other, resulting in segmentation.

Prospecting for CSD's can be time consuming, so fieldwork will be confined to the area at and around the boundary between the Provo and Nephi segments, near Payson. There, structure and stratigraphy are simpler than at other segment boundaries. Maps useful in detecting and defining CSD's include strike-line maps, maps of contours of values of bed dip, and structure contour maps (Wheeler, 1980; LaCaze and Wheeler, 1980; Wheeler and others, 1979, and references cited there). Most data needed for production of such maps have been obtained from compilations being prepared by I. J. Witkind and B. H. Bryant (oral and written commun., 1983-84), and from bed orientations plotted on numerous published and unpublished maps, mostly M.S. theses from Brigham Young University.

Geologic mapping. -- Inspection of the geologic and structural compilations just mentioned reveals several small areas where detailed remapping may aid evaluation of the proposed boundary between the Provo and Nephi segments. All are in or near the Payson Lakes quadrangle (fig. 4). In and adjacent to the northwestern portion of that quadrangle, the Wasatch fault of the Nephi segment extends northeastward along the west edge of Dry Mountain. East of Dry Mountain, the fault of the Provo segment extends southwestward; its

southwestern tip overlaps the northeastern tip of the fault of the Nephi segment (fig. 4). Between the two fault tips, Dry Mountain exposes Precambrian to upper Paleozoic rocks. Mapping of young faults between those two fault tips should aid in evaluating the proposed segment boundary.

In the north-central portion of the Payson Lakes quadrangle, Metter (1955) mapped exposures of Flagstaff Limestone throughout about one-fourth of a square kilometer. The Flagstaff Limestone is Eocene in age (MacLachlan, 1982), and Metter mapped the Bear Canyon thrust fault at its southeastern contact. The thrust fault is probably a splay within the Charleston-Nebo thrust complex. If remapping verifies that it cuts the Flagstaff Limestone, then some thrusting continued as late as Eocene.

In the central portion of the Payson Lakes quadrangle are two basins defined by concentric belts of outcrops of several Tertiary units. In the centers of the basins occur exposures of volcanic and sedimentary rocks of late Eocene to Oligocene age (Davis, 1983). The few available bed orientations from the basins, together with basin orientations and positions, are consistent with the hypothesis that the basins represent synclines separated by an anticline, all formed above a blind thrust that is part of the Charleston-Nebo thrust system. If remapping verifies that hypothesis, the basins would constitute further evidence of small amounts of thrusting as late as middle Tertiary time.

Demonstration of middle Tertiary thrusting would be pertinent to evaluating segmentation if the same Tertiary units are also exposed northeast of the Payson Lakes quadrangle, on the other side of the proposed segment boundary and about on strike with the exposures just described. If such rocks can be found, and if they are not folded, that would demonstrate at least

partial decoupling of the thrust complex across the segment boundary, and would support the inference of a CSD at the location of the segment boundary.

Jointing history and intensity. --Joint fabrics of thrust sheets can change into and across CSD's. Dixon (1979), Wheeler and Dixon (1980), and LaCaze and Wheeler (1980) found that systematic joints are more closely spaced inside Appalachian CSD's than outside them. Both greater size and greater abundance of joints produce smaller spacings (Wheeler and Dixon, 1980). If a CSD and its causative structures partly decoupled adjacent portions of a thrust complex during one or more episodes of joint formation, then jointing history may also change into or across a CSD, and so may help to detect and define it. Jointing history can be worked out by using joint shapes, fillings, and abutting relations, and delicate structures on joint faces such as plumose structures. Interpretation of such joint features to elucidate the evolution of single joints and of intersecting joints follows the principles of fractography, which were developed by ceramicists and applied to rocks in the field by Kulander and others (1979), Barton (1983), Verbeek and Grout (1983), Grout and Verbeek (1983), and R. L. Wheeler (unpub. data, 1978-84).

Examination of jointing history and intensity will be concentrated at and near the inferred boundary between the Provo and Nephi segments, near Payson. There, the most widely exposed rocks are the interbedded sandstones with some shales and limestones of the Oquirrh Formation of Pennsylvanian and Permian age. Synorogenic clastic units of Cretaceous age and postorogenic lacustrine and volcanic sedimentary units of Tertiary age are exposed locally. Thus, outcrop abundance and distribution require that the proposed jointing studies begin with the Oquirrh Formation, but application to inferred segmentation of Cenozoic structures requires that results be carried into the Cretaceous and Tertiary units. Rocks of the Oquirrh Formation have a long and

complex structural history. At least their older joint sets may predate Cretaceous thrusting or at least Tertiary extension, and so may be useful only for identifying widespread joint sets and CSD's. Only joints in Tertiary rocks are likely to bear directly on evolution of the Wasatch fault.

PRELIMINARY RESULTS

The sections of this chapter are organized to match those of the preceding chapter on investigations.

Paleoseismicity and Tectonic Geomorphology

How many trench sites?--The impact of the results of Swan and others (1980) and Schwartz and Coppersmith (1984) demonstrates the value of data obtained from trenches across fault scarps along the Wasatch Front. The importance and cost of such data make it worthwhile to estimate the number of trench sites that would be necessary to test the existence of segments. The following hypothetical examples illustrate that such a test would require more sites than presently exist. The examples also illustrate considerations and calculations that may be useful in optimizing future trenching operations.

Swan, Schwartz and coworkers actually trenched only the four central segments of the Wasatch Front, but surface observations in the two end segments allowed them to obtain information similar to that which could have been obtained there by trenching. Because they obtained most of the effect of six trench sites, the following discussion is phrased in terms of six sites.

The question to be answered is whether the recurrence intervals of scarp-forming events differ more between segments than they vary within segments. We will consider trench sites like the six of Schwartz and Coppersmith (1984), noting that a single site may contain more than one trench. For each example below, we use the randomization test (Conover, 1971, p. 357-364; Mosteller and Rourke, 1973, p. 12-15; Siegel, 1956, p. 152-157). In that test the P-value,

or descriptive level of significance P , is the ratio of the number of ways in which the observations can be arranged to give a result at least as extreme as the one observed, to the total number of ways in which the observations can be arranged. Let s be the number of trench sites, b be the number of segment boundaries, t be the recurrence interval in years that is determined for scarp-forming events at a given trench site, and d be the difference between t values obtained from two adjacent sites. For example, for the data of Schwartz and Coppersmith (1984), $s = 6$ and $b = 5$.

In each of the following examples, we calculate the smallest value of s for which it is possible to detect segmentation at the conventional significance level of 0.05. We cannot guarantee that having more sites than the minimum number will detect segmentation if it does not exist or is very subtly expressed, but we can be certain that having fewer sites will preclude detecting any segmentation that might be there.

Suppose we obtain only one value of t per site. That might occur because the structural and stratigraphic relationships and the amount of carbon recovered for that site allow only one value of t to be determined. It might also occur because we obtain several t values from a site but wish to average them in order to decrease variability. Figure 2 illustrates this example. We could then investigate whether the average of the values of t obtained for several sites in one segment differs significantly from the average from several sites in an adjacent segment. However sites suitable for trenching might not be concentrated within two adjacent segments. It would be safer to assume that suitable sites will be found in several different segments. Accordingly we examine values of d , not t , and ask whether the values of d that span segment boundaries are significantly larger than those that occur

within individual segments. For figure 2, we would ask whether d_1 , d_3 , d_5 , and d_6 are significantly larger than d_2 and d_4 .

In the most clear cut case, the b segment boundaries will be spanned by the b largest values of d . How many trench sites are needed for it to be possible to achieve significance at 0.05? In terms of the randomization test, $P = 1/C(s-1, b)$, and we wish to solve for the smallest value of s for which P does not exceed 0.05. For the segments of Schwartz and Coppersmith (1984), $b = 5$ so s must be at least 8.

If some of the boundary spanning values of d are small, they will overlap some of the d values that do not cross boundaries. Then the result is less clear and more sites are needed to test significance. For example, suppose that the boundary spanning values of d are not the b largest in the set of $s-1$ numbers, but are only among the $2b$ largest. Then we calculate s such that 0.05 equals or exceeds $P = C(2b, b)/C(s-1, b)$. We find that we need at least 19 sites.

Note several things about these examples. The t values will have uncertainties, and we would need to consider these uncertainties when comparing values of t and d . Correlating scarp-forming events between sites is not necessary for the calculation, but if it can be done it would aid in evaluating the uncertainties of the t values, and in determining which of any two values of d is the larger.

Also, if we obtain several t values at a site and average them to decrease variability, the averages will be more stable and reliable estimates of t than are the individual values, but our sample size will be smaller. Stabler estimates increase our ability to detect significant differences between segments, but smaller sample sizes decrease that ability. It is not clear which effect will dominate the other, so the analysis should be

performed both with and without averaging. If we averaged all t values from a site, then probably we would have few enough sites in each segment that we would have to work with d values, as described above. If we did not average t values at a site, then we might have enough t values that we could work directly with them. In that case, we could ask whether the several t values in one segment differ significantly from those in an adjacent segment. The better approach of the two will be the one that gives the smaller P-value.

The upshot of these calculations is that evaluating the segmentation hypothesis with more trench sites might be done with only a few more sites than have already been obtained by Swan and others (1980) and Schwartz and Coppersmith (1984), perhaps as few as eight in all. However, evaluation could require several times that many, for example at least 19.

Crestal elevations of the Wasatch Range. --Schwartz and Coppersmith (1984, their fig. 10) note that elevation of the crest of the Wasatch Range appears to change between segments, with some large changes occurring across segment boundaries. They suggest that those changes support the notion that the range is segmented, and that the segments have been uplifted independently. That suggestion can be tested as follows. For both tests below, we use the Kruskal-Wallis test (Siegel, 1956) because the calculations for the randomization test become long and tedious for all but very small samples or special cases. Figure 10 of Schwartz and Coppersmith (1984) shows crestal elevations at 39 points along the range.

First we ask whether the largest changes in crestal elevation, as measured between two adjacent points, span segment boundaries. They do not: the five elevation changes that span boundaries exceed the other 33 changes only at $P = 0.36$. A histogram of the two groups of numbers shows no obvious difference between the two groups.

Next we ask whether adjacent segments differ significantly in elevation. The northernmost (Collinston) segment is significantly lower than the adjacent Ogden segment, with $P = 0.01$. However, no other pair of adjacent segments differs significantly in elevation: the other four P -values exceed 0.10.

Thus for the Wasatch Front as a whole, and for the populous central segments, these crestal elevation data are consistent with the segmentation hypothesis, but can neither support nor deny it. However, there are only about six elevations per segment, and crestal elevation at single points may be affected by lithology and structure. Other measures that could yield more values, or that could average over larger areas might detect differential uplift between segments. For instance, more values could be obtained by determining median elevations of squares measuring 10 km on a side, over the entire range. Larger areas could be averaged by estimating total rock volume that lies above, say, 6,000 ft, within strips 10 km wide and spanning the range.

Pediments atop faceted spurs. --Hamblin (1976) and Anderson (1977) mapped and correlated pediment surfaces along the western face of the Wasatch Range in and near the Provo segment, from the Traverse Mountains southward to Payson Canyon. Can the pediment data of Anderson (1977) address the segmentation question? Several assumptions are needed for the following analysis. First, we accept Anderson's (1977) identification and morphologic correlations of pediment surfaces between ridges and across canyons. Second, we assume that pediment surfaces represent periods of little or no uplift, and that the slopes between pediments represent periods of comparatively rapid uplift (Hamblin and Best, 1980).

The slope between two vertically adjacent pediments cannot represent a scarp formed by a single event, because the slopes are typically 200 to 300 m high (Hamblin, 1976). Schwartz and Coppersmith (1984) estimate typical rates for uplift produced by scarp-forming events along the Wasatch Front at about 1 mm/yr, and typical scarp heights for single events at about 2 m. Given those estimates and the range of data about them, each intrapediment slope may represent tens to hundreds of scarp-forming events that occurred over a few hundred thousand to a few million years. Thus if pediments reflect segmentation in any way, that segmentation would act on time scales much longer than the Holocene. Such segmentation would be likely to continue for the next few millennia, the time period of most interest here. *? what about the decade?*

If a single pediment is followed north or south along the range front, it may branch into two pediments that continue at different elevations (Anderson, 1977; fig. 3). Branch points can be interpreted as the ends of portions of the range that underwent periods of uplift more or less as coherent blocks. If segments and their boundaries controlled that uplift and defined those blocks, then branch points should concentrate near segment boundaries.

Branches do not open preferentially to either north or south ($P = 0.26$ by the binomial test), so we seek departure from a uniform distribution of branch points along the Wasatch Front, rather than from a uniform northward or southward increase in numbers of branch points.

Anderson (1977) mapped 29 branch points in 590 linear kilometers of pediment, along 76 km of the range front. Pediment preservation, pediment detection, and range height vary along the front, so we normalize the number of branch points by kilometers of measured pediment length. Because branch points are few, and because locations and widths of segment boundaries are uncertain, we divide Anderson's (1977) 76 km traverse roughly into northern

and southern quarters and central half. We ask whether the number of branch points in the two end quarters, taken together, significantly exceeds the number in the central half, normalized for the fraction of the 590 km of pediment length that falls into each of the two parts of the traverse.

The binomial test gives a value for P between 0.4 and 0.5. We conclude that either Anderson's (1977) mapped branch points contain no evidence that segmentation operated at the time scale of pediment formation, or we have interpreted the pediments and branch points incorrectly, or both.

Spatial Associations

No work has been done on this topic yet, beyond considering which types of data to use, and collecting maps of such data.

Bedrock Structure

Structure maps. --Preliminary interpretation of partly compiled data suggests that a CSD may exist at or near the inferred boundary between the Provo and Nephi segments, east of Payson (fig. 4). The structure defined by the contact between Permian rocks and the underlying Oquirrh Formation, and the distribution of bed orientations in the outcrop area of the Oquirrh Formation, are consistent with the existence of a transverse ramp under the central portion of the Spanish Fork Peak quadrangle, and a flattening of southeastward dips in areas northeast of there. Southeast dips and upright orientations throughout the area sketched in figure 4 indicate that the area lies on the front limb of a large hanging wall anticline, the Nebo anticline of earlier workers (for example, Eardley, 1934). The lower elevations of the base of the Permian units to the northeast of the inferred transverse ramp suggest that the ramp may dip north (fig. 5).

Geologic mapping. --No work has been done yet, beyond collecting and compiling available maps and structural data.

Jointing history and intensity.--Two large roadcuts about 3 km apart in Spanish Fork Canyon expose sandstone beds of the Oquirrh Formation (circled S in fig. 5; Baker, 1972). There, four sets of calcite-filled systematic joints exhibit abutting and other relationships that define the order in which they formed; crystallization of joint fillings need not have occurred at the same time or in the same order as did jointing itself. Scattered observations elsewhere in the southern Wasatch Range indicate that this jointing history may be recognizable elsewhere in exposures of the Oquirrh Formation. Planar joints, many filled with calcite, occur in some roadcuts exposing synorogenic clastic units of Cretaceous age, and in natural exposures of the Flagstaff Limestone of Eocene age. Thus it may be feasible to develop jointing histories for those rocks. In and around the Payson Lakes quadrangle appears to be the best area to do that, and to attempt to relate jointing histories of younger rocks with that of the widely distributed and well-exposed Oquirrh Formation. Then jointing history and intensity could be compared across and into the segment boundary that is inferred to occur near Payson.

ACKNOWLEDGMENTS

I. J. Witkind and B. H. Bryant generously shared their knowledge of stratigraphic, structural, and map relationships throughout northern and central Utah. R. L. Bruhn, K. J. Coppersmith, D. R. Currey, L. Mayer, D. P. Schwartz, and R. B. Smith were generous with preprints and discussions of their unpublished results and my speculations. Discussions with R. E. Anderson sharpened my ideas.

REFERENCES CITED

- Algermissen, S. T., Perkins, D. M., Thenhaus, P. C., Hanson, S. L., and Bender, B. L., 1982, Probabilistic estimates of maximum acceleration and velocity in rock in the contiguous United States: U.S. Geological Survey Open-File Report 82-1033, 99 p., 6 pls.
- Anderson, T. C., 1977, Compound faceted spurs and recurrent movement in the Wasatch fault zone, north central Utah: Brigham Young University Geology Studies, v. 24, p. 83-101.
- Armstrong, R. L., 1968, Sevier orogenic belt in Nevada and Utah: Geological Society of America Bulletin, v. 79, p. 429-458.
- Baker, A. A., 1972, Geologic map of NE part of Spanish Fork quadrangle, Utah: U.S. Geological Survey Open-File Report 72-9, scale 1:24,000, 1 sheet.
- Barton, C. C., 1983, Systematic jointing in the Cardium Sandstone along the Bow River, Alberta, Canada: New Haven, Connecticut, Yale University Ph. D. dissertation, 302 p.
- Boyer, S. E., and Elliott, D., 1982, Thrust systems: American Association of Petroleum Geologists Bulletin, v. 66, p. 1196-1230.
- Conover, W. J., 1971, Practical nonparametric statistics: New York, John Wiley, 462 p.
- Currey, D. R., 1982, Lake Bonneville: Selected features of relevance to neotectonic analysis: U.S. Geological Survey Open-File Report 82-1070, 30 p., 1 pl.
- Davis, F. D., 1983, Geologic map of the southern Wasatch Front, Utah: Utah Geological and Mineral Survey Map 55-A, scale 1:100,000, 2 sheets.

Morgantown, West Virginia, West Virginia University Ph. D. dissertation, 143 p.

Eardley, A. J., 1934, Structure and physiography of the southern Wasatch Mountains, Utah: Michigan Academy of Science Papers, Arts and Letters, v. 19, p. 377-400.

Grout, M. A., and Verbeek, E. R., 1983, Field studies of joints -- Insufficiencies and solutions, with examples from the Piceance Creek basin, Colorado, in Gary, J. H., ed., Oil shale symposium, 16th, Golden, Colorado, April 13-15, 1983, Proceedings: Golden, Colorado School of Mines Press, p. 68-80.

Hamblin, W. K., 1976, Patterns of displacement along the Wasatch fault: Geology, v. 4, p. 619-622.

_____, 1984, Direction of absolute movement along the boundary faults of the Basin and Range-Colorado Plateau margin: Geology, v. 12, p. 116-119.

Hamblin, W. K., and Best, M. G., 1980, Patterns and rates of recurrent movement along the Wasatch-Hurricane-Sevier fault zone, Utah during late Cenozoic time, in Evernden, J. F., compiler, Proceedings of conference X, Earthquake hazards along the Wasatch and Sierra-Nevada frontal fault zones: U.S. Geological Survey Open-File Report 80-801, p. 601-633.

Harris, H. D., 1954, Geology of the Birdseye area, Thistle Creek Canyon, Utah: Compass of Sigma Gamma Epsilon, v. 31, no. 3, p. 189-208.

Harris, L. D., 1970, Details of thin-skinned tectonics in parts of the Valley and Ridge and Cumberland Plateau provinces of the southern Appalachians, in Fisher, G. W., Pettijohn, F. J., Reed, J. C., Jr., and Weaver, K. N., eds., Studies of Appalachian geology -- Central and southern: New York, John Wiley, p. 161-178.

- Hintze, L. F., 1962, Geology of the southern Wasatch Mountains and vicinity, Utah: Brigham Young University Geology Studies, v. 9, pt. 1, scale 1:126,720, 1 sheet.
- Jones, P. B., 1971, Folded faults and sequence of thrusting in Alberta foothills: American Association of Petroleum Geologists Bulletin, v. 55, p. 292-306.
- Kulander, B. R., Barton, C. C., and Dean, S. L., 1979, The application of fractography to core and outcrop fracture investigations: U.S. Department of Energy, METC/SP-79/3, 174 p.
- LaCaze, J. A., Jr., and Wheeler, R. L., 1980, Expression of a cross-strike structural discontinuity in Pennsylvanian rocks of the eastern Plateau province: Southeastern Geology, v. 21, p. 287-297.
- MacLachlan, M. E., 1982, Stratigraphic chart showing named units in the Basin and Range, Middle Rocky Mountains, and Colorado Plateaus provinces, in the field trip area, central Utah, in Nielson, D. L., ed., Overthrust belt of Utah: Utah Geological Association Publication 10, p. 291-297.
- Mayer, L., 1983, Morphometric tectonic geomorphology using multivariate discriminant analysis: Geological Society of America Abstracts with Programs, v. 15, no. 6, p. 638.
- Mayer, L., and Wentworth, C. M., 1983, Geomorphic differences east and west of the Stafford fault system, northeastern Virginia: Geological Society of America Abstracts with Programs, v. 15, no. 2, p. 56.
- McGuire, R. K., 1979, Adequacy of simple probability models for calculating felt-shaking hazard, using the Chinese earthquake catalog: Seismological Society of America Bulletin, v. 69, p. 877-892.

McGuire, R. K., and Barnhard, T. P., 1981, Effects of temporal variations in seismicity on seismic hazard: Seismological Society of America Bulletin, v. 71, p. 321-334.

Metter, R. E., 1955, The geology of a part of the southern Wasatch Mountains, Utah: Columbus, Ohio, Ohio State University, Ph. D. dissertation, 252 p., 2 pls.

Molnar, P., and Tapponnier, P., 1975, Cenozoic tectonics of Asia: Effects of a continental collision: Science, v. 189, p. 419-426.

_____, 1977, Relation of the tectonics of eastern China to the India-Eurasia collision: Application of slip-line field theory to large-scale continental tectonics: Geology, v. 5, p. 212-216.

Mosteller, F., and Rourke, R. E. K., 1973, Sturdy statistics: Nonparametrics and order statistics: Reading, Massachusetts, Addison-Wesley, 395 p.

Rawson, R. R., 1957, Geology of the southern part of the Spanish Fork Peak quadrangle, Utah: Brigham Young University Geology Studies, v. 4, no. 2, 34 p., 1 pl.

Schwartz, D. P., and Coppersmith, K. J., 19__, Fault behavior and characteristic earthquakes: Examples from the Wasatch and San Andreas fault zones: Journal of Geophysical Research, 54 ms. p., 15 figs., 4 tables [in press].

Siegel, S., 1956, Nonparametric statistics for the behavioral sciences: New York, McGraw-Hill, 312 p.

Smith, R. B., and Bruhn, R. L., 19__, Intraplate extensional tectonics of the western U.S. Cordillera: Inferences on structural style from seismic reflection data, regional tectonics and thermal-mechanical models of brittle/ductile deformation: Journal of Geophysical Research, 65 ms. p., 19 figs. [in press].

- Standlee, L. A., 1982, Structure and stratigraphy of Jurassic rocks in central Utah: Their influence on tectonic development of the Cordilleran foreland thrust belt: Rocky Mountain Association of Geologists, p. 357-382.
- Swan, F. H., III, Schwartz, D. P., and Cluff, L. S., 1980, Recurrence of moderate to large magnitude earthquakes produced by surface faulting on the Wasatch fault zone, Utah: Seismological Society of America Bulletin, v. 70, p. 1431-1462.
- Thenhaus, P. C., ed., 1983, Summary of workshops concerning regional seismic source zones of parts of the conterminous United States, convened by the U.S. Geological Survey, 1979-1980, Golden, Colorado: U.S. Geological Survey Circular 898, 36 p.
- Verbeek, E. R., and Grout, M. A., 1983, Fracture history of the northern Piceance Creek basin, northwestern Colorado, in Gary, J. H., ed., Oil shale symposium, 16th, Golden, Colorado, April 13-15, 1983, Proceedings: Golden, Colorado School of Mines Press, p. 26-44.
- Wheeler, R. L., 1980, Cross-strike structural discontinuities: Possible exploration tool for natural gas in Appalachian overthrust belt: American Association of Petroleum Geologists Bulletin, v. 64, p. 2166-2178.
- Wheeler, R. L., 19 , Stratigraphic evidence for Devonian tectonism on lineaments at Allegheny Front, West Virginia, in Glover, L., III, and McDowell, R. D., eds., Contributions to Appalachian geology, in honor of W. D. Lowry: Virginia Polytechnic Institute and State University, Department of Geological Sciences Memoir 3, 47 ms. p., 7 figs., 3 tables [in press].

Wheeler, R. L., and Dixon, J. M., 1980, Intensity of systematic joints:

Methods and application: *Geology*, v. 8, p. 230-233.

Wheeler, R. L., Winslow, M., Horne, R. R., Dean, S., Kulander, B., Drahovzal,

J. A., Gold, D. P., Gilbert, O. E., Jr., Werner, E., Sites, R., and

Perry, W. J., Jr., 1979, Cross-strike structural discontinuities in

thrust belts, mostly Appalachian: *Southeastern Geology*, v. 20,

p. 193-203; reprinted in O'Leary, D. W., and Earle, J. L., eds., 1981,

International Conference on Basement Tectonics, 3d, Durango, Colorado,

May 15-19, 1978, Proceedings: Denver, Colorado, Basement Tectonics

Committee Publication 3, p. 191-198.

Zhang, Zh. M., Liou, J. G., and Coleman, R. G., 1984, An outline of the plate

tectonics of China: *Geological Society of America Bulletin*, v. 95,

p. 295-312.

Zoback, M. L., 1983, Structure and Cenozoic tectonism along the Wasatch fault

zone, Utah, in Miller, D. M., Todd, V. R., and Howard, K. A., eds.,

Tectonics and stratigraphy of the eastern Great Basin: *Geological*

Society of America Memoir 157, p. 3-27.

FIGURE CAPTIONS

Figure 1.--Sketches showing geometries of structures that may occur in or under CSD's in thrust complexes. (a) Block diagram of footwall of a thrust fault. Open arrow shows direction of transport of hanging wall (not shown) over footwall. F shows flats, LR shows longitudinal ramps, and TR shows transverse ramp. (b) Block shown in (a), with addition of hanging wall block. Transport over distance D, in direction shown by arrows on front faces of blocks, produces hanging wall anticlines shown on top surface of block. (c) Geologic map of top surface of block shown in (b), with arrows showing trends of hanging wall anticlines and plunges of their noses. (d) Shape of bottom surface of a hanging wall block that has been cut by two thrust faults whose tips overlap and which die out past each other, en echelon. Sawteeth identify leading edges of both faults.

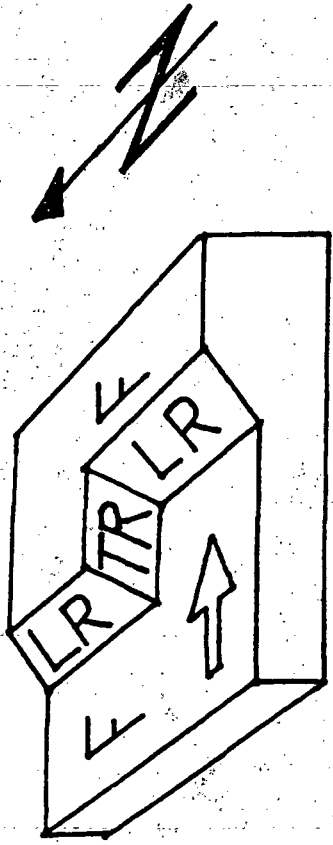
Figure 2.--Schematic diagram of hypothetical example for one value of t per site (see text). View is to east. Long horizontal brackets identify segments, from north to south along Wasatch Front. Circles enclose segment numbers, and squares enclose boundary numbers. Arrows point to locations of trench sites, at which t values are obtained. Here, in notation defined in text, $s = 7$, $b = 4$, and $d(i) = t(i+1) - t(i)$.

Figure 3.--Schematic diagram representing view eastward toward range front in Provo segment and adjacent ends of adjoining segments. Horizontal lines represent pediment surfaces. Dots on them represent branch points. Slopes between pediment surfaces represent periods of uplift, ranked approximately from youngest (circled 7) to oldest (circled 1).

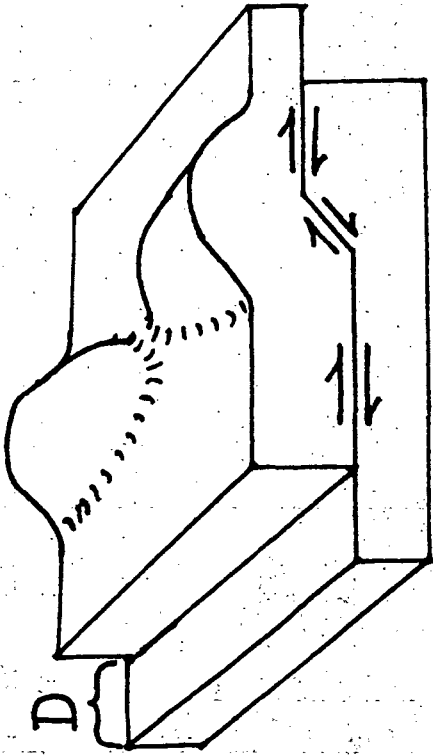
Figure 4.-- Sketch map summarizing preliminary evidence for a CSD at or near the segment boundary at Payson (circled P). 7.5 minute quadrangles shown are Spanish Fork (SF), Spanish Fork Peak (SP), Billies Mountain (BM), Santaquin (S), Payson Lakes (PL), and Birdseye (BE). Line with single hachures represents approximate locations of portions of the Wasatch fault that enter SP from the north, as the Provo segment, and S from the south, as the Nephi segment (after Davis, 1983). West sides are down. Line with double hachures represents the contact between the Oquirrh Formation and older rocks (Po) with overlying Permian and younger units (P), all upright and dipping southeasterly (after Davis, 1983). Double hachures show generalized directions of bed dips at and west of that contact. In BE, elevation of contact is mostly above 8000 feet, and in eastern SP and BM, mostly below 7000 feet. Numerous bed orientations (not shown) in SP, PL, and BE are from Harris (1954), Metter (1955), Rawson (1957), Hintze (1962), Baker (1972), and Davis (1983).

Circled S in center of SP shows location of road cuts of Oquirrh Formation in Spanish Fork Canyon, where systematic joints have been analyzed (see text).

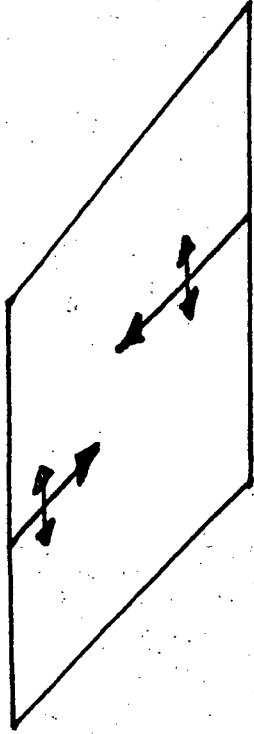
Figure 5.--Sketch maps showing inferred structure of buried footwall block (a) and exposed hanging wall block (b) in area surrounding Spanish Fork Peak quadrangle of figure 5. In (a), strike and dip symbols show dip directions of inferred longitudinal and transverse ramps. In (b), Po denotes exposed upper portion of Oquirrh Formation and older rocks, and P denotes exposed Permian and younger rocks. Hanging wall anticline in (b) overlies the southern of the two longitudinal ramps in (a). Structure in northern portion of area shown is speculative, as indicated by dashed lines and question marks.



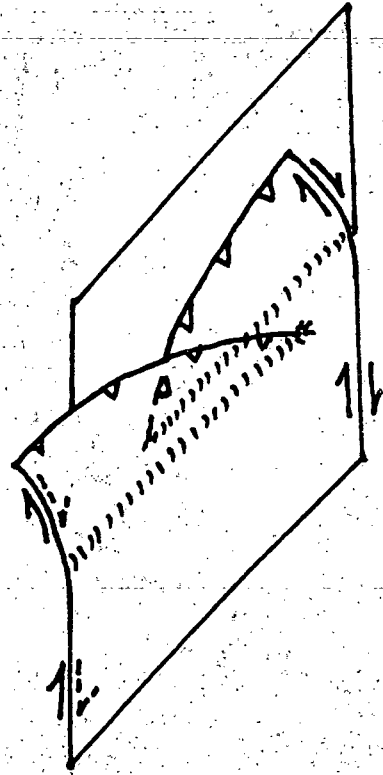
(a)



(b)



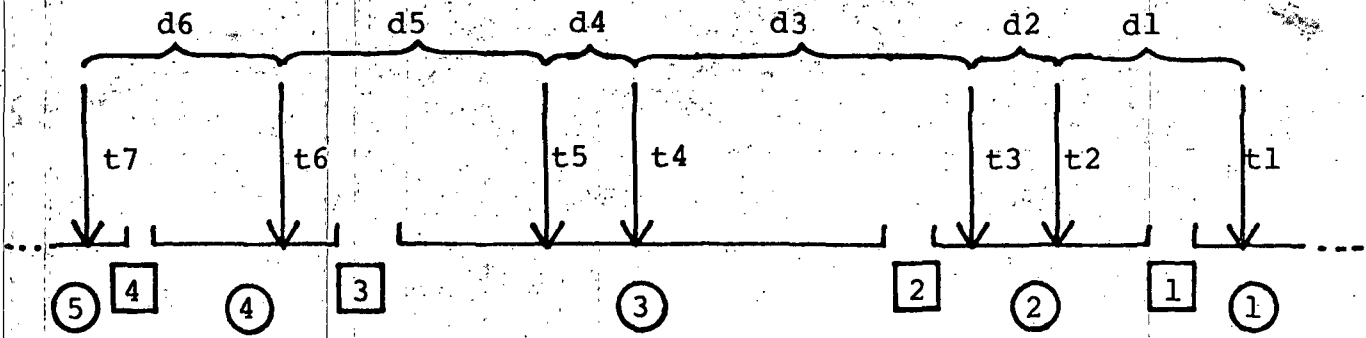
(c)



(d)

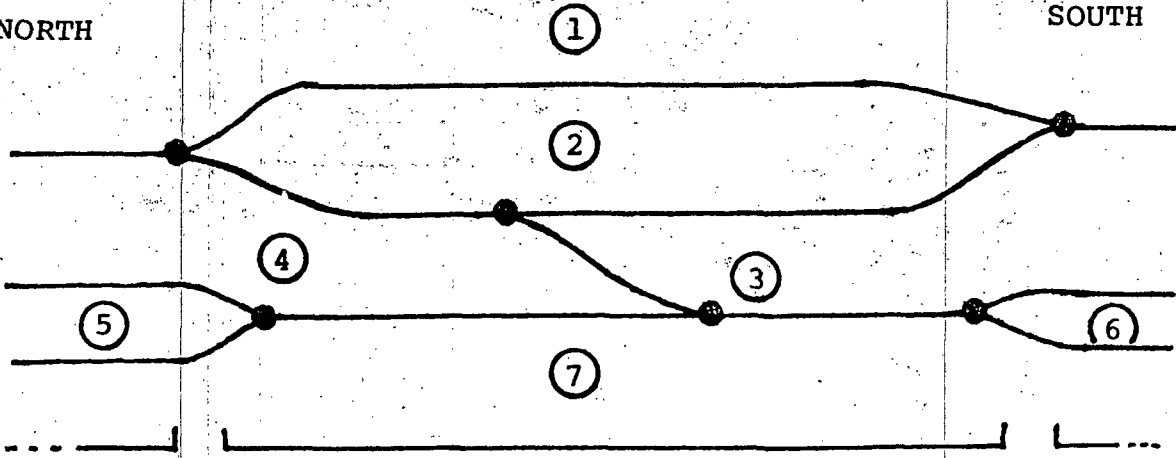
NORTH

SOUTH



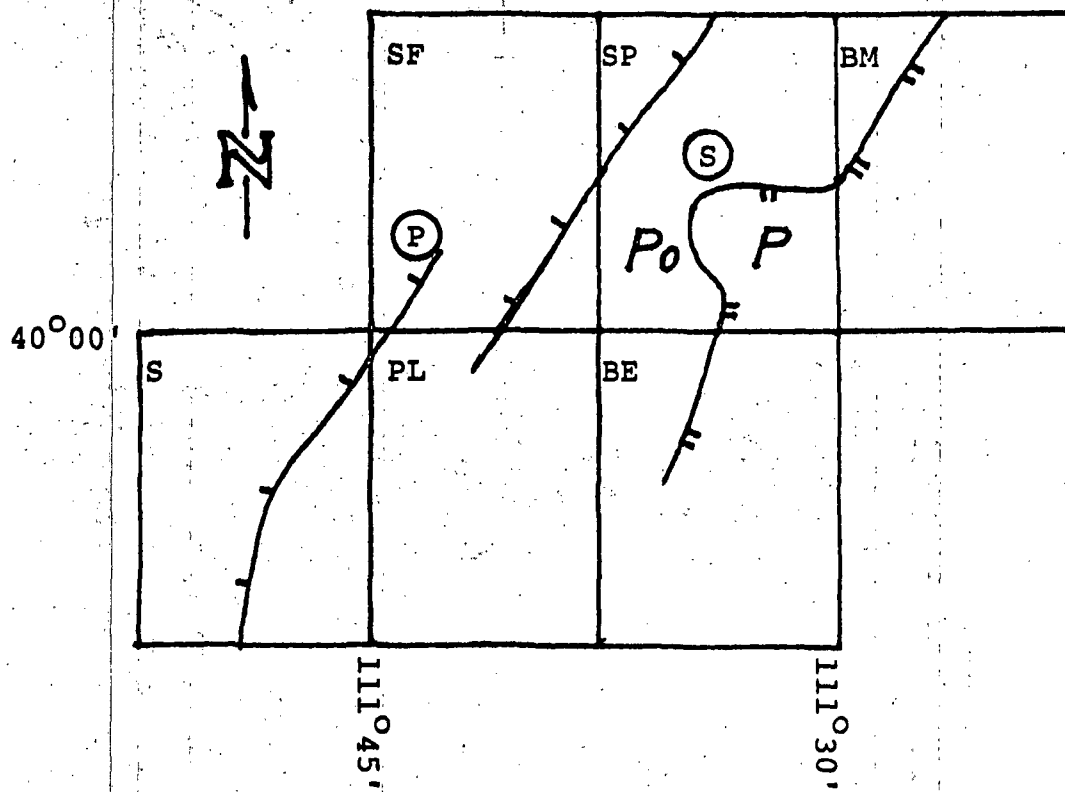
NORTH

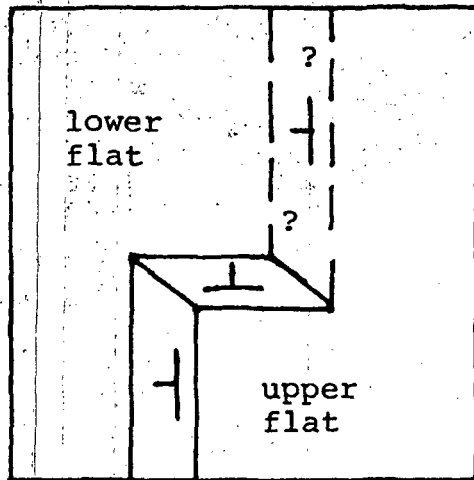
SOUTH



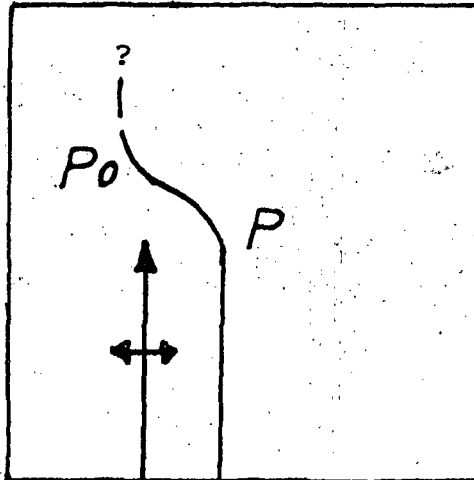
PROVO

SEGMENT





(a)



(b)



**NEAR-SURFACE FAULTING ASSOCIATED WITH HOLOCENE FAULT SCARPS,
WASATCH FAULT ZONE, UTAH: A PRELIMINARY REPORT**

by

Anthony J. Crone and Samuel T. Harding

U.S. Geological Survey,

Denver, Colorado 80225

INTRODUCTION

Abundant geologically young, fault scarps are clear evidence of recent major vertical displacements on the Wasatch fault zone in Utah (Swan and others, 1980; Schwartz and Coppersmith, in press). Earthquake hazard assessments assume that the formation of these scarps was associated with earthquakes of magnitude 7 or greater (Bucknam and others, 1980). However, it is uncertain how these scarps relate to subjacent near-surface faults and to deeper faults that may be the source of damaging earthquakes. Understanding the relationship of the scarps to deeper structures formed in high strength rocks and to the regional structural framework can provide a better basis for realistic earthquake hazard assessments.

During the past two years, we have collected high-resolution seismic reflection data with a MINI-SOSIE¹ system across Holocene fault scarps at

¹ Use of this name is for descriptive purposes only and does not constitute an endorsement by the U.S Geological Survey.

several locations along the Wasatch Front (Fig. 1). These profiles clarify the relationship between the scarps and the subjacent faults, and reveal the distribution of near-surface buried faults. From these data we can identify the areas adjacent to the scarps where ground rupture may occur during future large earthquakes. Where available, deep structural information from conventional reflection profiles can be used to relate the shallow buried faults and the scarps to deeper structures and to the regional structural patterns.

DATA COLLECTION AND PROCESSING

The MINI-SOSIE (MS) system is a small, versatile, high-resolution reflection technique that uses earth-tampers as energy sources. The foot of each tamper is fitted with a source sensor that triggers with each impact of the foot. Time breaks for the impacts are transmitted to a recording truck by radio. The tampers have a peak energy input at about 45 Hz but they also supply a considerable amount of higher-frequency energy above about 100 Hz that improves the resolution of shallow reflections (Wiles, 1979).

Input signals and time breaks from the tampers are cross-correlated in the field with the signals received by the geophones. The cross-correlated data are electronically stored while data from succeeding impulses are cross-correlated. Vibration point (VP) spacing is 16 m. For each vibration point, sufficient cross-correlated data were stacked to yield a good signal-to-noise ratio; in these surveys, a total of 1200 to 2400 impulses from three simultaneously operating tampers were stacked for each VP.

The field data were processed with a standard sequence of processing steps at the U.S. Geological Survey facilities in Denver. Processing steps included tape re-format and gain recovery, demultiplex, common-depth-point

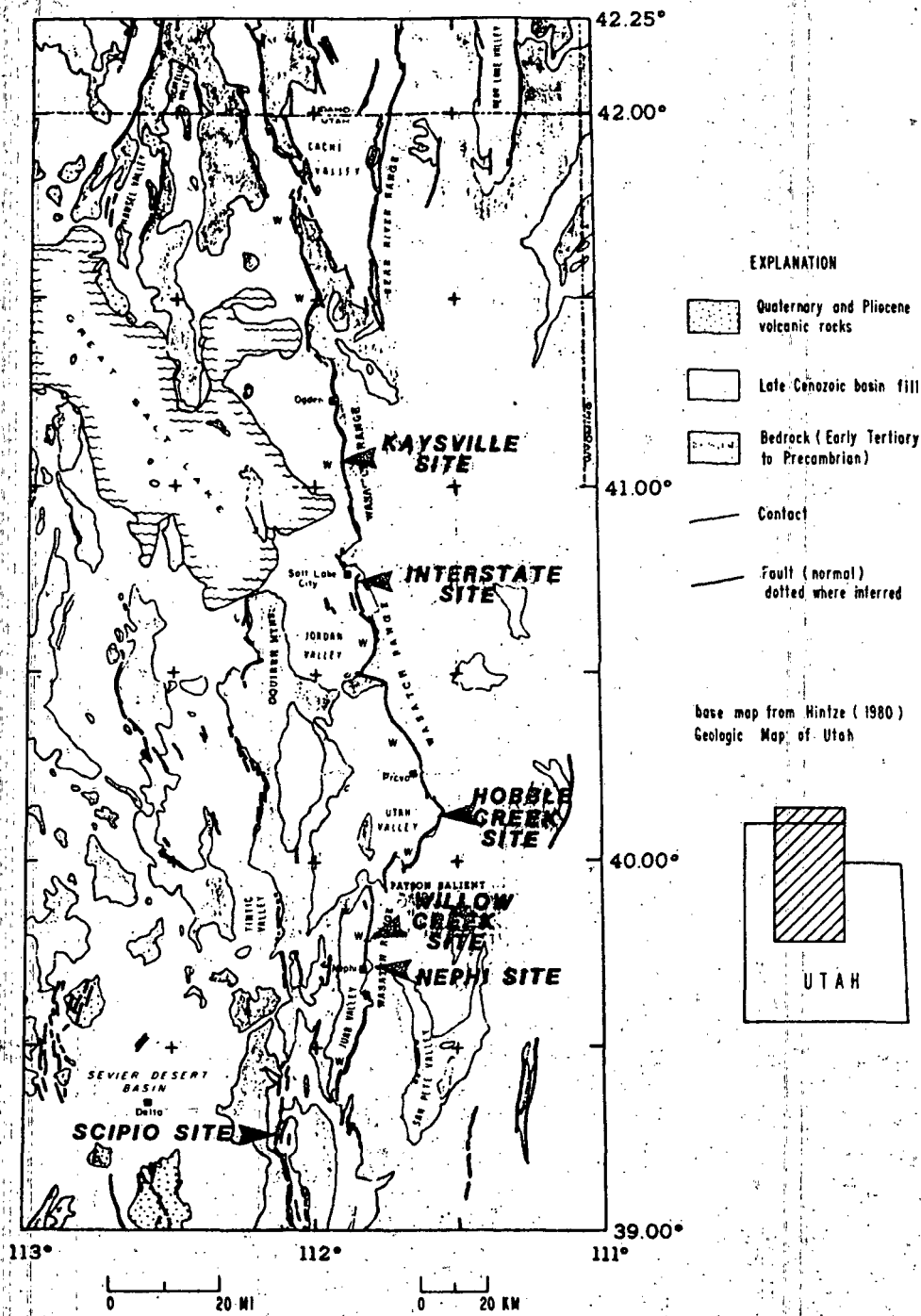


Figure 1.--Generalized geologic map of the Wasatch Front and environs, north-central Utah, and location of Mini-Sosie profile sites. Wasatch fault zone is indicated by "W." Modified from Zoback (1983b).

(CDP) sort, velocity analyses, normal moveout correction, datum and residual statics corrections, band pass filtering, final CDP stack, and wave migration. The resulting record sections consist of one-second, two-way travel time of 12-fold CDP data.

The MS technique has several distinct advantages over conventional reflection-profiling methods. Because of its small size, the system can be easily transported into remote areas with poor access. This advantage is particularly useful along some parts of the Wasatch Front where access is limited to steep, rugged roads and trails. The system is also capable of collecting reflection data in seismically noisy areas, a useful feature when working in urban areas. Where cultural noise is a problem, the number of impacts stacked for each VP can be increased until the reflection signal is strong enough to be distinguished from the undesirable noise. Another advantage of the MS is that it can operate in populated areas without the threat of vibration energy damaging nearby structures. Thus, the MS can fill gaps in conventional reflection data that are caused by cultural development.

REFLECTION PROFILES

To date, seven MS reflection profiles have been collected at six locations along the Wasatch Front (Fig. 1). All of the times cited in the following discussions are two-way travel times as shown on the figures. Depth estimates and displacements on faults were calculated from the stacking velocities used to process the profiles. Because of the uncertainties in the velocities, these values should be regarded only as general estimates.

Kaysville Site

Two parallel, east-west lines about 0.3 km apart, were run across the large fault scarps located approximately 3 km southeast of Kaysville (Fig. 2).

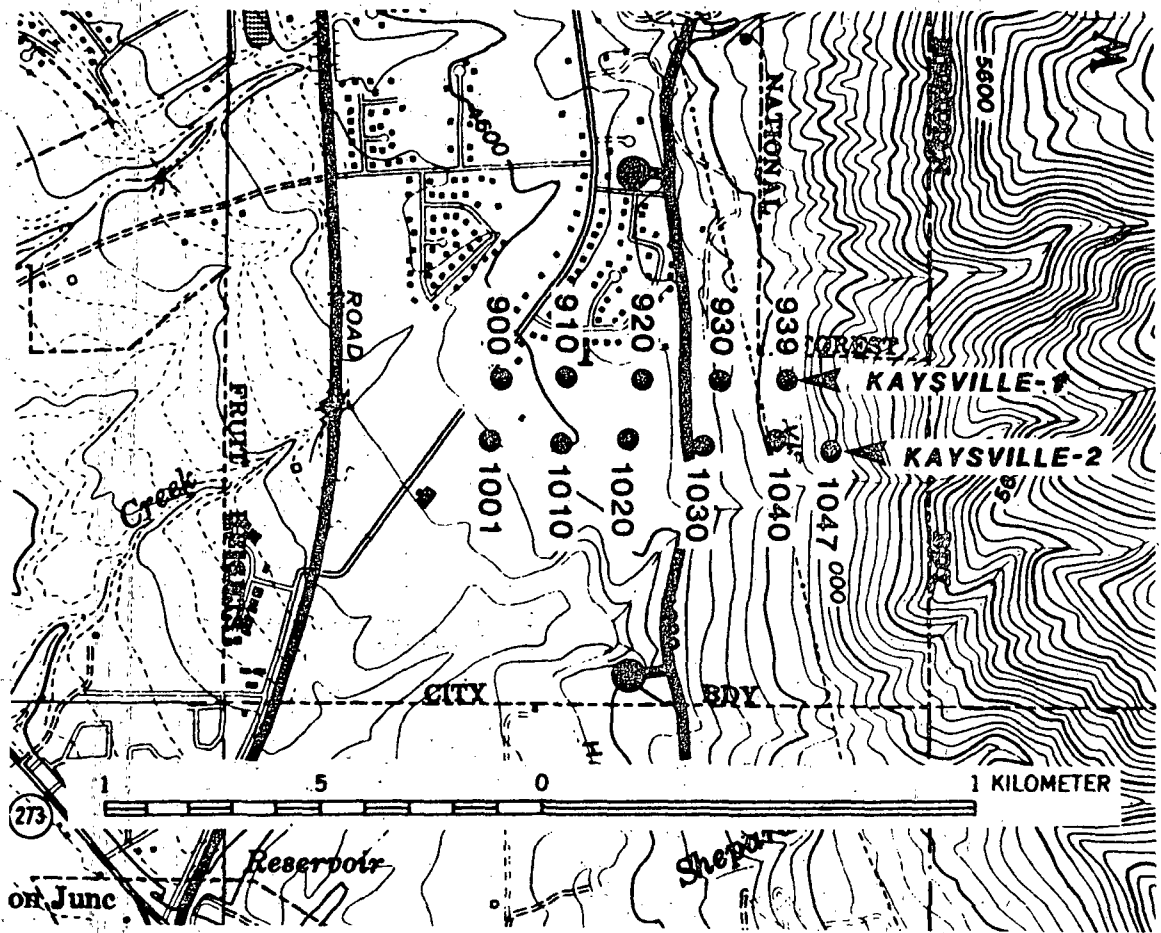


Figure 2. Vibration point (VP) map of Kaysville-1 and Kaysville-2 MS profiles plotted on the Kaysville 7.5-minute topographic quadrangle. Generalized location of main fault scarp from Cluff and others (1970) shown by heavy line; bar and ball on downthrown side. Antithetic fault west of main fault scarp not shown. Kaysville trench discussed by Swan and others (1980) was located at the scarp approximately midway between the two MS profiles. Distance between VPs is 16 m.

Here, an approximately 22-m-high, west-facing scarp marks the location of the most recently active major strand of the Wasatch fault; a 1 to 2.5-m-high antithetic fault scarp lies west of the main scarp.

Exploratory trenches and detailed mapping by Swan and others (1980) have documented several episodes of Late Pleistocene and Holocene surface faulting at this site. The stratigraphy in the trenches indicate at least three surface faulting events in the past 6,000 yrs producing a net vertical displacement of 10 to 11 m. Each event resulted in an estimated 1.7 to 3.7 m. of vertical displacement. Swan and others (1980) estimate a recurrence interval of about 1000 yrs for late Holocene for surface faulting.

The 0.75-km-long Kaysville-2 MS line (Fig. 2), located about 150 m south of trench A of Swan and others (1980), crosses the main fault scarp at VP 1029 and an antithetic scarp at VP 1023. Line Kaysville-1, 0.61 km long (Fig. 2), crosses the main scarp at VP 925 and an 1 to 2-m-high antithetic fault scarp at VP 919. At both lines, the graben formed by the two scarps is about 96 m wide (16 m/VP x 6 VP).

On Kaysville-2 (Fig.3), a strong, two-cycle (doublet) reflection between 0.1 and 0.2 s extends across much of the profile and shows the amount and distribution of near-surface faulting in this area. Beneath and east of the scarp, a continuous doublet reflection at about 0.095 s between VP 1027 and VP 1031 indicates that the fault associated with the scarp cannot be vertical. Just west of the main fault scarp a similar doublet reflection is at about 0.15 s. As will be discussed later, it is doubtful that these reflections originate from the same stratigraphic horizon. Nevertheless, the displacement between the two doublets (± 40 m) does identify the location of the main

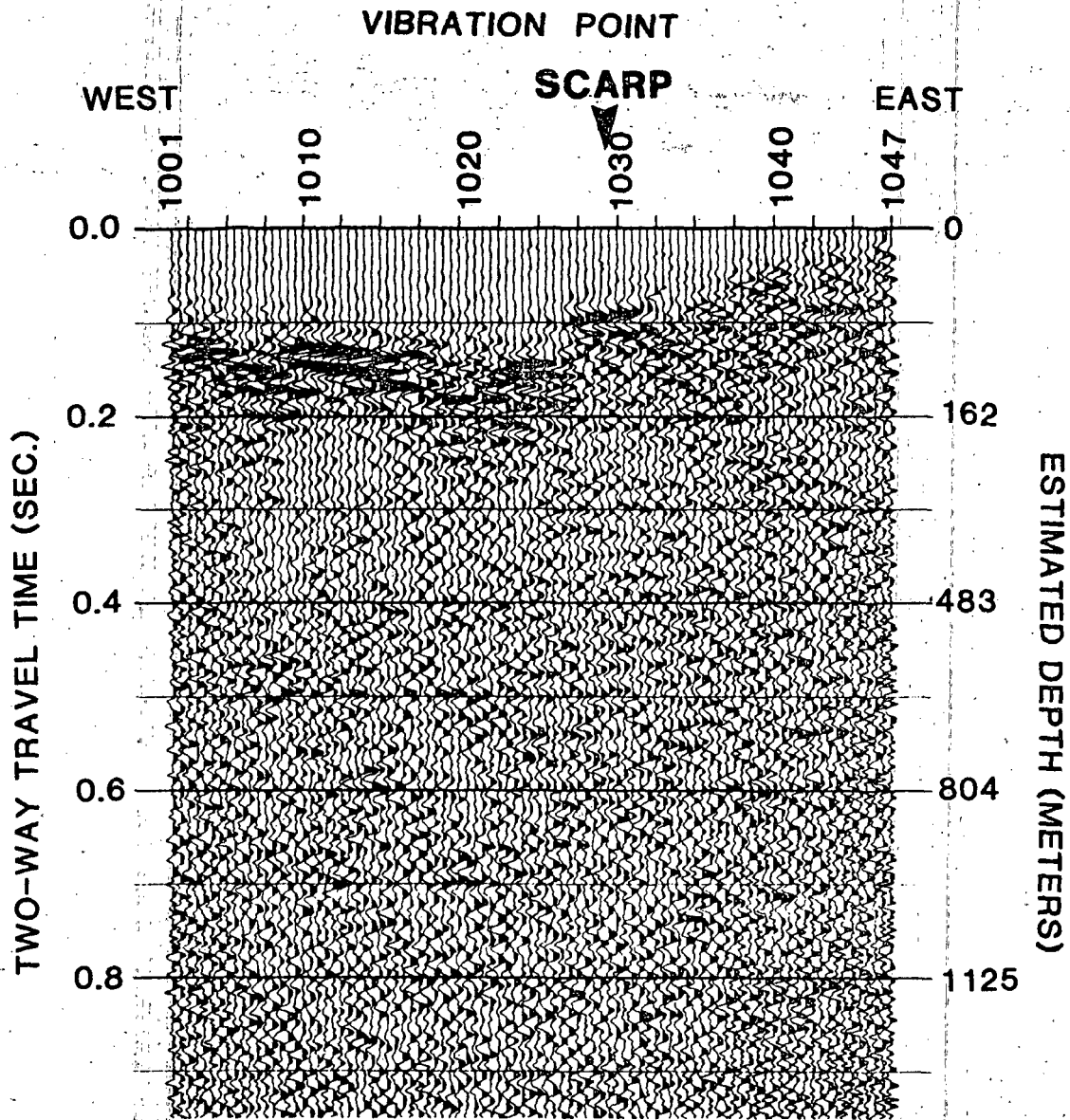


Figure 3. Kaysville-2 MS profile. Main scarp crosses the profile at vibration point (VP) 1029 and antithetic scarp (not shown) at VP 1023. Distance between VPs is 16 m.

fault. If the western termination of the shallow doublet at VP 1027 is projected upward to the scarp, the inferred near-surface dip of the fault is about 62° to a depth of 76 m.

The doublet west of VP 1027 is broken by a series of faults that form a broad graben. Down-to-the-west faults between VP 1023 and 1020 displace the doublet about 37 m to the low point of the graben. West from the low point, there are antithetic faults at VPs 1017 and 1014. The total displacement between the low point and the shallowest reflections west of the graben is about 72 m. The subsurface graben is about 250 m wide, approximately 2.5 times as wide as the graben on the surface.

Data from a water well, located about 0.6 km south of the west end of the Kaysville-2 line combined with criteria developed by Arnow and others (1970) in Salt Lake Valley to the south, suggests that the doublet reflection west of the main fault may mark the base of the unconsolidated Quaternary sediments on the MS line. In Salt Lake Valley, Arnow and others determined that the Quaternary-Tertiary contact (i.e. base of the Quaternary sediments) is marked by a distinctive carbonate cemented horizon, interpreted to be the remnants of the soil that formed on the Tertiary sediments prior to burial by Quaternary sediments. The well penetrated a sequence of unconsolidated sands, clays and gravels and, at of 88.7 m, it penetrated 3 m of cemented gravel in the bottom of the well. A reflector 88.7 m deep would generate a reflection at about 0.13 s, a travel time essentially the same as the doublet at the west end of the Kaysville-2 line.

There are no well data to identify the stratigraphic horizon responsible for the doublet at 0.1 s beneath and east of the fault scarp but it probably is generated by the contact between the bedrock and the overlying Quaternary and/or Tertiary sediments. If this doublet is correlated with the faulted

doublets west of the scarp then the net displacement across the entire fault zone on the profile is only about 5-10 m. However the trenches of Swan and others (1980) indicate a net Holocene displacement of 10 to 11 m. Also, the net displacement across scarps formed in late Pleistocene Lake Bonneville sediments is about 20 m. This implies that the doublet reflection east of the fault (VP 1027-1031) must correlate with a horizon that lies beneath the doublet west of the fault and that the net displacement indicated by the MS profile is a minimum value.

The reflections on line Kaysville-1 (Fig. 4) are generally poor but there is a strong doublet reflection at about 0.2 s between VP 917 and 909 (Fig. 4). To the east, there are few coherent reflections although at about 0.15 s at VP 925 there is some strong reflected energy and a suggestion of a weak doublet. Further east coherent reflections are absent. If the eastern termination of the doublet (0.21 s at VP 920), assumed to be the location of the fault at a depth of about 240 m, is projected up to the scarp, the fault has an apparent dip of about 72° .

West of the strong doublet near VP 907, there is also some strong but incoherent reflected energy. Although very speculative, if this energy and the doublet are correlative, they indicate a major down-to-the-east antithetic fault with about 35 m of vertical displacement. This antithetic fault would be the western boundary of a subsurface graben that is a minimum of 176 m wide, about 1.8 times wider than the surface graben.

The doublet reflection on Kaysville-1 has an apparent west dip whereas the reflections on Kaysville-2 are essentially horizontal or have an east dip. The stacking velocities for Kaysville-1 show that the apparent west dip results from a westward decrease in the velocities across the profile. Depth estimates show that the doublet actually has an estimated 10° to 15° east dip.

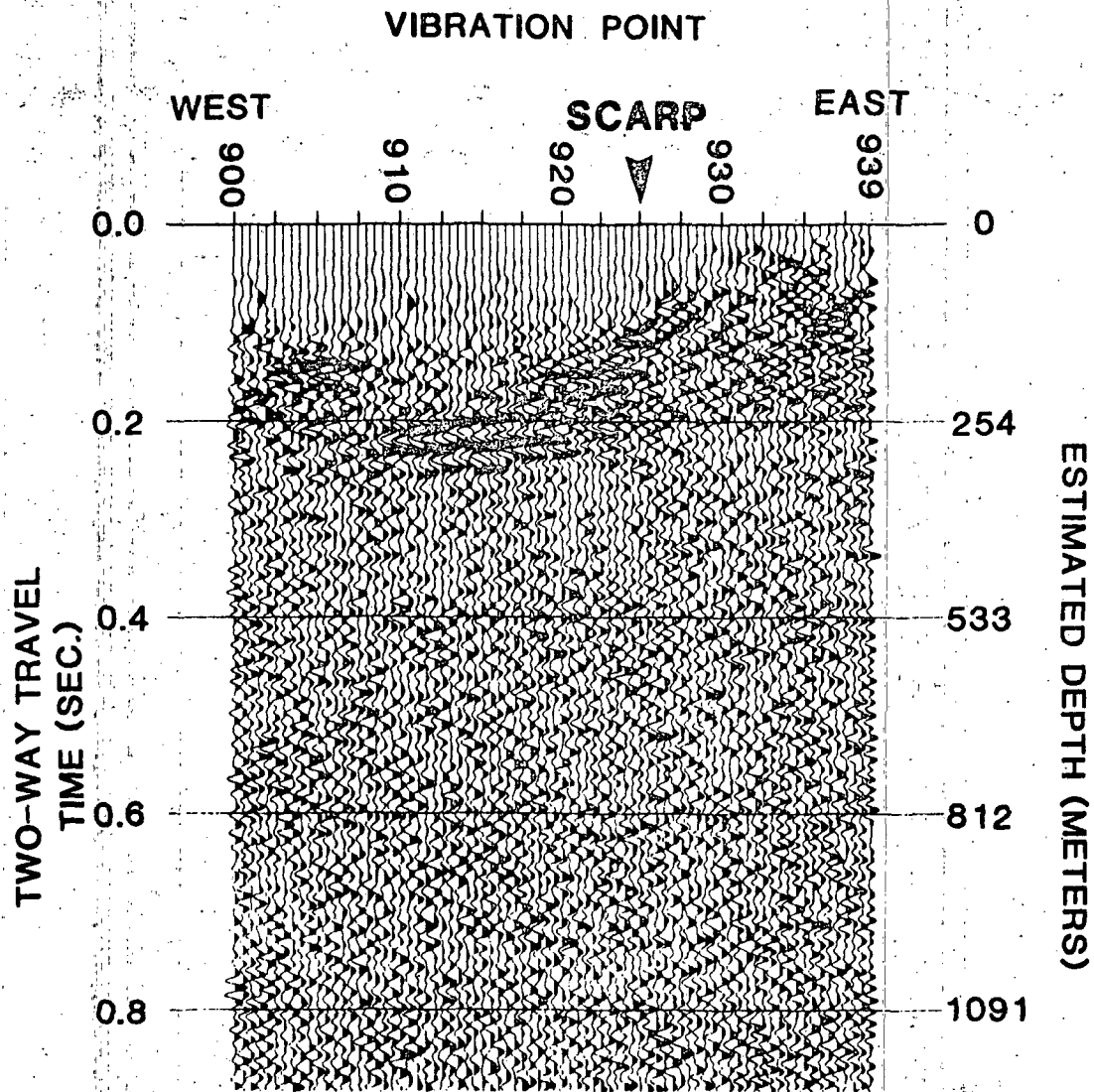


Figure 4. Kaysville-1 MS profile. Main scarp crosses the profile at vibration point (VP) 925 and antithetic scarp (not shown) at VP 919. Distance between VPs is 16 m.

The two-way travel times of the doublet reflections on Kaysville-1 and Kaysville-2 are noticeably different. Part of the difference may be real but much of it result from lateral velocity changes between the profiles and possibly variations in statics corrections.

There is a major difference in the number of faults on the two Kaysville profiles. The doublet reflection on Kaysville-1 is essentially unbroken across much of the inferred graben whereas numerous faults displace the doublets on Kaysville-2. This suggests that large variations in the number of individual faults can occur within short distances along the strike of the fault zone.

Interstate 80-Salt Lake City

Limited geologic information suggests that the East Bench fault scarp, a prominent topographic feature that extends through Salt Lake City and lies west of the main range front escarpment, may be the major structure separating the Jordan Valley graben from the Wasatch Range. East of the fault but west of the range front, a bedrock piedmont lies close to the surface, buried by a veneer of younger deposits (Marsell, 1969). West of the fault in the Valley, the bedrock is several thousand feet below the surface (Mattick, 1970). Locally the scarp is as much as 49 m high, and geologic studies show that some movement has probably occurred along the fault in the past 5,000 yrs (VanHorn, 1972). All of these data combined suggest that the East Bench fault may pose a significant earthquake hazard within Salt Lake City.

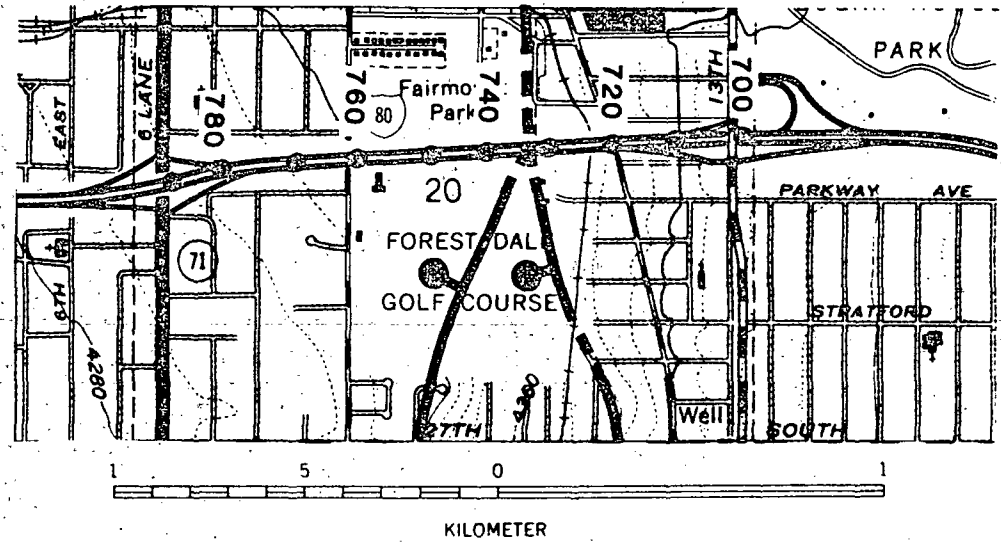
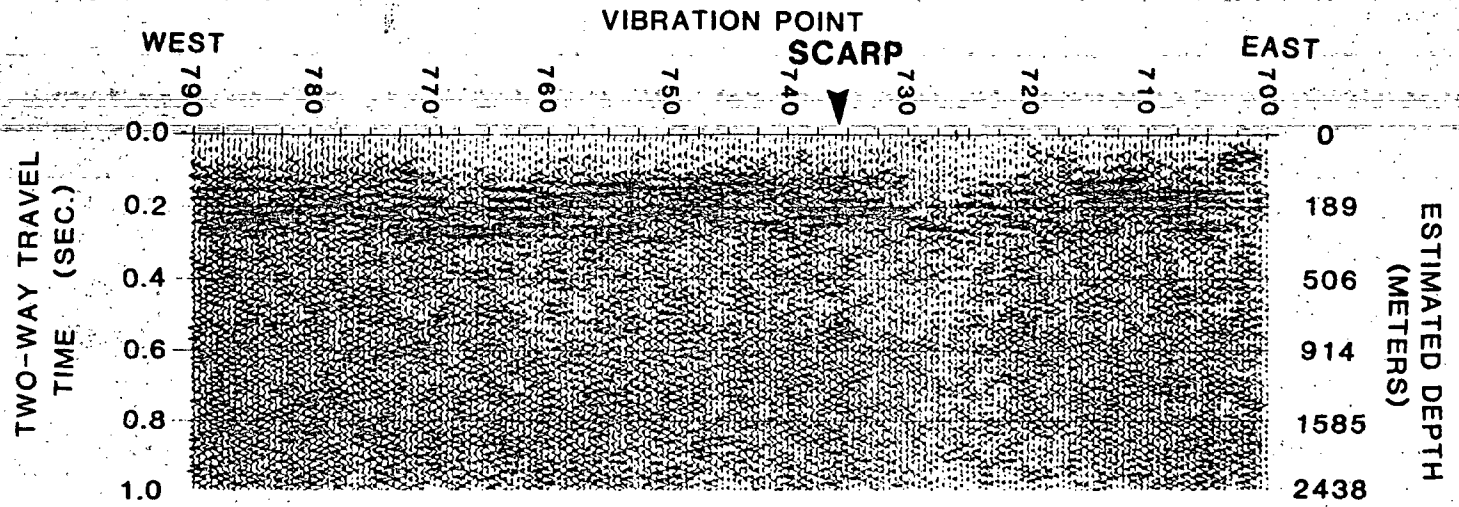


Figure 5. Interstate-80 MS profile and vibration point (VP) map. Fault scarp crosses the profile at about VP 736. Distance between VPs is 16 m. VP map is plotted on the Sugar House 7.5-minute topographic quadrangle. Fault scarps from VanHorn (1972) are shown as heavy line, dashed where concealed; bar and ball on downthrown side. Small solid dots are VPs in increments of ten.

A 1.44-km-long MS line was run across the East Bench fault along Interstate 80 between 1300 East and 700 East to clarify the relationship of the scarp to subjacent faults. Despite the extremely noisy conditions for recording seismic data, the record section shows a series of strong reflections between 0.1 and 0.3 s (Fig. 5).

At several places on the record section, lateral variations in the coherency of the reflections locally result in poor discontinuous reflections. The area of poor reflections between VP 716 and VP 730 is generally coincident with the 1200 East Overpass and is thought to be related to a decrease in fold near the overpass. Correlation of the strong reflections at about 0.2 s on either side of the poor data are not definitive but one reasonable correlation suggests no vertical displacement.

The East Bench fault scarp crosses the profile at about VP 736 (Fig. 5) and, westward from this point to about VP 760, the coherency noticeably decreases and the character of the reflections change. Within this less coherent zone, there is a suggestion of essentially horizontal reflections but individual reflections seem to be laterally discontinuous. The strong reflections to the east and to the west cannot be traced into the zone. There are no bridges, overpasses or other cultural features that might account for the reduced signal quality in this zone.

West of this poor signal quality zone is a series of coherent reflections at 0.1-0.3 s between VP 760 and VP 770. The strong, two-cycle reflection at 0.25 s in this area is similar to a reflection near VP 734. Correlating these two-cycle reflections across the low coherency zone suggests a vertical displacement of about 85 m. Construction has obliterated the scarp along the highway but, on the golf course directly to the south (Fig. 5), it is conspicuous and about 3-4.5 m high (Marsell, 1969).

The well data near the MS line helps identify some reflections on the profile. A water well 0.9 km east of the east end of the line drilled a sequence of interbedded gravels and clays without encountering bedrock (Iorns and others, 1966), but, from a depth of about 94 m to the bottom of the hole at 175 m, the driller's log reports that the gravels are cemented. These cemented gravels may be part of the Tertiary Salt Lake Group. The 94 m depth converts to about 0.12 s, a travel time similar to that of the first strong reflection on the eastern part of the profile. The series of strong reflections on this part of the profile may be generated within the upper part of the Salt Lake Group and the shallowest reflection may correlate with the base of the Quaternary sediments. If identification of the reflections and the correlations are correct then the MS profile indicates about 85 m of vertical slip on the East Bench fault during the Quaternary.

Estimates of long-term slip rates on the East Bench fault are very poorly constrained because the age of the base of the Quaternary sediments in the Salt Lake City area is not well known. Quaternary sediments in the area are a minimum of 600,000 yrs old (Scott and others, 1982, p. 24). The age of the upper part of the Salt Lake Group is generally considered to be Pliocene. McDonald (1976, p. 306) reports that a well north of Salt Lake City (T. 3N., R. 1W.) is believed to have drilled into upper Pliocene sedimentary rocks. On

the basis of this information, we will use a maximum age of about 2 million yrs for purposes of this discussion. The long-term slip rates calculated using these ages are a maximum of 0.14 m/ka and a minimum of 0.04 m/ka. These estimated rates are much smaller than the Holocene slip rates (Swan and others, 1980; Schwartz and Coppersmith, in press) but similar to the pre-Bonneville rates of Machette (this volume).

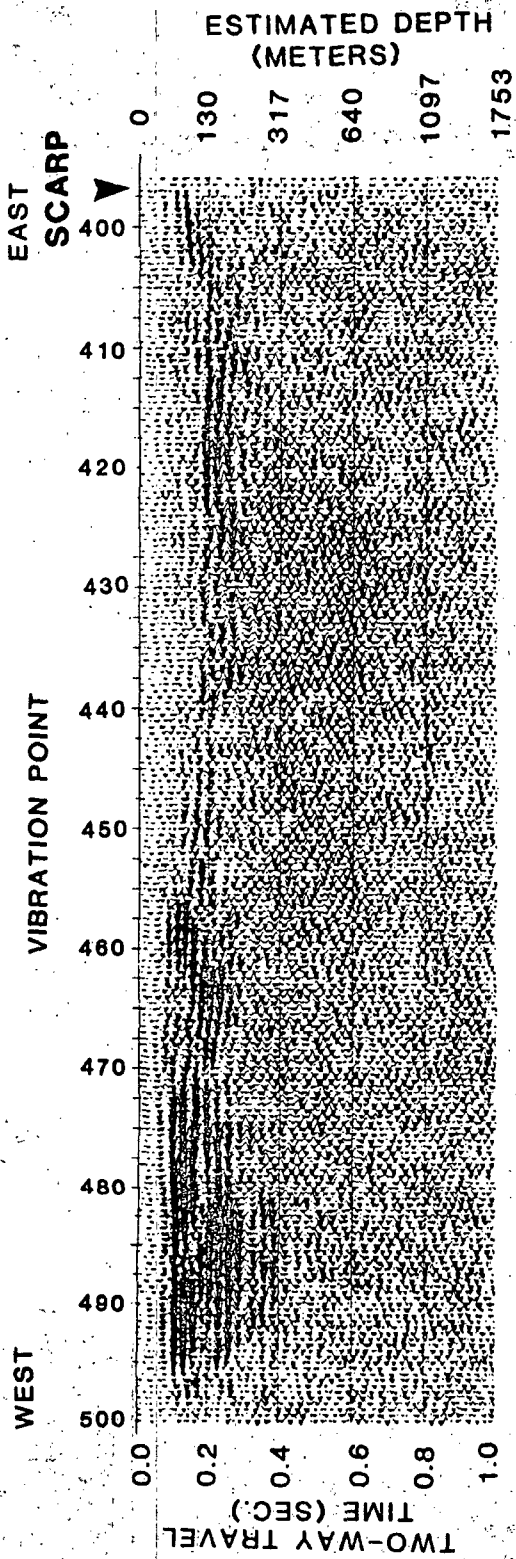
A water well located less than 0.5 km north of VP 755 penetrated 147 m of interbedded Quaternary gravels and clays (Marine and Price, 1963). This depth converts to a travel time of approximately 0.2 s, shallower than any strong reflections on nearby parts of the MS line.

Hbble Creek Site

The Hbble Creek MS site, located about 12 km southeast of Provo, Utah (Fig. 1), examines the relationship between near-surface structure and faulting, and a deformed late Quaternary (Provo lake level) terrace that has been backrotated by movement on the Wasatch fault. A topographic profile parallel to but about 250 m to the north of the MS line shows that the originally west-sloping Provo terrace now slopes to the east for a distance of 385 m from the fault (Profile L-L'; Swan and others, 1980).

Detailed mapping and trench studies near the Hbble Creek site by Swan and others (1980) indicate six or seven surface faulting events in the past 12,000 to 13,000 yrs resulting in a net vertical displacement of 11.5 to 13.5 m. Less precise data suggest movement on the Wasatch fault has vertically displaced Lake Bonneville sediments 18.5 to 38.5 m.

The Hbble Creek MS line is 1.66 km long and crosses the west-facing main fault scarp at the extreme east end (VP 397, Fig. 6). A two- to three-cycle reflection occurs at about 0.14 s (150 m) below VP 397 and continues unbroken



EAST SCARP

VIBRATION POINT

WEST

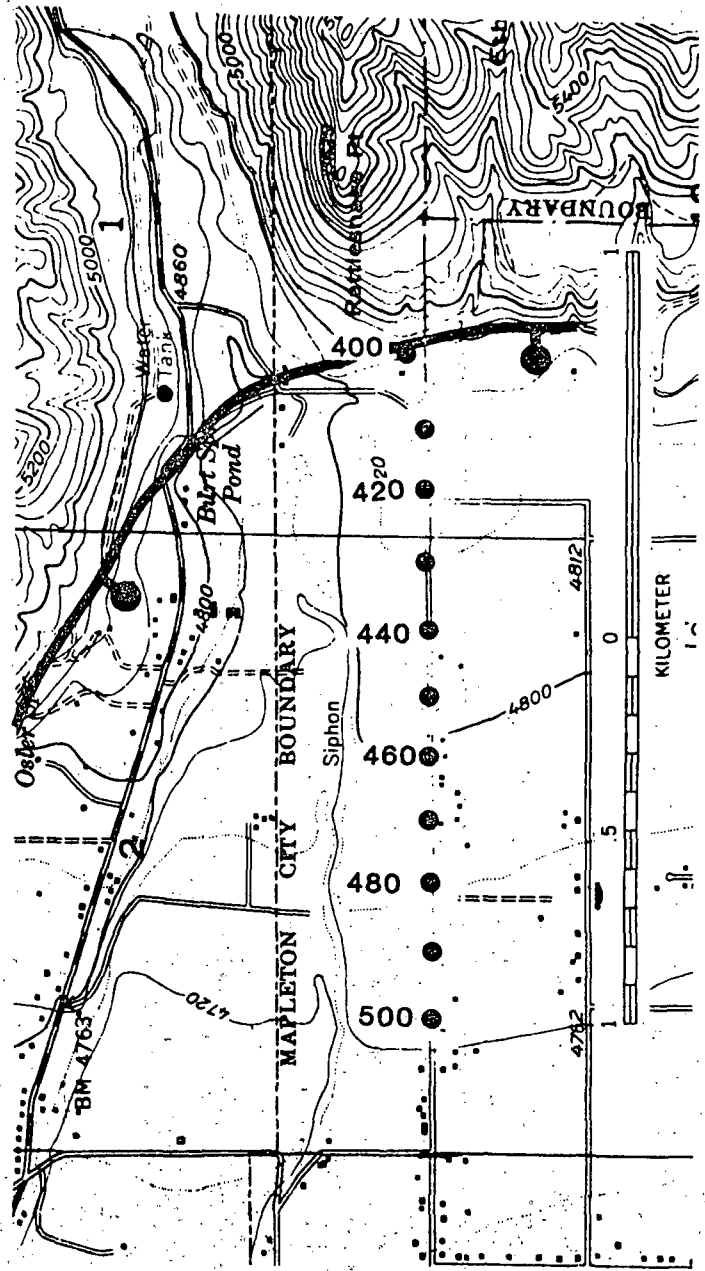


Figure 6. Hubble Creek MS profile and vibration point (VP) map. Fault scarp crosses the profile at the east end at VP 397. Distance between VPs is 16 m. VP map is plotted on the Springville 7.5-minute topographic quadrangle. Fault scarp generalized from Cluff and others (1973) is heavy line; bar and ball on downthrown side. Small dots are VPs in increments of ten.

with a gentle west dip for nearly 100 m to VP 403. West of VP 403, the reflections appear to be downdropped, however calculations indicate that the reflections to the east and to the west of VP 403 are at similar depths; differences in stacking velocities are probably responsible for the apparent vertical displacement. However the difference in stacking velocities for the reflections east and west of VP 403 suggest that there may be an important structural boundary in this area. There are insufficient velocity analyses to determine if the west dip of these reflections is apparent or real.

The reflections between VPs 397 and 403 constrain the near-surface geometry of the main strand of the fault. If the fault lies east of the reflections, it is nearly vertical; if it lies west of the reflections, it has a shallower dip. Although inconclusive, the MS data favor a nearly vertical fault interpretation. The similar depths of the reflections east and west of VP 403 argues against extending the main strand of the fault west of the reflections, especially considering the large amount of post-Bonneville displacement.

The MS profile shows that warping of the Provo terrace is not simply a surface phenomena but occurs in the shallow subsurface. Westward from VP 403, a weak multi-cycle reflection is distinguishable to VP 410 where it becomes continuous and coherent to VP 423. This reflection has a distinct eastward

dip and an inflection point that coincides with the inflection point of the overlying warped terrace. This backrotation is similar to the "reverse drag" believed to be associated with listric normal faults (Hamblin, 1965), but the small size of the backrotated block (i.e. distance between the inflection point and the end of the east-dipping reflections) suggests that a listric fault responsible for this backrotation would probably flatten at shallow boundary of this backrotated block would be the main strand of the range-bounding fault.

An inflection point in the reflections at VP 474 suggests that a large backrotated block may extend across much of the profile. From VP 474, east to VP 403, all of the reflections have a gentle but obvious eastward dip. The east-dipping reflections are broken by several faults between VPs 452 and 472, none with any obvious surface expression. Some of the faults have as much as 50-55 m of vertical displacement, but the net displacement across all of them is small. A listric fault responsible for this broad area of backrotation would extend to greater depths and perhaps be tectonically more significant than a listric fault associated with the inflection point of the warped Prove terrace.

A series of strong, unbroken, flat reflections extend westward from the inflection point at VP 474 to the end of the profile. The general continuity of these reflections indicates little near-surface faulting along this part of the MS line.

Well control in the vicinity of the Hubble Creek profile is sparse. A drillers log of a 93-m-deep well located less than 200 m north of VP 420 shows prominent lithology changes at depths of 29 m and 73 m but these are shallower than all of the distinct reflections on the MS line. About 2.2 km south of VP 465, a 205-m-deep well (Cordova, 1969) drilled through a sequence of clays,

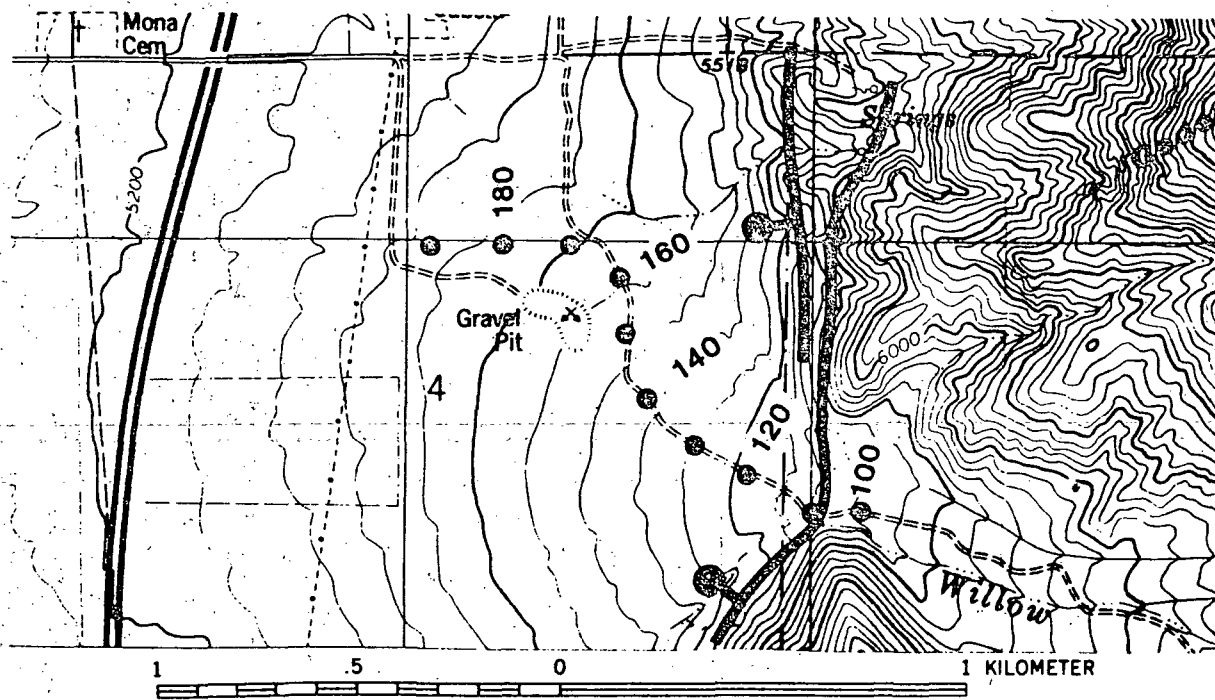
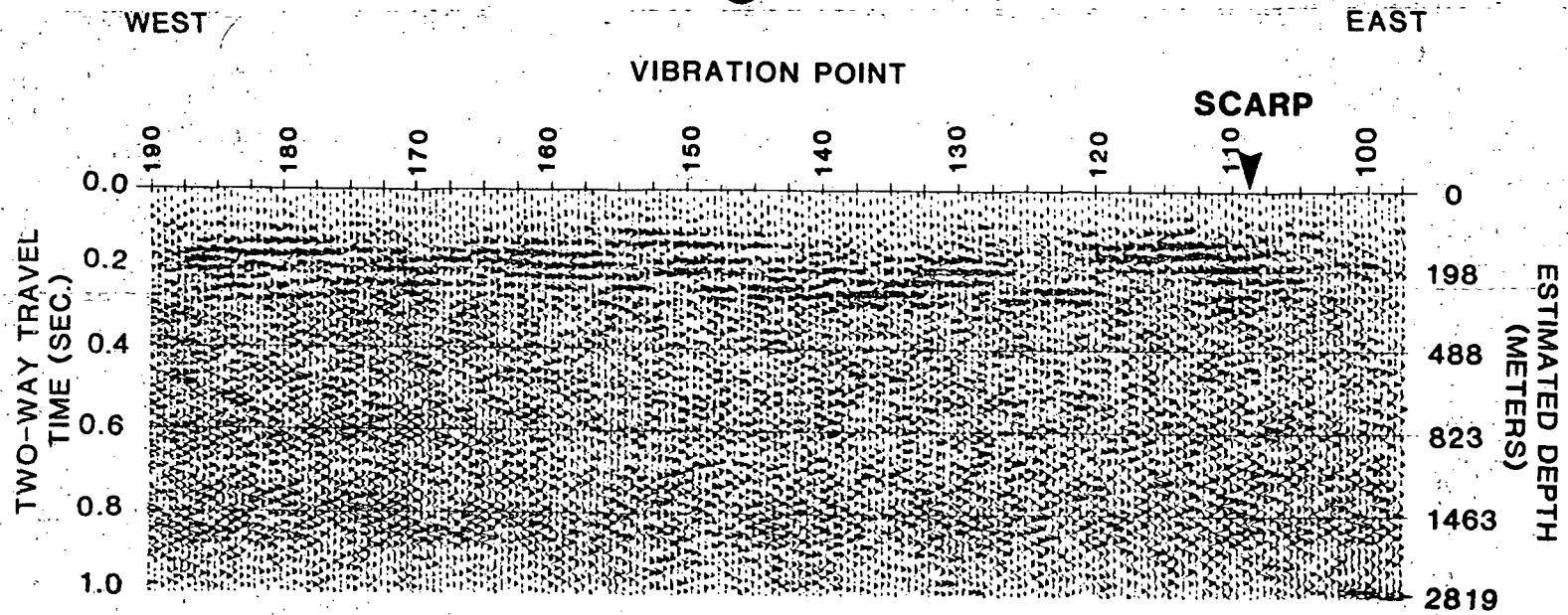
gravel and sand that are probably Quaternary in age. The 205 m depth converts to about 270 ms travel time on the MS profile suggesting that all of the reflections on the profile are from Quaternary sediments. The lack of specific age information precludes estimates of long-term slip rates.

Willow Creek Site

There is more than 2.1 km of topographic relief between the crest of the Wasatch Range and the floor of Juab Valley (Fig 1) near the town of Mona. Displacement on the Wasatch fault zone has probably produced much of the relief although preexisting topography may have contributed to the total (Eardley, 1933). Trenching studies and the morphology of the youthful fault scarp along this part of the range suggest that the last major displacement may have been only 300 to 500 yrs ago (Schwartz and Coppersmith, in press).

To investigate the near-surface structure associated with this young fault scarp, we collected MS data along a 1.47-km-long line extending generally westward near Willow Creek Canyon, about 2.7 km southeast of Mona (Fig. 7). At the mouth of the canyon at VP 109 the profile crosses an approximately 6-m-high scarp (Machette, this volume). In the canyon east of the scarp, Pennsylvanian-Permian Oquirrh Formation (Hintze, 1980) is covered by a veneer of stream alluvium. In Juab Valley west of the fault, locally as much as 610 m of basin-fill overlies the downfaulted bedrock (Eardley, 1933).

The part of the profile in the canyon has few coherent reflections but west of the scarp, there are a series of reflections between 0.1 and 0.2 s (85-213 m) from within the basin-fill. From the scarp to westward VP 140, correlation of the reflections shows a gentle westward dip of about 2.5° toward the valley. This is interpreted as a primary depositional dip.



20

Figure 7. Willow Creek MS profile and vibration point (VP) map. Fault scarp crosses the profile at the mouth of Willow Creek Canyon at VP 109.

Distance between VPs is 16 m. The VP map is plotted in the Mona 7.5-minute topographic quadrangle. Fault scarps generalized from Cluff and others (1973) are heavy lines; bar and ball on downthrown side. Small dots are VPs in increments of ten.

The quality of the reflections from the basin-fill clearly deteriorates at two locations west of the scarp, a zone between VP 120 and 126, and near VP 140. The zone of poor reflections between VP 120-126 is perplexing. Good quality reflections to the east and west at 0.15-0.2 s abruptly disappear and, within the zone, a distinct doublet is present at about 0.25 s. The continuity of the doublet shows that there are no large faults within the zone but does not eliminate faults at either edge. Correlation of reflections across the zone suggest little net displacement. Near VP 140 the character of the reflections gradually changes westward, making it difficult to confidently correlate reflections to the east with those to the west. Along the western part of the line, changes in wave amplitude and frequency suggest that facies changes may occur within the basin-fill. The poor correlations caused by the discontinuous reflections makes it difficult to recognize possible small faults, but there is sufficient continuity across most of the profile to demonstrate the absence of any major near-surface faults other than the fault associated with the scarp.

Nephi Site

Near the town of Nephi (Fig.1), a major change occurs in the range-front physiography and in the distribution of Holocene scarps. North of town, the range crest towers over Juab Valley, and multiple surface faulting events have

produced large Holocene scarps. South of Nephi, the relief between the range crest and valley is much less and there is a 17-km-long gap in Holocene scarps. Where present south of the gap, the scarps are small, single-event scarps (Schwartz and Coppersmith, in press). These changes suggest that Nephi is located near a segment boundary of the Wasatch fault zone and that the long-term behavior of the two segments is very different (Schwartz and Coppersmith, in press).

The deep structure at this important boundary has been studied by Zoback (1983a; 1983b) using conventional seismic reflection and gravity data, but these data do not clearly reveal the location or distribution of near-surface faults. Specifically, the conventional reflection profile has no data in the upper 0.2 s and a large "drop-out" of "deep" data in Nephi. To fill this critical gap, we collected 3.97 km of MS data along the route of the conventional reflection line from east of the Wasatch fault in Salt Creek Canyon to beyond the west edge of town (Fig. 8).

An additional objective of the Nephi MS line was to identify the locations of potential surface faulting in town during future earthquakes. The scarps to the north die out before they reach Nephi (Fig 8), thus the surface faulting hazard is uncertain.

The general attitude of the reflections on the MS profile (Fig. 9) and the stacking velocities both suggest that there is a boundary between the bedrock in the range and basin-fill at about VP 340. From the east end of the line in Salt Creek Canyon where bedrock is exposed, to about VP 340 (Fig. 8), the reflections at 0.1-0.2 s are locally faulted but have a uniform westward dip, and stack at velocities of 1981-3048 m/s. From VP 340 to the west end of the line, all of the reflections at about 0.2 s are subhorizontal or have a slight eastward dip and stack at velocities between 1372-1676 m/s. The

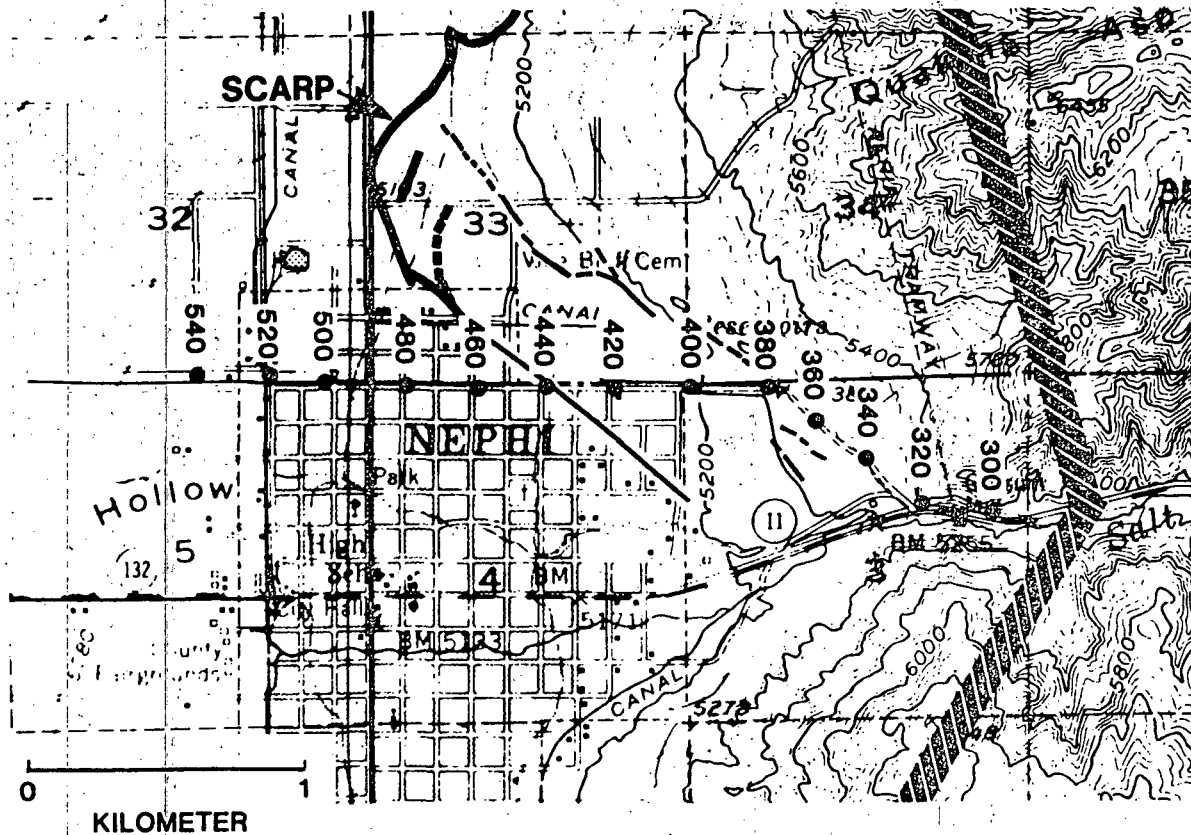


Figure 8. Nephi MS-profile vibration point (VP) map. Map is modified from sheet 10 of Cluff and others (1973). Fault scarps are heavy lines, dashed where approximate. Fine lines are possible surface faults with little or no vertical relief; dashed where approximate. Distance between VPs is 16 m. Small dots are VPs in increments of ten.

relatively high stacking velocities east of VP 340 indicate that these reflections are probably associated with the lithified Mesozoic and early Tertiary sedimentary bedrock, and the lower velocities to the west suggest that the reflections are associated with basin-fill sediments. The record section falsely implies that the reflections east and west of VP 340 are

vertically displaced; both sets of reflections have estimated depths of about 122 m.

The bedrock and basin-fill boundary at VP 340 most likely coincides with the location of a buried fault. A broad zone of incoherent noise and weak reflections between VP 340 and 380 on the MS profile supports this interpretation. The noisy zone with poor reflections starts at the boundary (VP 340) and continues to VP 380 where the reflections become strong and distinct. The part of the profile with the poor reflections trends northwestward, subparallel to the local trend of the range and essentially parallel to the expected strike of a fault. The good quality reflections occur where the line turns westward, away from the range and away from the fault (Fig. 8). The zone of weak reflections and noise is probably related to disruption and "out-of-plane" reflections from the fault zone. The similar estimated depths for the reflections on either side of VP 340 suggest that there has been little recent vertical displacement on this fault.

The fault interpretation for this boundary is also supported by the possible fault-related lineaments (Fig. 8) parallel to and adjacent to the northwest-trending part of the MS line (Cluff and others, 1973). A questionable small fault on the MS profile at VP 383 may also be related to these lineaments. A lineament that crosses the MS line at VP 440 does not appear to be fault related.

Correlations of the strong, continuous, two- to three-cycle reflection at about 0.2 s across the central 1.66 km of the MS profile (Fig. 9) indicate probable faults at VPs 468, 473, and 478. The faults at VPs 468 and 473 define a narrow graben; the vertical displacement of about 46 m on the down-to-the-west fault at VP 468 and 35 m on the antithetic fault at VP 473 yields a net displacement of about 11 m across the graben. A small down-to-the-west

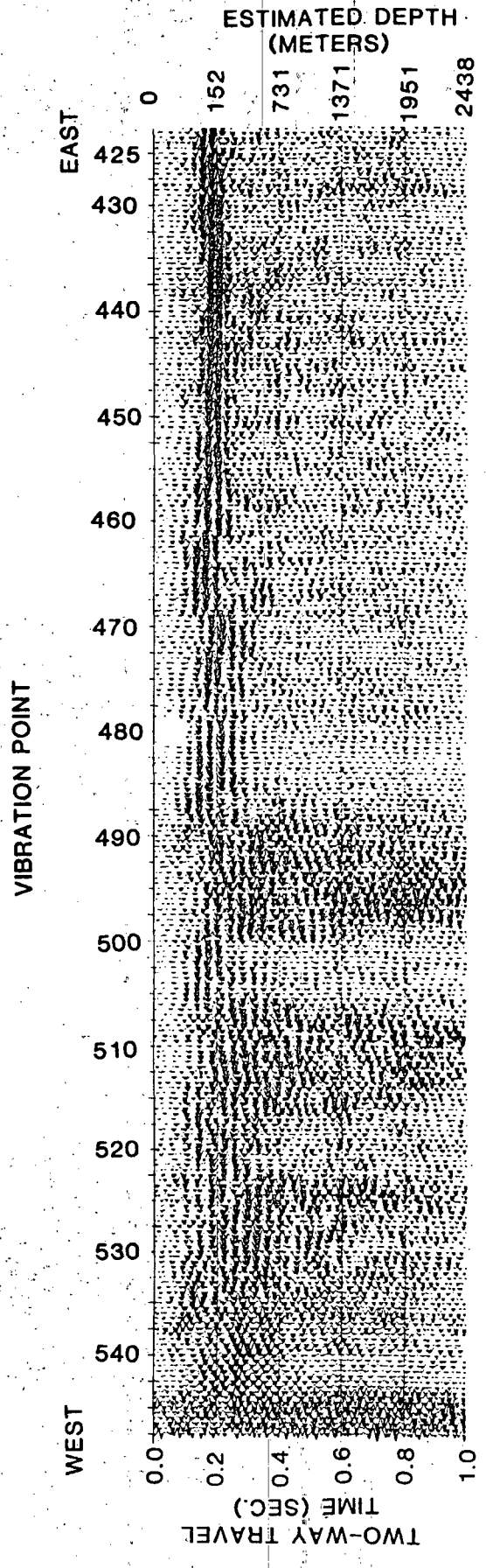
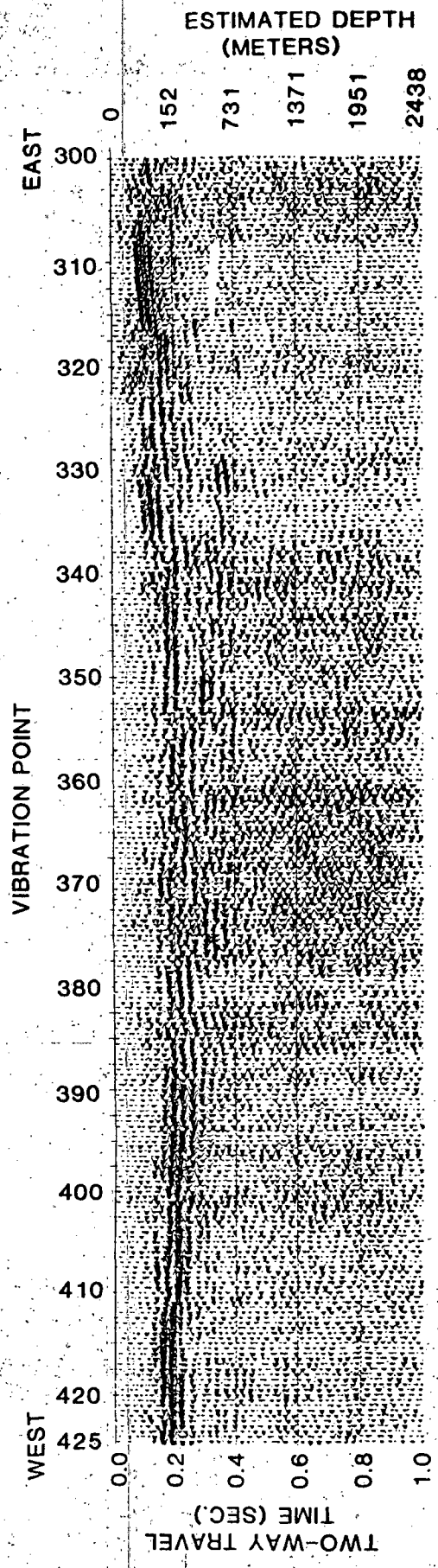


Figure 9. Nephi MS profile. Profile is broken into two segments that overlap between VPs 423-425. Distance between VPs is 16 m. See text for discussion of the profile.

fault at VP 478 has about 9 m of displacement.

From these faults to the west end of the line, the quality of the reflections varies; in the areas of good data, subhorizontal reflections are visible down to about 0.4 s. The subhorizontal reflections at about 0.3 s on the MS line probably correspond to a strong reflection at a similar travel time on the conventional reflection profile. Some areas of poor MS data are probably related to junctions with major roads and bends in the line.

Gravity data combined with the MS and the conventional reflection data show that the major fault zone separating the basin in Juab Valley from the Wasatch Range is probably located near VPs 468-478, not near the fault at VP 340. A two-dimensional model of the gravity data shows Juab Valley contains a maximum of 1.2 km of basin-fill just west of Nephi (Zoback, 1983b). Stacking velocities for the conventional reflection profile show that bedrock is not deeply buried on the downthrown side of the fault at VP 340. This requires the presence of another fault zone west of VP 340 that is the major boundary of the east side of the basin. The near-surface faults between VPs 468-478 probably identify the location of this eastern boundary. The MS stacking velocities show that the near-surface faults are formed in the basin-fill, but they occur where the conventional reflection profile constrains the location of the eastern margin of the basin (M. L. Zoback, 1984, oral commun.). Movement on the near-surface faults is probably controlled by movement on the subjacent basin-margin faults. The configuration of this part of Juab Valley indicated from all of these data is a bedrock bench, buried by a comparatively

thin cover of basin-fill, that extends westward from near the range front (VP 340) to the eastern basin-margin fault zone located near VPs 468-478. The east edge of the bedrock bench is probably bounded by a fault that has little recent vertical movement.

The near-surface faults at VP 468-478 are generally on strike with but about 0.3 km south of the prominent scarps mapped by Cluff and others (1973). They displace reflections as shallow as approximately 150 m. Based on the MS data, it seems likely that the faults associated with the scarps to the north extend southward into Nephi. Although the most recent movement on this part of the Wasatch fault zone apparently did not produce surface faulting within Nephi, our interpretation indicates that the near-surface faults in Nephi are probably continuous with the faults that have recently formed scarps to the north and are associated with deeper faults that have a long history of movement. Thus, during future earthquakes, displacement on the near-surface faults might produce surface ruptures in town.

Scipio Valley Profile

Scipio Valley is located about 55 km south-southwest of Nephi (Fig. 1) and lies within the transition zone between the Colorado Plateau and the Great Basin. There are numerous scarps in the Valley, some with associated well-defined grabens. A prominent scarp near the northern end of the Valley shows evidence of Holocene movement superimposed on a pre-Holocene scarp (Bucknam and Anderson, 1979).

The 0.75-km-long Scipio Valley profile (Fig 10) shows that an approximately 5-m-high scarp represents a young displacement on a subjacent fault zone. The fault most directly related to the scarp has an average dip of $\pm 69^{\circ}$ E. Segments of coherent reflections only occur in the upper 0.5 s

providing no data on the fault geometry below about 400 m. The variable quality of the reflections makes correlations across the interpreted faults tenuous. Reflections C, east of the fault zone, do not have any correlative reflections to the west but if the correlation of reflections D is correct, one strand of the fault has a vertical displacement of about 68 m. This suggests multiple episodes of movement.

In Scipio Valley, the North Horn Formation and Flagstaff Limestone of Late Cretaceous and early Tertiary age, underlie the alluvium, and locally, sinkholes and collapse features form where accelerated groundwater dissolution occurs in faulted and fractured carbonate bedrock (Bjorkland and Robinson, 1968). It seems unlikely that this process would produce recurrent movement on the long, high scarps described by Bucknam and Anderson (1979) or produce the differential movement on a moderately dipping fault as interpreted on the MS profile. Scarps in Japanese Valley, about 12 km to the east, have been attributed to salt diapirism (Witkind, 1982), but lack of deep data does not permit this possible mechanism to be evaluated at the Scipio site.

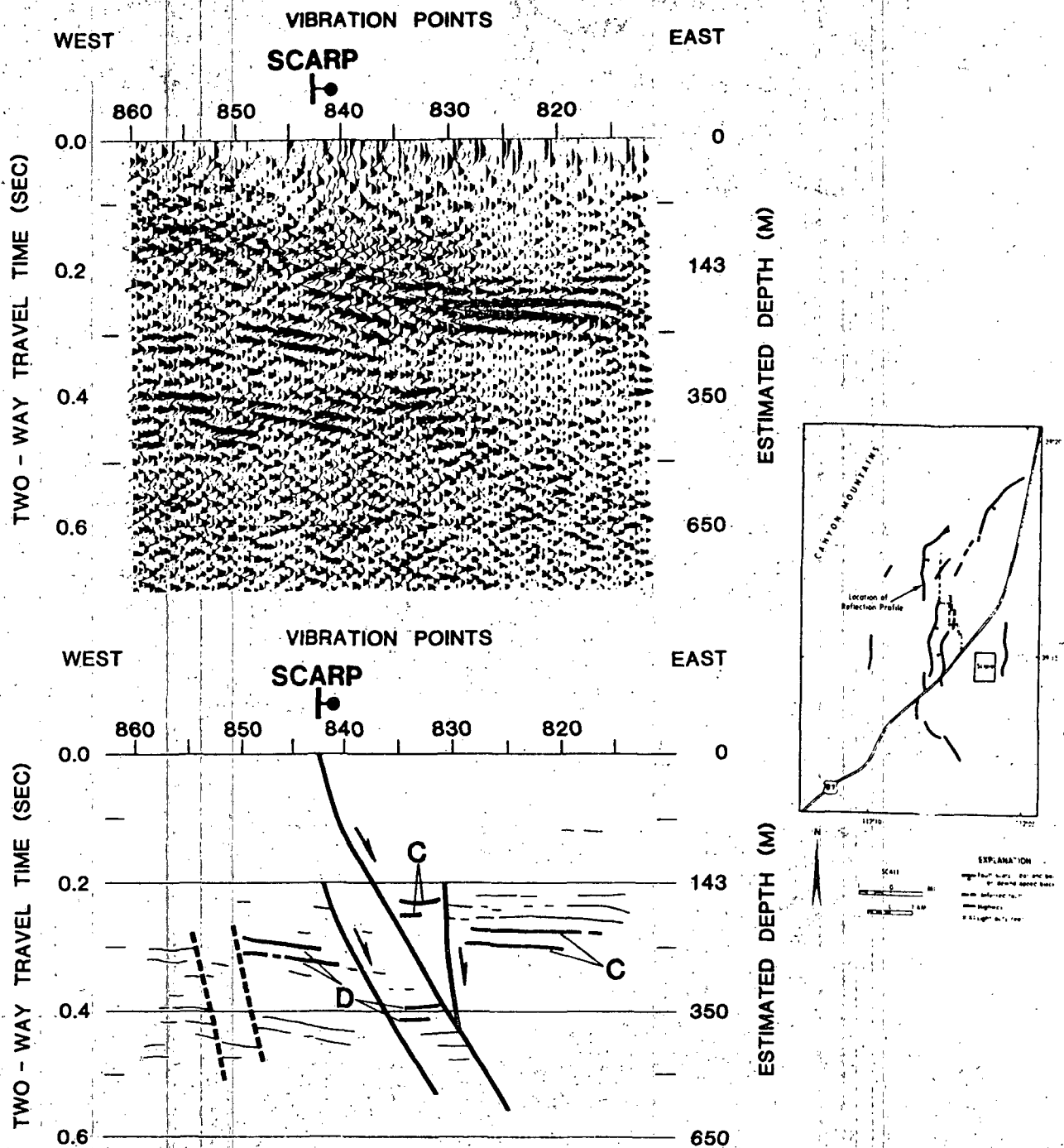


Figure 10. Scipio Valley MS profile, line drawing, and generalized location map. Fault scarp crosses the profile at vibration point 843. Reflections C and D are discussed in the text.

PRELIMINARY CONCLUSIONS

The MS system is an effective means of examining the near-surface structure and faulting associated with Holocene fault scarps along the Wasatch Front. Future studies will examine the near-surface structure at proposed segment boundaries such as at the salient north of Salt Lake City, and investigate the potential for surface faulting in urban areas from movement on intra-basin faults. To date, important observations on the profiles include:

1) The main fault scarps overlie either vertically displaced reflections, zones of incoherent noise, or zones of weak reflections. The MS profiles show that many inferred faults or fault zones, some with substantial vertical displacements, are not associated scarps.

2) The zone of faulting and deformation in the shallow subsurface is commonly more extensive than expressed at the surface by young fault scarps. Defining the areas of potential surface faulting on the basis of Holocene scarps may underestimate the surface faulting hazard.

3) The two adjacent profiles at Kaysville show that large variations in the number of individual faults can occur within a short distance along the strike of the fault zone.

4) The East Bench fault at Interstate-80 in Salt Lake City may have as much as 85 m of vertical displacement during the Quaternary. Although very poorly constrained, the available data indicate that the Quaternary slip rate for the fault is considerably slower than the Holocene slip rates estimated from trenching studies of other parts of the Wasatch fault zone.

5) At Hobbie Creek a broad area of backrotation in the shallow subsurface extends west of the scarp for more than a kilometer. A more local area of backrotation coincides with the warped Provo terrace described by Swan and others (1980). The backrotation may be evidence of listric faults in the area.

6) At Nephi, the combination of gravity data, the MS line, and conventional reflection data suggest that the major basin-margin fault zone is not located at the range front but, to the west, within the town. Movement on near-surface faults associated with the fault zone may produce surface faulting in the town during future earthquakes.

ACKNOWLEDGEMENTS

The data at the Kaysville site were collected with the support and assistance of D. P. Schwartz, F. H. Swan, III, and K. L. Hanson of Woodward-Clyde Consultants, San Francisco, California. K. A. Monger compiled much of the well data. Numerous helpful comments on the manuscript by R. E. Anderson are appreciated.

REFERENCES CITED

- Arnow, Ted, VanHorn, Richard, and LaPray, Reed, 1970, The pre-Quaternary surface in Jordan Valley, Utah: U.S. Geological Survey Professional Paper 700-D, p. D257-D261.
- Bjorkland, L. J. and Robinson, G. B. Jr., 1968, Ground-water resources of the Sevier River basin between Yuba Dam and Leamington Canyon, Utah: U. S. Geological Survey Water-Supply Paper 1848, 79 p.
- Bucknam, R. C., Algermissen, S. T., and Anderson, R. E., 1980, Patterns of late Quaternary faulting in western Utah and an application in earthquake hazard evaluation: in Proceedings of Conference X, Earthquake Hazards along the Wasatch and Sierra Nevada Frontal Fault Zones, U.S. Geological Survey Open-File Report 80-801, p. 299-314.
- Bucknam, R. C., and Anderson, R. E., 1979, Map of fault scarps in unconsolidated sediments, Delta 1⁰x 2⁰ quadrangle, Utah: U.S. Geological Survey Open-File Report 79-366, 21 p., 1 pl.
- Cluff, L. S., Brogan, G. E., and Glass, C. E., 1970, Wasatch fault, northern portion; Earthquake fault investigation and evaluation: unpublished report prepared for Utah Geological and Mineralogical Survey by Woodward-Clyde and Associates, Oakland California, 27p.

- _____, 1973, Wasatch fault, southern portion; Earthquake fault investigation and evaluation: unpublished report prepared for Utah Geological and Mineralogical Survey by Woodward-Lundgren and Associates, Oakland, California, 79 p.
- Cordova, R. M., 1969, Selected hydrologic data, Southern Utah and Goshen Valleys, Utah: U.S. Geological Survey Utah Basic-Data Release No. 16, 35 p.
- Eardley, A. J., Strong relief before block faulting in the vicinity of the Wasatch Mountains, Utah: Journal of Geology, v. XLI, p. 243-267.
- Hamblin W. K., 1965, Origin of "reverse drag" on the downthrown side of normal faults: Geological Society of America Bulletin, v.76, p. 1145-1164.
- Hintze, L. F., 1980, compiler, Geologic map of Utah: Salt Lake City, Utah, Utah Geological and Mineral Survey, scale 1:500,000, 2 sheets.
- Iorns, W. V., Mower, R. W., and Horr, C. A., 1966, Hydrologic and climatologic data collected through 1964, Salt Lake County, Utah: U.S. Geological Survey Utah Basic-Data Release No. 11, 91 p.
- Marine, W. I., and Price, Don, 1963, Selected hydrologic data, Jordan Valley Salt Lake County, Utah: U.S. Geological Survey Basic-Data Report No. 4, 30 p.

Marsell, R. E., 1969, The Wasatch fault zone in north central Utah: in Jensen, M. L., ed., Guidebook of northern Utah, Utah Geological and Mineralogical Survey Bulletin 82, p. 125-139.

Mattick, R. E., 1970, Thickness of unconsolidated and semiconsolidated sediments in Jordan Valley, Utah: U.S. Geological Survey Professional Paper 700-C, p. C119-C124.

McDonald, R. E., 1976, Tertiary tectonics and sedimentary rocks along the transition: Basin and Range province to plateau and thrust belt province, Utah, in Hill, J. G., ed., Geology of the Cordilleran hingeline: Denver, Colorado, Rocky Mountain Association of Geologists, p. 281-317.

Schwartz, D. P., and Coppersmith, K. J., in press, Fault behavior and characteristic earthquakes: Examples from the Wasatch and San Andreas fault zones: Journal of Geophysical Research.

Scott, W. E., Shroba, R. R., and McCoy, W. D., 1982, Guidebook for the 1982 Friends of the Pleistocene, Rocky Mountain Cell, field trip to Little Valley and Jordan Valley: U. S. Geological Survey Open-File Report 82-845, 58 p.

Swan, F. H., III, Schwartz, D. P., and Cluff, L. S., 1980, Recurrence of moderate to large magnitude earthquakes produced by surface faulting on the Wasatch fault zone, Utah: Bulletin of the Seismological Society of America, v. 70, p. 1431-1462.

VanHorn, Richard, 1972, Map showing relative ages of faults in the Sugar House quadrangle, Salt Lake County, Utah: U.S. Geological Survey Map I-766-B, scale 1:24,000.

Wiles, C. J., 1979, MINI-SOSIE: New concept in high-resolution seismic surveys: Oil and Gas Journal, v. 66, no. 11, p. 94-97.

Witkind, I. J., 1982, Salt diapirism in central Utah: in Nielson, D. L., ed., Overthrust belt of Utah, Utah Geological Association Publication 10, p. 13-30.

Zoback, M. L., 1983a, Structural style along the Sevier frontal thrust zone in central Utah: Geological Society of America Abstracts with Programs, v. 15, no. 5, p. 377.

_____, 1983b, Structure and Cenozoic tectonism along the Wasatch fault zone, Utah: in Miller, D. M., Todd, V. R., and Howard, K. A., eds., Tectonic and stratigraphic studies in the eastern Great Basin, Geological Society of America Memoir 157, p. 3-27.

AN EFFORT TO DETERMINE POISSON'S RATIO
IN SITU FOR NEAR-SURFACE LAYERS

by

Don W. Steeples and Richard D. Miller
Kansas Geological Survey
Lawrence, Kansas

and

K. W. King
U.S. Geological Survey
Denver, Colorado

For presentation at the
Workshop on Regional and Urban
Earthquake Hazards Evaluation
Wasatch Front, Utah

Salt Lake City, Utah

August 14-16, 1984

AN EFFORT TO DETERMINE POISSON'S RATIO
IN SITU FOR NEAR-SURFACE LAYERS

Don W. Steeples and Richard D. Miller
Kansas Geological Survey
Lawrence, Kansas
and
K. W. King
U.S. Geological Survey
Denver, Colorado

INTRODUCTION

Intensity of ground shaking during an earthquake is determined in part by local near-surface geological conditions. Intensity differences of three to four units on the MM scale at sites no more than a few kilometers apart have been well established for nearly a century (Lawson et al., 1908). Because of these differences, prediction of individual site response is an important part of earthquake hazard reduction.

To help with urban earthquake hazard evaluation, we are developing and testing shallow P- and S-wave reflection techniques that will allow direct in situ measurement of engineering properties of materials within a few hundred feet of the earth's surface. Medvedev (1965) showed that seismic shear impedance (the product of density and S-wave velocity) can be used to make estimates of relative ground response. The potential for amplification of shaking increases as the impedance contrast between layers increases, provided other parameters are constant.

It is rapidly becoming feasible to produce shallow P-wave and S-wave reflection profiles along the same surface line. This will allow interpretation of far more geological information than use of P-waves or S-waves alone. In addition to determination of velocities, it will be possible to determine Poisson's ratio as a function of depth.

Techniques

Seismic reflection techniques have been used in petroleum prospecting for about a half century. Although examples are occasionally cited in the literature, shallow reflection techniques in engineering and groundwater applications have met with only limited success, because of the difficulty encountered in identifying reflections from layers at shallow depths. The shallowest reflections (other than our work) documented in the literature appear to be those at 30 meters by Hunter et al. (1981). The amplitudes of the reflected waves at commonly recorded frequencies, when present, are smaller than the amplitudes of unwanted waves, particularly ground roll composed of Rayleigh waves and Love waves. Furthermore, the generation and recording of frequencies much above 100 Hz has not been possible on land, or at least has not been adequately recorded in the literature.

Typical energy sources that have been tried include sledge hammer (Hunter et al., 1981, and Meidav, 1969), weight drop (Doornenbal and Helbig, 1983), and small explosive charges (Pakiser and Warrick, 1956). These energy sources produce seismic waves with dominant frequencies of less than 100 Hz. In order to provide better resolution (both precision and accuracy) of shallow reflective interfaces, high frequencies are needed. Since direct resolution of "thin beds" is practically limited to about $1/4$ wavelength of the seismic energy (Widess, 1973), the improvement in resolution (and imaging of shallower reflectors) can be obtained directly by increasing the frequency of the energy that is recorded.

A worthy goal of shallow reflection surveys is to provide bed resolution in the approximate dimension of one foot. Typical velocities

of near-surface soil and/or alluvial materials range from about 1000 to about 4000 per second. Using the $1/4$ wavelength criterion, we can obtain the dominant P-wave frequency needed from the fact that velocity is directly proportional to both wavelength and frequency. The desired one-foot resolution cannot be obtained with a frequency less than 250 Hz for a P-wave velocity of 1000 feet/second. If the P-wave velocity is as high as 4000 feet/second, dominant frequencies higher than 1000 Hz are required for one foot bed resolution.

During the past two years, we have made substantial progress in improving shallow P-wave reflection techniques. We have been able to detect reflections in the depth range of 5 to 50 meters in alluvial valleys by using projectile impacts from ordinary hunting rifles as energy sources. We have built a gun mount that allows rifles to be safely fired vertically into the ground without danger to personnel and equipment. We have test-fired a 30.06 high-power rifle onto a one-inch thick steel plate lying on the ground beneath the mount with no escape of particulate debris. We designed, built, and tested a gun mounted at about 50° from vertical as a source of shear-wave energy in August of 1983.

FIELD EXPERIMENTS

Early in 1984, the USGS and the KGS entered into a cooperative agreement to develop capability of obtaining shallow P- and S-wave reflection data along the same seismic profile. The work discussed in the remainder of this paper reflects results of the first few months' effort on the project.

Geological Field Setting of Test Site

The area selected for our initial field experiments was examined geophysically previously by Steeples (1970) and is located in the Kansas River valley near Manhattan, Kansas. Bedrock beneath the valley fill is composed of alternating beds of Permian-aged limestones and shales ranging in thickness from a few inches to a few tens of feet. The alluvial fill is clearly of Pleistocene age and it varies in thickness from zero at the valley walls to as much as 35 meters at the deepest part of the bedrock valley.

Field Methods

We use an Input/Output, Inc. DHR 2400 seismic recording system with 24 channels to amplify, filter, and digitize the data (word size 11 bits plus sign) in the field and to record the data on digital tape. Our amplifier gains can be adjusted from 42 to 120 dB, depending upon the distance from the shot point to the geophone for the individual channels. The upper limit of amplifier gains, to avoid clipping of signal, is limited by digital word size rather than by the amplifier gains available. Our low-cut filters have 24 dB/octave rolloff to decrease the amplitude of ground roll. Data sample interval on each channel is 1/4 msec for P-wave studies and 1 msec for S-wave studies with a total record length of 1000 samples per channel. High-cut filters are used to attenuate energy at frequencies above the alias frequency.

Relatively severe low-cut filters have the beneficial effect of eliminating substantial amounts of cultural noise. Cultural noise in urban areas is relatively severe at frequencies below 50 Hz, but vehicular traffic and other vibratory noise sources do not produce much energy above 100-150 Hz. The noise that is produced at these high

frequencies attenuates rapidly with distance from the source because of the low-pass nature of the earth's transfer function.

Data Processing

Data shown in Table 1 indicate the type of processing that we have applied to the P-wave reflection data. The processing is very similar to that used in the petroleum industry, except that special care is exercised in muting non-reflected energy.

S-wave processing is similar to P-wave processing, except that an extra step is added to combine two separate data sets that are obtained by our S-wave reflection field procedure (as explained later). The two data sets are differenced (multiply one set by -1 and then add) to enhance S-waves and to cancel P-waves.

ACCOMPLISHMENTS TO DATE

We have succeeded in recording P-wave and S-wave reflections along the same seismic profile near Manhattan, Kansas. A typical field record of P-wave data with no processing is shown in Figure 1. In Figure 2, a 12-fold common depth point (CDP) stack of the P-wave data is shown. Note that the prominent reflector at about 60 msec on the stacked sections (Figure 2) is also visible on the field record of Figure 1. These data were recorded with single 100 Hz geophones using 220 Hz low-cut recording filters and single 180 grain 30.06 rifle bullets fired vertically into the ground. Split spread geometry was used with geophone interval of four feet and shot point to nearest geophone distance of eight feet.

Figure 3 shows a typical field record of the S-wave reflection data. The S-wave survey was done using single 100 Hz horizontal geo-

TABLE 1TYPICAL COMMON DEPTH POINT PROCESSING FLOW FOR
VERY SHALLOW REFLECTIONS

- 1) Surface statics and geometry specification
- 2) Editing
- 3) Mute first breaks and other linear arrivals
- 4) Sort into CDP gathers
- 5) Preliminary velocity analysis
- 6) Spectral analysis (determine bandpass)
- 7) Brute stack (preliminary velocity function and filtering)
- 8) Detailed velocity analysis
- 9) Determine automatic statics
- 10) Apply:
 - a. Final velocity function,
 - b. filter,
 - c. correct for normal moveout, and
 - d. automatic statics to the sorted data.
- 11) Residual statics
- 12) Stacked section
- 13) Decon. to remove multiples (if necessary)

phones with identical geometry as that discussed in the previous paragraph. Source energy was obtained by firing a single 180 grain 30.06 rifle bullet into the ground at approximately a 45° angle from vertical. Figure 4 shows a 12-fold CDP stacked section of records obtained from the horizontal geophones along the same seismic profile as that shown in Figure 2.

The 100 Hz geophones that we use are omnidirectional in the sense that they are sensitive to motion along their long axis, regardless of their orientation relative to vertical. This allows the phones to be used in either the vertical mode or the horizontal mode, provided they are mounted with their long axes vertical or horizontal, respectively. We have built geophone holders that allow these geophones to be easily changed to horizontal (S-wave) mode in the field.

One might ask why we believe the data in Figure 4 to be primarily S-wave reflections. In addition to the data in Figure 4 that were obtained by shooting the rifle 45° downward pointing north, we repeated the same line shooting 45° downward pointing south (data not shown). This process should reverse polarity of the horizontal component of S-waves, but not of P-waves. The two data sets were then subtracted from one another, trace-for-trace. This procedure should tend to cancel P-waves while tending to enhance S-waves. In Figure 5, the data from this subtraction stack are shown as a "pseudo-24-fold CDP profile." Note that the data in Figure 5 show reflections somewhat better than the data of Figure 4. If the reflection events were primarily P-waves, the subtraction stack would tend to degrade rather than enhance the quality of the reflections. We therefore conclude that a substantial portion of the reflected events shown on Figures 4 and 5 is composed of S-waves.

Note in comparing Figures 2 and 5 (the P-wave section and the S-wave section, respectively) that the reflections come in at substantially different times (i.e. 60 msec for P vs 260 msec for S).

While the difference between P- and S-wave velocities for solid rock is roughly a factor of 2, it may approach a factor of 7 for unconsolidated materials (Hasbrouck, 1982). If the reflected energy is coming from the same horizons for both P and S, then a factor of 4 difference in P and S velocity is implied. It is not yet clear that we are observing the same horizon, but note a synform structure exists on both Figure 2 and Figure 5 between CDP's 222 and 242. This suggests that the two sections may be observing the same structure, though this conclusion is still speculative.

Field experiments have been conducted at another location in north-central Kansas, but data processing is incomplete at this writing.

RECOMMENDATIONS FOR FURTHER RESEARCH

There are several improvements in technique and additional experiments that need to be performed in order to reach our objective of in situ determination of Poisson's ratio.

1. We need to improve the accuracy of our shot time-break so that high frequency components in the data are not attenuated. This can be done by optical or opto-electronic means. We presently use a geophone attached to the rifle to provide a time-break voltage. The time-break errors of two to three milliseconds are unacceptably large.
2. The 100 Hz horizontal geophones we have been using are perhaps not of low enough frequency to obtain S-waves at some localities.

Experiments should be done with horizontal geophones in the 20 to 50 Hz natural frequency range.

3. Air blast has been a major problem, particularly with the P-wave experiments. We have built an air-blast containment device (ABCD) that eliminates at least 36 dB of air blast noise. Further development and refinement is needed, including improved portability.

4. We need to establish that the P-wave reflections and S-wave reflections are coming from the same horizon. This entails careful choice of a new experimental locality where the geologic section is extremely well known, and/or the performance of experiments such as up-hole checkshot surveys to determine both the P-wave velocity and the S-wave velocity.

5. We need to perform additional experiments to determine the important parameters of bullet selection for S-wave reflection surveys. The use of 150 grain bullets occasionally results in poor energy generation caused by lack of penetration into the earth. The bullets occasionally shatter on impact or ricochet into a steel safety plate. It is likely that the use of 220 grain bullets will alleviate much of this problem.

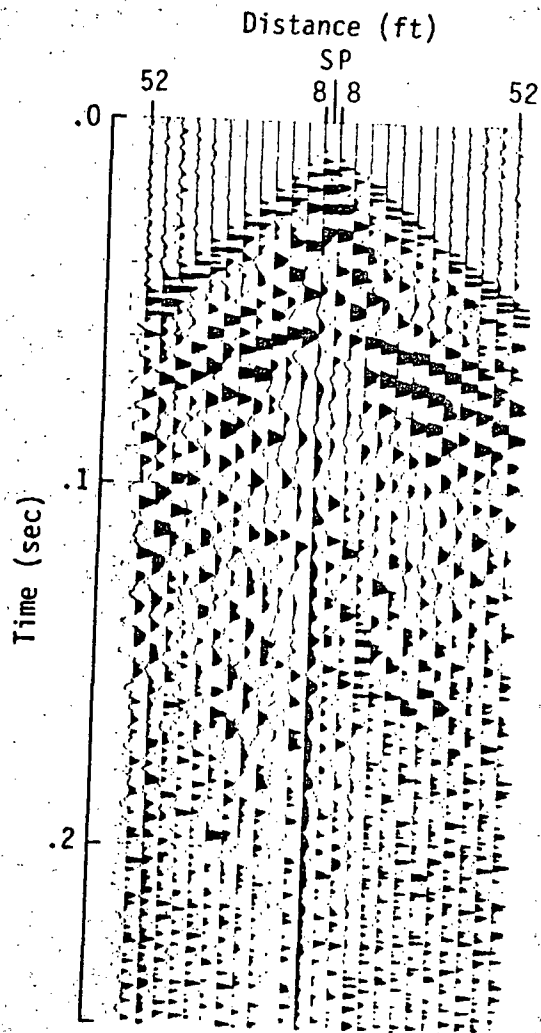
6. At this writing, the subtraction stack of S-wave reflections must be done in the computer processing. We are in the process of obtaining hardware to reverse polarity in the field during data recording. This will allow more flexibility in recognizing S-wave reflections on the field records.

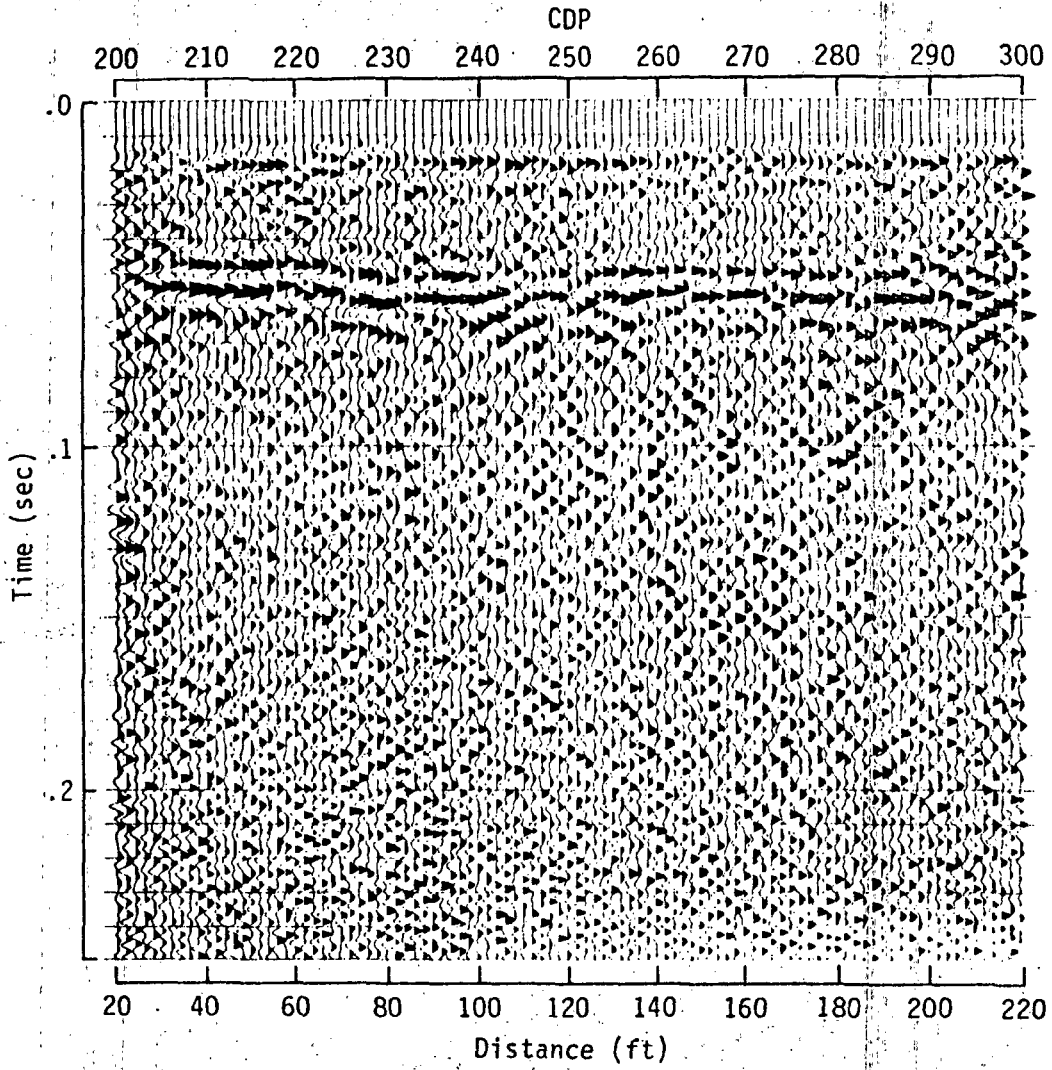
BIBLIOGRAPHY

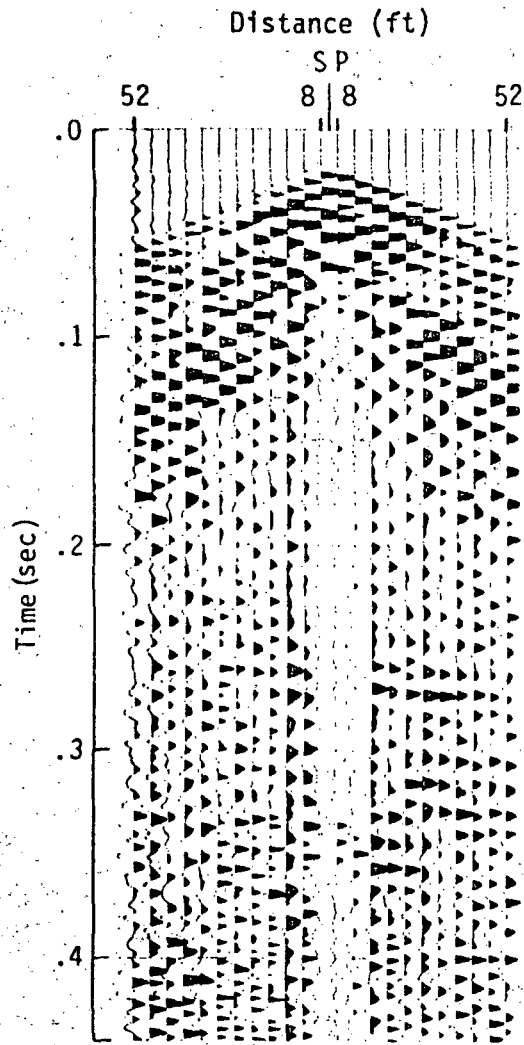
- Doornenbal, J.C. and Helbig, K., 1983, High resolution seismics on a tidal flat in the Dutch Delta acquisition, processing and interpretation, First Break, May 1983 issue, p. 9-20, Geospace Corporation, Houston, Texas.
- Hasbrouck, W.P. and Padget, N., 1982, Use of shear wave seismics in evaluation of strippable coal resources: Utah Geological and Mineral Survey, Bull. 118, p. 203-218.
- Hunter, J.A., Burns, R.A., and Good, R.L., 1981, Optimum field techniques for bedrock mapping with the multichannel engineering seismograph, (abstract): Geophysics, v. 46, p. 451.
- Lawson, A.C., 1908, The California earthquake of April 18, 1906: Report of the State Earthquake Investigation Commission, v. I, Carnegie Institute of Washington, Washington, D.C.
- Medvedev, S.V., 1965, Engineering seismology; National Technical Information Service, NTIS no. TT65-50011, 260 p.
- Meidav, T., 1969, Hammer reflection seismics in engineering geophysics: Geophysics, v. 34, p. 383-395.
- Pakiser, L. and Warrick, R., 1956, A preliminary evaluation of the shallow reflection seismograph: Geophysics, v. 21, p. 388-405.
- Steeple, D.W., 1970, Resistivity methods in prospecting for groundwater: M.S. Thesis, Dept. of Geology, Kansas State University, Manhattan, Kansas.
- Widess, M.B., 1973, How thin is a thin bed?: Geophysics, v. 38, p. 1176.

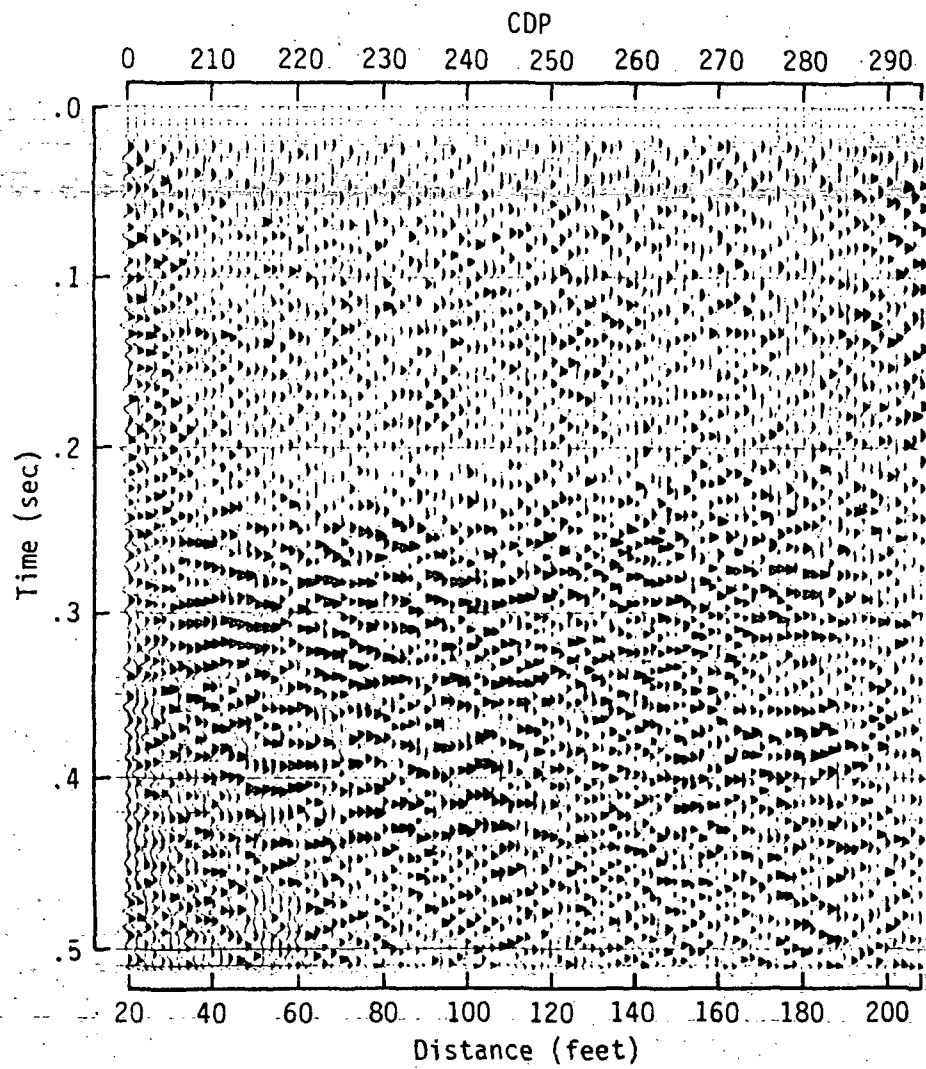
FIGURE CAPTIONS

- FIGURE 1. Unprocessed seismic field record showing prominent P-wave reflection at 60 msec.
2. Processed 12-fold CDP stack in alluvial valley near Manhattan, Kansas. Data from Figure 1 was included in this seismic section. Note prominent reflections in the 50 to 70 msec range and apparent stratigraphic variations. Dominant frequency is 150 to 200 Hz.
 3. Unprocessed seismic field record showing prominent S-wave reflection at 270 msec and subtle reflectors at later arrival times.
 4. Processed 12-fold CDP stack of S-wave data at same CDP points as Figure 2.
 5. Processed pseudo 24-fold CDP section obtained by subtraction stack of section in Figure 4 and data obtained at same CDP, with rifle fired in opposite horizontal direction.









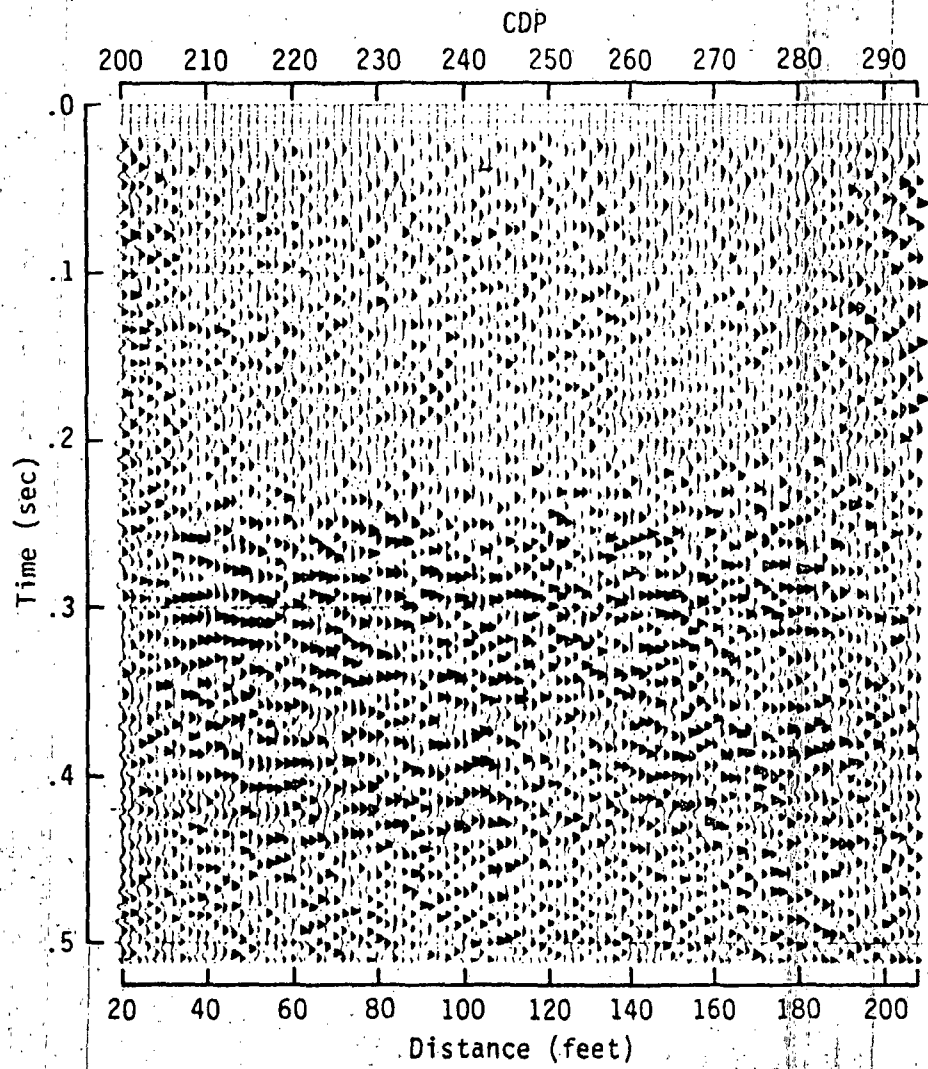


Fig. 5

INVESTIGATIONS OF AN M_L 4.3 EARTHQUAKE IN THE WESTERN SALT LAKE VALLEY
USING DIGITAL SEISMIC DATA

by

James C. Pechmann and Bergthora Thorbjarnardottir

Department of Geology and Geophysics

University of Utah

Salt Lake City, Utah 84112-1183

INTRODUCTION

Earthquakes in the Utah region have been recorded digitally by the University of Utah seismic network since January 1981. To date, digital seismograms from more than 2000 earthquakes have been archived on magnetic tape. Together with colleagues at the University of Utah, we have begun to systematically test and apply techniques for extracting information on source properties of small earthquakes from these data. Our goal is to try to obtain a better understanding of how these earthquakes are related to cycles of strain accumulation and release on major faults along the Wasatch Front. To illustrate the type of research we are pursuing, we present here a study of an M_L 4.3 earthquake that occurred approximately 10 km west of downtown Salt Lake City, Utah, at 11:57 GMT on October 8, 1983 (Figure 1). This earthquake occurred within a region of the western Salt Lake Valley that has been characterized by persistent seismicity since at least 1962, when instrumental

location of Utah earthquakes was begun at the University of Utah (Arabasz et al., 1980). Past activity in this region has included an M_L 5.2 earthquake located approximately 8 km northwest of Magna, Utah, on September 5, 1962, and an earthquake swarm several kilometers north and northwest of Magna during February and March of 1978 (largest event M_L 3.2) (Arabasz, et al., 1979; Cook, 1979). Earthquakes in this region are of particular interest because of their proximity to Salt Lake City and the possibility of an association with the Wasatch fault which dips westward beneath the Salt Lake Valley (Figure 1).

MAINSHOCK LOCATION AND FOCAL MECHANISM

The M_L 4.3 mainshock on October 8, 1983 was located using the computer program HYPOINVERSE (Klein, 1978) and the velocity model in Table I. This velocity model is from a refraction line extending southward from the Bingham Canyon copper mine 35 km southwest of Salt Lake City (Keller et al., 1975). A 7.9 km/sec half space at 42 km depth has been added in order to fit observed travel time data from earthquakes at distances greater than about 250 km.

The constraint of the arrival time data on the source depth was carefully examined. For our initial location, we used stations out to a distance of 300 km. Figure 2 demonstrates that the velocity model fits the observed travel-time data from the earthquake very well even at large distances. The hypocentral depth obtained, 4 km, is constrained primarily by the P_n crossover distance which is well defined by the data. The accuracy of this depth determination depends on the accuracy of the velocity model, in particular the crustal thickness. A crustal thickness of 28 km and a P_n velocity of 7.6 km/sec was obtained by Braille et al. (1974) from a refraction line extending

northeastward from the Bingham Canyon mine. If the depth of the moho is changed from 25.4 km to 28 km in the velocity model in Table I the earthquake locates at a depth of 8 km. If stations beyond the P_n crossover distance (120-130 km) are not used in the location a hypocentral depth of 11 km is obtained. In this case the depth control comes from the arrival time at the closest station RBU, which is 15 km from the epicenter. If a less reliable P-wave arrival time from the Wood-Anderson instrument at SLC, 12 km from the epicenter, is added to the data set the depth of 11 km remains unchanged. However, because even the closest stations are more than one focal depth away from the epicenter the arrival times at these stations do not provide a strong constraint on focal depth. We conclude that the depth of the M_L 4.3 mainshock probably lies between 4 and 11 km, but it is not possible to constrain the depth any more accurately than this with the data at hand.

The focal mechanism obtained for the mainshock is shown in Figure 3. The two sets of nodal planes illustrate the range of possible solutions. The takeoff angles used for this mechanism are for a source depth of 4.2 km. Despite the uncertainty in focal depth we are confident that these takeoff angles are realistic because of the excellent agreement between the travel time data and the model (Figure 2). If a focal depth of 8 km and a crustal thickness of 28 km are used to compute the takeoff angles the mechanism obtained is virtually identical to the one shown by the dashed nodal planes in Figure 3. Note that both nodal planes are very well constrained by the data.

The mechanism of Figure 3 indicates normal faulting on a north-northwest-striking fault that dips either 68° - 80° east or 10° - 22° west. Our knowledge of the subsurface geology is insufficient to choose between these

two possibilities. If the westward-dipping plane is the fault plane and if the Wasatch fault beneath the Salt Lake Valley is listric, then the possibility that this earthquake occurred along the Wasatch fault cannot be ruled out. However, there are undoubtedly other faults in this region along which the earthquake could have occurred.

ESTIMATION OF SOURCE RADIUS AND STRESS DROP

The method of Frankel and Kanamori (1983) was used to estimate the source radius of the M_L 4.3 mainshock. This technique involves measurement at nearby stations of a parameter designated $\tau_{1/2}$, the time between the P-wave onset and the first zero crossing. $\tau_{1/2}$ was measured at four stations for the mainshock and eleven aftershocks. At each station, $\tau_{1/2}$ was found to remain nearly constant with decreasing magnitude for aftershocks less than about magnitude 2, as was found by Frankel and Kanamori (1983), O'Neill (1984), and O'Neill and Healy (1973) for earthquakes in California. This is interpreted to signify that the waveforms of the events smaller than magnitude 2 represent the combined impulse response of the path between the source and receiver and the instrument itself. When the values of $\tau_{1/2}$ for the smallest aftershocks are subtracted from those measured for the mainshock at each station (in effect deconvolved), the corrected values of $\tau_{1/2}$ show excellent agreement from one station to another (Table II). These corrected values of $\tau_{1/2}$ are estimates of the half-duration of the source time function for the mainshock (see Frankel and Kanamori, 1983).

The corrected $\tau_{1/2}$ measurements are converted to estimates of source radius r using

$$r = \tau_{1/2} v / (1 - (v/c) \sin \theta)$$

where c is the P-wave velocity, v is the rupture velocity, and θ denotes the angle between the normal to the fault plane and the outgoing seismic ray (Sato and Hirasawa, 1975). We use 5.9 km/sec for c (Table I) and assume that the rupture velocity v is 0.9 times the corresponding shear wave velocity of 3.5 km/sec (Keller et al., 1975). Values for θ are taken from the focal mechanism in Figure 3. The value obtained for r is either 1.1 or 1.4 km, depending on which plane is chosen as the fault plane. This estimate for the size of the fault plane is comparable to the size of the aftershock area for this earthquake (Figure 1).

We estimate the moment for this earthquake from the Wood-Anderson magnitude and a moment-magnitude relation for Utah earthquakes determined by Doser and Smith (1982):

$$\log M_0 = 1.1 M_L + 18.4$$

The moment obtained is about 1.3×10^{23} dyne-cm. The stress drop $\Delta\sigma$ can be calculated from this moment and the fault radius determined above using the solution for a circular crack in an elastic medium determined by Eshelby (1957) and Keilis-Borok (1959):

$$\Delta\sigma = (7/16) M_0 / r^3$$

The calculated stress drops are 43 and 21 bars, depending on whether 1.1 or 1.4 km is used for the source radius. These are typical stress drop values for earthquakes, neither unusually high nor unusually low. However, since the moment was not determined directly for this earthquake and since all stress

drop estimates are model-dependent caution must be used in comparing this stress drop with those reported in the literature for other earthquakes.

WAVEFORMS OF PRESHOCKS AND AFTERSHOCKS

All earthquakes with preliminary locations within 20 km of the mainshock during the time period January 1981 through November 1983 were relocated relative to the mainshock using the master event technique of Johnson and Hadley (1976) with the computer program HYPOINVERSE. The results (Figure 1) show a clustering of activity centered 12 km northeast of the mainshock epicenter during the three year period preceding this earthquake. Waveforms for the earthquakes in this cluster and for aftershocks were examined at several stations. Figure 4 shows the seismograms recorded at a typical station, MOU (Figure 1). The clear difference in P/SV amplitude ratios between the "preshocks" and the aftershocks suggest a systematic difference in focal mechanism. The waveforms of all five preshocks are very similar to one another over the entire record. This suggests that all of these events had similar mechanisms and occurred within about $1/4$ wavelength of each other (Geller and Mueller, 1980), in this case within about 150-200 m. The waveforms of the aftershocks are not all the same, although groups of similar earthquakes can be identified within the aftershock sequence. The tight clustering of the preshock hypocenters and some of the aftershock hypocenters implied by the waveform data suggests that the location of small earthquakes may be controlled by stress concentrations on fault asperities. Analysis of this waveform data is continuing.

CONCLUSIONS

An earthquake of M 4.3 occurred on October 8, 1983, within a seismically active region of the western Salt Lake Valley. The depth of this earthquake is problematic, but probably lies within the range of 4-11 km. A well-constrained focal mechanism for this event indicates normal faulting on a north-northwest striking fault plane that dips either steeply to the east or gently to the west. The method of Frankel and Kanamori (1983) was successfully applied to determine a source radius of about 1 to 1-1/2 km and a stress drop of a few tens of bars. Similarity of waveforms for a group of preshocks located 12 km northeast of the mainshock epicenter suggests clustering within a source volume less than 200 m in extent. The aftershock waveform data suggests that some of these events are tightly clustered as well.

Groups of similar earthquakes have also been observed elsewhere in the world and may be related to concentrations of stress such as might be expected along fault asperities (see Pechmann and Kanamori, 1982). Continued study of earthquakes using digital network data will hopefully lead to a better understanding of earthquake tectonics and perhaps to the development of techniques for using small earthquakes as indicators of potential for moderate-to-large earthquakes.

Table I. Wasatch Front Velocity Model
(Modified from Keller et al., 1975)

P-Wave Velocity of Layer	Depth Below Datum (1500 m) of Top of Layer
3.4 km/sec	0.0 km
5.9	1.4
6.4	15.5
7.5	25.4
7.9	42.0

Table II. $\tau_{1/2}$ Measurements

Station	Delta (km)	Azimuth (deg)	Minimum $\tau_{1/2}$ (sec)	Mainshock $\tau_{1/2}$ (sec)	Corrected $\tau_{1/2}$ (sec)
GMU	26.0	134	0.06	0.26	0.20
CWU	34.2	198	0.05	0.25	0.20
JLU	47.5	108	0.10	0.35	0.25
MOUT	51.9	9	0.04	0.22	0.18

REFERENCES

- Arabasz, W.J., R.B. Smith, and W.D. Richins, 1980, Earthquake studies along the Wasatch Front, Utah: Network monitoring, seismicity and seismic hazards, Bull. Seism. Soc. Am., 70, p. 1479-1499.
- Arabasz, W.J., R.F. Smith, and W.D. Richins (editors), 1979, Earthquake Studies in Utah, 1850 to 1978, University of Utah, Salt Lake City, Utah, 552 p.
- Braile, L.W., R.B. Smith, G.R. Keller, R.M. Welch, and R.P. Meyer, 1974, Crustal structure across the Wasatch Front from detailed seismic refraction studies, J. Geophys. Res., 79, p. 2669-2677.
- Cook, K.L., 1979, Effects of the earthquakes in the Magna area, Salt Lake County, Utah, during February-March 1978, in Earthquake Studies in Utah, 1850 to 1978, W.J. Arabasz, R.B. Smith, and W.D. Richins (editors), University of Utah, Salt Lake City, Utah, p. 474-485.
- Doser, D.I. and R.B. Smith, 1982, Seismic moment rates in the Utah region, Bull. Seism. Soc. Am., 72, p. 525-551.
- Eshelby, J.D., 1957, The determination of the elastic field of an ellipsoidal inclusion and related problems, Proc. R. Soc. London, Ser. A, 241, p. 376-396.
- Frankel, A., and H. Kanamori, 1983, Determination of rupture duration and stress drop for earthquakes in Southern California, Bull. Seism. Soc. Am., 73, p. 1527-1551.
- Geller, R.J., and C.S. Mueller, 1980, Four similar earthquakes in central California, Geophys. Res. Lett., 7, p. 821-824.
- Johnson, C.E., and D.M. Hadley, 1976, Tectonic implications of the Brawley earthquake swarm, Imperial Valley, California, January 1975, Bull. Seism. Soc. Am., 66, p. 1133-1144.
- Keilis-Borok, V., 1959, On estimation of the displacement in an earthquake source and of source dimensions, Ann. Geofis., 12, p. 205-214.

Keller, G.R., R.B. Smith, and L.W. Braille, 1975, Crustal structure along the Great Basin-Colorado Plateau transition from seismic refraction studies, J. Geophys. Res., 80, p. 1093-1098.

Klein, F.W., 1978, Hypocenter location program HYPOINVERSE, U.S. Geol. Survey Open-File Report 78-694, 113 p.

O'Neill, M.E., 1984, Source dimensions and stress drops of small earthquakes near Parkfield, California, Bull. Seism. Soc. Am., 74, p. 27-40.

O'Neill, M.E., and J.H. Healy, 1973, Determination of source parameters of small earthquakes from P-wave rise time, Bull. Seism. Soc. Am., 63, p. 599-614.

Pechmann, J.C., and H. Kanamori, 1982, Waveforms and spectra of preshocks and aftershocks of the 1979 Imperial Valley, California earthquake: Evidence for fault heterogeneity?, J. Geophys. Res., 87, p. 10579-10597.

Sato, T., and T. Hirasawa, 1973, Body-wave spectra from propagating shear cracks, J. Phys. Earth, 21, p. 415-432.

41° 15'
111° 30'

40° 30'
112° 30'

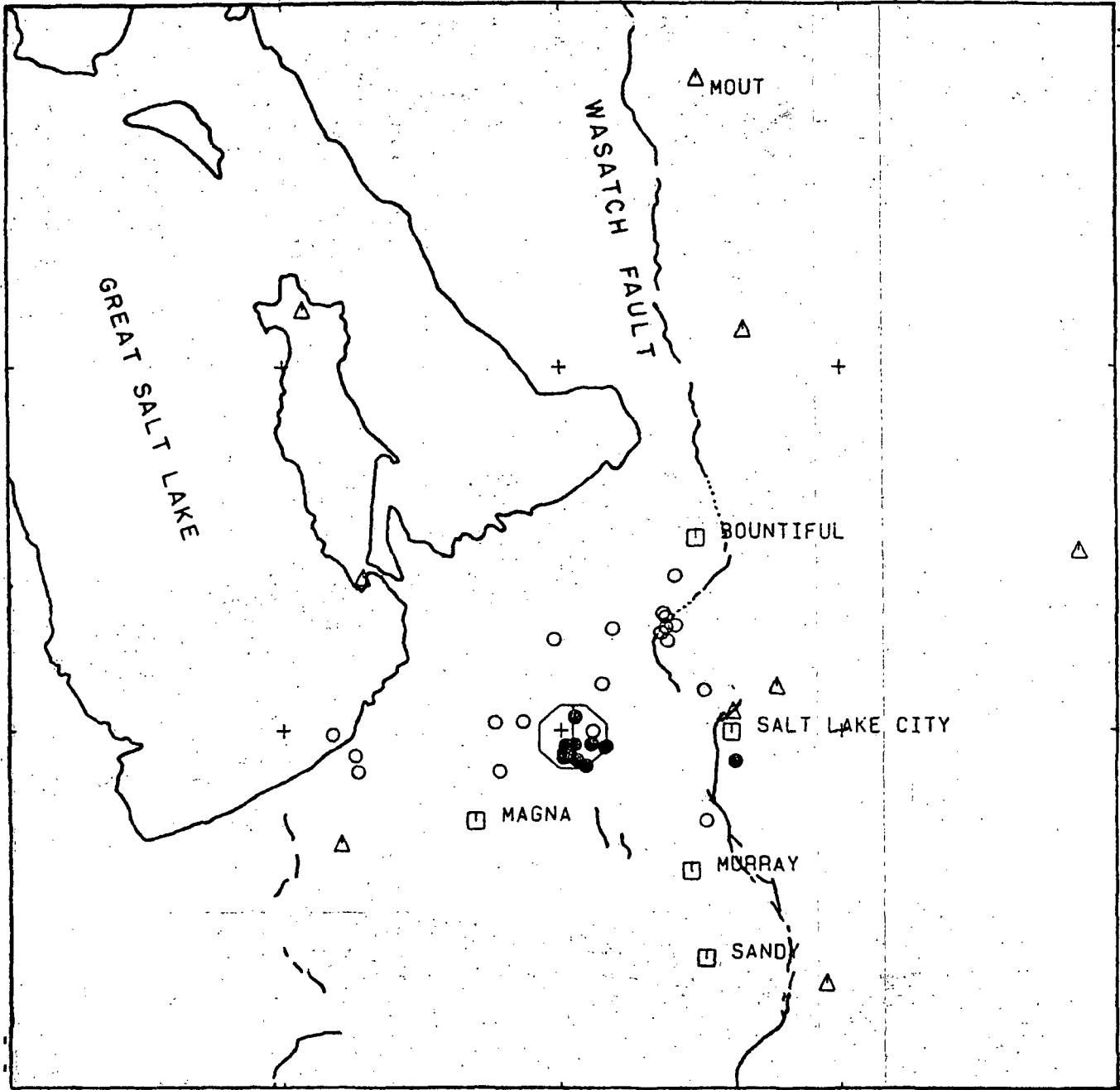
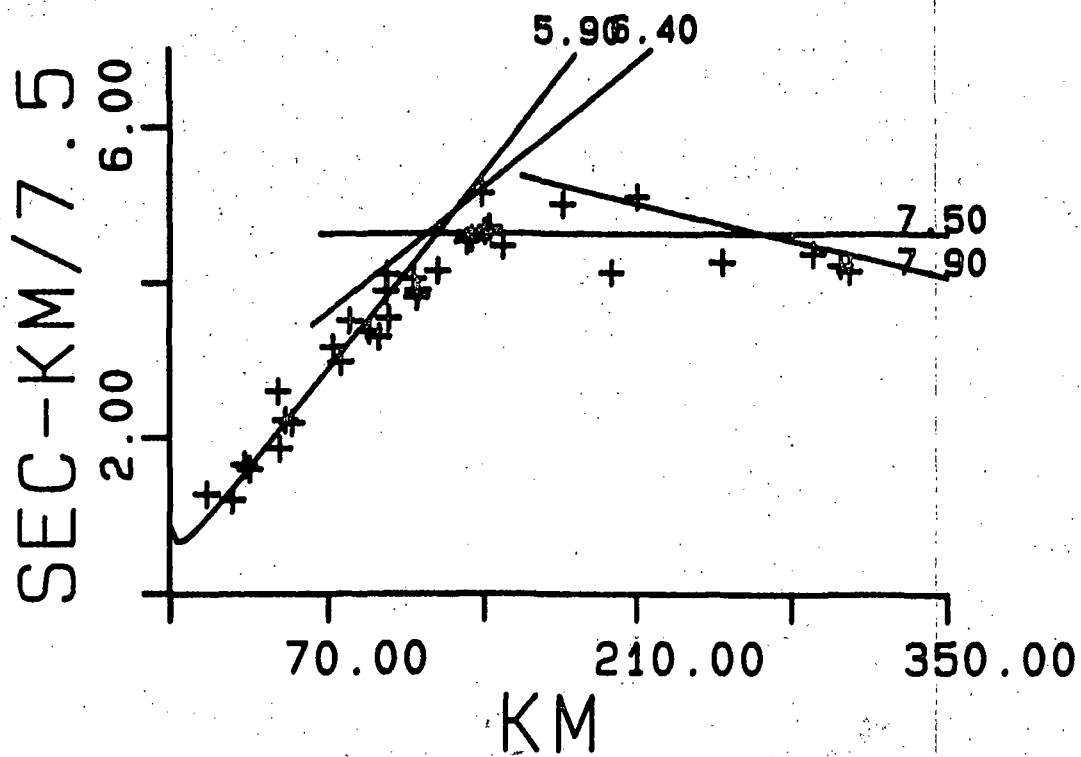


Figure 1. Map showing epicenter of the M_L 4.3 earthquake at 11:57 on October 8, 1983 (large octagon) and relocated epicenters of all events within a 20 km radius of this earthquake during the period January 1981 up until the time of this earthquake (open circles) and from immediately after the earthquake through November 1983 (solid circles). Triangles are seismic stations and squares are cities.



0 <AZ< 360 DEPTH=4.18
 DATE=83-10-08 TIME=1157

Figure 2. Reduced travel-time plot for the mainshock. Solid lines show travel times calculated from the velocity model in Table I.

OCTOBER 8, 1983 11:57
ML=4.3 DEPTH=4.2

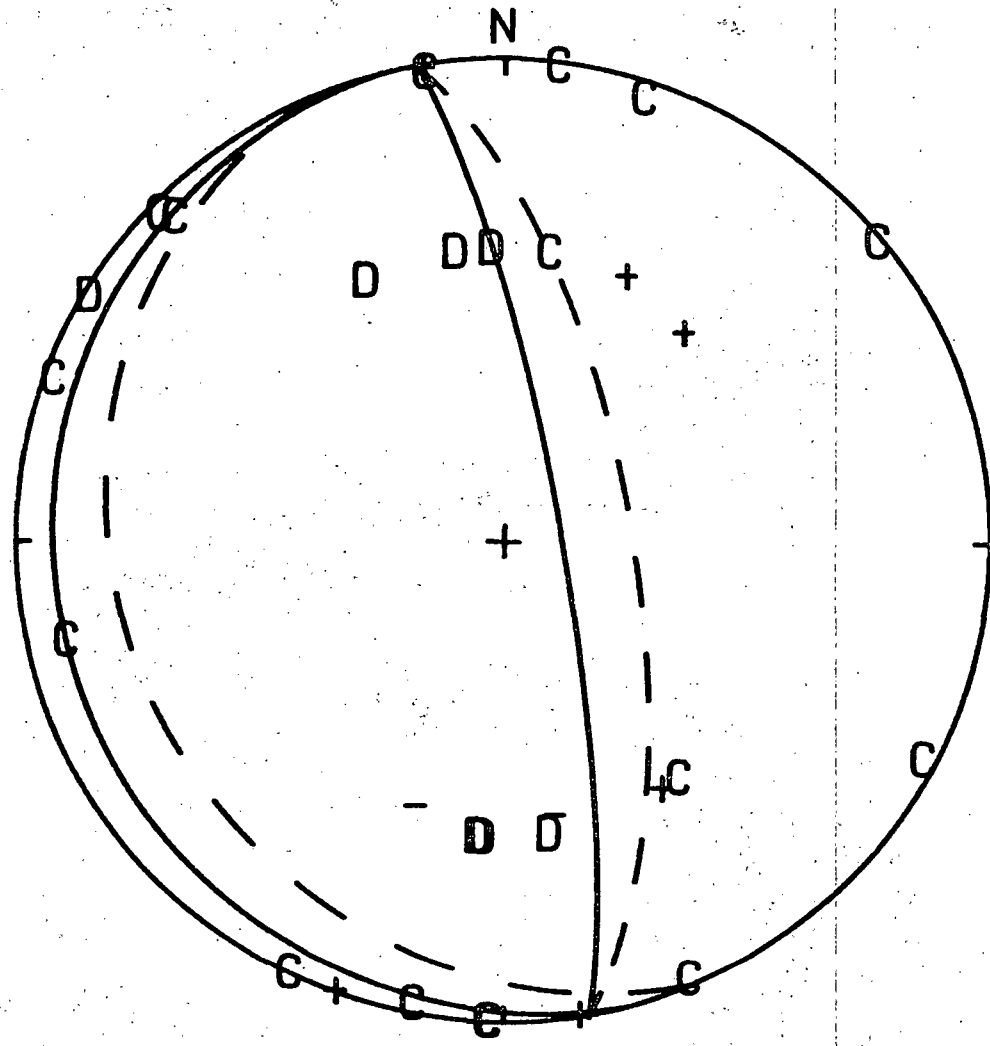


Figure 3. Lower hemisphere P-wave fault plane solution. C's and D's indicate compressions and dilatations, respectively. Pluses and minuses indicate less certain compressional and dilatational first-motion readings.



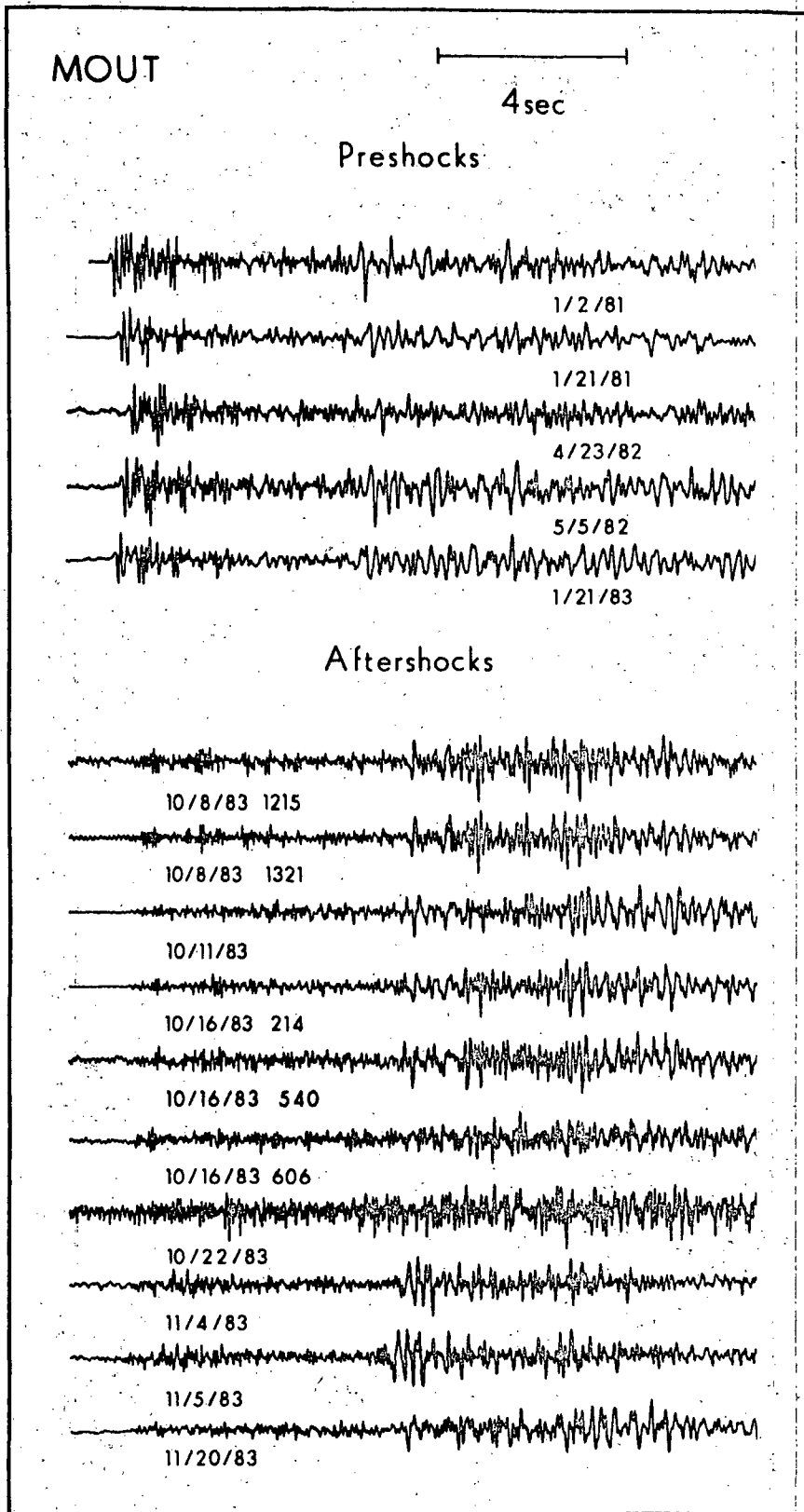


Figure 4. Vertical component seismograms recorded at station MOUT for (1) preshocks from the cluster of activity 12 km northeast of the mainshock epicenter and (2) aftershocks within 3 km of the mainshock epicenter (Figure 1). All seismograms are plotted with the same maximum amplitude.

NEAR-SOURCE CHARACTERISTICS OF
STRONG GROUND MOTION FOR MODERATE TO LARGE EARTHQUAKES--
AN UPDATE AND SUGGESTED APPLICATION TO THE WASATCH FAULT ZONE
OF NORTH-CENTRAL UTAH

by

Kenneth W. Campbell

U.S. Geological Survey, Golden, Colorado

ABSTRACT

The near-source scaling relationships for peak horizontal acceleration and velocity developed previously (Campbell, 1981a, 1982, 1983) have been revised to incorporate the results of further investigations into the near-source characteristics of strong ground motion. Although preliminary in nature, these revisions are significant enough to warrant presentation at this time in hopes that they will stimulate further discussion and research on these important issues. Major revisions have included changes in the definition of source-to-site distance and building size and embedment variables, as well as the way in which local site geology is treated. These preliminary results indicate that both peak acceleration and peak velocity become independent of earthquake magnitude (i.e., saturate) at the source of an earthquake, consistent with geophysicists' interpretations of rupture mechanics. Although preliminary, the scaling relations are considered stable enough to warrant their use in estimating strong ground motion for the near-source region of moderate-to-large earthquakes on the Wasatch fault zone of northcentral Utah for purposes of zoning or planning.

INTRODUCTION

Previous studies (Campbell, 1981a, 1982, 1983) have investigated the near-source scaling characteristics of peak ground motion parameters through the relationship

$$\ln Y = a + bM - d \ln [R + c_1 \exp(c_2 M)] + \sum e_1 K_1 + \varepsilon \quad (1)$$

where Y is the peak ground motion parameter to be predicted, M is magnitude defined as M_L for $M < 6.0$ and M_g for $M \geq 6.0$, R is shortest distance between the recording site and the fault rupture surface, K_1 is a set of variables representing the effects of fault mechanism, building embedment, etc., and ε is a random error term with mean of zero and standard deviation equal to the standard error of the regression. The data base was comprised of strong motion data recorded within 50 km of a set of worldwide earthquakes with $M \geq 5.0$. The coefficients a through e were determined from weighted nonlinear regression analysis, where weights were used to control the influence of well-recorded earthquakes.

While only minor revision of the data base used previously has been made, further investigations have indicated that several of the variables require modification to better represent the near-source characteristics of peak ground motion parameters. These modifications are summarized below.

Distance. The distance measure used previously was defined as the shortest distance between the recording station and the fault rupture surface. While found to be superior to either epicentral or hypocentral distance in modeling the near-source attenuation characteristics of strong ground motion for moderate-to-large earthquakes (Campbell, 1981b), its

application to predicting ground motion from earthquakes of magnitude 5.5 and greater is complicated by ambiguity as to the appropriate value for the depth to rupture. For very small earthquakes one can reasonably assume that fault rupture is restricted to the basement rock beneath the sediments. However, for events of $M \geq 5.5$, rupture may or may not propagate into the sedimentary deposits. Even for larger earthquakes for which rupture clearly extends to the ground surface, it is unlikely that the small stresses associated with rupture within the sediments can contribute any substantial energy to ground motions recorded at the surface of the earth.

Taking this into consideration, the distance measure was revised to more closely represent the distance to that part of the rupture surface believed to contribute significantly to the strongest shaking recorded at a site. This revised distance is defined as the shortest distance between the site and the seismogenic zone of rupture, determined from either the depth of aftershocks associated with an earthquake or the depth to basement rock. Use of this revised distance measure was found to reduce the standard error of the regression on peak horizontal acceleration.

Site Geology. Previously it was found that shallow soil sites, sites with 10 m or less of fill or soil over rock, were associated with higher accelerations than either deeper soil sites or rock. Once these sites were removed, no significant difference was found in accelerations recorded on soil or rock. A preliminary analysis of peak velocity indicated that basement rock sites were associated with velocities approximately 50 percent less than soil sites and that shallow soil sites behaved as rock sites.

Because of complexities associated with many of the rock sites in the data base, it was decided that the revised analyses should include only soil sites. This restriction eliminated only a small percentage of the sites,

mostly those located on the abutments of dams where there is a potential for substantial modification of the ground motion by ground topography and response of the dam. Having removed rock sites, it was found that peak horizontal velocity was significantly influenced by the depth of the sediments beneath the site. Velocities were found to increase with sediment depth up to a depth of approximately 4 or 5 km after which little additional increase was observed. This effect has been reasonably modeled with a hyperbolic tangent function. A similar dependence on sediment depth was observed for moderate-to-low frequency components of Fourier amplitude spectra by Trifunac and Lee (1978).

Building Effects. In the previous analyses, large embedded buildings (buildings of three stories or greater in height) were found to be associated with peak horizontal accelerations approximately 24 percent lower than non-embedded instruments. Embedded buildings of less than three stories in height were found to be associated with accelerations approximately 11 percent lower than non-embedded instruments. Large buildings, whether embedded or not, were found to have peak horizontal velocities approximately 20 percent higher than small buildings and freefield sites.

Further investigations on peak horizontal acceleration have indicated that the effect of building embedment is distance dependent, with reductions in acceleration due to embedment decreasing with increasing distance. This apparently reflects a shift to lower predominant frequencies as distance increases. In addition, this effect was found to be a function of building size, with buildings of ten stories or greater having larger reductions at all distances as compared to three to nine story buildings. Embedded buildings less than three stories high were not observed to have accelerations significantly lower than non-embedded instruments. Because the observed

reductions were found to decrease more rapidly with distance at short distances and approach some limiting value at larger distances, a hyperbolic tangent function was used to model these embedment effects.

Further investigations on peak horizontal velocity indicate that building size affects the rate at which velocity increases with sediment depth. Larger buildings (buildings greater than four stories in height) exhibit velocities that increase faster with depth than smaller buildings and freefield sites. However, for depths greater than about 5 km, for which the effect of sediment depth remains relatively constant, the larger buildings exhibit peak velocities only about 10 percent larger than other recordings. This difference may reflect the effects of soil-structure interaction as it relates to the fundamental frequencies of the structure and the ground motion.

Source Directivity. While the effects of source directivity have not been fully investigated, a few sites exhibited such strong amplification effects for peak velocity that their observed values fell more than four standard errors above their median predicted values. These sites were all located on deep sedimentary deposits and situated along the direction of unilateral fault rupture. This may represent an extreme amplification effect. This bias was so severe that these sites had to be represented by a scaling variable in the regression analysis to control their influence on the other variables. While not as strong, a similar effect was found for peak horizontal acceleration.

GROUND MOTION MODELS

The weighted nonlinear regression analysis technique described by Campbell (1981a) was used to establish the coefficients a through e and ϵ in.

Equation (1) for both peak acceleration and peak velocity. For peak horizontal acceleration (PHA), the resulting scaling relationship is given by the expression

$$\ln \text{PHA} = -2.817 + 0.702M - 1.20 \ln [R + 0.0921 \exp(0.584M)] + \sum e_i K_i \quad (2)$$

where PHA is the mean of the two horizontal components of peak acceleration in units of g (fraction of gravity). The coefficients e_i are given in Table 1. The standard error associated with this relationship is 0.30, representing an 84th-percentile value of PHA that is 35 percent higher than the median.

For peak horizontal velocity (PHV), the resulting scaling relationship is given by the expression

$$\ln \text{PHV} = -0.798 + 1.02 M - 1.26 \ln [R + 0.0150 \exp(0.812M)] + \sum e_i K_i \quad (3)$$

where PHV is the mean of the two horizontal components of peak velocity in cm/sec and the coefficients e_i are given in Table 2. The standard error associated with this relationship is 0.26, representing an 84th-percentile value of PHV that is 30 percent higher than the median.

The near-source behavior of PHA and PHV is summarized in Table 3, where median values are given for fault distances of 5, 10, 25 and 50 km and for magnitudes of 5.5, 6.5 and 7.5. These values represent the ground motion recorded on a freefield instrument from a strike-slip earthquake. For PHA, the recording is that expected on a soil site, while for PHV, the recording is that expected on a deep sedimentary site ($D > 5$ km). Table 4 gives a similar

summary for a site located on basement rock. For these estimates it was assumed that near-source values of PHA are similar on soil and basement rock (Campbell, 1981a). For PHV, sediment depth was assumed equal to zero ($D=0$ km).

Equation (3) indicates that PHV attenuates more rapidly with distance than does PHA. This results in ratios of PHV to PHA that decrease slightly with distance for fixed magnitude. This trend is inconsistent with past investigations (e.g. McGuire, 1978; Joyner and Boore, 1981; Nuttli and Herrmann, 1984), and may be a result of source directivity effects at the near-source distances of concern in this study. The relatively low frequencies associated with PHV make it strongly influenced by source directivity. Preliminary inspection of the data indicates that the majority of recordings near the fault are situated where source directivity would tend to amplify the motions. Accounting for this would lower the near-fault predictions of PHV relative to those at further distances, thereby decreasing the effective rate of attenuation. The relatively high frequencies associated with PHA would make it less susceptible to source directivity effects. Thus, the net effect of including source directivity effects in the analysis would be to reduce the rate of attenuation of PHV with respect to PHA, making it more compatible with other investigations.

Setting aside the possible bias associated with source directivity, it is possible to assess the reasonableness of the predictions offered by Equations (2) and (3) by comparing them with the results of past studies. A brief comparison is presented below.

Upper bounds. Table 4 indicates that both PHA and PHV saturate with magnitude at the fault rupture surface ($R=0$). As defined in this study, the fault rupture surface represents that portion of the rupture confined either

to basement rock or the seismogenic zone of rupture as determined by the depth distribution of aftershocks. The median values of PHA and PHV saturate to values of 1.05 g and 88 cm/sec, respectively, at $R=0$. Upper bounds may be estimated from these values by taking some multiple of σ , the standard error. If we may approximate the upper bound of PHA and PHV by a 2 to 3 σ value, then upper bounds for these parameters are estimated to be in the range 1.9 to 2.6 g for PHA and 150 to 190 cm/sec for PHV. These values are reasonably consistent with those estimated independently by geophysicists (e.g. McGarr, 1982).

Magnitude Scaling. The magnitude dependence of PHA and PHV at far-source distances is given by the coefficient b in Equation (1). Equations (2) and (3) indicate this magnitude coefficient to be 0.70 and 1.02 for PHA and PHV, respectively. These coefficients may be compared directly with values of 0.89 for PHA and 1.07 for PHV as determined by McGuire (1978) and with values of 0.58 and 1.13 determined for PHA and PHV by Joyner and Boore (1981). From spectral scaling studies, Nuttli and Herrmann (1984) established theoretical m_b magnitude scaling coefficients for PHA and PHV, assuming predominant frequencies of 5 and 1 Hz, respectively. Since their values represent m_b , they cannot be directly compared to the coefficients of Equations (2) and (3). However, they do give a relationship between m_b and M_s which may be used to convert their coefficients to a more compatible scale (Nuttli and Herrmann, 1982). So doing, their theoretically derived magnitude coefficients are 0.58 and 1.15 for PHA and PHV, respectively. Considering our restriction to near-source recordings, the far-source magnitude scaling characteristics of Equations (2) and (3) are quite consistent with those proposed by other investigators.

The near-source magnitude scaling characteristics of Equations (2) and

(3) cannot be compared with either of the previously referenced studies. McGuire as well as Joyner and Boore assumed magnitude scaling to be independent of distance, thereby restricting their results to the moderate-to-far-source distances representing the majority of their data. In addition, McGuire used hypocentral distance and Nuttli and Herrmann used epicentral distance as their measures of distance, measures found to result in substantially different near-source magnitude scaling characteristics than the fault distance measure used in this study (Campbell, 1981b). These differences also make it difficult to compare the near-source distance attenuation characteristics of the various relationships.

Site Geology. Table 2 indicates that PHV is strongly affected by the depth of the sediments beneath the site. Deep sites were found to be associated with velocities approximately 88 percent higher than sites underlain by very shallow sediments. While Trifunac and Lee (1978) have found a similar depth dependence for Fourier amplitude spectra, no similar study is available for PHV. We can, however, roughly compare differences in PHV between soil and rock established by other investigations with the results of this study. For example, Joyner and Boore (1981) found that soil sites exhibit peak horizontal velocities approximately 50 percent higher than rock sites, while Seed and Idriss (1982) suggest differences of about a factor of two. Both results are reasonably consistent with the results of this study. McGuire (1978), on the other hand, finds that PHV is relatively independent of site geology, but the small number of rock sites in his data base makes his results for rock subject to error.

PHV/PHA ratios. Ratios of PHV to PHA for deep sediment and basement rock sites are summarized in Tables 3 and 4. These may be compared with ratios suggested by others to assess the validity of the results. Seed and Idriss

(1982) indicate that recordings obtained within 50 km of the fault are consistent with PHV/PHA ratios of 55 cm/sec/g for rock and 110-135 cm/sec/g for soil. If we approximate the conditions representative of these ratios as an average of the ratios for $R=5-50$ km and $M=6.5-7.5$ in Tables 3 and 4, then we obtain corresponding ratios of 62 and 118 cm/sec/g for basement rock and deep sediments, respectively, in close agreement with those suggested by Seed and Idriss.

Newmark and Hall (1982) suggest PHV/PHA ratios of 92 and 122 cm/sec/g for rock and soil and Mohraz (1976) finds values of 65 and 85-133 cm/sec/g for rock and alluvium, respectively. While it is not clear for which magnitude and distance ranges these values are appropriate, they are found to be in general agreement with the average values given above. Campbell (1984) has estimated the ratios of PHV to PHV for a freefield site located approximately 15 km from a 7.5 M_g earthquake by several methods and suggests ratios of 70 and 125 cm/sec/g for basement rock and soil, respectively, in close agreement with ratios given in Tables 3 and 4.

Finally, the scaling relations of McGuire (1978) may be used to estimate PHV/PHA ratios to be compared with this study. Using $R=25$ km and $M=6.5$ as a means of comparison (this is near the centroid of data used in this study), McGuire's predictions give a ratio of 100 cm/sec/g for sites founded on soil, whereas this study (Table 3) gives a ratio of 97 cm/sec/g. Using $R=40$ km and $M=6.0$ as a means of comparison (this is near the centroid of the data used by McGuire), the ratio from McGuire's relations is again 100 cm/sec/g for soil sites, while that estimated from Equations (2) and (3) is 79 cm/sec/g. Again, the two studies are found to be in reasonably good agreement. Because of the limited number of rock sites in McGuire's data set, ratios for rock are considered unreliable and no comparisons were made.

CONCLUSIONS

Strong-motion data recorded on soil sites in the near-source region of moderate-to-large earthquakes have been used to update scaling relations for peak horizontal acceleration and velocity. These models may be used to predict ground motion parameters from earthquake magnitude, distance to the seismogenic zone of rupture, and other source, site and structure variables. For peak acceleration, such variables as fault mechanism, source directivity, building size, and instrument embedment are found to be important. For peak velocity, important variables are fault mechanism, source directivity, building size, and depth to basement rock. Both acceleration and velocity are found to become independent of magnitude at the source of $M \geq 5.0$ earthquakes, attaining median values of 1.05 g for peak horizontal acceleration and 88 cm/sec for peak horizontal velocity. Median plus 2 to 3 σ values for these parameters are found to agree with upper bounds suggested by geophysicists as interpreted from simple models of rupture mechanics.

A comparison of this study with the results of other recent investigations indicates that the scaling relations developed in this study are quite consistent with these other studies with respect to magnitude scaling, site geology, and ratios of velocity to acceleration. One area of disagreement involves the relative attenuation rate of peak acceleration and peak velocity. Although not statistically significant, this study has found acceleration to attenuate at a slightly lower rate than velocity, whereas other recent studies have found velocity to attenuate at either the same or at a slightly lower rate than acceleration at similar distances. This discrepancy may result from the effects of source directivity in the data,

which tend to bias near-fault values of peak velocity to higher values, resulting in a greater rate of attenuation than would otherwise be found.

Because of the provisional nature of the distances and sediment depths used in this study, the scaling relations presented in this paper are subject to some revision in the future. However, no substantial modification is anticipated and any revision would probably be no greater than that resulting from a periodic revision of the relations as new data become available.

RECOMMENDATIONS FOR APPLICATION TO THE WASATCH REGION

The scaling relations presented in this paper are believed to be generally applicable to the prediction of ground motion parameters in the near-source region of moderate-to-large earthquakes associated with the Wasatch fault zone. The attenuation characteristics of the northcentral Utah region have been found to be similar to that of California (King and Hays, 1977; McGuire, 1984) from which the majority of the strong-motion recordings used in this study have come. In any event, differences in anelastic attenuation are not important at these near-source distances.

Of some concern is the fault mechanism of earthquakes on the Wasatch fault zone. Geologic investigations indicate that the predominant mode of faulting is normal or normal-oblique. McGarr (1982) suggests from stress considerations that such events are associated with lower amplitudes of ground motion than those from strike-slip faults, and still even lower amplitudes than those from reverse or thrust faults. This study offers empirical justification for differences in the later two fault mechanisms (strike-slip versus reverse), but the current data are not sufficient to empirically establish differences between normal mechanisms and either strike-slip or

reverse mechanisms. This will have to await the addition of normal fault recordings to the data base. For the time being, it is recommended that one make predictions using a strike-slip mechanism with the understanding that these estimates may be somewhat higher than actually observed.

While rock records were specifically excluded from this study, estimates for rock may be obtained using the following guidelines. Consistent with the results of Campbell (1981a, 1983, 1984) and Joyner and Boore (1981), freefield predictions of peak horizontal acceleration for rock may be assumed to be equivalent to those for soil. In this case, Equation (2) should be used with K_4 through K_6 set equal to zero. For peak horizontal velocity, Equation (3) may be used for both soil and rock by using an appropriate value for D, the depth to basement rock (Table 2). Predictions for basement rock may be obtained by setting $D=0$. For soil and sedimentary rock sites, freefield predictions of peak velocity may be estimated by setting D equal to the depth of sediments for the site of interest, setting K_3 and K_4 equal to zero.

Since near-source scaling relations for response spectra are not yet available, it is suggested that the procedure recommended by Newmark and Hall (1982) for developing spectra from peak acceleration and velocity be used when estimates of pseudo-relative velocity are required (see their Tables 1 and 2 and Figure 5). To establish the low-frequency portion of the spectrum, an estimate of peak horizontal displacement (PHD) will be required. Using the recommendation of Newmark and Hall, this parameter may be estimated from peak acceleration and velocity from the dimensionless ratio $(PHA \cdot PHD)/(PHV)^2$. Newmark and Hall (1982) suggest a value of 6.0 for this ratio, independent of site geology, whereas Mohraz (1976) suggests values of 4.0 for alluvium and 5.0 for rock.

REFERENCES

- Campbell, K. W. (1981a). Near-source attenuation of peak horizontal acceleration, Bull. Seism. Soc. Am., v. 71, p. 2039-2070.
- Campbell, K. W. (1981b). A ground motion model for the central United States based on near-source acceleration data, Proc. of Earthquakes and Earthquake Engineering: The Eastern U.S., Knoxville, Tennessee, 1981, v. 1, p. 213-232.
- Campbell, K. W. (1982). Near-source scaling characteristics of peak horizontal acceleration for moderate-to-large earthquakes, Proc. of Conference XVI - Workshop on the Dynamic Characteristics of Faulting as Inferred from Recordings of Strong Ground Motion, Incline Village, California, 1981, U.S. Geological Survey Open-File Rept. 82-591, v. I, p. 120-184.
- Campbell, K. W. (1983). The effects of site characteristics on near-source recordings of strong ground motion, Proc. of Conference XXII - Workshop on Site Specific Effects of Soil and Rock on Ground Motion and their Implications for Earthquake-Resistant Design, Santa Fe, New Mexico, 1983, U.S. Geological Survey Open-File Rept. 83-845, p. 280-309.
- Campbell, K. W. (1984). An empirical assessment of near-source strong ground motion for a $6.6m_b$ ($7.5M_s$) earthquake in the eastern United States, U.S. Nuclear Regulatory Commission Report (in press).
- King, K. W. and W. W. Hays (1977). Comparison of seismic attenuation in northern Utah with attenuation in four other regions of the western United States, Bull. Seism. Soc. Am., v. 67, p. 781-792.
- Joyner, W. B. and D. M. Boore (1981). Peak horizontal acceleration and velocity from strong-motion records including records from the 1979

no
page 15

- Imperial Valley, California, earthquake, Bull. Seism. Soc. Am., v. 71, p. 2011-2038.
- McGarr, A. (1982). Upper bounds on near-source peak ground motion based on a model of inhomogeneous faulting, Bull. Seism. Soc. Am., v. 72, p. 1825-1841.
- McGuire, R. K. (1978). Seismic ground motion parameter relations, J. Geotech Engrng. Div., ASCE, v. 104, p. 481-490.
- McGuire, R. K. (1984). Estimation of seismic ground motion in northern Utah, Dames and Moore report to U.S. Geological Survey, Golden, Colorado.
- Mohraz, B. (1976). A study of earthquake response spectra for different geological conditions, Bull. Seism. Soc. Am., v. 66, p. 915-935.
- Newmark, N. M. and W. J. Hall (1982). Earthquake Spectra and Design, Earthquake Engineering Research Institute Monograph, Berkeley, California.
- Nuttli, O. W. and R. B. Herrmann (1982). Earthquake magnitude scales, J. Geotech. Engrng. Div., ASCE, v. 108, p. 783-786.
- Nuttli, O. W., and R. B. Herrmann (1984). Ground motion of Mississippi Valley earthquakes, J. Tech. Topics in Civil Engrng., v. 110, p. 54-69.
- Seed, H. B. and I. M. Idriss (1982). Ground motions and soil liquefaction during earthquakes, Earthquake Engineering Research Institute Monograph, Berkeley, California.
- Trifunac, M. D. and V. W. Lee (1978). Dependence of Fourier amplitude spectra of strong motion acceleration on the depth of sedimentary deposits, Univ. of So. California Dept. of Civil Engrng. Rept. CE78-14, Los Angeles, California.

TABLE 1

Summary of Coefficients e_1 in Equation (2)
(Peak Horizontal Accelerations)

Index (i)	Variable (K_i)	Function	Coefficient (e_i)
1	Fault Mechanism	$K_1=0$ (Strike-slip) $K_1=1$ (Reverse & reverse oblique)	0.32
2	Shallow Soil	$K_2=0$ (Soils >10m deep) $K_2=1$ (Soils \leq 10m deep)	0.41
3	Source Directivity (Deep sediments)	$K_3=0$ (Other rupture configurations) $K_3=1$ (Rupture towards site)	0.52
4	Small Embedded Building	$K_4=0$ (Other recordings) $K_4=1$ (Basements of 3-9 story bldgs.)	-0.85
5	Large Embedded Building	$K_5=0$ (Other recordings) $K_5=1$ (Basements of \geq 10 story bldgs.)	-1.14
6	Small & Large Embedded Building (Distance Variable)	$K_6=(K_4+K_5) \tanh(0.068 R)$	0.87

TABLE 2

Summary of Coefficients e_1 in Equation (3)
(Peak Horizontal Velocity)

Index (1)	Variable (K_1)	Function	Coefficient (e_1)
1	Fault Mechanism	$K_1=0$ (Strike-slip) $K_1=1$ (Reverse & reverse oblique)	0.47
2	Source Directivity (Deep sediments)	$K_2=0$ (Other rupture configurations) $K_2=1$ (Rupture towards site)	0.95
3	Building Size	$K_3=0$ (Buildings ≥ 5 stories) $K_3=1$ (Freefield and bldgs. < 5 stories)	0
4	Sediment Depth (Freefield & Small Bldgs.)	$K_4=K_3 \tanh(0.39 D)$	0.63
5	Sediment Depth (Large Bldgs.)	$K_5=(1-K_3) \tanh(0.75 D)$	0.72

TABLE 3

Median Predictions of Peak Horizontal Ground Motion for
Freefield Soil or Deep Sediment Recordings of a Strike-Slip Earthquake

Distance ^(b) (km)	Magnitude (M)	PHA (g)	PHV (cm/sec)	PHV/PHA (g/cm/sec)
5(0)	5.5	0.26	23	88
	6.5	0.41	47	115
	7.5	0.57	81	142
10(9)	5.5	0.14	11	79
	6.5	0.24	26	108
	7.5	0.38	52	137
25(24)	5.5	0.054	3.8	70
	6.5	0.10	9.7	97
	7.5	0.18	23	128
50(50)	5.5	__(a)	__(a)	__(a)
	6.5	0.047	4.3	91
	7.5	0.089	11	124

(a) There is no data at this distance.

(b) Distance to the seismogenic zone of rupture. Value in parentheses represents the corresponding distance to the surface trace of a vertical fault with 5 km of sediments.

TABLE 4

Median Predictions of Peak Horizontal Ground Motion for
Freefield Basement Rock Recordings of a Strike-Slip Earthquake

Distance ^(b) (km)	Magnitude (M)	PHA (g)	PHV (cm/sec)	PHV/PHA (g/cm/sec)
0	5.5	1.05	88	84
	6.5	1.05	88	84
	7.5	1.05	88	84
5(0)	5.5	0.26	12	46
	6.5	0.41	25	61
	7.5	0.57	43	75
10(9)	5.5	0.14	5.8	41
	6.5	0.24	14	58
	7.5	0.38	28	74
25(24)	5.5	0.054	2.0	37
	6.5	0.10	5.1	51
	7.5	0.18	12	67
50(50)	5.5	---(a)	---(a)	---(a)
	6.5	0.047	2.3	49
	7.5	0.089	5.8	65

(a) There is no data at this distance.

(b) Distance to the seismogenic zone of rupture. Value in parentheses represents the corresponding distance to the surface trace of a vertical fault with 5 km of sediments.

APPLICATION OF GROUND FAILURE MAPS TO EARTHQUAKE HAZARD REDUCTION

By

T. Leslie Youd

U.S. Geological Survey

Menlo Park, CA 94025

and

Brigham Young University

Provo, UT 84602

INTRODUCTION

The National Program for Earthquake Hazards Reduction stipulates that regional earthquake hazards assessments be conducted in urban areas "identified as having moderate to high risk, including analyses of potential ground shaking and ground failure on a regional scale and the demonstration of specific hazard assessment techniques unique to each region. (This does not include block-by-block analyses (microzoning), which are more properly performed at the State and local level.)" In response to this requirement, techniques have been developed for compiling maps of liquefaction and ground failure potential on a regional scale, and maps for several regions have been completed.

Methods for applying these maps by state and local governments, financial, insurance, and other private groups to reduce earthquake hazards, however, are still largely in the developmental state. The purpose of this paper is to examine some applications and benefits that are presently being derived from these maps.

AVAILABILITY OF LIQUEFACTION AND GROUND FAILURE MAPS FOR UTAH

Utah State University and Dames and Moore Consulting Engineers (Anderson, this volume) are preparing a series of liquefaction potential maps for several counties in the State under sponsorship of the U.S. Geological Survey. A map for Davis County has been completed and maps are in preparation for Salt Lake and Utah Counties. Contracts are being prepared for compilation of liquefaction potential maps for additional counties in the northern part of the state and also for evaluation of regional landslide hazards along the steep Wasatch Mountain front. These maps are regional in scale and are more valid for comparing the relative hazard in one area or zone versus another than for making decisions about the hazard at a particular site. Site specific geotechnical studies are required to make the latter determination.

APPLICATION OF LIQUEFACTION AND GROUND FAILURE MAPS

Considerable progress has been made in compiling maps showing areas subject to liquefaction; application of these maps, however, to reduce or mitigate liquefaction hazards is still in a developmental-experimental state. There are three general areas where effort is being made to use these maps - land use planning, building code provisions, and bases for insurance rate and other financial decisions.

Land use planning.--The broadest attempt to date in this country to mitigate earthquake hazards through land use planning is the required inclusion of a seismic safety element in the general plan of each county and community in the

state of California. Each seismic safety element considers liquefaction and ground failure along with other earthquake hazards. With respect to liquefaction and ground failure, the elements generally define the processes and associated hazards, give general information on areas in the community where susceptible materials might lie, state general plan requirements for potentially hazardous areas, and suggest zoning and engineering measures to mitigate the hazard. A statement from the Fremont, California Seismic Safety Element is given here as an example:

The areas subject to general ground failure presently have General Plan designations of industrial use, public open space use, medium density residential use, and transportation facilities, including portions of the Fremont Airport. These areas are located in the westernmost portion of the Northern Plain, in the Baylands, and in the industrial area. The most westerly of these lands are classified by the U.S. Soil Conservation Service as Land Capability Class VIII. Such lands will be designated Open Space when the Baylands Area plan is amended to implement the Open Space Element of the General Plan. The remainder of the soils in this area have a Land Capability Classification of III and would not be designated Open Space. Development need not be totally prohibited in either of these areas. However, thorough testing of the liquefaction potential of any proposed development site should be required. In general, these areas will be more appropriate for light, low structures and for low intensity uses than for tall structures and intensive uses.

Seismic Safety Elements are being used as a valuable aid to California communities for understanding their earthquake hazards and for implementing planning and regulatory measures to mitigate the consequences. Examples of

planning measures that have been implemented based on information produced for the elements are set-backs from active faults and improved building code provisions. Additional benefits and more conscious use of the available information will likely develop as more experience is gained.

Building codes.--The influence of soil conditions on the response of buildings to earthquake shaking has long been recognized and criteria incorporated into some building codes to account, at least in part, for that influence. Code provisions to consider the effects of liquefaction and ground failure, however, are only now being developed. A pioneering effort in this area is occurring in the City of San Diego, California. A tentative code element has been drafted and approved by several key committees and final inclusion in the city building code and city approval is expected (oral communciation, Andrew Dawson, Woodward-Clyde Consultants, March 1984). The San Diego element (see appendix to this paper) primarily requires specific engineering investigation for various classes of construction where these developments are to be located in potential liquefaction areas as delineated in the Seismic Safety Element of the General Plan. In this instance, the Building Code and the Seismic Safety Element are complimentary. This element might serve a as model for other communities, including those in Utah with potential liquefaction problems. If adopted and implemented, this element should significantly reduce the risk of damage from liquefaction to major new construction in San Diego, while allowing wavers for relatively low-cost, low-occupancy construction, such as residential housing, where the owner is willing to accept the risk rather than pay for the expense of an engineering investigation.

Financial and Insurance Considerations

Although liquefaction and ground failure potential maps appear to be well suited for use by insurance companies to set rates based on risk and by other financial companies as a factor in the decision making processes, this writer knows of very little application in these areas. Possible incentives from favorable financial decisions and insurance rates and financial requirements for safe siting of constructed works could have considerable beneficial impact for earthquake hazard mitigation. Such measures could also provide means for local property owners and communities to repair or reconstruct damaged facilities without calling for emergency help from state and federal governments.

Appendix - Code Element on Liquefaction

Tentatively Approved For San Diego, California Building Code

(condensed and slightly reworded by the author)

Soil Liquefaction: These requirements are applicable to "potential liquefaction" areas as identified in the Seismic Safety Element of the General Plan for the City of San Diego.

Exception: An evaluation of the liquefaction potential and mitigation measures if necessary are required for any site, regardless of location, if an essential facility is to be located at the site (see item 1.A., below).

1. Investigations: An investigation conforming to Section 2905 shall be made of subsurface soils to evaluate their susceptibility to liquefaction from earthquake-induced ground shaking for the following structure or occupancy categories.

A. Essential facilities.

Essential facilities are those structures or buildings which must be safe and usable for emergency purposes after an earthquake in order to preserve the health and safety of the general public. Such facilities shall include but not be limited to:

1. Hospitals and other medical facilities having surgery or emergency treatment areas.
2. Fire and police stations.
3. Municipal government disaster operation and communication centers deemed to be vital in emergencies.

B. Buildings with an importance factor greater than 1.0 as specified in the tabulation below:

<u>Type of Occupancy</u>	<u>Importance Factor</u>
Essential facilities	1.5
Any building where the primary occupancy is assembly of more than 300 persons (in one room)	1.25
All others	1.0

C. All buildings over two stories in height.

D. All buildings containing the following occupancies:

1. Any building with an assembly room and a stage or with an assembly room with an occupant load of 300 or more without a stage, including such buildings used for educational purposes.
2. Any building used for educational purposes through the 12th grade by 50 or more persons for more than 12 hours per week or four hours in any one day.
3. a. Buildings for storage, handling, use, or sale of hazardous and highly flammable or explosive materials other than flammable liquids. b. Buildings for storage, handling, use, or sale of Classes I, II, and III-A liquids (includes dry cleaning plants, paint stores with bulk handling, paint shops, spray-painting rooms and shops).
4. a. Nurseries for the full-time care of children under the age of six accommodating more than five persons.
b. Hospitals, sanitariums, nursing homes with nonambulatory patients and similar buildings (each accommodating more than five persons).
c. Mental hospitals, mental sanitariums, jails, prisons, reformatories and buildings where personal liberties of inmates are similarly restrained.

- E. All buildings with an occupant load of more than 300 (as determined from Table 33-A of the building code).
- F. Tanks of more than 20,000 gallons capacity intended for storage of toxic, hazardous or flammable contents.
- G. Tanks over 35 feet high.
- H. Towers over 35 feet high.
- I. Other structures not included in categories A through H, except construction of a minor nature as determined by the Building Official, must either have an investigation made to evaluate if hazards are posed by the effects of liquefaction, and if so, to incorporate measures to mitigate the hazards or obtain a waiver from the Building Official. The waiver, which shall be executed by the legal owner, approved by the Building Official and recorded by the County Recorder, shall state the applicable facts relative to potential liquefaction and shall attest to the legal owners's knowldege thereof.

LEGAL ISSUES RELATED TO HAZARD MITIGATION POLICIES

by

James E. Slosson, Ph.D.

SLOSSON AND ASSOCIATES, INC.

14046 Oxnard Street

Van Nuys, California 91401

Professionals involved in design, construction, and maintenance of structures, facilities, and graded areas have become the target of litigation within the past decade when failures and losses have occurred. Recent out-of-court (or pre-trial) and Superior Court decisions in California indicate a recognizable trend toward holding the professional responsible when there is an indication of negligence and/or work that falls below that which a prudent and responsible professional would do. Prior to this change in philosophy by the courts, the professional had only to reach the level of quality commonly attained by other members of the prescribed discipline in the geographic area in which the professional worked; that locally-applicable level of quality has been called "standard practice".

Some judges have suggested it may be possible for "standard practice" in a given geographic area to be substandard relative to professional standards elsewhere. A professional who uses a lower standard adopted by a lax governmental jurisdiction for a project within that jurisdiction, but who meets or utilizes higher standards elsewhere, can be held responsible for a failure or loss resulting from the use of the lower standards, even though the lower standards are accepted by local government.

It will be interesting to monitor the course of the Utah courts during the next decade as they determine whether professionals and/or their firms, which offer service in both Utah and California, are allowed to ignore the higher standards (related to site analysis and design criteria) to which they are compelled to adhere in California in order to use the lower requirements acceptable in Utah. In cases involving severe damage to structures and loss of life, will the professional be able to argue that he or she knowingly dropped professional standards to address only the lower standards of care accepted in Utah with full knowledge that failure and loss of life might occur?

It is the opinion of the author that the courts will hold the professionals responsible for the highest standards that they meet in strict jurisdictions such as the city of Los Angeles or the State of California. Furthermore, the engineering geologist will most likely be held responsible to meet or exceed the standard of care outlined in the guidelines for reports developed more than a decade ago by the Association of Engineering Geologists (see attached). These guidelines were adopted by the California Division of Mines and Geology in 1973 (CDMG Notes #37) and the California Board of Registration for Geologists in 1979.

#####

GUIDELINES TO GEOLOGIC/SEISMIC REPORTS

The following guidelines are taken from "Geology and earthquake hazards: Planners guide to the seismic safety element" prepared by Grading Codes Advisory Board and Building Code Committee of the Southern California Section, Association of Engineering Geologists, July, 1973. They are reprinted here courtesy of the Association of Engineering Geologists.

I. Introduction

This is a suggested guide or format for the seismic section of engineering geologic reports. These reports may be prepared for projects ranging in size from a single lot to a master plan for large acreage, in scope from a single family residence to large engineered structures, and from sites located on an active fault to sites a substantial distance from the nearest known active fault. Because of this wide variation, the order, format, and scope should be flexible and tailored to the seismic and geologic conditions, and intended land use. The following suggested format is intended to be relatively complete, and not all items would be applicable to small projects or low risk sites. In addition, some items would be covered in separate reports by soil engineers, seismologists, or structural engineers.

II. The Investigation

A. Regional Review

A review of the seismic or earthquake history of the region should establish the relationship of the site to known faults and epicenters. This would be based primarily on review of existing maps and technical literature and would include:

1. Major earthquakes during historic time and epicenter locations and magnitudes, near the site.
2. Location of any major or regional fault traces affecting the site being investigated, and a discussion of the tectonic mechanics and other relationships of significance to the proposed construction.

B. Site Investigation

A review of the geologic conditions at or near the site that might indicate recent fault or seismic activity. The degree of detail of the study should be com-

patible with the type of development and geologic complexity. The investigation should include the following:

1. Location and chronology of local faults and the amount and type of displacement estimated from historic records and stratigraphic relationships. Features normally related to activity such as sag ponds, alignment of springs, offset bedding, disrupted drainage systems, offset ridges, faceted spurs, dissected alluvial fans, scarps, alignment of landslides, and vegetation patterns, to name a few, should be shown on the geologic map and discussed in the report.
2. Locations and chronology of other earthquake induced features caused by lurching, settlement, liquefaction, etc. Evidence of these features should be accompanied with the following:
 - a. Map showing location relative to proposed construction.
 - b. Description of the features as to length, width and depth of disturbed zone.
 - c. Estimation of the amount of disturbance relative to bedrock and surficial materials.
3. Distribution, depth, thickness and nature of the various unconsolidated earth materials, including ground water, which may affect the seismic response and damage potential at the site should be adequately described.

C. Methods of Site Investigation

1. Surface investigation
 - a. Geologic mapping.
 - b. Study of aerial photographs.
 - c. Review of local ground water data such as water level fluctuation, ground water barriers or anomalies indicating possible faults.
2. Subsurface investigation
 - a. Trenching across any known active faults and suspicious zones to determine location and recency of movement, width of disturbance, physical condition of fault zone materials, type of displacement, and geometry.

(over)

b. Exploratory borings to determine depth of unconsolidated materials and ground water, and to verify fault-plane geometry. In conjunction with the soil engineering studies, obtain samples of soil and bedrock material for laboratory testing.

c. Geophysical surveys which may indicate types of materials and their physical properties, ground water conditions, and fault displacements.

III. *Conclusions and Recommendations*

At the completion of the data accumulating phase of the study, all of the pertinent information is utilized in forming conclusions of potential hazard relative to the intended land use or development. Many of these conclusions will be revealed in conjunction with the soil engineering study.

A. *Surface Rupture Along Faults*

1. Age, type of surface displacement, and amount of reasonable anticipated future displacements of any faults within or immediately adjacent to the site.
2. Definition of any areas of high risk.
3. Recommended building restrictions or use-limitations within any designated high risk area.

B. *Secondary Ground Effects*

1. Estimated magnitude and distance of all relevant earthquakes.
2. Lurching and shallow ground rupture.
3. Liquefaction of sediments and soils.
4. Settlement of soils.
5. Potential for earthquake induced landslide.

IV. *Presentation of Data*

Visual aids are desirable in depicting the data and may include:

A. *General data*

1. Geologic map of regional and/or local faults.
2. Map(s) of earthquake epicenters.
3. Fault strain and/or creep map.

B. *Local or site data*

1. Geologic map.
2. Geologic cross-sections illustrating displacement and/or rupture.
3. Local fault pattern and mechanics relative to existing and proposed ground surface.
4. Geophysical survey data.
5. Logs of exploratory trenches and borings.

V. *Other Essential Data*

A. *Sources of data*

1. Reference material listed in bibliography.
2. Maps and other source data referenced.
3. Compiled data, maps, plates included or referenced.

B. *Vital support data*

1. Maximum credible earthquake.
2. Maximum probable earthquake.
3. Maximum expected bedrock acceleration.

C. *Signature and license number of geologist registered in California*

JES 8/73

WASATCH FRONT HAZARDS INFORMATION SYSTEM

by

Arthur C. Tarr, U.S. Geological Survey, Denver, CO 80225

and

Don R. Mabey, Utah Geological and Mineral Survey,

Salt Lake City, UT 84108

INTRODUCTION

If data are to be widely used by a diverse group of users, the data should be organized in a fashion that permits easy identification and access. The Information Systems component of the "Regional and Urban Earthquake Hazards Evaluation: Wasatch Front, Utah" addresses that requirement. A large but unorganized amount of data relating to the earthquake hazard along the Wasatch Front already exists in published maps, reports, and computerized data sets. As research studies continue and mature, the data base will grow. If these data are properly organized, the resultant data base would be an extremely valuable resource to a wide variety of user groups.

OBJECTIVES

The objectives of this component are: 1) to make quality data readily available to meet the needs of researchers and policymakers, 2) to create an information system that assures that new data will be available in the form most useful to meeting program objectives, 3) to devise a system whereby potential users will have easy access to data in media, scales, and formats that will be most useful to them, and 4) to provide continuing information on objectives and progress of the program element. Accomplishing these objectives will require: 1) inventorying

existing data sets, 2) developing data standards for critical data sets, 3) identifying user groups and their needs, 4) developing strategies for data management and data dissemination, and 5) assuring that pertinent hazards data are available to the user community.

IMPLEMENTATION

Accomplishing the above objectives will require the concerted efforts of many individuals and institutions. We realized that establishing a kind of information "clearinghouse" early on would provide a focus for the Information Systems component and further, would expedite accomplishing the more difficult objectives. One initial manifestation of the clearinghouse concept is the Information Directory, an informally-produced and regularly-updated guide to all kinds of resources: personnel, publications, computers and other tools, data bases, and software. The Information Directory is intended, in part, to be the repository of lists of existing data sets, computer programs, base materials, and project personnel. The Information Directory is also intended to provide access to key contacts, people who can answer questions easily and fast, and access to procedures that can provide a needed item (such as a base map) rapidly.

Another manifestation of the clearinghouse concept is the Newsletter that will be prepared and published quarterly by the USGS and UGMS. The Newsletter will contain ephemeral and newsy items of interest to participants and associates in the form of brief progress reports of scientific studies, lists of new publications, an event calendar listing technical meetings and conferences with abstract due dates, short articles written by participants, and descriptions of new projects. The

Newsletter and Information Directory are intended to be complementary in their scope of information dissemination.

The inventory of existing resources has identified two areas of particular interest. For example, the UGMS supports a computerized bibliography of geotechnical literature about Utah that potentially could be extremely valuable for literature searches. The bibliography is, however, not as comprehensive or complete in the geophysical literature as we believe desirable for the Urban Hazards Evaluation. The UGMS has targeted the upgrade of the bibliography as a priority task this year. Another example is the need for a single, accepted earthquake catalog of Utah. The absence of a standard catalog perpetuates confusion and the appearance of disagreement when no substantial disagreement may actually exist. We believe a committee of experts should be convened to resolve the conflicts among the existing Utah earthquake catalogs, and the resultant catalog and an accompanying map published.

Progress has been made in developing data management and dissemination strategies. Procedures for accessing bibliographies of Utah geology and Wasatch Front base materials have been incorporated into the Information Directory. An upgrade of the UGMS computer system to increase its capability for data communications and advanced data processing is underway. Following completion of the upgrade, communications tests and other experiments are planned to expedite exchange of data sets and software between computer centers.

SEISMICITY AND EARTHQUAKE HAZARDS OF UTAH AND THE WASATCH FRONT:

PARADIGM AND PARADOX

(An Extended Abstract)

by

Robert B. Smith, and William D. Richins.

University of Utah

Department of Geology and Geophysics

University of Utah Seismograph Stations

Salt Lake City, Utah 84112-1183

I. INTRODUCTION

The impressive topographic break at the base of Wasatch Range east of Salt Lake City marks the location where colonizer Brigham Young said in 1847 "This is the place." The mountains to the east rise 2000 m above the densely populated valley floor to the west and indeed mark the place where large earthquakes have played a prophetic role in the structural evolution of the Wasatch Front.

Crustal uplift during the past 15 million years has produced 4500 m of total displacement along the Wasatch fault, no doubt accompanied by large prehistoric earthquakes. The youthful Wasatch fault is considered tectonically active today. Thus, residents of the Wasatch Front should recognize that they live in an active tectonic environment where contemporary mountain-building

processes produce a continuing state of readjustment and concomitant earthquakes. The geologic symbiosis between the development of fertile valleys on the west and the spectacular Wasatch Mountains on the east results in a unique location for a major urban center, but it also necessitates a thorough evaluation of its attendant earthquake hazards.

Much of our new information on earthquakes in Utah has been gathered by the University of Utah Seismograph Stations, a modern computer-recorded 76-station radio telemetered network that monitors the active fault zones of the southern Intermountain Seismic Belt in Utah and surrounding areas, but focuses on the Wasatch Front urban corridor. Utilizing seismological, geodetic, and geologic data we will review the tectonic framework, structural style, geology, and temporal-spatial variations of seismogenic zones. Fault zone characteristics inferred from mapping and analyses of active faults combined with geophysical and geological information provide a tectonic model for potential large earthquakes. New studies of fault segmentation, maximum magnitudes expected, inversion of seismic moment tensors, and statistical evaluation of recurrence intervals provide estimates of earthquake potential. Ultimately, these data taken together with engineering requirements and plans for urban development can provide the fundamental information for delineation and evaluation of earthquake hazards in the Wasatch Front urban region. Our principal focus will be on the Provo-Salt Lake City-Ogden urban corridor, but will include information from the surrounding areas in Utah and in neighboring states where earthquake hazards are similar.

In the past decade, we and our colleagues at the University of Utah have investigated many aspects of seismicity in Utah. Many of our discussions here

rely upon our combined research efforts for which we appreciate the collaborative contributions of our colleagues. The paper presented here also relies heavily upon seismic reflection data, geometry of the fault zone, and general conclusions on potential earthquake nucleation on normal faults that were defined by Smith and Bruhn (1984).

Earthquake hazards of the Wasatch Front were first recognized by G. K. Gilbert, a pioneering geologist of the 19th century, who in a letter to the Salt Lake Tribune on September 16th, 1883 (Gilbert, 1883) described the location of fault scarps along the Wasatch Front and warned of impending large earthquakes;

"It is useless to ask when this disaster will occur. Our occupation of the country has been too brief for us to learn how fast the Wasatch grows; and, indeed, it is only by such disasters that we can learn. By the time experience has taught us this, Salt Lake City will have been shaken down."

Gilbert further recognized the location and, hence, the importance of the Wasatch fault;

"When the earthquake comes, the severest shock is likely to occur along the line of the great fault at the foot of the mountains."

Gilbert's astute observations on the geometry and structural style of the Wasatch fault were summarized in a U.S. Geological Survey Professional Paper titled "Studies of Basin-Range Structure" (Gilbert, 1928).

Following the work by Gilbert, many geophysicists and geologists of University, U.S. Geological Survey, and private consultant affiliations have studied earthquake hazards and active faulting throughout the Wasatch Front and Utah. Their results will not be repeated here, but the interested reader is referred to a summary of "Earthquake Studies of Utah, 1850-1978," edited by

Arabasz, Smith, and Richins (1979) for a detailed documentation of earthquake information for the state of Utah current to 1978. Subsequent earthquake catalogs are available for the Utah region in Richins et al. (1981) and Richins et al. (1984b). Estimates of possible earthquake losses in the Salt Lake City area were investigated by the U.S. Geological Survey (1976). Further assessment of earthquake hazards of the Wasatch Front is contained in the USGS Open-File Report 80-801 (1980), that includes discussions by Bucknam et al. (1980) and Hayes et al. (1980) regarding probability of exceedance of ground acceleration and empirical scaling of strong ground motion. Results from trenching and mapping of individual segments of the Wasatch fault were summarized by Swan et al. (1980).

Current interest in understanding and mitigating earthquake hazards of the Wasatch Front by the U. S. Geological Survey, Earthquake Hazards Reduction Program is focused on the Salt Lake City-Ogden-Provo urban corridor. This national program places highest priority on delineation of earthquake hazards and risk assessment. Discussions in this paper will focus primarily on the tectonic framework, source zone characterization, and mechanism of normal fault earthquake nucleation on the Wasatch Front--properties required to assess earthquake hazard and risk.

II. PARADIGM AND PARADOX

The occurrence of the M7.3 Borah Peak, Idaho, earthquake, October 28, 1983, not only shocked our senses regarding the potential of large magnitude earthquakes in the eastern Basin-Range environment, but provided important incentives and lessons for evaluating the potential for earthquake hazards for the geologically similar Wasatch fault. This important geological event not

only stirred our scientific curiosity, but reminded us of the potential crustal deformation and ground shaking that could accompany a large earthquake on the Wasatch Front as well as providing new scientific models of earthquake nucleation that may be applied to the Wasatch fault (Richins, et al., 1984a; Doser, 1984).

The past half decade has been a period of renewed studies of earthquakes in the Intermountain region accentuated by new techniques such as determining strain rates from the seismic moment tensor (Doser and Smith, 1982) and from geodetic methods (Snay et al., 1984). Detailed evaluations of the M7.5, 1959 Hebgen Lake earthquake, Montana, (Doser, 1984) and the M7.3, 1983 Borah Peak earthquake (Richins et al., 1984a) provided important insights into the nucleation process of normal fault events. Detailed microearthquake studies in central Utah by McKee and Arabasz (1981), investigation of the seismogenic potential of normal faulting by Smith and Bruhn (1984), and detailed studies of faults using gravity by Zoback (1983) provided important insights into the earthquake generation process of the Intermountain region.

The recent investigations incorporating early findings provide a new framework for evaluating normal faulting earthquakes. They not only provide answers to important issues, but raise several new questions. We suggest several of the important paradigms and paradoxes below:

1. In the past 30 years, the three largest earthquakes in the western United States were associated with normal faulting that occurred in the Basin-Range environment (1954, Fairview Peak, Nevada, M7.1; 1959 Hebgen Lake, Montana, M7.5; 1983 Borah Peak, Idaho, M7.3). These large earthquakes nucleated at depths of ~15 km near the bottom of the seismogenic layer on planar 40°-65° dipping faults that are displaced laterally 10-15 km from the surface rupture. Will large normal fault earthquakes on the Wasatch Front be of the same form, i.e. will large earthquakes nucleate beneath the populated central and

western areas of Wasatch Front valleys?

2. New seismic reflection data, regional tectonics, and rheologic models suggest that large normal faults in the eastern Basin-Range have planar to listric geometries with near-surface steep dips in unconsolidated sediments but moderate dips of 40° - 65° at depths of 4 to 10 km.
3. The temporal behavior of individual fault segments along the Wasatch Front may not be necessarily random and independent of adjacent zones. Are individual segments active for hundreds to tens of thousands of years while adjacent segments remain quiescent? Will future large earthquakes of M7+ occur along segments of known Quaternary-Holocene displacement on the Wasatch Front?
4. Contemporary strain rates from cumulative seismic moment tensors and geodetic measurements show general E-W extension at maximum rates of order 1 mm/yr in the Hansel Valley region of northwest Utah, but 1-2 orders of magnitude less on the Wasatch Front. Strain rates associated with prehistoric faulting inferred from Quaternary-deformation based on mapping and trenching, however, are significantly greater. Will areas of seismic quiescence be interrupted by large earthquakes equilibrating the long-term strain accumulation?
5. Empirical measurements of peak ground accelerations from normal faulting earthquakes may be 2 to 3 times smaller than accelerations from equivalent magnitude thrust-type earthquakes (McGarr, 1984). Does this conclusion apply to earthquake hazards assessment on the Wasatch Front?
6. Asymmetric back-tilt from hypothetical M7+ normal-fault earthquakes along the Wasatch Front can produce a heretofore uninvestigated hazard; inundation from adjacent bodies of water, i.e. the Great Salt Lake, Utah Lake, and Willard Bay. Flooding could encroach eastward several kilometers into developed urban, commercial and agriculture lands. This hazard is accentuated by high water stands.

III. WESTERN UNITED STATES PERSPECTIVE

The Intermountain Seismic Belt (ISB) is the general zone of seismicity that extends from southeastern Utah, through eastern Idaho, western Wyoming, and Montana and marks an intraplate boundary of the North American plate (Smith and Sbar, 1974). It is clearly less seismically active than the San Andreas fault, a major transform boundary, and relatively less active than the Walker Lane, central Nevada seismic zone (Figure 1). The map (Figure 1) of

modern instrumentally recorded earthquakes for the western United States (taken from Smith, 1978) demonstrates intense activity along the San Andreas fault in California where one magnitude eight and several magnitude 7+ earthquakes have occurred in historic time. In comparison, four magnitude 7+ earthquakes have occurred in the central Nevada seismic zone, and two magnitude 7+ earthquakes have occurred in the Intermountain region; the M7.5, 1959 Hebgen Lake, Montana, and the M7.3 1983 Borah Peak, Idaho, earthquakes.

The largest historic earthquakes in Utah were the 1934 Hansel Valley event of M_L 6.6 and the 1901 Richfield earthquake, M_L 6.5 (Figure 2). Only the Hansel Valley earthquake produced surface faulting with a 50 cm maximum vertical displacement along a north-south fault at the north end of Great Salt Lake. Six M_L 6.0-6.5 earthquakes have occurred throughout the Utah region but apparently none have produced surface rupture.

In general, the seismicity of the Intermountain Seismic Belt is characterized by occurrence rates of magnitude 7+ earthquakes on the order of hundreds to thousands of years compared to tens to hundreds of years for the San Andreas fault. Maximum magnitudes are not expected to exceed $M7-3/4$ for the Utah region, but may exceed magnitude 8 for the San Andreas fault.

An interesting observation from historical seismicity is that more large earthquakes (magnitude 7+) have occurred in the past 30 years in the Basin-Range environment of normal faulting ($M7.1$, Dixie Valley earthquake, 1954; $M7.5$ Hebgen Lake, Montana, earthquake, 1959; and $M7.3$ Borah Peak, Idaho, earthquake, October 1983) than have occurred during the same time period along the San Andreas fault. Prior to 1954 only three $M7+$ occurred in the Great Basin in the 19th century and early 20th century.

On a regional scale, Figure 2 shows that at least 17 historic earthquakes of $M \geq 6$ have occurred in the Intermountain region, notably at locations where general changes in direction of this major interplate seismicity zone occur. Arabasz and Smith (1981) noted that the Intermountain Seismic Belt extends 1300 km, but is segmented into several sectors with divergent trends. The larger $M6+$ earthquakes were generally located near the sector boundaries.

The ISB is difficult to define as a linear zone of earthquakes such as along the San Andreas fault. Rather diffuse seismicity extends across 100-200 km-wide zones with focal depths generally shallower than 15 km (Smith, 1978). A rather important conclusion noted by Smith and Sbar (1974) and since by several investigators is the poor correlation of earthquakes with major active faults.

The paucity of large $M7+$ surface-faulting earthquakes in historic time, despite abundant late Quaternary and Holocene fault scarps, further complicates the problem of earthquake evaluation using the seismic and geologic information independently. This makes it difficult to assess earthquake hazards on the basis of epicenter locations alone or by the presence of active fault zones alone. As will be described later, hazard evaluation requires the integration of information on assessment of the fault geometry with depth, its relationship to laterally displaced seismicity, and the relationship to timing and distribution of surface faulting.

An important observation from Figure 2 is the location of the Borah Peak $M7.3$ earthquake that occurred along a major northwest trending Lost River fault, with Quaternary-Holocene displacement but for which no earthquakes had been recorded in historic time, even by sensitive local microearthquake

surveys. Hait (1978) noted several Holocene displacement events along the segment of the Lost River fault that broke during the Borah Peak earthquake with a maximum vertical displacement of ~2.5 m. This earthquake occurred in one of three apparently active segments of the Lost River fault zone, with the southeastern segments having displacements 30,000 years and older. This observation suggests that Basin-Range normal faults may have temporal properties where individual segments are active for thousands of years with several scarp-forming events, while adjacent segments remain quiescent for tens of thousands of years. If this property is valid for the Wasatch Front it has important ramifications for evaluating earthquake hazards along the defined segments of the Wasatch fault.

III. EARTHQUAKES IN UTAH

The pattern of early historic earthquakes and Late Cenozoic faulting in Figure 3 (taken from Arabasz and Smith, 1979) shows the generally broad N-S trending zone of seismicity in Utah. Note that Cenozoic faults capable of generating earthquakes occur throughout most of the central and western portion of Utah, not only along the Wasatch fault. In this figure the largest earthquakes for the period 1850-1978 of approximately magnitude 4 or greater are shown. Epicenters for the early historic data are based upon personal felt reports and were not recorded instrumentally, thus the error in epicenters could be as large as $\pm 10-20$ km. Nonetheless, the epicenter patterns clearly delineate the active belt of diffuse seismicity characteristic of the southern Intermountain Seismic Belt.

A depiction of the past 22 years of instrumentally-recorded and computer located earthquakes in Utah is shown in Figure 4. In this diagram earthquakes

of magnitude 2.5 or greater were plotted from the University of Utah data file. Also, superimposed on the map is an outline of the Wasatch Front study area. Several papers have discussed the general trends, magnitude distribution, and relationship to geology of earthquakes in the Utah region and will not be repeated here. However, the reader is referred to the papers by Cook and Smith (1967), Smith and Sbar (1974), and most importantly to a volume published by the University of Utah Seismograph Stations titled "Earthquake Studies in Utah, 1850-1978" by Arabasz, Smith, and Richins (1979). The later document describes in detail the earthquake distributions as a function of time, methodologies for locating and calculating earthquake epicenters and magnitudes, and general studies of individual earthquakes.

Three general zones of seismicity in Utah are apparent from the detailed epicenter map (Figure 4): (1) a southwest-northeast trend 100-200 wide zone that extends from St. George to the vicinity of Richfield, (2) a central to northern Utah diffuse zone of earthquakes that trends generally north-south along either side of the Wasatch fault but with limited earthquake activity except at its northern and southern boundaries, and (3) a change to a northeast trend at the Utah-Idaho border including the two areas of significant activity; (a) the Pocatello Valley earthquake at the Utah-Idaho border, and (b) earthquake swarms near Soda Springs in southeastern Idaho. Induced seismicity related to extraction of coal in eastern Utah is clearly visible as three clusters of activity 100 km southeast of Provo. An important observation from the seismicity map is that practically the entire state of Utah has had earthquakes of magnitude 2.5 and greater in historic times demonstrating the on-going tectonic significance of this major intraplate region.

A rather important property of seismicity is the time variation of earthquake occurrence. For example, the seismic behavior of the Wasatch fault north and south of Salt Lake City since at least 1962 shows persistent zones of seismic quiescence or gaps in seismicity. Yet, we know very little about the timing of large earthquakes in Utah because none have occurred during historic time. Thus, the cyclic nature of earthquakes in terms of mainshock and aftershock distributions and their relationship to surface faulting is poorly understood for the Wasatch Front.

It is possible, however, to examine the spatial distribution of earthquakes as a function of time. To view the space-time patterns of earthquakes in Utah a computer-generated movie has been produced with the help of Einar Kjartansson, Assistant Professor of Geophysics, University of Utah. In this production, earthquakes are plotted on a color-graphics CRT where earthquake epicenters are located on a background map and magnitudes are scaled in color from the cool, blue-green colors for low magnitude to warm, orange-red colors for larger magnitudes. Two periods are presented: (1) the early historic record from December, 1853 through June, 1962; and (2) a modern historic record from July, 1962 through December, 1983. Discussions of the space-time variations from aftershock distributions and possible precursory manifestations will be discussed during the movie to be shown during the Workshop on "Evaluation of Regional and Urban Earthquake Hazards and Risk in Utah," August, 1984, meeting in Salt Lake City.

V. WASATCH FRONT: SEISMICITY AND FAULTING

A detailed epicenter and fault map of the general Wasatch Front region is shown in Figure 5. Here earthquakes from 1974 through 1982 are plotted on a

generalized tectonic map with bedrock geology, Laramide-Sevier thrust faults, and Late Cenozoic normal faults to examine the relationship between earthquakes and tectonic features. The most notable earthquake activity during the 1974-1982 period occurred in the Pocatello Valley-Hansel Valley area of northern Utah-southern Idaho where a magnitude 6.0 event occurred in March 1975 (Arabasz et al., 1979).

The most continuous zone of earthquake activity extends southward beneath the Bear River Range on the east side of Cache Valley terminating 20 km east of Salt Lake City. Earthquakes then occur along an east-west zone across the Salt Lake City-Magna area, in the vicinity of the M5.2 1962 Magna earthquake. This zone also has had prominent occurrences of earthquake swarms. Concentrated zones of activity extend across the Traverse Range south of the Salt Lake Valley and at the southern end of Utah Lake. A magnitude 3.9 event in 1982 occurred near Orem and near the Wasatch fault. Activity continues south as a notable trend along the Juab Valley displaced west of the Wasatch fault. Activity east of Ephraim is primarily mining induced activity.

The Wasatch fault, shown by a heavy line, extends from near Malad, Idaho, southward 370 km on the west side of the Wasatch Range (Figure 5). The notable quiescence of earthquakes along the Wasatch fault north of Salt Lake City, on the east side of the Salt Lake Valley, and south of Provo have been earlier recognized as seismic gaps by Smith and Sbar (1974) and Arabasz and Smith (1981), i.e. areas of seismic quiescence that otherwise would be expected to have earthquake activity along an active fault segment. One interpretation of the zones of low seismicity is taken from an analogy with plate tectonics where averaged over centuries or more, movement can be

expected at all points along the intraplate boundary. Thus, gaps in the seismic activity could be developed along a boundary such as the Wasatch fault as a result of the past occurrence of large earthquakes. Eventually these gaps will be filled in by future earthquakes. If this interpretation is valid, then areas of unusually low seismicity and areas of previous faulting may be regarded as having a higher probability for future large earthquakes.

Other possible explanations for the apparent low seismicity along the quiet zones of the Wasatch fault are: (1) release of strain energy by aseismic creep and by crustal rebound of Lake Bonneville, and (2) the return rate for large earthquakes is sufficiently large that the time window of the past ~100 years of recording was too small to sample the long-term seismicity. An important hypothesis to be tested, suggests that earthquakes occurring along the west side of the Wasatch fault, for example at Salt Lake City near Magna and along the Santaquin-Nephi-Levan area may reflect earthquakes associated with the westward extension of the Wasatch fault zone at depth. This topic will be discussed later.

To examine the role of pre-existing structures on the origin of the Wasatch fault, Smith and Bruhn (1984) hypothesized that the influence of pre-existing Laramide thrust sheets correlate in a general way with the surface delineation of fault zone segmentation as proposed by Schwartz and Coppersmith (1984). In Figure 6, a map of the distribution of thrust sheets and the Wasatch fault shows an interesting correlation of the segment boundaries with lateral terminations of the thrust sheets.

To examine the hypothesized westward extension of the Wasatch fault geometry, Smith and Bruhn (1984) interpreted several seismic reflection

profiles across the East Cache fault, the Wasatch fault, and adjacent fault zones in the Great Salt Lake. Figure 7 shows two seismic reflection profiles, one across the East Cache Fault near Logan where seismic reflections dipping westward beneath the Cache Valley may be interpreted as a low-angle listric fault that flattens at depths of approximately 4 km beneath the valley fill. Eastward stratal tilt of Quaternary and Tertiary sediments suggests the valley fill has rotated along this active fault zone.

A seismic reflection profile across the mouth of the Weber Canyon, south of Ogden (Figure 7), shows a lack of reflection truncation beneath or west of the projected location of a steeply dipping Wasatch fault. Rather a very low angle zone of reflection truncations begins near the fault and flattens to zero dip at ~ 2 km beneath the valley. Whether this reflection represents a fault can not be equivocally interpreted, but it is clear that the Wasatch fault is not imaged as a steeply dipping major through-going structure.

Additional seismic reflection profiles discussed by Smith and Bruhn (1984) and unpublished reflection data for the Brigham City area, the Great Salt Lake, the north Salt Lake City area, and near Levan show that the Wasatch fault zone varies in dip from values as steep as $\sim 60^\circ$ to as shallow as $\sim 40^\circ$ -- all suggestive of westward projection beneath the populated Wasatch Front. Thus, while the seismic reflection data do not provide a unique interpretation of the attitude and extent of faulting, it is clear that we must recognize that this structural style of normal-faulting may characterize M7+ earthquakes in an extensional environment.

VI. LESSONS FROM THE M 7.3 BORAH PEAK, IDAHO, EARTHQUAKE

On October 28, 1983 an M7.3 earthquake occurred along a segment of the Lost River fault zone, central Idaho. This major earthquake produced a 34-km long fault scarp with up to 2.5 m of near-vertical displacement along a known Quaternary fault. The Borah Peak earthquake was extensively instrumented by the University of Utah, the U.S. Geological Survey, and other collaborative investigators with up to 50-portable stations and provided extensive data for analysis (Richins et al., 1984a; Doser, 1984). The importance of the Borah Peak earthquake to the Wasatch Front is that its age and structural style are similar to that of the Wasatch Front.

Primary results of the Borah Peak earthquake analyses show that the main shock nucleated at a depth of ~ 16 km, but displaced 10-15 km laterally SW from the end of the surface rupture. Aftershocks extend along a zone parallel to the surface rupture, but displaced 10-20 km SW of the surface fault. Cross-sections of accurately determined foci of aftershocks show that they define a zone that dips southwesterly at $\sim 45^\circ$ (Richins et al., 1984a). A plane passing through the aftershock cluster intersects the hypocenter of the main shock whose fault plane solution (Doser, 1984) indicates a 49° southwest dip. Thus, it appears that the Borah Peak earthquake occurred on a moderately dipping planar fault zone where the main shock nucleated at the base of the seismogenic structure and propagated both upfault and northwestward along at least a 34 km segment.

An interesting observation from the central portion of the Borah Peak scarp near its point of maximum displacement is the attitude of the hanging-wall bedrock surface that dips at $\sim 45^\circ$ and projects southwest along the

subsurface extension of the fault plane mapped by the aftershock hypocenters. On the east side of the Salt Lake Valley, Gilbert (1928) noted that the adjacent hanging-wall blocks of the Wasatch fault had 45° W dips that he suggested project westward on the main Wasatch fault surface. Although Gilbert's (1928) interpretation of the shallow dip of the Wasatch fault has been controversial, the similarities of structural geometries between the Borah Peak earthquake and the Wasatch Front are striking.

VII. GEOMETRY OF FAULTING AND 'LIKELY' LOCATIONS OF FUTURE LARGE WASATCH FRONT EARTHQUAKES

During the past decade accelerated research on the Wasatch fault principally by trenching and detailed mapping (Schwartz and Coppersmith, 1984) have noted several important features: (1) the Wasatch fault can be divided into segments that appear to break as independent zones, and (2) individual segments have statistically different repeat times and displacement histories. Smith and Bruhn (1984) noted (also see Figure 6) that the Wasatch fault segmentation also correlates with the lateral termination of major Laramide thrust structures that disrupt fault plane continuity. We regard the current delineation of fault segmentation as preliminary with need for additional statistical and geological conformation they can provide a basis for a working model of Wasatch Front earthquakes.

By definition a segment is a sector of a major fault zone that may break independent of adjacent segments with each segment having its own displacement rate characteristics and history. Thus, one segment may become active while adjacent segments remain quiescent. The Borah Peak earthquake apparently occurred on one of approximately three segments that Hait (1978) showed has

had repeated displacement in Holocene time while the adjacent segments have been quiescent for the past 30,000 years. If these arguments are valid for the Wasatch fault then the segments themselves may be a starting point for estimating the location of likely future large earthquakes.

To compare the structural geology of large normal faulting events in the Basin-Range, Figure 8 shows cross-sections through the fault zones of three large, M7+ earthquakes, their inferred fault planes, fault plane solutions, and fault plane dip: (1) the 1954 Dixie Valley, Nevada, M7.1; (2) the 1959 Hebgen Lake, Montana, M7.5, and (3) the 1983 Borah Peak, Idaho, M7.3. These large earthquakes have occurred in the same intraplate extensional stress regime as the Wasatch Front and on planar faults with from 40° - 65° dip and nucleation depths ~ 15 km.

A hypothetical working model for large Wasatch Front earthquakes is one in which a westward-dipping fault zone could nucleate a large earthquake at a depths of ~ 15 km beneath the adjacent valley. This model has important implications because it suggests that the major earthquakes would occur beneath the populated centers of the Wasatch Front. Note that the histograms of aftershocks and on-going seismicity for the three major earthquakes in the Great Basin, including aftershocks as large as M6+ occur in the shallower seismogenic layer from the near-surface to the maximum depth of the major event (Figure 8).

Smith and Bruhn (1984) hypothesized that large M7+ shocks may nucleate at the base of a brittle layer perhaps in the upper part of a ductile layer where shear stresses are at a maximum. Thus, the intraplate extensional deformation of the Basin-Range could drive the energy system to maximum values of a few

hundred bars. This energy is then released by a major earthquake at the base of the seismogenic layer that propagates to the surface as a major surface faulting event. Aftershocks and inter-event seismicity in the upper-crust may reflect antithetic normal faulting and a homogeneous strain release in the deformed volume.

A plot of space-time seismicity from 1962 through 1978 along the Wasatch Front clearly demonstrates the development of zones of seismic quiescence or seismic gaps (Figure 9). The sector from Parry southward through the Ogden area is clearly aseismic at the M3+ level. A distinct increase in the seismicity occurs north of Salt Lake City along the east-west zone of the Salt Lake salient and in the Magna area where persistent earthquake swarms and a magnitude 5.2 earthquake in 1962 have occurred. This zone seems to mark the northern edge of the Salt Lake segment where most of these earthquakes occur 10 to 20 km west of the Wasatch fault. The south end of the Salt Lake segment is marked by activity along the Traverse Range, but seismic quiescence is apparent from Orem southward to approximately Santaquin at the north end of the Nephi segment. Notable activity occurs near the Wasatch fault and westward beneath the Levan segment beneath the Juab Valley (McKee and Arabasz, 1982).

The question then arises, are the zones of seismic quiescence truly seismic gaps and at what magnitude level are they significant? If one applies the westward-dipping hypothetical Wasatch fault model (Figure 10), earthquakes occurring west of the Wasatch fault such as near Magna, the Traverse Range, and the extensive zone south of Santaquin may represent down-dip activity associated with past large Wasatch Front events. While this hypothesis cannot

be tested without detailed seismic reflection profiling and accurate earthquake monitoring, it nevertheless provides a plausible explanation.

Also, note that the Traverse Range and Salt Lake City-Magna earthquake zones occur near bedrock salients that extend westward from the main fault a few kilometers and may further act as stress concentrators or asperities at the ends of individual segments. Here the seismicity may be related to additional stored energy from stress heterogeneities.

VIII. EARTHQUAKE PRODUCED FLOODING

An important result of faulting associated with large normal-fault earthquakes is the asymmetric back-tilt of the footwall block. This property was well developed in the M7.5 Hebgen Lake earthquake where a maximum of 6.1 m displacement occurred at the surface fault, with back-tilt extending ~18 km in width and 30 km in length at the top of the footwall block. Recognizing that large bodies of water occur in close proximity to the Wasatch fault, eastward tilt in response to a large earthquake on the Wasatch fault could introduce an unrecognized hazard. For the purposes of comparison we have superposed the observed subsidence from the M7.5 Hebgen Lake earthquake and calculated the ground deformation for this hypothetical event at three locations along the Wasatch fault, at: (1) Bountiful, (2) Salt Lake City, (3) Provo-Springville. The effect of the backward tilt is flooding into the zones of subsidence (Figure 10). Selecting the high water mark of 4209 feet for the Great Salt Lake allowed inundation eastward into the Bountiful area with flooding extending eastward to the Interstate I-15. In the Salt Lake City example, flooding extended southeast from the north end of Salt Lake City to approximately 6th West. In central Utah, Utah Lake at a undeformed level of 4494 feet could

inundate areas east of the Interstate I-15, between Provo and Springville. Note that these hypothetical models are simply a hazard scenario that, heretofore, has been unrecognized and cannot be applied to the Wasatch fault without more investigations. For example, the extent of inundation depends upon location of faulting, dip, and total displacement, parameters that are not yet known accurately for the Wasatch Front.

IX. RECOMMENDATIONS

The above discussions highlight data and new concepts of earthquake nucleation for the Wasatch Front principally focusing on recent seismicity, fault zone geometry, explanations of Wasatch Front seismicity, possible locations of future large earthquakes--all ingredients of an accurate assessment of earthquake hazards. Based on our investigations we would like to recommend to the U.S. Geological Survey and the National Science Foundation for incorporation into the National Earthquake Hazards Reduction Program and to the coordinated USGS-UGMS program the following considerations:

1. Detailed investigations of major Quaternary-Holocene normal fault zones emphasizing information from adjacent bedrock exposures, mechanical, and chemistry properties of fault zones, geometric and geomorphic information on inferred fault zones, and most importantly incorporating geophysical information such as seismic reflection, refraction, and gravity techniques to map the fault with depth beneath adjacent valleys.
2. At least three, deep penetration seismic reflection profiles designed to image dipping structures should be recorded across all major segments of the Wasatch fault and adjacent fault zones to provide high-resolution information on fault zone geometry, structure, style, depth, etc. This research effort will compliment borehole and fault zone evaluation.
3. Detailed evaluation of fault zone segmentation is required to examine with statistical uncertainties: segment lengths, end-points, fault geometries. etc. Deep boreholes should be drilled in each of the segments of the Wasatch fault to penetrate the fault for

purposes of determining Quaternary-Holocene stratigraphy, borehole properties, geochemical/geopressure information, in situ stress, etc.

4. Expanded efforts in trenching of at least two to three sites per fault segment is necessary to establish statistical certainties, areal distribution of recurrence rates, slip rates, displacement histories, and maximum magnitudes.
5. Increased research on probabilistic and deterministic models of temporal and spatial occurrence of earthquakes to incorporate all of the existing information on dating, fault area, recurrence intervals, fault geometry, stress, etc.
6. Expanded geodetic (horizontal and vertical) networks across major fault zones should be implemented with more frequent reobservations to assess pre-seismic, co-seismic and post-seismic deformation.
7. Theoretical modeling and implementation of a strong motion network to predict and evaluate peak ground accelerations associated with active segments of the Wasatch fault will be an important contribution to engineering assessments of risk.
8. Long-term stable funding is required for effective operation of the southern Intermountain Seismic Belt regional seismograph network with the addition of three-component broad-band seismographs at selected digital stations and ancillary seismological studies of the dynamics and kinematics of normal faulting. Emphasis on normal fault mechanisms including precursory phenomena, modeling of ground motion, modeling space-time histories, etc. are needed.

References

- Arabasz, W. J., and R. B. Smith (1979). Introduction, What you've always wanted to know about earthquakes in Utah, in Earthquake Studies in Utah; 1850-1978, edited by W. J. Arabasz, R. B. Smith, and W. D. Richins, University of Utah Seismograph Stations, University of Utah, Salt Lake City, 1-14.
- Arabasz, W. J., and R. B. Smith (1981). Earthquake prediction in the Intermountain seismic belt--An intraplate extensional regime in Earthquake Prediction--An International Review, D. W. Simpson and P. G. Richards, Editors, Am. Geophys. Union, Maurice Ewing Series, 4, 238-258.

- Arabasz, W. J., R. B. Smith, and W. D. Richins, editors (1979). Earthquake Studies in Utah: 1850-1978, University of Utah Seismograph Stations, Department of Geology and Geophysics, University of Utah, Salt Lake City, 552 p.
- Arabasz, W. J., W. D. Richins, and C. J. Langer (1979). The Pocatello Valley (Idaho-Utah border) earthquake sequence of March to April 1975, Bull. Seism. Soc. Am., 71 803-826.
- Arabasz, W. J., R. B. Smith, and W. D. Richins (1980). Earthquake studies along the Wasatch Front, Utah: Network monitoring, seismicity, and seismic hazards, Bull. Seismol. Soc. Am., 70, 1479-1499.
- Bucknam, R. C., S. T. Algermissen, and R. E. Anderson (1980). Patterns of late Quaternary faulting in western Utah and application in earthquake hazard evaluation, U.S. Geol. Surv. Open-File Rept. 80-801, 299-314.
- Cook, K. L., and R. B. Smith (1967). Seismicity in Utah, 1850 through June 1965, Bull. Seism. Soc. Am., 57, 689-718.
- Doser, D. I. (1984). Source Parameters and faulting processes of the August 1959 Hebgen Lake Montana earthquake sequence, Ph.D. Thesis, University of Utah, Salt Lake City.
- Doser, D. I. (1984). The 1959 Hebgen Lake, MT and the 1983 Borah Peak, ID, earthquakes: Examples of large normal fault events in the Intermountain region, Earthquake Notes, 55, (in press).
- Doser, D. I., and R. B. Smith (1982). Seismic moment rates in the Utah region, Bull. Seismol. Soc. Am., 72, 525-551.
- Gilbert, G. R., (1883). Earthquakes, The Daily Tribune, Salt Lake City. Sunday Morning, September, 16, 1883.
- Gilbert, G. R., (1928). Studies of Basin Range structure, U.S. Geol. Survey Prof. Paper 153, 92 pp.
- Hait, T. M., Jr. (1978). Holocene faulting, Lost River Range, Idaho, Geol. Soc. America, Abstracts with Programs, Rocky Mountain Section, Geological Society of America, Provo, Utah, 217.
- Hayes, W. W., R. D. Miller and K. W. King (1980). Research to define the ground shaking hazard along the Wasatch fault zone, Utah, U.S. Geol. Surv. Open-File Rept. 80-801, 172-180.
- McGarr, A. (1984). Scaling of ground motion parameters, state of stress and focal depth, J. Geophys. Res., (in press).
- McKee, M. E., and W. J. Arabasz (1981). Microearthquake studies across the Basin and Range-Colorado Plateau transition in central Utah, Earthquake Notes, 52 (1), 62.

- McKee, M. E., and W. J. Arabasz (1982). Microearthquake studies across the Basin and Range-Colorado Plateau transition in Central Utah, in Overthrust Belt of Utah, D. L. Nielson, Editor, Utah Geol. Assoc. Publ., 10, 137-149.
- Okaya, D. A., and G. A. Thompson (1984). Geometry of Cenozoic extensional faulting: Dixie Valley, Nevada, Tectonics, (in press).
- Richins, W. D., W. J. Arabasz, G. M. Hathaway, P. J. Oehmich, L. L. Sells, and G. Zandt (1981). Earthquake Data for the Utah Region: July 1, 1978 to December 31, 1980, University of Utah Seismograph Stations, University of Utah, Salt Lake City, 125 pp.
- Richins, W. D., R. B. Smith, J. J. King, C. J. Langer, C. W. Meissner, J. C. Pechmann, W. J. Arabasz, J. E. Zollweg (1984a). The 1983 Borah Peak, Idaho, earthquake: A progress report on the relationship of aftershocks to the mainshock, surface faulting, and regional tectonics, Earthquake Notes, 55, (in press).
- Richins, W. D., P. J. Oehmich, L. L. Sells, G. M. Hathaway, and W. J. Arabasz (1984b). Earthquake Data for the Utah Region: January 1, 1981 to December 31, 1983 University of Utah Seismograph Stations, University of Utah, Salt Lake City, (in press).
- Schwartz, D. P., and K. J. Coppersmith (1984). Fault behavior and characteristic earthquake: Examples From the Wasatch and San Andreas fault zone, J. Geophys. Res., 89, 5681-5698.
- Smith, R. B. (1978). Seismicity, crustal structure, and intraplate tectonics of the interior of the Western Cordillera, in Cenozoic Tectonics and Regional Geophysics of the Western Cordillera, edited by R. B. Smith and G. P. Eaton, Geol. Soc. Am., Memoir 152, 111-144.
- Smith, R. B., and M. Sbar (1974). Contemporary tectonics and seismicity of the western United States with emphasis on the Intermountain seismic belt, Bull. Geol. Seismol. Soc. Am., 85, 1205-1218.
- Smith, R. B., and R. L. Bruhn (1984). Intraplate extensional tectonics of the Western U.S. Cordillera: Inference on structural style from seismic reflection data, regional tectonics, and thermal-mechanical models of brittle-ductile deformation, J. Geophys. Res., 89, 5733-5762.
- Snay, R. A., R. B. Smith, and T. Soler (1984). Horizontal strain across the Wasatch Front near Salt Lake City, Utah, J. Geophys. Res., 89, 1113-1122.
- Swan, F. H., III, D. P. Schwartz, and L. S. Cluff (1980). Recurrence of moderate-to-large magnitude earthquakes produced by surface faulting on the Wasatch fault zone, Bull. Seismol. Soc. Am., 70, 1431-1462.
- U. S. Geological Survey, (1976). A Study of Earthquake Losses in the Salt Lake City, Utah Area: U.S. Geol. Survey, Open-File Report 76-89.

U.S. Geological Survey (1980). Earthquake Hazards Along the Wasatch and Sierra-Nevada Frontal Fault Zones: U.S. Geol. Survey, Open-File Report 80-801.

Zoback, M. L. (1983). Structure and Cenozoic tectonism along the Wasatch fault zone, Utah, Mem. Geol. Soc. Am., 157, 3-27.

FIGURE CAPTIONS

- Figure 1. Epicenter map of western United States with data principally from 1950 through 1976. Taken from Smith (1978).
- Figure 2. Epicenter map of the Intermountain Seismic Belt with largest historic earthquake high lighted by large dots (modified from Smith, 1978 and Arabasz and Smith, 1979).
- Figure 3. Epicenter map of largest historical earthquakes in Utah, 1850-1978 (from Arabasz and Smith, 1979).
- Figure 4. Epicenter map of Utah: 1962-1983. Wasatch Front study area shown by black box; solid lines show locations of the Wasatch fault (west) and the East Cache fault (east).
- Figure 5. Epicenter and regional tectonic map of the Wasatch Front (taken from Smith and Bruhn, 1984). Epicenters from University of Utah files for period: 1974-1982.
- Figure 6. Tectonic map of Wasatch Front and adjacent mountain ranges illustrating the Quaternary normal fault segments proposed by Schwartz and Coppersmith (1984). Figure taken from Smith and Bruhn (1984).
- Figure 7. Seismic reflection profiles and interpretations across: a) East Cache fault, south of Logan, Utah and b) Wasatch fault, south of Ogden, Utah.
- Figure 8. Cross-sections across fault zones of the three largest historic Basin-Range type earthquakes with hypothetical model for a large earthquake on the Wasatch Front, Salt Lake City area. 1959, M7.5, Hebgen Lake, Montana earthquake data from Doser, 1984; 1983, M7.3 Borah Peak, Idaho earthquake data from Richins, et al. (1984a) and 1954, M7.1 Dixie Valley, Nevada earthquake data from Okaya and Thompson (1984).
- Figure 9. Space-time distribution of earthquakes within 10 km of the Wasatch fault, 1962-1978 (from Arabasz, Smith, and Richins, 1980).
- Figure 10. Hypothetical model for nucleation of large earthquakes that could plausibly occur on the main westward dipping Wasatch fault and

subsidiary faults. Fault plane geometries inferred from comparison with other large Basin-Range earthquakes and data from Smith and Bruhn (1984).

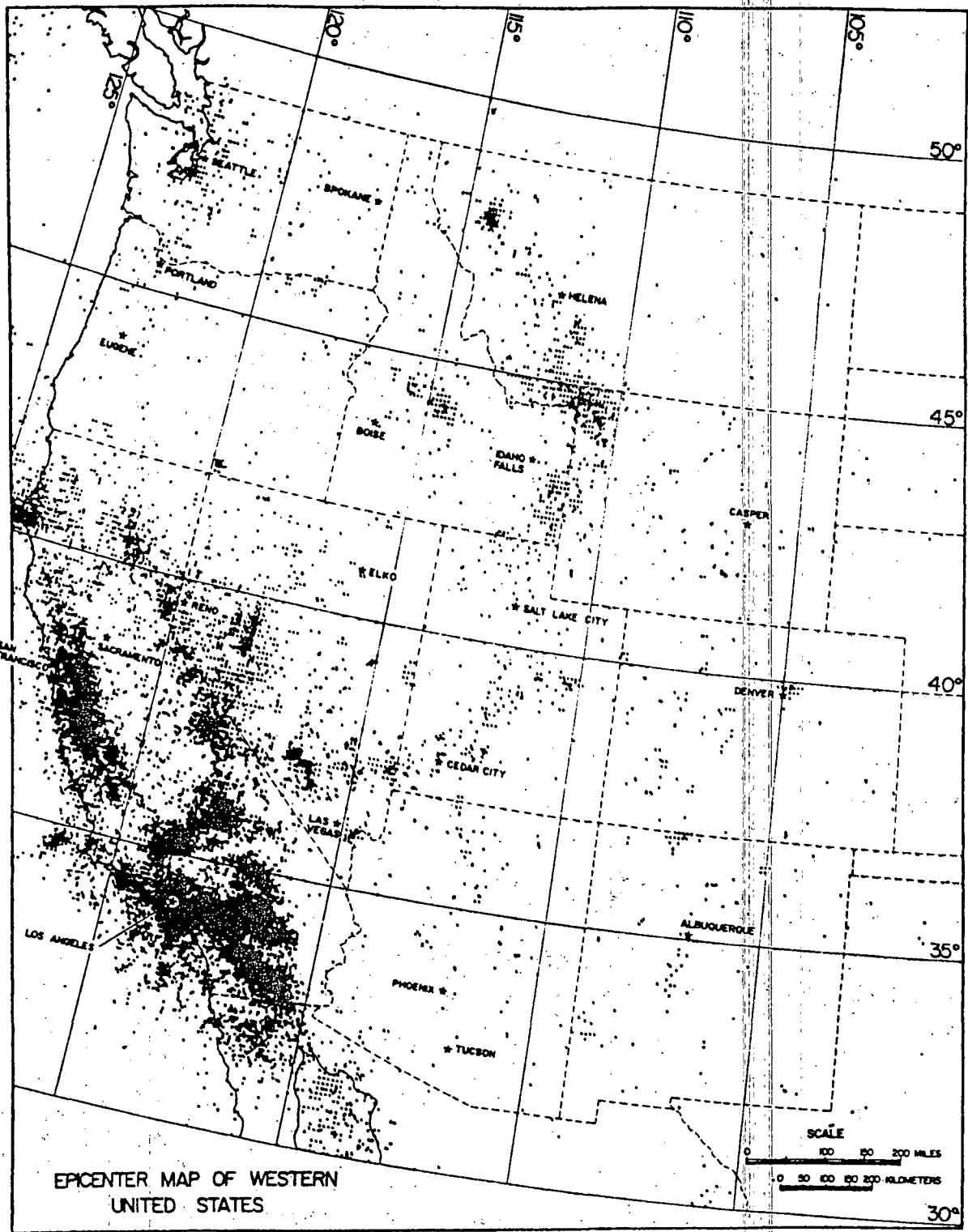


Figure 1.

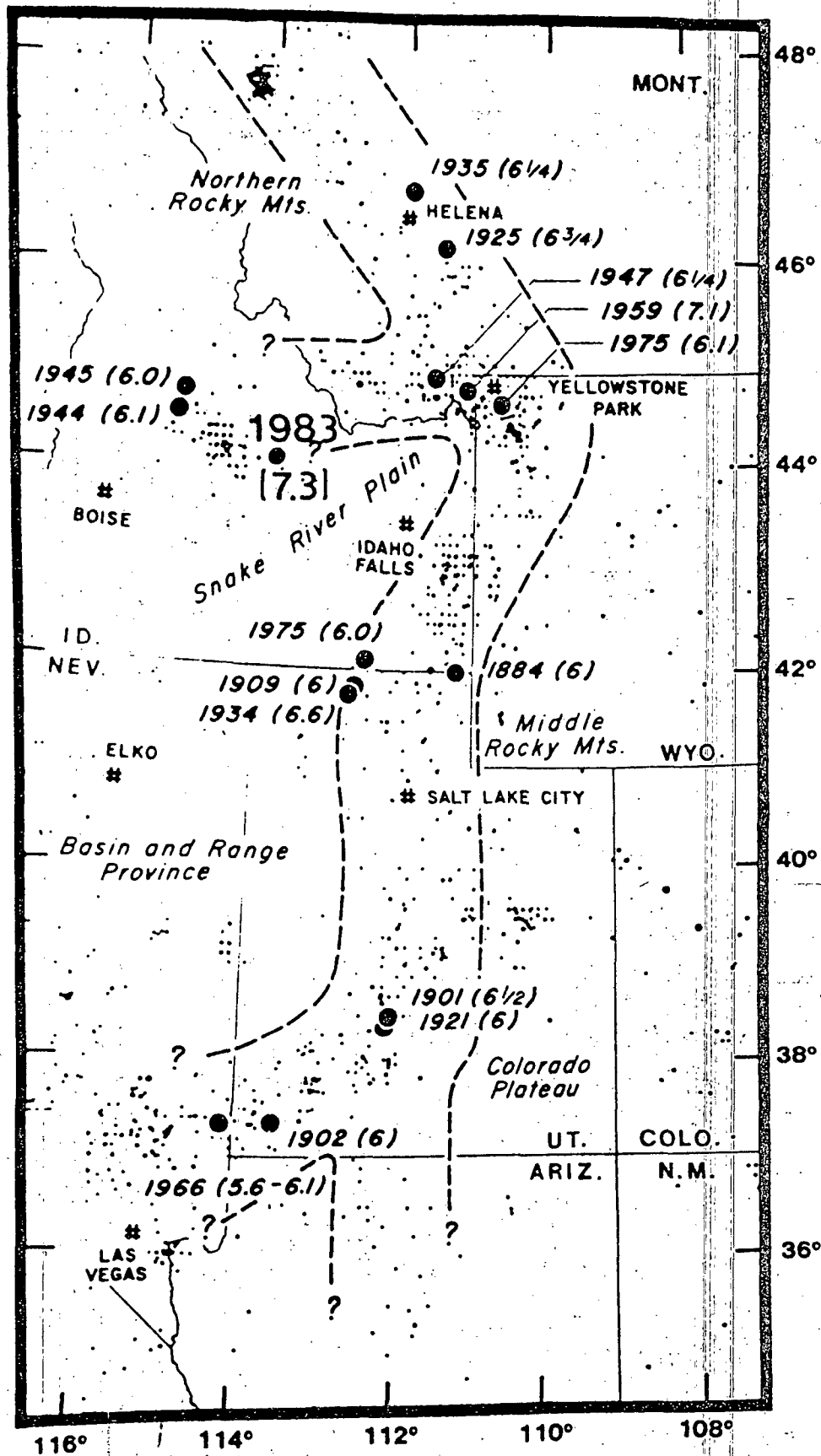


Figure 2.

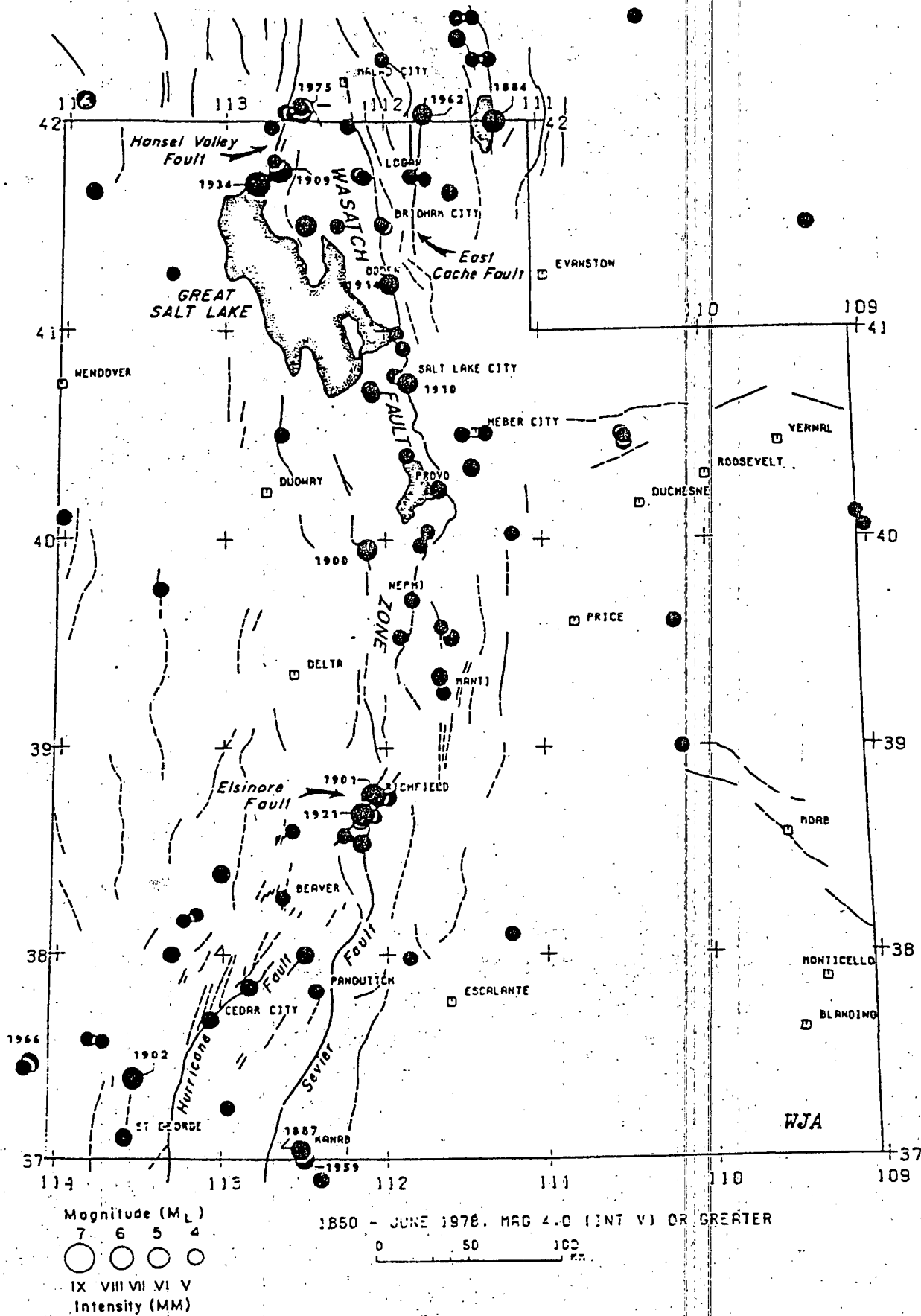


Figure 3.

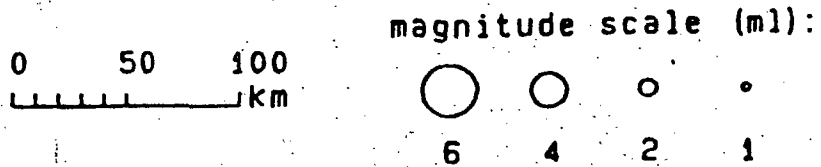
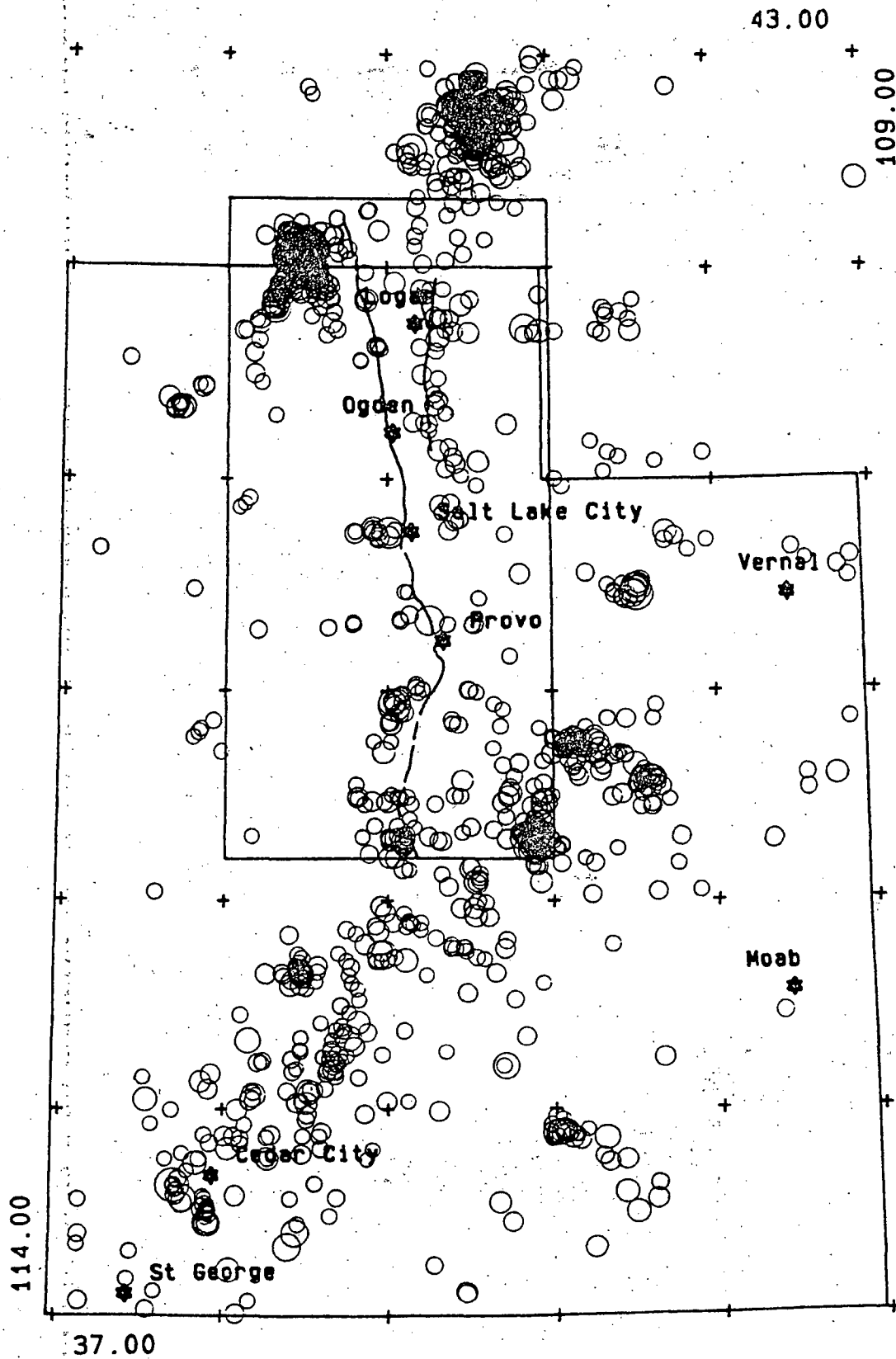


Figure 4.

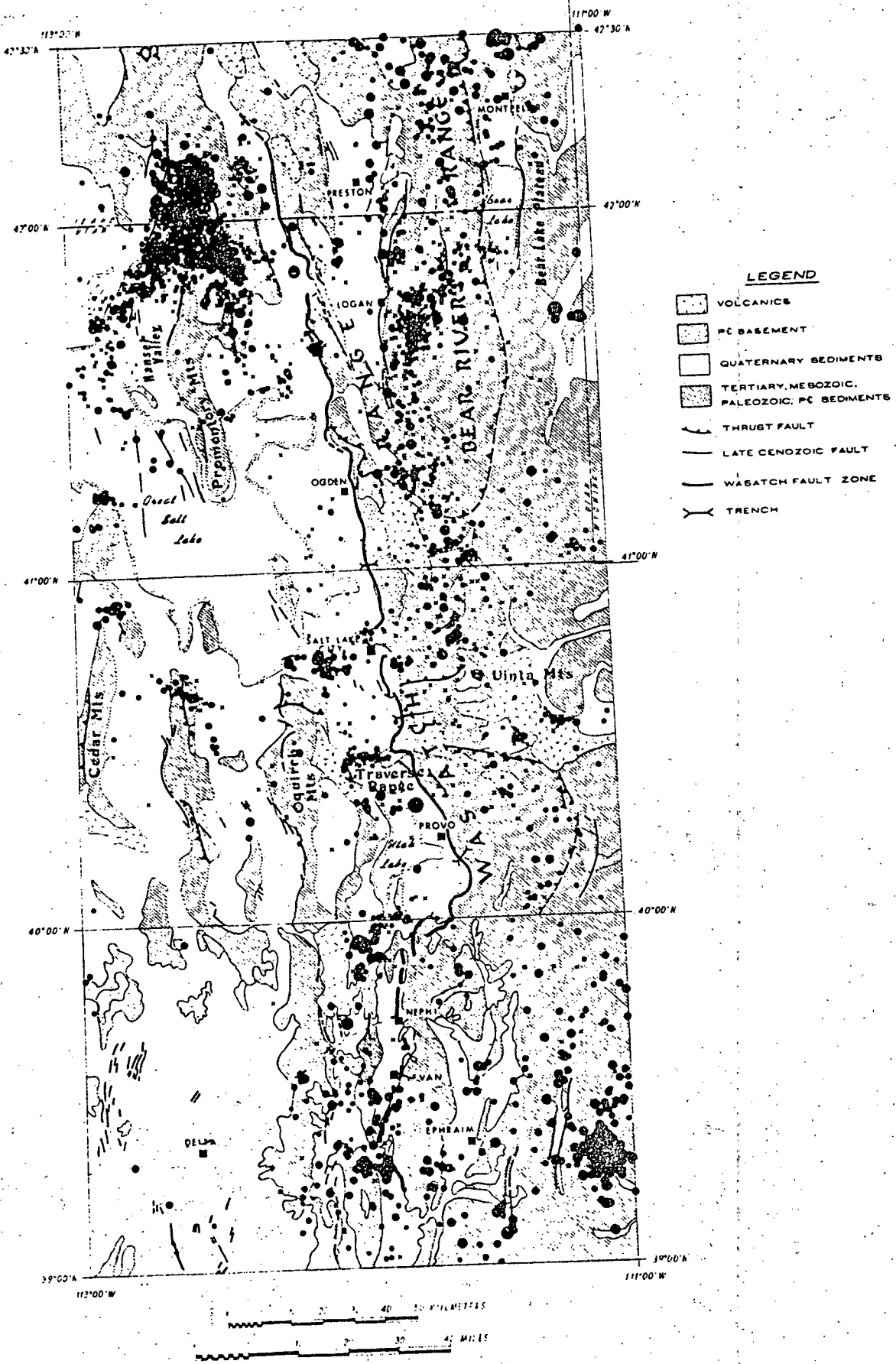


Figure 5.

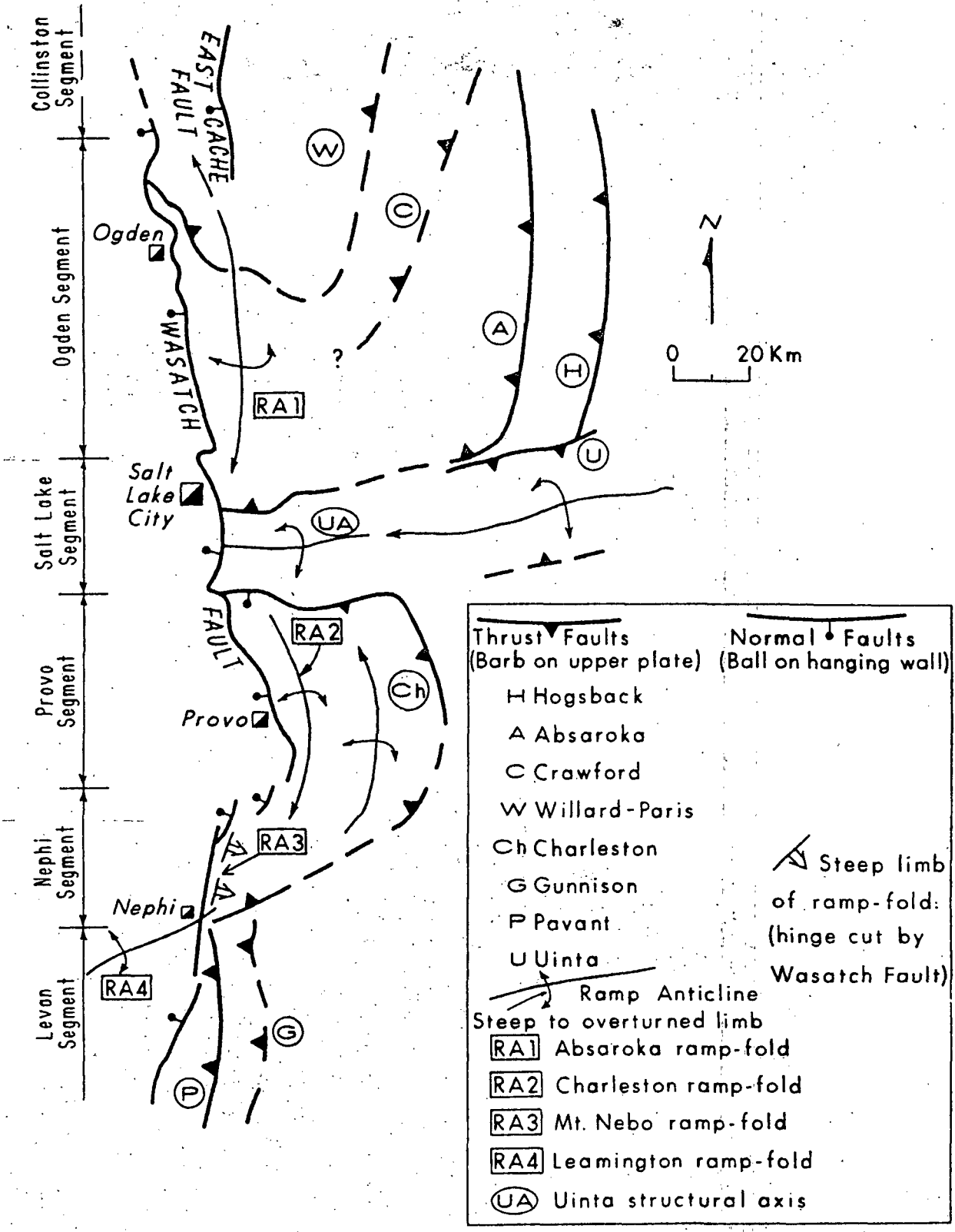


Figure 6.

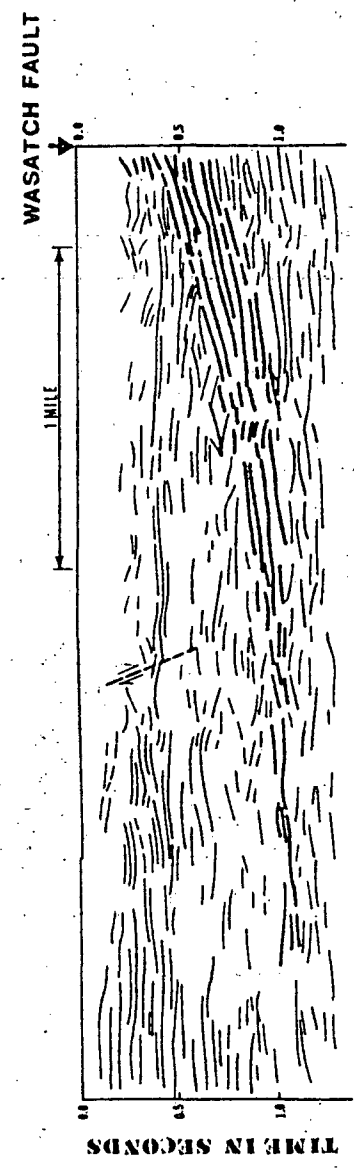
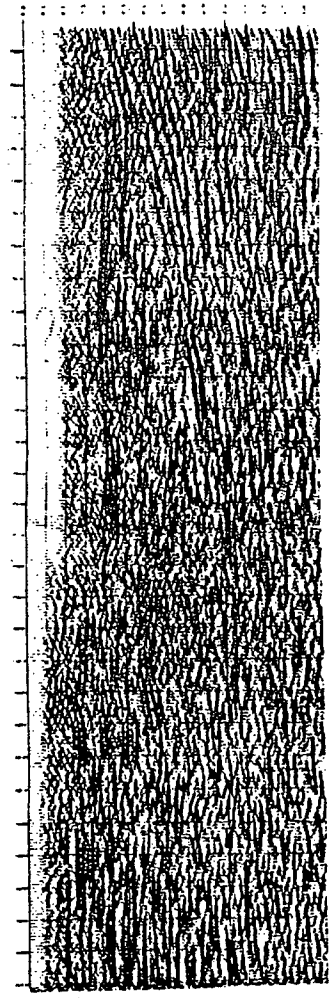
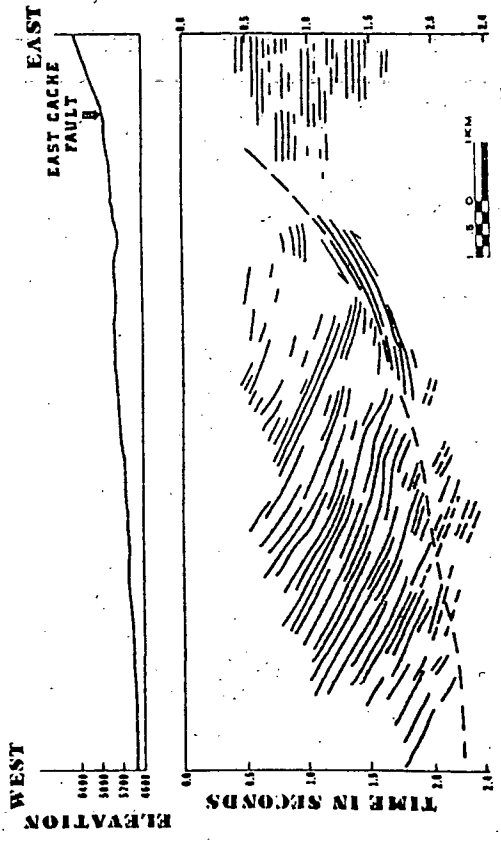
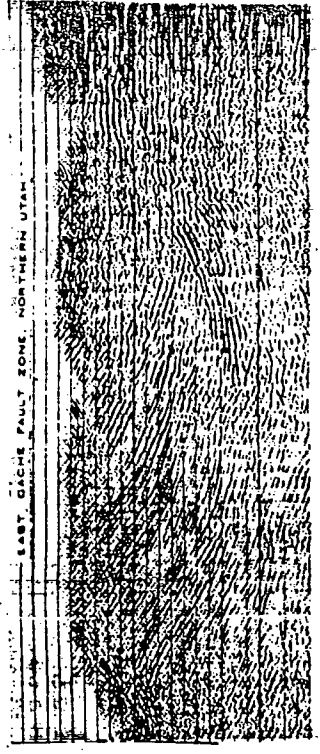


Figure 7.

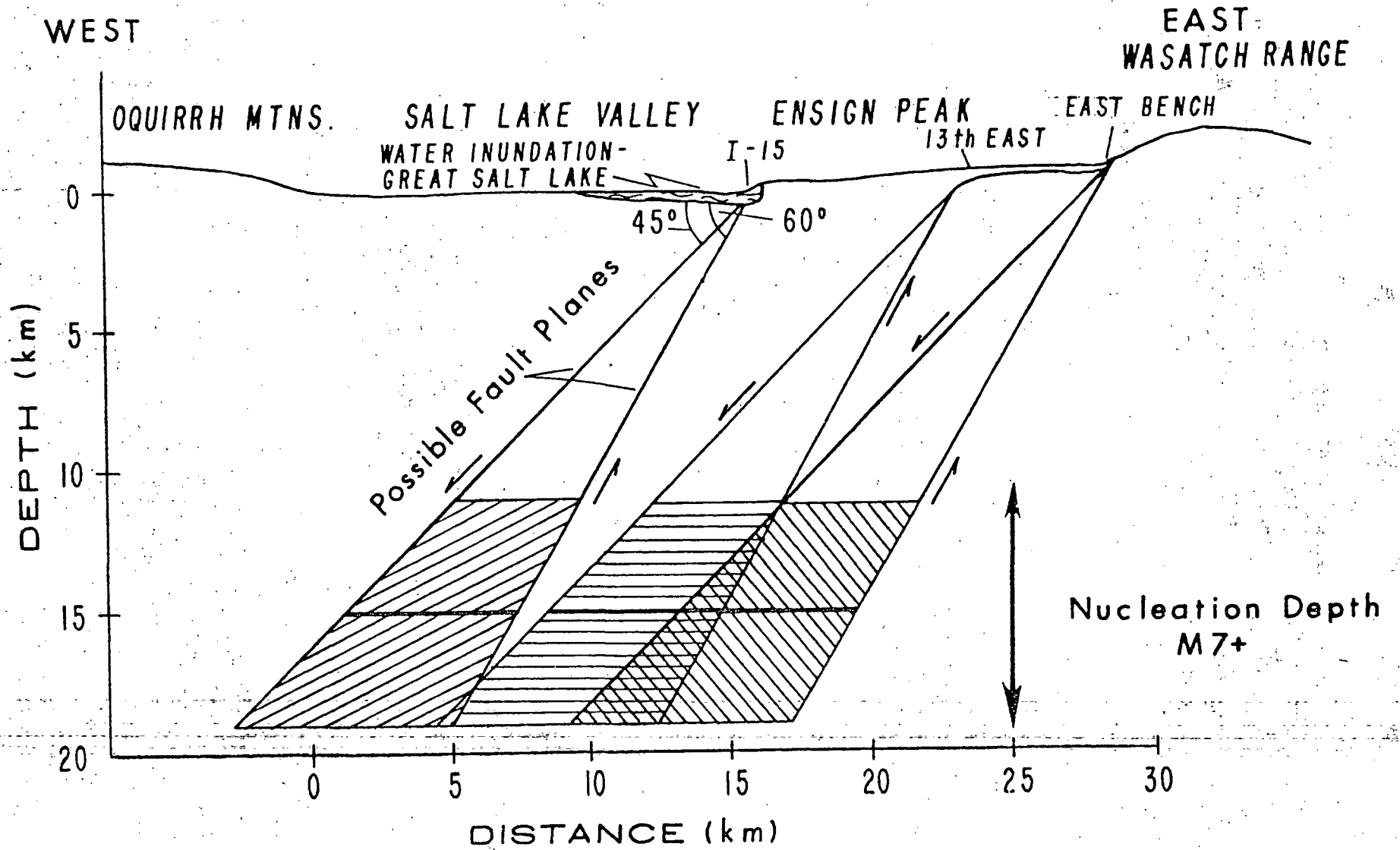


Figure 8.

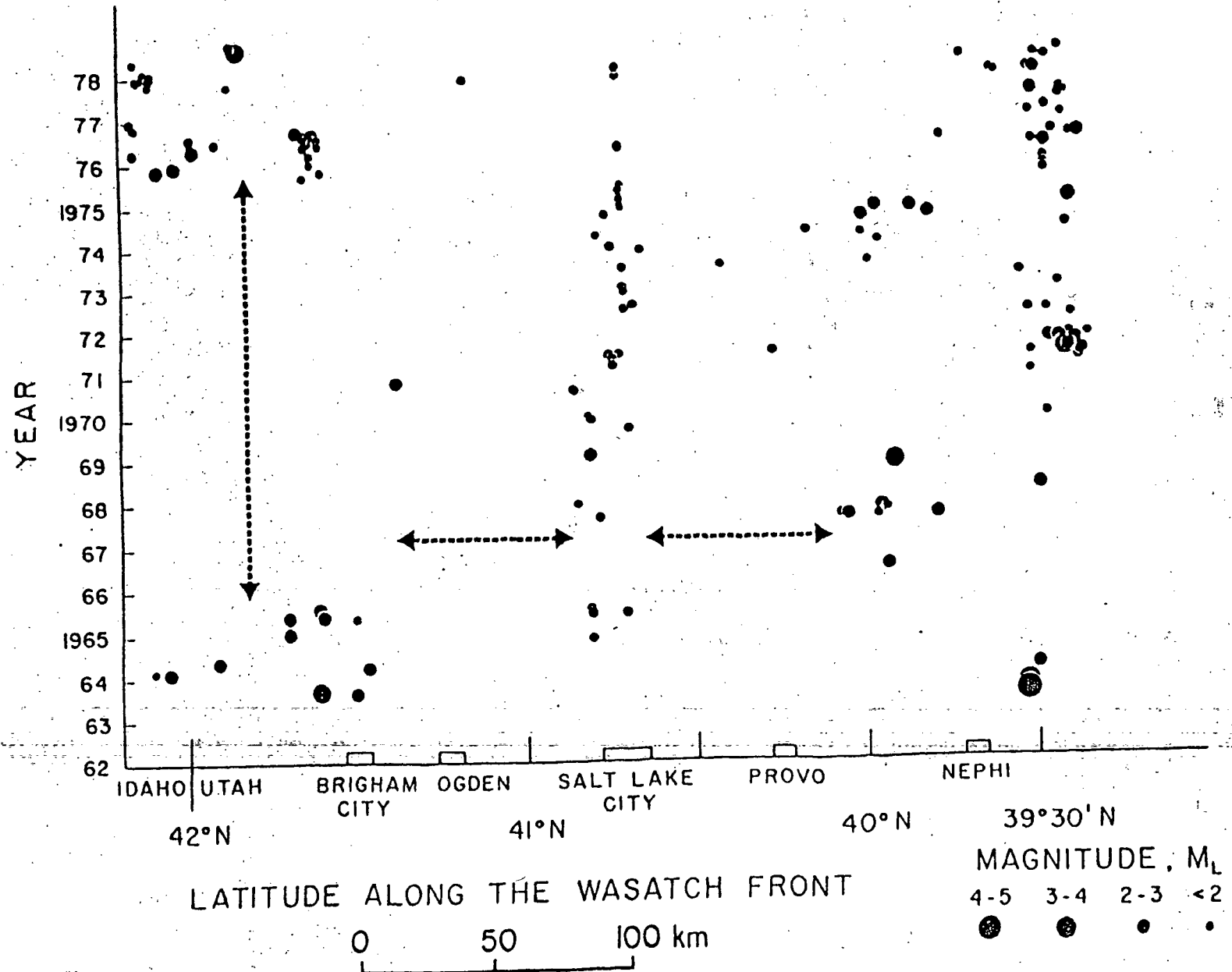
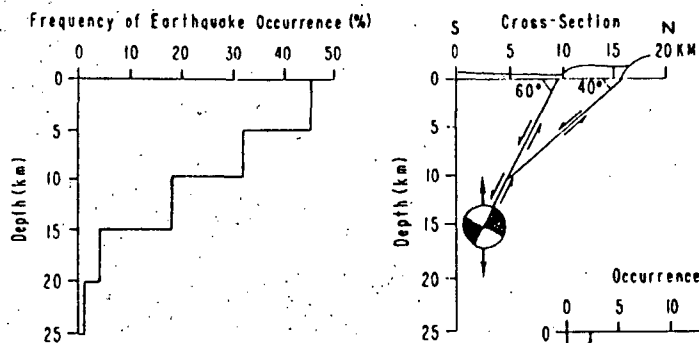
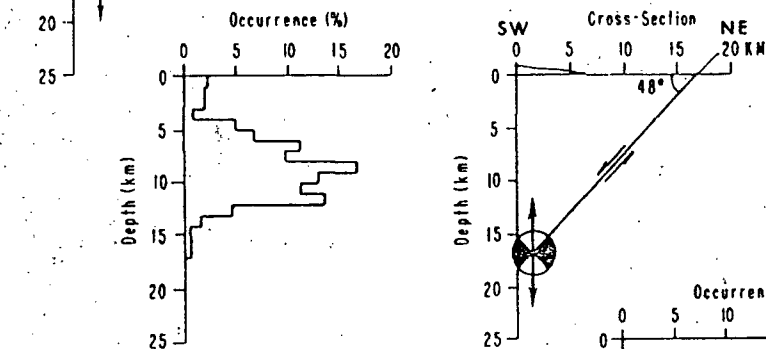


Figure 9.

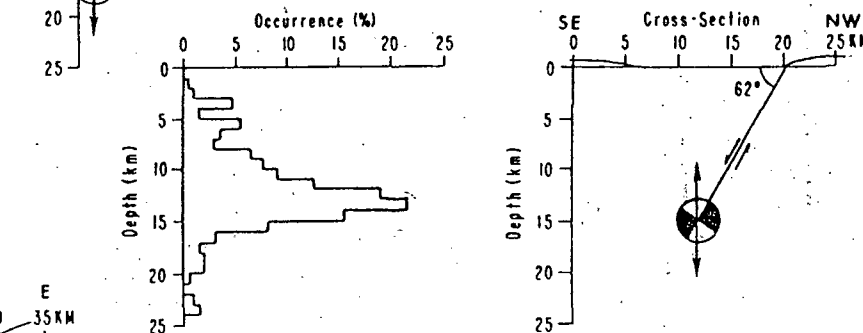
HEBGEN LAKE, MONTANA, M7.5
August 17, 1959



BORAH PEAK, IDAHO M7.3
October 28, 1983



DIXIE VALLEY, NEVADA M7.1
December 16, 1954



WASATCH FRONT SALT LAKE VALLEY
Hypothetical M7+ Earthquakes

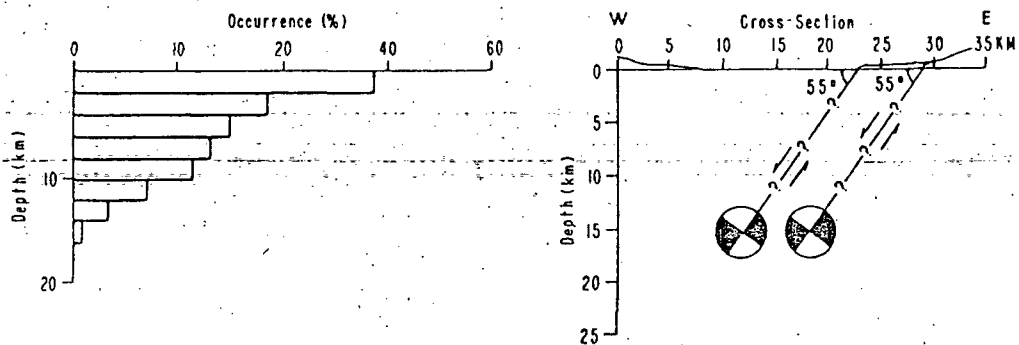


Figure 10.

FAULT BEHAVIOR AND EARTHQUAKE RECURRENCE ALONG
THE WASATCH FAULT ZONE

D. P. Schwartz, F. H. Swan, III, L. S. Cluff

Woodward-Clyde Consultants

100 Pringle Avenue

Walnut Creek, CA 94596

INTRODUCTION

The Wasatch fault zone is an active intraplate normal fault that extends for approximately 370 km along the western front of the Wasatch range. The majority of Utah's population lives along the Wasatch Front and all of the principal urban areas and most of the larger towns are located adjacent to the Wasatch fault zone and associated faults such as the East Cache fault.

Paleoseismological studies of these faults show they have been the sources of repeated past large magnitude earthquakes in the range of M 6-3/4 - 7-1/2 (Swan and others, 1980, 1982), although no surface faulting earthquakes have occurred on these faults since settlement of the area in 1847. Because of this, an understanding of the future behavior of these faults, especially the size of future earthquakes, the amount of surface displacement and style of ground deformation associated with the events, the probable location and timing of the events, and the ground motions produced during the earthquakes is critical to the mitigation of seismic hazards along the Wasatch Front.

In 1977, the first trenches were excavated across the Wasatch fault zone at the Kaysville site (Figure 1) for the specific purpose of quantifying

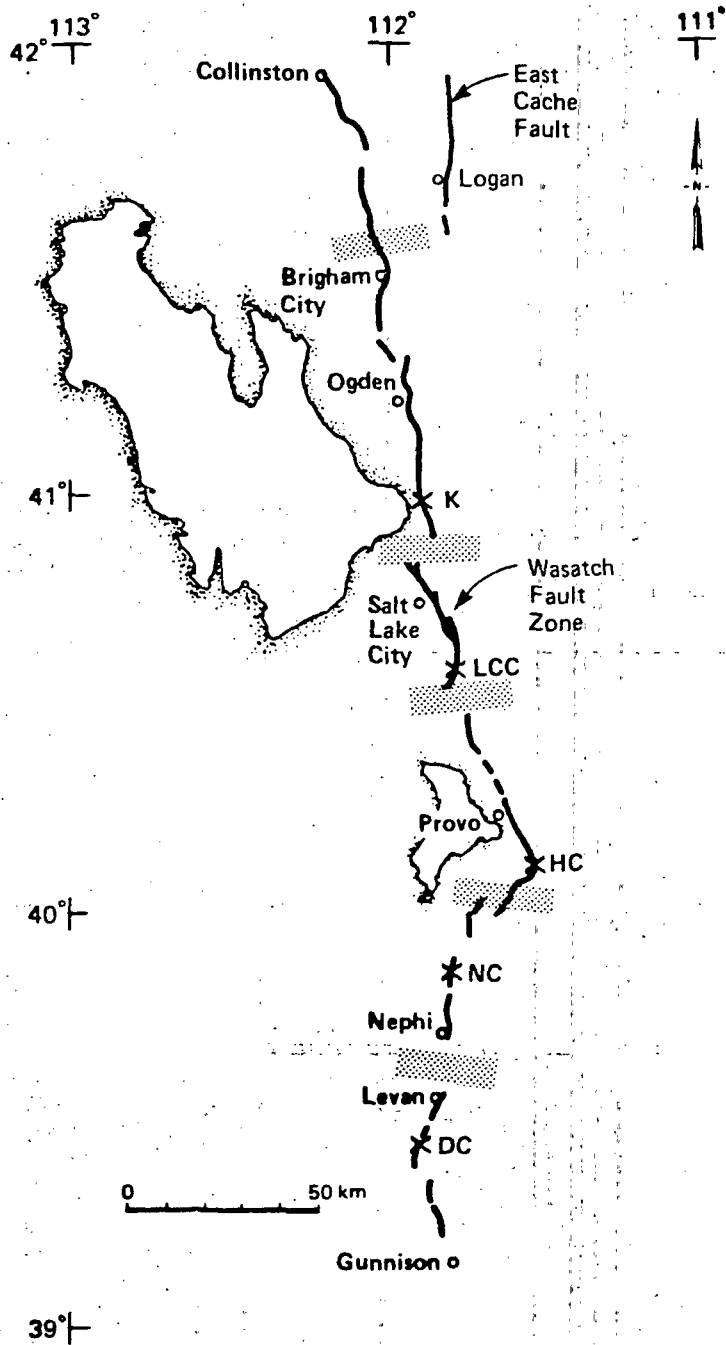


Figure 1. Locality Map for Wasatch and East Cache Fault Zones. Sites Described in the Text Are K = Kaysville, LCC = Little Cottonwood Canyon, HC = Hobble Creek, NC = North Creek, DC = Deep Creek. Stippled Bands Define Proposed Boundaries of Major Fault Segments.

earthquake recurrence. Since then, investigations have been conducted at the Hobble Creek, Little Cottonwood Canyon, and North Creek sites along the Wasatch fault zone and at Logan along the East Cache fault (Figure 1). These investigations have yielded information on slip rate, recurrence intervals for past surface faulting earthquakes, displacement per event for past earthquakes, and fault segmentation, and they provide a basis for evaluating the late Pleistocene-Holocene behavior of the Wasatch fault zone. Results from these investigations have been presented by Swan and others (1980), Schwartz and others (1983), and Schwartz and Coppersmith (1984). The present paper summarizes the data collected at all sites and discusses the implications of these data to fault behavior and earthquake recurrence.

SLIP RATE

Slip rates provide a means for comparing relative behavior of different parts of a fault zone. In addition, slip rates can be used to model earthquake recurrence. Slip rate data for the Wasatch fault zone are summarized in Table 1. Late Pleistocene-Holocene rates for the Wasatch fault zone range from essentially > 0 along the segment of the fault north of Brigham City to 1.36 mm/yr along the Nephi segment. The rate for the East Cache fault is 0.1-0.2 mm/yr. These slip rates were developed from topographic profiling of displaced geomorphic features, including surfaces that grade to the Provo shoreline, glacial moraines, alluvial fans, and stream terraces. However, rates based on different-aged datums may not be exactly comparable. Also, care must be exercised in extrapolating rates calculated at a point for long distances along the trace of the fault. Considering these factors, we view the slip rates as representing a generally constant rate of strain

TABLE 1
 FAULT BEHAVIOR DATA
 WASATCH FAULT ZONE

Segment	Site	Slip Rate (mm a ⁻¹) ^a	Displacement per Event (m)		Recurrence		Elapsed Time (yr) ^c	Reference
			Measured	Average ^b	Interval	Average (yr)		
Collinston	-	≥ 0 (13,500)	-	-	-	-	$\geq 13,500$	Schwartz and others (1983)
Ogden	Keyaville	1.3 (+0.5, -0.2) ^e (8,000; +1000, -2000)	1.6 1.7	-	2 (after 1580) ^d	2000	≤ 500	Swan and others (1980)
Salt Lake City	Little Cottonwood Canyon	0.76 (+0.6, -0.2) (19,000 \pm 2000)	-	2 (2)	-	2400-3000	-	Swan and others (1981); Schwartz and Coppermith (1984)
Provo	Hobble Creek	0.85 - 1.0 ^e (13,500)	2.7	1.6-2.3 (6-7)	6-7 (after 13,500)	1700-2600	> 1000	Swan and others (1980)
Nephi	North Creek	1.27-1.36 (\pm 0.1) (4580) ^d	2.0-2.2 2.0-2.5 2.6	2.3 (3)	2 (between 4580 and 3640) ^d 1 (after 1100) ^d	1700-2700	300-500	Schwartz and Coppermith (1984)
Levan	Deep Creek	$\leq 0.35 \pm 0.05$ (7300) ^d	2.5	-	1 (after 7300) ^d	-	<1750 ^d	Schwartz and Coppermith (1984)
East Cache	Logan	0.1-0.2 (14,000-15,000)	1.35 1.4	-	1 (between 15,000 and 13,500) 1 (after 13,500)	-	6000-10,000	Swan and others (1982)

a Age of displaced datum (years B.P.) on which slip rate is based is shown in parentheses.

b Number of events on which average is based is shown in parentheses.

c Time in years since the most recent surface faulting earthquake.

d Age in 14 C yr B.P.

e Modified from Swan et al. (1980).

accumulation of about 1 mm/yr along the Wasatch fault zone between Nephi and Brigham City during Holocene time. This rate of strain accumulation is one to two orders of magnitude greater than the rate for faults in other parts of the Basin and Range province.

DISPLACEMENT PER EVENT

Information on the amount of displacement per event for past surface faulting earthquakes is important for assessing the magnitude of past earthquakes, for developing models of earthquake recurrence, and for developing estimates of the amount of displacement that might occur where lifelines such as water and gas pipelines cross fault traces. The thickness of colluvial deposits (colluvial wedges) adjacent to the fault observed in trenches, profiling of fault scarps, and measuring the heights of tectonic terraces inset into the upthrown block of the fault are the methods generally used for evaluating the size of paleodisplacements.

Displacement per event data are summarized in Table 1. Investigations of historical surface ruptures on normal faults in the Basin and Range, such as the 1915 Pleasant Valley and the 1983 Borah Peak earthquakes, show systematic variation in displacement along the surface trace of the fault. For the Wasatch fault zone, we do not know where individual trench sites are located with respect to past surface ruptures, and there is some uncertainty as to whether an individual measurement represents a minimum, an average, or a maximum displacement for that surface faulting event. Despite this, the data clearly show that displacement per event has been consistently large. The measured values range from 1.6 to 2.6 m, and the average displacement per

event is about 2 m. The data also indicate that displacements at the same location along the fault have been essentially the same during successive events.

EARTHQUAKE RECURRENCE INTERVALS

Factors that affect the evaluation of earthquake recurrence at a specific location along a fault include the completeness of the stratigraphic record, the local erosional and depositional environment, and the threshold earthquake magnitude that produces recognizable surface-fault rupture. Recurrence estimates at individual sites along the Wasatch fault zone have been based on a combination of trenching and mapping. Trenching of normal fault scarps has shown the usefulness of scarp-derived colluvial deposits in quantifying the number of past surface faulting events. In trenches, these are commonly seen as stacked units or wedges grading away from the main fault scarp. Mapping is especially important because it helps establish many stratigraphic and structural relationships that clarify observations made in trenches and it aids in identifying secondary features such as tectonic terraces and segmented alluvial fans that also provide evidence of recurrence.

Data on the recurrence of surface faulting earthquakes at individual sites along the Wasatch fault zone are shown in Table 1. Recurrence intervals clearly vary along the length of the zone. Average intervals are shortest along the four central segments of the zone between Brigham City and Nephi, where they range from 1700 to 3000 years. In contrast, the ends are less active. A minimum interval of 5000 years occurred along the southern segment of the zone prior to its most recent event, and the northern segment does not

appear to have had a recognizable scarp-forming event during the past 13,500 years. Where radiocarbon dates constrain the actual interval between events, it is evident that the actual recurrence is not uniform and may vary from the average by at least a factor of two. At the North Creek site, for example, there have been three surface faulting earthquakes during the past 4,580 ¹⁴C yr B.P.; two of these occurred between 4,580 and 3,640 ¹⁴C yr B.P. and the most recent event is estimated to have occurred within the past 300 to 500 years. At this location, the interval between successive events was not uniform and varied from somewhat less than 1,000 years between the oldest and middle events to longer than 3,000 years between the middle and most recent events. This non-uniformity of earthquake recurrence is typical of faults in intraplate environments.

Swan and others (1980) suggested an average recurrence interval along the entire Wasatch fault zone of 50 to 430 years. This was calculated by using minimum (500 yr) and maximum (2600 yr) intervals estimated at the Kaysville and Hobble Creek sites, respectively, and assuming that these were representative of 6 to 10 independent fault segments. Additional investigations have shown that the fault zone is most likely composed of six segments, the recurrence interval can differ significantly between segments, and the recurrence along a given segment can also be highly variable. Based on these additional data, and the behavioral variability they indicate, Schwartz and Coppersmith (1984) have revised the estimate of the average recurrence for the zone by using the number of events observed or estimated in the geological record along each segment of the fault over a particular interval, which in this case was selected as the past 8000 years on the basis of available radiocarbon dates and the ages of displaced datums. Using this

approach, they calculated a range of 400 to 666 and a preferred value of 444 years for the average recurrence interval for a surface faulting earthquake along the entire Wasatch fault zone. This is similar to the longer interval suggested by Swan and others (1980), and we feel it is presently the best estimate of the average recurrence for the zone.

The occurrence of successive large and similar displacement events along the Wasatch fault zone coupled with the variability in timing between these events and the lack of evidence of small-displacement events, has led to the development of the characteristic earthquake recurrence model (Schwartz and Coppersmith, 1984). This recurrence model suggests that: a) linear frequency-magnitude distributions over a full range of earthquake magnitudes may not be appropriate for individual faults or fault segments and moderate magnitude events smaller than the characteristic earthquake may be relatively less likely to occur than the larger event, b) the magnitude of the characteristic earthquake may approximate the maximum earthquake ($M 7 - 7\frac{1}{2}$ for the Wasatch fault zone) and, c) stress application appears to be non-uniform and faults may fail in response to localized, rapid increase in stress. Similar behavior appears to characterize other Basin and Range normal faults.

SEGMENTATION

A normal fault as long as the Wasatch fault zone (370 km) will only rupture along part of its total length during a surface faulting earthquake. A major question is does rupture occur randomly along the fault or are there distinct rupture segments, perhaps controlled by the geometry of the fault and by older

structural trends, that behave consistently through time? Quantifying the number of potential rupture segments is a key factor in evaluating recurrence for the entire fault zone and in estimating where the next rupture is most likely to occur.

Swan and others (1980), on the basis of rupture lengths of historical Basin and Range surface faulting earthquakes with $M > 6\frac{1}{2} < 7\frac{1}{2}$ suggested that the Wasatch fault zone consists of 6 to 10 segments, although the individual segments were not specifically identified. Based on additional data, we now believe there are six major segments. Selection of each segment is based to varying degrees on fault geometry, scarp morphology, slip rate, and timing the most recent event, gravity data, and geodetic data. The proposed fault segments are shown on Figure 1. From north to south, the segments and their length and orientation are: 1) Collinston, >30 km, N20W; 2) Ogden, 70 km, N10W; 3) Salt Lake City, 35 km, convex east N20E to N30W; 4) Provo, 55 km, N25W; 5) Nephi, 35 km, N11E; and 6) Levan, 40 km, convex west. The Collinston segment has had no identifiable surface faulting during the past 13,500 years. The Ogden segment has experienced multiple displacements, including two within the past 1580 ^{14}C yr B.P. and with the most recent of these within the past 500 years. The Salt Lake City and Provo segments have each had repeated Holocene events; the timing of the most recent event along the Salt Lake City segment is not known, and the youngest event on the Provo segment appears to have occurred more than 1000 years ago. Along the Nephi segment one event has occurred within the past 1100 ^{14}C yr B.P. and possibly as recently as 300 years ago; two earlier events occurred on this segment between 4580 and 3640 ^{14}C yr B.P. The Levan segment has experienced only one event

during the past 7300 ¹⁴C yr B.P. and this event occurred less than 1750 ¹⁴C yr B.P. ago.

Proposed segment boundaries are not sharply defined. The boundaries may represent structurally complex transition zones a few to more than ten kilometers wide. To varying degrees, boundaries selected on the basis of paleoseismic and geomorphic observations are coincident with changes in the trend of segments; major salients in the range front; intersecting east-west or northeast structural trends observed in the bedrock geology of the range (Smith and Bruhn, 1984); saddles, cross faults, and transverse structural trends interpreted from gravity data (Zoback, 1983); and geodetic changes (Snay and others, 1984).

WHERE DO WE GO FROM HERE?

Two aspects of the investigations undertaken to date deserve especially close attention in future studies for evaluating seismic hazards. These are refinement of fault zone segmentation and development of tighter constraints on earthquake recurrence with emphasis on the timing of the most recent surface faulting earthquake along each segment.

The delineation of segments and evaluation of their past behavior through several seismic cycles has a major impact on the evaluation of seismic hazards along the Wasatch Front. The segments may provide a basis for constraining the location and length of rupture during single events. The potential rupture length is an important parameter for estimating maximum earthquake magnitude and it can be combined with displacement per event and fault width

data to estimate the most realistic maximum earthquake for that segment.

The elapsed time since the most recent event, the average recurrence interval, and the standard deviation of recurrence from the mean can be used to calculate real-time probabilities of occurrence of the next event on a segment during a selected interval (e.g., the next 50, 100, and 200 years). With better constrained, systematic data on elapsed time and average recurrence along the zone, it is possible to identify the segment of the fault that has the greatest likelihood of producing the next large earthquake. For example, the elapsed time since the most recent event along the proposed Salt Lake City and Provo segments, which lie astride the largest population centers, are not constrained by radiocarbon dating, although geomorphic observations suggest that the elapsed time since the most recent event on at least the Provo segment is significantly longer than on the adjacent Nephi segment to the south or on the Ogden segment north of Salt Lake City (Table 1). Therefore, elapsed time data are extremely important, and these two segments deserve close attention in this regard.

REFERENCES

- Schwartz, D.P., Hanson, K.L., and Swan, F.H., III, 1983, Paleoseismic investigations along the Wasatch fault zone: An Update: in Crone, A.J., (ed) Paleoseismicity along the Wasatch Front and Adjacent Areas, Central Utah, Geological Society of America Rocky Mountain and Cordilleran Sections Meeting, Guidebook Part 2, Utah Geological and Mineral Survey Special Studies 62, 45-49.
- Schwartz, D.P. and Coppersmith, K.J., 1984, Fault behavior and characteristic earthquakes: examples from the Wasatch and San Andreas faults: Journal of Geophysical Research, v. 89, p. 5681-5698.
- Smith, R.B. and Bruhn, R.L., 1984, Intraplate extensional tectonics of the eastern Basin-Range: inferences on structural style from seismic reflection data, regional tectonics, and thermal-mechanical models of brittle-ductile deformation: Journal of Geophysical Research, v. 89, p. 5733-5762.
- Snay, R.A., Smith, R.B., and Soler, T., 1984, Horizontal strain across the Wasatch front near Salt Lake City, Utah: Journal of Geophysical Research, v. 89, p. 1113, 1122.
- Swan, F.H., III, Schwartz, D.P., and Cluff, L.S., 1980, Recurrence of moderate to large magnitude earthquakes produced by surface faulting on the Wasatch fault, Utah: Bulletin of the Seismological Society of America, v. 70, no. 5, p. 1431-1462.

Swan, F.H., III, Hanson, K.L., Schwartz, D.P., and Kneupper, P.L., 1981, Study of earthquake recurrence intervals on the Wasatch fault at the Little Cottonwood Canyon site, Utah: U.S. Geological Survey, Open-File Report No. 81-450, 30 p.

Swan, F.H., III, Hanson, K.L., and Schwartz, D.P., 1982, Study of earthquake recurrence intervals on the Wasatch fault, Utah: Eighth semi-annual technical report prepared for the U.S. Geological Survey under Contract No. 14-07-0001-19842 (East Cache fault).

Zoback, M.L., 1983, Structure and Cenozoic Tectonism along the Wasatch fault zone, Utah: GSA Memoir 157, 3-27.

LIQUEFACTION POTENTIAL
AND SLOPE STABILITY
WASATCH FRONT AREA

by
Loren R. Anderson
Utah State University
Logan, Utah 84322

Introduction

The effects of earthquakes can cause loss of life and costly property damage; therefore, in areas of high seismic activity, earthquake hazard reduction must be an important consideration for intelligent land use planning. Damage during earthquakes can result from surface faulting, ground shaking, ground failure, generation of large waves (tsunamies and seiches) in bodies of water, and regional subsidence or downwarping. All of these causes of damage need to be considered in reducing earthquake hazards.

Ground failure associated with earthquake-induced soil liquefaction has caused major damage in various parts of the world during past earthquakes. The seismic history of the Wasatch front area in north-central Utah clearly indicates that ground motion of sufficient intensity and duration to induce liquefaction of susceptible soils is very likely to occur in the relatively near future.

Deposits of loose fine sand, highly susceptible to liquefaction, exist along the Wasatch front. Areas of shallow ground water are also widespread. In addition, evidence of liquefaction was observed following the 1934 Hansel Valley earthquake in Box Elder County, Utah and again following the Cache Valley earthquake of 1962.

The seismic history, subsurface soil and ground water conditions, and evidence of liquefaction in Utah indicate that liquefaction is a significant hazard which must be assessed as an important element in seismic hazard reduction planning.

In addition to earthquake hazards a number of other geologic hazards exist along the Wasatch Front and should also be considered in land use planning. During approximately three months in the spring of 1983, the state of Utah, with a population of about 2 million people, sustained direct damages from landslides, debris flows, mud floods, and flooding in excess of \$250 million. These disastrous events were so widespread and extensive that 22 of the 29 counties in the state were declared national disaster areas.

Considering all of these geologic hazards in a rational manner will require using a risk analysis framework. It is important that this framework be defined as soon as possible so that the format for individual hazard mapping programs can be adjusted to accommodate combining the results of several different studies.

Liquefaction Potential Mapping

As part of the U.S. Geological Survey's Earthquake Hazard Reduction program "Liquefaction Potential Maps" have been prepared for Davis, Salt Lake and Utah Counties and a study for the Northern Wasatch Front is pending. Liquefaction potential was evaluated from existing subsurface data and from supplementary subsurface investigations performed during the studies.

For this regional assessment, liquefaction implies liquefaction-induced ground failure. The liquefaction potential is classified as high, moderate,

low and very low depending on the probability that a critical acceleration will be exceeded in 100 years. The critical acceleration for a given location is defined as the lowest value of the maximum ground surface acceleration required to induce liquefaction. The categories of high, moderate, low and very low correspond to probabilities of exceeding the critical acceleration in the ranges of greater than 50 percent, 10 to 50 percent, 5 to 10 percent and less than 5 percent, respectively.

The Liquefaction Potential Maps that were developed show that for a significant portion of the Wasatch Front the probability of exceeding the critical acceleration in 100 years is greater than 50 percent. Hence, liquefaction induced ground failure is a significant seismic hazard.

Ground slope information, as well as the subsurface conditions documented on Soils and Ground Water Data Maps, can be used in combination with the Liquefaction Potential Maps as a means of assessing the type of ground failure likely to occur. Three slope zones have been identified from the characteristic failure modes induced by liquefaction during historic earthquakes (Youd, 1981, personal communication).

At slope gradients less than about 0.5 percent, loss of bearing capacity is the type of ground failure most likely to be induced by soil liquefaction. Stratified soil conditions, which exist in the study areas, provide vertical confinement for liquefiable layers and may tend to reduce the probability of bearing capacity failures. Buildings imposing light loads on the subsurface soils may not be affected by loss of bearing capacity during an earthquake. Heavy buildings, on the other hand, might be severely affected. Additionally, during earthquakes, heavy buildings subjected to movement from

deformation of the subsurface soils might cause damage to adjacent lightly-loaded structures.

Buried tanks, even those full of water or gasoline, could "float" to the surface if the soils surrounding them were to liquefy. For this to happen, however, the tanks would have to be buried in very thick deposits of sand. The stratified nature of the soils in the study areas generally tend to reduce the likelihood of this type of failure.

Slope gradients ranging from about 0.5 percent to about 5.0 percent tend to fail by lateral spread processes as a result of soil liquefaction. Evidence exists in Davis County for five large lateral spread landslides. Consequently, it appears that these kinds of failures have occurred in response to earthquakes within the past few thousand years.

Lateral spread landslides present the greatest concern because of the potential consequences. A small amount of movement can do a great deal of damage. Lifelines (buried utilities) are particularly vulnerable. A large area along the Wasatch Front area falls within the slope range characterized by lateral spread landslides induced by soil liquefaction.

Slopes steeper than about 5 percent tend to fail as flow slides if the mass of soil comprising the slope liquefies. In the study area, the stratified nature of the geologic materials suggests that flow-type failures are likely to be relatively rare. Instead, translational landslides or lateral spreads are likely to result from liquefaction on slopes steeper than about 5 percent.

The results of our research on the liquefaction potential along the Wasatch Front leads us to conclude that lateral spread landsliding is the type

of ground failure most likely to accompany soil liquefaction. The probability of extensive damage due to this type of ground failure is very high. All types of structures could be damaged by liquefaction-induced ground failure; lifelines are especially susceptible to damage.

Landslide Potential Research

During the unusually heavy spring snowmelt period of 1983, over ninety landslides occurred along the Wasatch Front between Bountiful and Kaysville, Utah. Many of these landslides, commonly referred to as "debris slides" or "soil slips", came to rest only a short distance downslope from the zone of initiation. However, some of them mobilized into debris flows which transported large boulders up to five miles. One debris flow inundated nine square blocks of the town of Farmington with over 90,000 cubic yards of debris and caused extensive damage.

Readings on open stand-pipe piezometers which were installed near five of the landslides shortly after slope failure show complex groundwater behavior with sharp fluctuations in piezometric pressure. Artesian pore water pressures were observed on a slope with a gradient in excess of 30 degrees indicating a strong influence of confining layers within the soil strata. Visual observations by landslide hazard warning teams during the height of landslide activity and photographic documentation shown that a time delay exists between initial ground cracking and subsequent ground failure and debris flow mobilization.

In response to the landslide activity during 1983 a number of research projects were initiated that will lead to a better understanding of the landslide hazard along the Wasatch Front. These projects are listed below.

<u>Project</u>	<u>Research Group</u>	<u>Sponsored by</u>
Seismic Slope Stability Map of the Urban Corridor of Davis and Salt Lake Counties	Dames & Moore Utah State University	USGS
Debris Slide Initiation	Utah State University	NSF
Probabilistic Landslide Potential Delineation	Utah State University	USFS, USU, NSF
Potential for Debris Flow Along the Wasatch Front	U.S. Geological Survey	USGS
Landslide Surveillance	University of Utah	UGMS, Utah CEM
Numerous Landslide Reconnaissance Investigations	Utah Geological and Mineral Survey	UGMS
Numerical Modeling of Debris Flows	Utah State University	USU
Monitoring Debris Flows	U.S. Geological Survey	USGS

Photographic documentation and eyewitness accounts during the spring of 1983 indicated that landslides which triggered debris flows were often preceded by ground cracking on steep mountain slopes. When the cracks were identified, the time lag between initial slope cracking and subsequent complete slope failure sometimes provided a reaction period during which threatened residents could be either evacuated or put on alert.

Anticipating further landslide activity in the spring of 1984, a reconnaissance aerial photography program was initiated with the support of the Boise Air National Guard to systematically identify incipient landslides which could mobilize debris flows. The program emphasized a quick turn-around time of 3 to 4 days from the date of photography to the interpretation of the photographs. When signs of instability were identified, the potential hazards were reported to the Utah Geological and Mineral Survey and the USDA Forest Service for follow-up investigation and appropriate action. The program

successfully identified several areas on the basis of ground cracking which subsequently failed and mobilized into debris flows.

In addition to the aerial photography coverage that was obtained from the Boise Air National Guard other coverage of the Wasatch Front has been obtained and is available for landslide studies.

Conclusion

There are numerous geologic hazards along the Wasatch Front that must be considered as part of intelligent land use planning activities. Three studies sponsored by the U.S.G.S. Earthquake Hazard reduction program indicate that there are significant areas in Davis, Salt Lake and Utah Counties with high liquefaction potential. Furthermore, the events of 1983 indicate that landslides, debris flows and floods are of significant concern. An important step must be taken soon to coordinate hazard mapping studies so that they can be integrated in a Risk Analysis Framework.

THE GROUND-SHAKING HAZARD ALONG THE WASATCH FAULT ZONE, UTAH

W. W. Hays (I)
K.W. King (II)

SUMMARY

This paper combines probabilistic estimates of bedrock ground motion and empirical soil-transfer functions for sites in the Salt Lake City, Ogden, and Provo area to evaluate the earthquake ground-shaking hazard along the Wasatch fault zone, Utah. The Wasatch fault zone, which has the potential for generating moderate to large earthquakes, could cause peak bedrock accelerations of and velocities of as much as 0.28 g and 16 cm/s, respectively. The ground-shaking hazard in the Salt Lake City, Ogden, and Provo area is greatest for sites underlain by thick, fine-grained silts and clay because they amplify ground motion in some period bands by as much as a factor of ten.

INTRODUCTION

Salt Lake City, Ogden, and Provo are located adjacent to the Wasatch fault zone, Utah (Fig. 1). The Wasatch fault zone has the potential for generating moderate to large earthquakes which could cause serious social and economic disruption to approximately 900,000 people (about 80 percent of the population of Utah). Moderate and large earthquakes would cause damage from ground-shaking, surface fault rupture, earthquake-induced landslides, and liquefaction.

Evaluation of the earthquake hazards of ground shaking, surface fault rupture, and earthquake-induced ground failure along the Wasatch fault zone is a complex research task, as illustrated in Fig. 2. Evaluation of the ground-shaking hazard in each urban area requires: 1) identification of the seismogenic zones, 2) definition of an earthquake-occurrence model for each seismogenic zone, 3) formulation of a regional seismic-wave attenuation model, and 4) evaluation of the site-specific effects of soil and rock on ground motion.

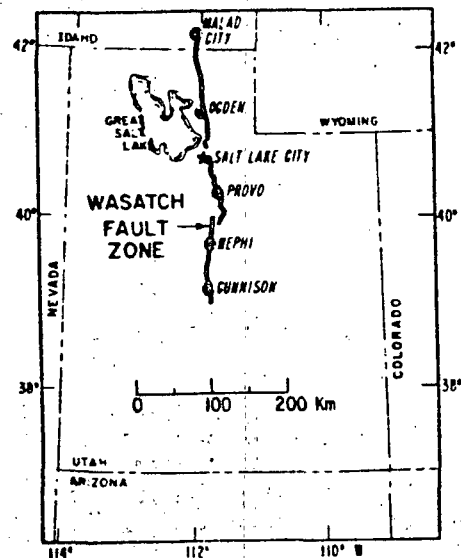


Figure 1.—Map showing Salt Lake City, Ogden, and Provo, and the Wasatch fault zone.

- I Geophysicist, U.S. Geological Survey, Reston, Virginia, USA 22092
II Geophysicist, U.S. Geological Survey, Denver, Colorado, USA 80225

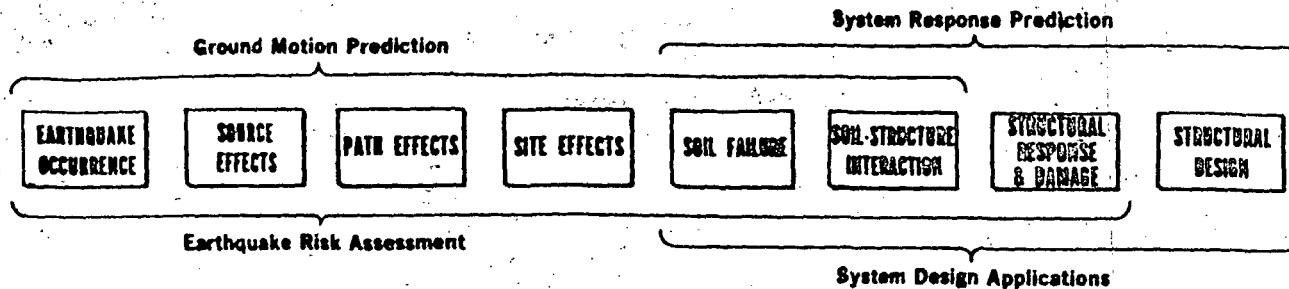


Figure 2.—Schematic illustration of the steps involved in evaluating the earthquake hazards of ground shaking, surface fault rupture, and earthquake-induced ground failure. Evaluation of the ground-shaking hazard requires consideration of the first four steps.

THE RESEARCH PROBLEM

The fundamental problem in the evaluation of the ground-shaking hazard in Salt Lake City, Ogden, and Provo is the lack of scientific and engineering data. Only one strong motion accelerogram, recorded in the 1962 of earthquake of magnitude 5.7 in Cache Valley, exists in Utah. No strong ground-motion data exist to define regional seismic-wave attenuation relations and site response. Because of these significant gaps in data, evaluation of the ground-shaking hazard requires an approach that combines probabilistic estimates of the bedrock ground motion and empirical estimates of the site response. The following sections briefly describe the information used to evaluate the ground-shaking hazard in the Salt Lake City, Ogden, and Provo area, emphasizing the evaluation of site response.

Earthquake Occurrence - Although the Wasatch fault zone, a 370-km-long north-trending zone of young, active, normal faulting has produced many earthquakes, it has not produced an earthquake as large as magnitude 6 since 1850 (Ref. 1). The geologic and geomorphic records clearly show that individual faults in this zone have been active for millions of years (Ref. 2.) and have the potential for generating an earthquake of magnitude 7.5. Exploratory trenching and analysis of scarp morphology and scarp-derived colluvial deposits at two locations along the fault zone suggest that the recurrence interval of moderate to large earthquakes (i.e., magnitudes of 6.5 to 7.5) for the Wasatch fault zone ranges from about 50 to 430 years (Ref. 3).

Maps of Bedrock Ground Motion - Maps of the ground-shaking hazard for bedrock have been prepared for the United States (Ref. 4). In terms of peak bedrock acceleration, these maps show that the Wasatch front has a significant ground-shaking hazard compared with other areas of the Nation (Fig. 3). For Utah, historical seismicity and geologic information were integrated to define seismogenic zones (Fig. 4). Using these zones, an assumed attenuation function, and a probability of nonexceedance of 90 percent during an exposure time of 50 years, values of 0.28 g and 16 cm/s were calculated as the maximum values of peak horizontal bedrock ground acceleration and ground velocity along the Wasatch front. (Fig 5.).

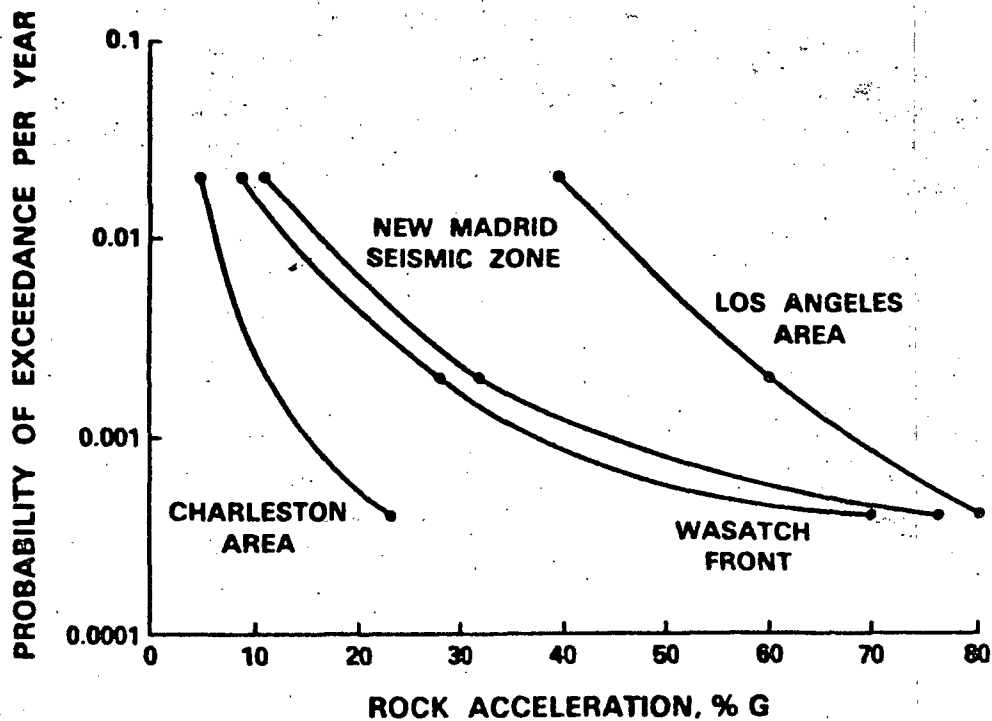


Figure 3.—Curves comparing the bedrock ground-shaking hazard in various geographic areas. Each curve represents a 90 percent probability of nonexceedance (from Ref. 4).

Because empirical data showing the characteristics of ground response under low-to high-strain ground shaking are lacking along the Wasatch fault zone, a special effort, described in the following sections, was made to quantify the physical properties of the unconsolidated materials along the Wasatch front and to define their response to ground shaking. Sites underlain by unconsolidated materials subjected to a peak acceleration of 0.28 g and a peak velocity of 16 cm/s are generally expected to have larger values of ground shaking due to amplification of ground motion (Ref. 5). Some researchers (for example, Ref. 6) disagree with this conclusion when the peak bedrock acceleration is 0.2 g or greater.

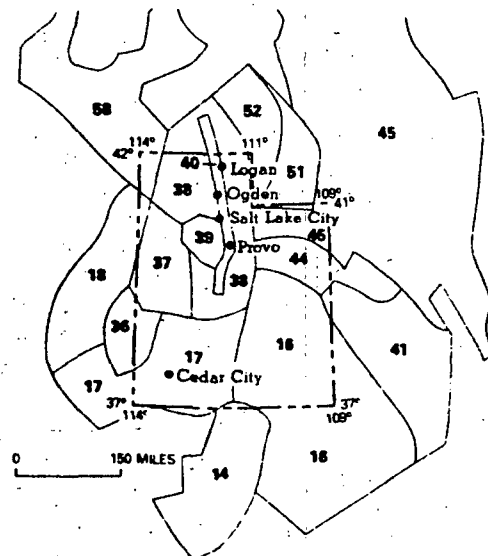


Figure 4.—Map showing seismicogenic zones in Utah (from Ref. 4).

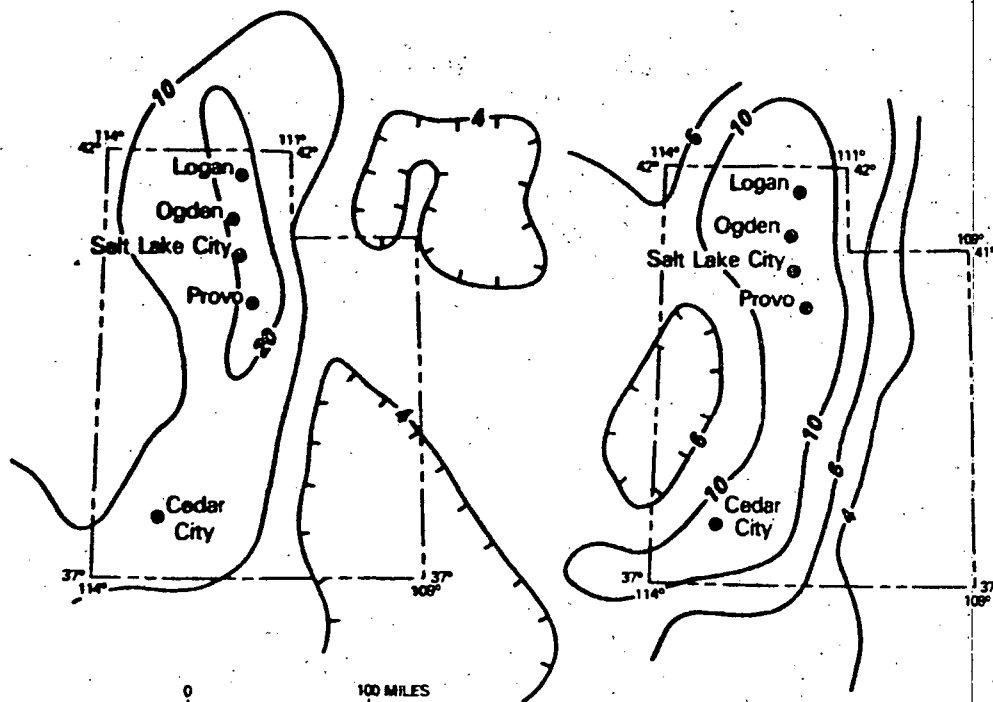


Figure 5.—Maps of the probabilistic bedrock peak horizontal ground acceleration (left) and peak horizontal ground velocity (right) for Utah. Each map represents a 90 percent probability of nonexceedance in a 50 year exposure time. The maximum values of acceleration and velocity are 0.28 g and 16 cm/s (from Ref. 4).

Physical Properties of Unconsolidated Materials - The surficial materials underlying Salt Lake City, Ogden, and Provo (Ref. 7) are related to the deposits of several lakes, (the last being Lake Bonneville) that filled the Great Salt Lake Basin during the Pleistocene Epoch. Salt Lake City, Ogden, and Provo are founded on several different types of unconsolidated materials which have been classified in terms of depositional environments: onshore, nearshore, and offshore.

Salt Lake City is founded on several different types of nearshore deposits which have been studied fairly extensively. The deposits range in thickness from about 100 to 900 m, have shear-wave velocities that average about 200 m/s, and have a natural moisture content by weight of about 43 percent.

In Ogden and Provo, less information is available; however, the available data suggest that the physical properties of the unconsolidated materials underlying these cities are similar to those underlying Salt Lake City. A borehole in the Provo area indicates a shear-wave velocity of about 155 m/s. These two values (155 m/s and 200 m/s) compare with values ranging from 55 to 310 m/s for soil types in the San Francisco Bay region (Ref. 8), suggesting that the shear strength (at failure) of the unconsolidated materials in the two geographic areas is roughly the same.

Ground Motion Measurements - Ground motion from nuclear explosions at the Nevada Test Site was measured at 40 locations in Salt Lake City, 13 locations in Ogden, and 11 locations in Provo, using portable broadband velocity seismographs. These data were used to derive empirical site-transfer functions. Some of the recording sites in each city were located on the Wasatch front and underlain by rock (for example, limestone, shale, sand-stone, and quartz monzonite); the others were underlain by unconsolidated materials. The recording sites satisfied the following criteria: 1) they encompassed all of the depositional environments (onshore, nearshore, and offshore), 2) they exhibited a wide range of physical properties, and 3) they were located within about 30 km of the Wasatch fault zone. Measurements at some sites were duplicated to verify the transfer functions.

Soil Transfer Functions - Soil transfer functions derived from nuclear-explosion ground-motion data recorded in Salt Lake City, Ogden, and Provo, show that the consolidated and unconsolidated materials underlying these three major cities have distinctive characteristics of ground response. A transfer function (which is defined as the average ratio of the 5-percent damped, horizontal, velocity response spectra for a pair of sites underlain by soil and rock) correlates with changes in thickness and type of unconsolidated material (Refs. 9-15). Empirical data suggest that a reliable transfer function can be determined for some soil types from either earthquake or nuclear-explosion ground-motion data in spite of differences in their ranges of peak ground acceleration and dynamic shear strain. The level of dynamic shear-strain is defined as the ratio of the peak particle velocity induced in the soil column to the shear-wave velocity of the soil. Past studies (Ref. 12) indicate that the response of some soil types remains linear under levels of strain of about 0.5 percent (i.e., the ratio of 115 cm/s and 200 m/s corresponding to the peak particle velocity observed in the 1979 Imperial Valley earthquake and the shear-wave velocity of the near-surface soil). The value of 0.5 percent is the greatest level of dynamic shear strain represented by the current strong-motion data sample. The maximum level of shear strain expected along the Wasatch front in a 50 year period would be about 0.08 percent (the ratio of 16 cm/s and 200 m/s). Ground motions corresponding to higher levels of shear strain than 0.5 percent (i.e., produced in laboratory measurements) have not been recorded.

The transfer functions for the Salt Lake City area (Figs. 6, 7) show that the site response varies markedly. The response for sites underlain by thin deposits of gravel and coarse sand is about a factor of 2, relative to a rock site on the Wasatch front, across most of the spectrum. However, the response for sites underlain by thick deposits of silt and clay is as much as a factor of 10 in some period bands.

The transfer functions for the Ogden and Provo areas show features similar to those in the Salt Lake City area. For the Provo area, the response for sites underlain by unconsolidated materials reaches a factor of about 8, in some period bands, relative to a rock site on the Wasatch front. The relative response is about 5 in the Ogden area.

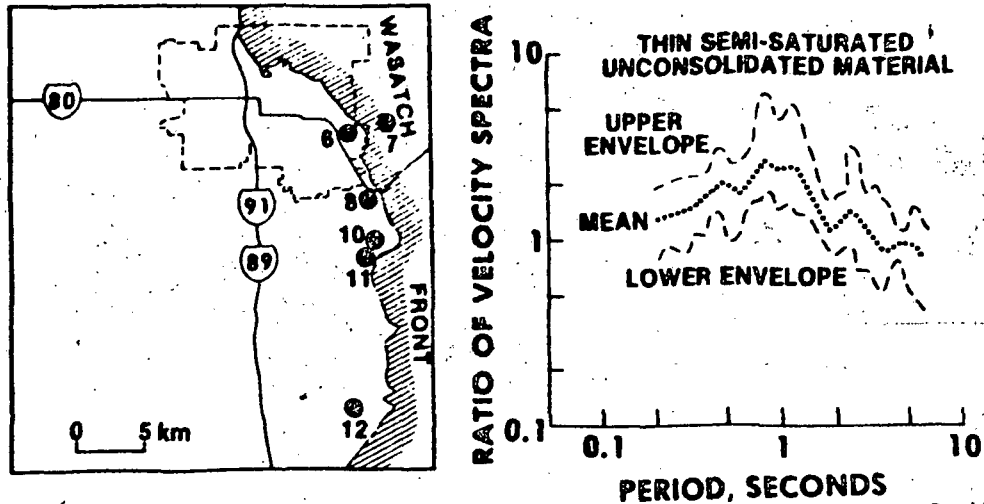


Figure 6.—Range of transfer functions showing horizontal response of sites underlain by thin (150 m or less) unconsolidated onshore deposits (stations 6, 8, 10, 11, 12) relative to a rock site (station 7) on the Wasatch front, Salt Lake City area.

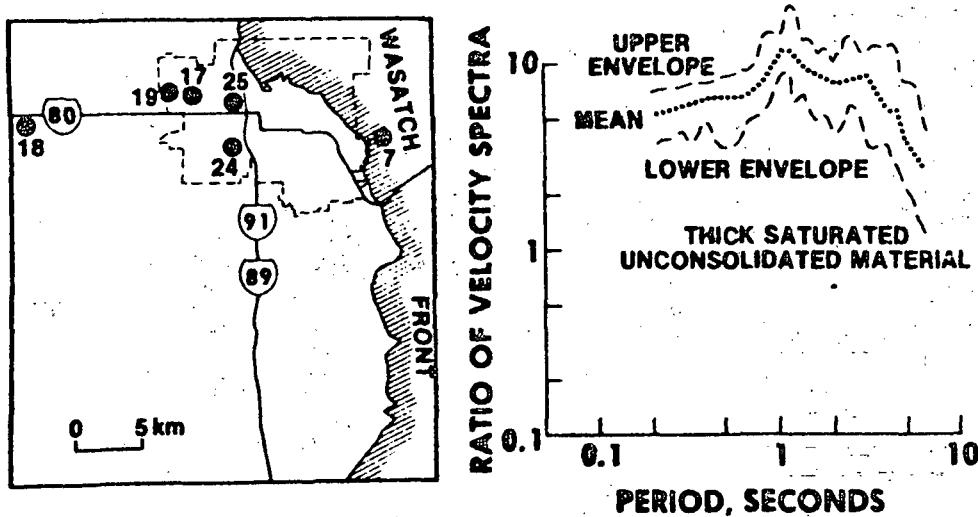


Figure 7.—Range of transfer functions showing horizontal response of sites underlain by thick (450-750 m) unconsolidated nearshore and offshore deposits (stations 17, 18, 19, 24, 25) relative to a rock site (station 7) on the Wasatch front, Salt Lake City area.

THE GROUND-SHAKING HAZARD

Combining the probabilistic maps of bedrock ground motion and the empirical data on site response indicates that a significant ground-shaking hazard exists along the Wasatch front (Figs. 8, 9). The most significant implication is that site amplification of as much as a factor of 10, in the period band that coincides with the natural periods of vibration of 2-7 story buildings, can occur in the Salt Lake City, Ogden, and Provo areas. For Salt Lake City, the map of site response (Fig. 8)

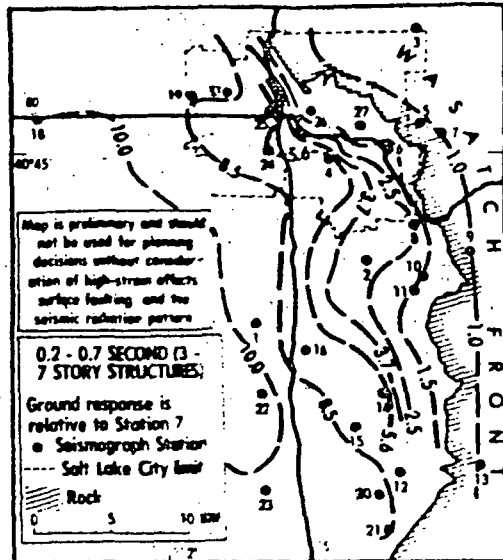


Figure 8.—Map of estimated horizontal site response for the period band 0.2-0.7 sec., Salt Lake City area. Values on contours were taken from the transfer functions. This period band corresponds to the natural period of vibration of 2-7 story buildings. Recording stations are shown by solid circles. Corporate limits of Salt Lake City are dashed.

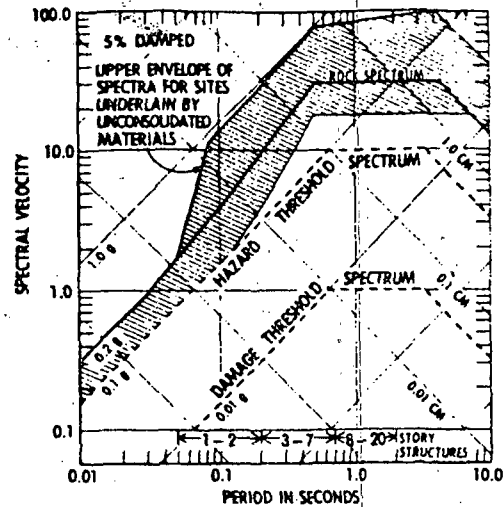


Figure 9.—Graph showing the estimated ground-shaking hazard in Salt Lake City, Ogden, and Provo based on the assumption of a magnitude 7.5 earthquake occurring on the Wasatch fault zone and producing a peak bedrock acceleration of 0.2 g. The variation shown corresponds to differences in the site response indicated by the site-transfer functions.

shows that the response of sites underlain by unconsolidated materials increases as distance from the Wasatch fault zone increases and is greatest in regions of thick, fine-grained deposits of silts and clay near the center of the Jordan River Valley. The effect of water saturation on site response is not clear. The data suggest that a broad area in each city would be exposed to about the same level of ground shaking and expected to undergo extensive damage. Although the strain dependence of soils along the Wasatch front is unknown, some empirical data (Ref. 10) suggest that even in large earthquakes linear ground response would be expected beyond about 2 km from the Wasatch fault zone.

REFERENCES

1. Arabasz, W. J., Smith, R. B., and Richens, W. D., (1979), Earthquake studies in Utah, 1850 to 1978: University of Utah Seismograph Station, Department of Geology and Geophysics, 552 p.
2. Hamblin, W. K., (1976), Patterns of displacement along the Wasatch fault: *Geology*, v. 4, p. 619-622.
3. Swan, F. H., Schwartz, D. P., and Cluff, L. S., (1980), Recurrence of moderate-to-large magnitude earthquakes produced by surface faulting on the Wasatch fault zone: *Seismological Society of America Bulletin*, v. 70, p. 1431-1462.

4. Algermissen, S. T., and Perkins, D. M., (1976), A probabilistic estimate of maximum acceleration in rock in the contiguous United States: U.S. Geological Survey Open-File Report 76-416, 45p.
5. Joyner, W. B., Warrick, R. E., and Fumal, T. E., (1981), The effect of Quaternary alluvium on strong ground motion in the Coyote Lake, California, earthquake of 1979: Seismological Society of America Bulletin, v. 71, p. 1333-1349.
6. Seed, H. B., Murarka, R., Lysmer, J., and Idriss, I. M., (1976), Relationships of maximum acceleration, maximum velocity, distance from source, and local site conditions for moderately strong earthquakes: Seismological Society of American Bulletin, v. 66, p-1323-1342.
7. Miller, R. D., (1980), Surficial geologic map along part of the Wasatch Front, Salt Lake Valley, Utah: U.S. Geological Survey Miscellaneous Field Studies Map, MF-1198, (Scale: 1:100,000).
8. Gibbs, J.F., Fumal, T.E., and Borchardt, R. D. , (1976), In situ measurements of seismic velocities in the San Francisco Bay region, Part III: U.S. Geological Survey Open-File Report 76-731, 145 p.
9. Borchardt, R. D., editor, (1975), Studies for seismic zonation of the San Francisco Bay region: U.S. Geological Survey Professional Paper 941-A, 102 p.
10. Hays, W. W., Algermissen, S. T., Miller, R. D., and King, K. W., (1978), Preliminary ground response maps for the Salt Lake City area: International Conference on Microzonation, 2nd, San Francisco, California, Proceedings, v. 2, p. 497-508.
11. Rogers, A. M., and Hays, W. W., (1978), Preliminary evaluation of site transfer functions developed from nuclear explosions and earthquakes: International Conference on Microzonation, 2nd, San Francisco, California, Proceedings, v. 2, p. 753-764.
12. Hays, W. W., Rogers, A. M., and King, K. W., (1979), Empirical data about local ground response: U.S. National Conference on Earthquake Engineering, 2nd, Stanford, Calif., Proceedings, p. 222-232.
13. Hays, W. W., (1980), Procedures for estimating earthquake ground motion: U.S. Geological Survey Professional Paper 1114, 95p.
14. Rogers, A. M., Covington, P. A., and Borchardt, R. D., (1980), A comparison of ground response in the Los Angeles Region from nuclear explosions and the 1971 San Fernando earthquake: World Conference on Earthquake Engineering, 7th, Istanbul, Turkey, Proceedings, v.2, p. 625-632.
15. Rogers, A. M., Algermissen, S. T., Hays, W. W., Perkins, D. M. (geologic and seismological portion), Van Strien, D. O., Hughes, H. C., Hughes, R. C., Lagorio, H. J., and Steinbrugge, K. V. (engineering analyses portion), (1976), A study of earthquake losses in the Salt Lake City, Utah, area: U.S. Geological Survey Open-File Report 76-89, 357p.

EARTHQUAKE BEHAVIOR IN THE WASATCH FRONT AREA: ASSOCIATION
WITH GEOLOGIC STRUCTURE, SPACE-TIME OCCURRENCE, AND STRESS STATE

by

Walter J. Arabasz

Dept. of Geology and Geophysics

University of Utah

Salt Lake City, Utah 84112-1183

INTRODUCTION

The potential in Utah for a large disastrous earthquake--notably along the Wasatch fault--has been recognized and documented for more than a century. Geological observations, the record of earthquake activity since 1850, and modern methods of probabilistic analysis firmly establish a significant level of earthquake risk. This risk relates not only to the occurrence of a large (magnitude 6-1/2 to 7-3/4) surface-faulting earthquake but also to cumulative exposure to moderate-size (magnitude 5 to 6-1/2) earthquakes, perhaps below the threshold for surface rupture. Distinction between these two threats is useful because they appear to require attention to separate aspects of the tectonic framework of the Wasatch Front area--and different, albeit complementary, research strategies.

The purpose of this invited contribution is to stimulate discussion of specific risk-related issues raised by organizers of this workshop. Some of

these issues amenable to a seismological perspective include: historical seismicity versus tectonics, seismic cycle, characteristic earthquakes, seismic gaps, and mechanics of the Wasatch fault zone. For convenience, these issues will be discussed within the context of three general topics: (1) the association of seismicity with geological structure, (2) space-time patterns of earthquake occurrence, and (3) stress state. Because the Wasatch fault itself during historical time has had no large earthquakes and few (perhaps no) moderate-size earthquakes, consideration of earthquake experience within a broader region is inescapable.

ASSOCIATION OF SEISMICITY WITH GEOLOGICAL STRUCTURE

A fundamental obstacle for understanding fault behavior and earthquake generation in the Utah region is the problematic correlation of diffuse seismicity with mapped Cenozoic faulting (e.g., Smith, 1978; Arabasz and others, 1980; Arabasz and Smith, 1981; McKee and Arabasz, 1982). Problems include: (1) uncertain subsurface structure, which typically is more complex along the main seismic belt than apparent from the surface geology; (2) observations of discordance between surface fault patterns and seismic fault slip at depth (Arabasz and others, 1981; Zoback, 1983); (3) a paucity of historic surface faulting; and (4) inadequate focal-depth resolution from regional seismic monitoring (discussed later). Investigations of diffuse seismicity should also consider the possibility of depth-varying stress orientation (for which there is no good evidence yet in the Intermountain area), and variations in seismicity patterns with earthquake size or stress level (see McKee and Arabasz, 1982).

The characterization of subsurface structure will not be pursued here. See Smith and Bruhn (1984) for a summary of seismic-reflection data that indicate the widespread presence of low-angle and downward-flattening faults in the subsurface, and an intimate relationship between pre-Neogene thrustbelt structure and young normal faults, along the eastern Basin and Range margin. Seismological evidence to date indicates that, at least for small to moderate earthquakes, seismic slip in this region predominates on fault segments with moderate ($>30^\circ$) to high-angle dip (Arabasz, 1983; Zoback, 1983).

There has been only one instance of historic surface faulting in the Utah region--the 0.5-m vertical displacement associated with the $M_L 6.6$ Hansel Valley earthquake of 1934. The occurrence of seven other historical earthquakes of magnitude $6.0 \leq M_L < 6.6$ without surface rupture (see Arabasz and others, 1979) suggests a relatively high threshold for such faulting in the region. Bucknam and others (1980), summarize data on documented surface faulting in the Basin and Range province and note that all historic earthquakes in the Great Basin of $M_L 6.3$ or greater (7 earthquakes) have produced surface rupture. The two smallest earthquakes in their tabulation, $M_L 5.6$ and 6.3 , had maximum displacements of 0.2 m and 0.1 m, respectively; earthquakes of $M_L 6.8$ or less (5 earthquakes) all had a maximum displacement less than one meter.

Rigorous efforts were not made to search for evidence of surface faulting immediately following many of Utah's larger historical earthquakes, say $M_L \geq 5$, so the threshold for small surface displacements up to a few tenths of a meter is debatable. Moreover, the minimum magnitude for surface rupture depends on variable parameters of an earthquake source, including focal depth, fault geometry, stress drop, seismic moment, rupture-propagation dynamics, and

the like. No evidence was found for tectonic surface faulting accompanying the M_L 6.0 Pocatello Valley earthquake in 1975, but observations were made of non-tectonic surface cracking in frozen snow cover in the alluviated valley, and up to 13 cm of localized subsidence in the valley may have been coseismic (see Arabasz and others, 1981, p. 819f).

Given the relatively high threshold of surface faulting and observations noted earlier of discordance between surface fault patterns and seismic slip at depth, one can argue that--with the sole exception of the 1934 Hansel Valley earthquake--no other of Utah's 15 historical earthquakes of M_L 5.5 or greater (Arabasz and others, 1979, p. 9) can be confidently associated with a mapped surface fault. Further, our present incomplete understanding of the association of seismicity with geological structure in the Utah region allows the following assertion. Within the domain of Utah's main seismic belt, future seismicity below the threshold of surface faulting (M_L approx. 6 to 6-1/2) cannot be confidently precluded by knowledge of the surface geology alone. Where subsurface structure is complex, moderate size earthquakes may occur on "blind" subsurface structures that have no direct surface expression.

Crustal structure along the eastern Great Basin is now known to involve vertically stacked plates separated by low-angle detachments resulting from relict pre-Neogene thrustbelt structure and/or Neogene extension (Allmendinger and others, 1983; Smith and Bruhn, 1984; Standlee, 1983). On the basis of special earthquake studies in the southern Wasatch Front area, neighboring parts of central Utah, and southeastern Idaho, the following working hypothesis is offered to explain observations of diffuse background seismicity. Background seismicity is fundamentally controlled by variable mechanical behavior and

internal structure of individual horizontal plates within the seismogenic upper crust. Diffuse epicentral patterns result from the superposition of seismicity occurring within individual plates, and also perhaps from favorable conditions for block-interior rather than block-boundary microseismic slip.

To illustrate this hypothesis, Figure 1 summarizes evidence for a spatially discontinuous distribution of seismicity with depth, above and below about 5-6 km below datum, in the vicinity of the Sevier Valley near Richfield, Utah. Aftershock foci of a magnitude 4.0 earthquake on the eastern side of the valley (lower right, Figure 1) abruptly terminate at this level; foci of background earthquakes along the western side of the valley (lower left, Figure 1) decrease markedly in frequency below this level.

A schematic diagram in the upper part of Figure 1 shows that the depth-discontinuities in seismicity approximately coincide with an identified jump in P-wave velocity. Nearby drill-hole data, local geological information, and evidence from both COCORP (Allmendinger et al., 1983) and industry seismic reflection data (Frank Royse, Chevron, U.S.A., personal communication, 1983) suggest that the seismicity discontinuities coincide with a regional near-horizontal detachment fault at that level. One outstanding implication is the possibility of decoupling between surface faulting (and shallow seismicity) and deeper extension (e.g., see Cape et al., 1983). Because the Richfield area has been the site of some of the most significant magnitude 6 to 6-1/2 earthquakes in the Utah region, the critical question arises whether such strain release was related to very shallow or deeper extension.

Results of a special field study of earthquake swarm activity ($M \leq 4.7$) near Soda Springs, Idaho, in October 1982 by Richins et al. (1983) also

suggest the influence of a low-angle structural discontinuity upon seismic deformation within the upper crust. Comparison of accurately located earthquake foci from that study (Figure 2) with subsurface seismic reflection data from that same area (Dixon, 1982) indicate (1) that seismicity is not simply identifiable with late Cenozoic faulting (the earthquake foci define a NW-trending high-angle structure within and not simply bounding a major range block), and (2) that an apparent discontinuity in the frequency distribution of earthquakes with depth coincides with the pre-Cenozoic Meade thrust fault. Abundant seismicity above 7 km in Figure 2 occurs within the Meade thrust plate; subjacent foci lie within the Absaroka thrust plate. Focal mechanisms indicate a predominance of strike-slip faulting on NW-trending steeply-dipping fault segments--both above and below the near-horizontal thrust fault. There is some mixing of normal-faulting mechanisms in spatial compartment 3, but no indication of seismic slip on a low-angle plane.

One important point of these examples is that precise hypocenters, adequately concentrated seismicity, and abundant single-event focal mechanisms are required to unravel the association of seismicity with structure. Our fixed-network station spacing is simply inadequate for the critical resolution achievable with supplementary short-term efforts with portable seismographs. A second point is that precisely resolving the focal depth of background seismicity may be crucial for effective surveillance in the ISB. Because large earthquakes expectedly nucleate at the base of the seismogenic layer (Sibson, 1982; Das and Scholz, 1983), at about 10-15 km in the Utah region (Smith and Bruhn, 1984), the pattern of background seismicity at this depth may in some cases be masked or blurred by greater flux of small to moderate-size earthquakes within an overlying plate. Such an hypothesis requires

"linkage" or some rupture pathway between the deep nucleation points of large earthquakes and existing surface fault scarps.

Figure 3 schematically shows some aspects of the working hypothesis proposed here as relating diffuse seismicity to vertically stacked plates in the upper crust. These aspects (by no means exhaustive) include: (a) local predominance of background microseismicity within a lower plate, such as at 7-12 km depth in Goshen Valley, southwest of Provo, Utah (McKee and Arabasz, 1982); (b) nucleation of a large normal-faulting earthquake near the base of the seismogenic layer, on an old thrust ramp, and with linkage or an established rupture pathway to a major surface fault; (c) occurrence of a moderate-size earthquake within a lower plate--manifesting structural discordance with surficial geology, and with surface rupture inhibited by no established linkage to a shallow structure; (d) occurrence of a moderate-size earthquake and aftershocks on a secondary structure where an underlying detachment restricts deformation to the upper plate; (e) diffuse block-interior microseismicity predominating within an upper plate--perhaps responding to extension enhanced by gravitational backsliding on an underlying detachment; and (f) diffuse block-interior microseismicity within a lower plate where frequency of occurrence is markedly lower than in the overlying plate. In the case of location (b), note that focal-depth resolution would be critical to discriminate background earthquakes associated with the deeper nucleation zone from background seismicity associated with an overlying shallow structure. This situation may be analogous to that in the western Salt Lake Valley.

SPACE-TIME PATTERNS OF EARTHQUAKE OCCURRENCE

Observations have earlier been published regarding space-time patterns of earthquake behavior in the Utah region. These include discussion of persistent microseismicity gaps along the Wasatch fault zone (Arabasz and others, 1980), and extended discussion of a systematic examination of the Utah earthquake record for foreshock occurrence, precursory quiescence and clustering, migration of mainshocks, and seismicity gaps (Arabasz and Smith, 1981; see also Griscom, 1980). The intention here is to provide an up-dated perspective on seismicity gaps associated with the Wasatch fault zone on a local and regional basis. The same data allow comment on characteristic earthquakes and seismic cycle.

Figure 4, reproduced from Arabasz and others (1980), indicates two elliptical zones of anomalously low seismicity along the Wasatch fault that have been described as seismicity gaps. It should be emphasized that the boundaries of these zones, located to the north and south of Salt Lake City, were based directly on observations of Smith (1974) of pre-1974 seismicity-- not on the post-1974 seismicity shown in Figure 4. Nevertheless, the zones demarcate a remarkable paucity of microseismicity within the broadly active earthquake belt of the Wasatch Front. The 3.75-yr period of Figure 4 represents the initial period of modern instrumental monitoring. Figure 5 is an updated 5.5-yr sample of seismicity of the Wasatch Front area subsequent to that of Figure 4. Comparison of the two figures suggests a basically stationary pattern of background seismicity during the two time samples. In terms of the seismicity gaps, Figure 5 shows a persistent paucity of earthquake epicenters in the northern zone. In the southern zone, however, an earthquake of

magnitude 3.9 occurred on February 20, 1981, near the town of Orem, northwest of Provo. A distinctive aspect of this earthquake was the relative absence of aftershocks compared to sequences associated with other comparable mainshocks in the region. Only a single microaftershock was located by the local network.

Arabasz and others (1980) discuss the depicted seismicity gaps along the Wasatch fault, including their initiation and considerable uncertainty in relating them to sectional behavior of the fault. Indeed, one need only recall problems raised in the preceding section. It is apparent, however, that specific features of small-earthquake occurrence in the vicinity of the Wasatch fault are open to investigation. These notably include (1) epicentral clustering along the fault trace north of Brigham City, (2) episodic earthquake activity west of the fault beneath the Salt Lake Valley and beneath Goshen Valley southwest of Provo, and (3) diffusely scattered seismicity in the vicinity of the southernmost Wasatch fault (see Pechmann and Thorbjarnardottir, this volume; McKee and Arabasz, 1982; Arabasz, 1984, regarding relevant special studies).

There is minimal microseismicity along the 20- to 30-km-long segment of the Wasatch fault north of Nephi, possibly associated with the youngest (< 300 yr?) surface rupture anywhere on the Wasatch fault (Schwartz and Coppersmith, 1984). Relatively intense but dispersed seismicity to the south belies simple correlation with the southernmost Wasatch fault, which markedly changes character south of Nephi. Preliminary results suggest predominant background seismicity shallower than about 7 km within Jurassic and younger sedimentary rocks involved in complex structure (see Standlee, 1983).

As argued by Arabasz and Smith (1981), the microseismicity gaps along the Wasatch fault north and south of Salt Lake City are not necessarily indicative of a late (i.e., pre-earthquake) stage of a seismic cycle. Uncertainties include the timing of the last surface-faulting event and the variation of interevent times at sites within the gaps. They observed, however, that the microseismicity gaps are encompassed by a more extensive regional zone of anomalous seismicity for earthquakes of $M_L 3.5$ or greater. Those observations will next be updated and examined.

Figure 6, reproduced from Arabasz and Smith (1981), summarizes the observation of a 300 km by 100 km N-S trending seismicity gap ($M_L \geq 3.5$) along the main axis of the Intermountain seismic belt between 38.9° N and 41.5° N latitude. (Only independent mainshocks are considered.) This spatial compartment, hereafter referred to as the Wasatch Front (WF) compartment, encompasses 80 percent of the Wasatch fault zone. No mainshock larger than Modified Mercalli intensity VII, or about magnitude 5-1/2, has occurred in this area since 1915. Despite background microseismicity (e.g., Figure 4), the hachured space-time compartment in Figure 6 shows that only one mainshock of $M_L 3.5$ or greater occurred from 1968 through March 1980. Figure 7 gives an updated view of earthquakes within the WF compartment above magnitude thresholds of 2.5 and 3.5.

As shown in Figure 7b, four independent mainshocks of $M_L 3.5$ or greater occurred in the WF compartment during 1980-1983. (A fifth shock near its southeast extremity is in an area of known mining-related seismicity and is justifiably excluded.) The largest event had a magnitude of 4.4 and was investigated by McKee and Arabasz (1982). The next largest event of magnitude 4.3

is the subject of a companion report by Pechmann and Thorbjarnardottir (this volume). Epicentral distributions in both Figures 7a and 7b suggest random occurrence throughout the main seismic belt during the 5.5-yr sample period. The WF compartment does not appear to be anomalously quiet in either sample. Inspection of Figure 7a, however, shows that seismic flux is relatively low within the part of the WF compartment north of 40°N lat.--similar to the relative flux seen in the epicenter map of Figure 6 for a 130-yr period.

In view of its location within the densest part of the University of Utah's seismic network, it is noteworthy that the northern part of the WF compartment exhibits minimal clustering compared to neighboring areas (Figure 7a). The possibility that some source zones in this area may exhibit suppressed aftershock behavior--perhaps indicative of high stress (Sanders and Kanamori, 1984)--is the subject of current investigation.

With updated information in hand, the earthquake record of the WF compartment was re-examined using two approaches. First, a homogeneous space-time sample with a reasonable number of events was established by considering all independent earthquakes (aftershocks excluded) of Modified Mercalli epicentral intensity (I_0) V or greater, or M_L 4.3 or greater, complete since 1950 (see Arabasz and others, 1980 regarding thresholds of completeness and equivalence between I_0 and M_L). The instrumental record begins in 1962 with confidence in completeness at least for M_L 3.5 and greater.

The cumulative distribution for the selected sample of events is shown in the lower part of Figure 8a. For comparison, the cumulative distribution for all earthquakes of I_0 IV or greater since 1950 and M_L 3.5 or greater since 1962 is also shown. The latter sample, however, cannot simply be demonstrated to be

homogeneous. One reason for plotting it is that the change in rate for the former sample lies suspiciously close to the juncture between the non-instrumental and instrumental earthquake catalogs. In either case, there appears to be a significant decrease in rate of seismicity during the 1960's. Changes in rates are apparent in 1963 for $M_L \geq 4.3$ and in 1968 for $M_L \geq 3.5$. The significance of differences in the mean rates before and after these two respective points was tested using the normal deviate (z) test (e.g., Habermann, 1981). In both cases, the compared sample means can be considered different with 99 percent confidence.

A second approach that was taken was to look critically at the worst-case sample for $M_L \geq 4.3$, which includes interevent times as long as 7.7 and 9.2 years, to test whether the associated time sequence of events was non-random. Assuming the mean rate of occurrence from the 34-year sample for the WF compartment, application of the Kolmogorov-Smirnov test, shown in Figure 8b, indicates that we cannot reject at the 95-percent confidence level the hypothesis that the observed distribution is non-Poisson. Neither can the sample for $M_L \geq 3.5$ similarly be shown to be non-Poisson. In other words, the occurrence of only a single shock of $M_L 3.5$ or greater during the 1968-1980 period, as shown in the hachured space-time compartment of Figure 6, can be argued to have been due to a random Poisson process. Arabasz and Smith (1981) argued that the anomaly was non-Poisson by considering the average rate of occurrence throughout the main seismic belt in Utah. The critical issue is whether the WF compartment has a long-term rate of flux for small to moderate-size earthquakes that is different--and lower--than that for neighboring parts of the seismic belt.

The issue of characteristic earthquake occurrence on the Wasatch fault is worth examining in the context of flux of moderate-size earthquakes. Schwartz and Coppersmith (1984) use the paucity of moderate-size earthquakes in the historical record to support the idea that the Wasatch fault tends to generate essentially same-size or characteristic large earthquakes. We can use the average recurrence interval of 444 years estimated by them for surface-faulting earthquakes on the Wasatch fault and compare it with the historical record. During the last 100 years, the number of moderate-to-large earthquakes ($M \geq 5.5$) that can be associated with the Wasatch fault is 0 to 2 (Arabasz and others, 1980).

Assuming (1) a Poisson process, (2) that surface-faulting earthquakes of magnitude 6-3/4 or greater occur once every 444 years on the Wasatch fault, and (3) that the minimum number of observations is 18--the number of probable surface-faulting events upon which the recurrence interval of 444 years was based, we can compute the probability of having no earthquakes of $M_L 5.5$ or greater on the Wasatch fault during the last 100 years (see, for example, Benjamin and Cornell, 1970). For a low b-value of 0.5, the lowest published value for a historical catalog in the Intermountain seismic belt (see Arabasz and others, 1980), 0.95 events per century of $M_{5.5}$ or greater would be expected, and with 95 percent confidence the probability of having no such earthquakes in 100 years would be 0.50. Alternatively, for a b-value of 1.0, 4.01 events per century of $M_L 5.5$ or greater would be expected and the corresponding probability of no such earthquake would be 0.06. Assignment of two historical moderate-size earthquakes to the Wasatch fault alters the argument considerably. In sum, implications of the historical record for the characteristic earthquake hypothesis should be considered with care.

It is arguable whether space-time patterns of earthquake occurrence in the Wasatch Front area can be used as indicative of stage within a seismic cycle. Relatively low seismic flux, compared to active plate boundaries, and the absence of a complete seismic cycle in the historic record diminish our statistical and scientific confidence. Temporal decreases in seismicity ambiguously characterize both the early post-aftershock stage and the late pre-mainshock stage of a seismic cycle (e.g., Ellsworth and others, 1981). Nevertheless, the microseismicity gaps along the Wasatch fault and the seemingly anomalous behavior of the broader Wasatch Front spatial compartment deserve serious attention. They provide investigative targets for geodetic monitoring and for studies of the characteristics of small earthquakes to test for indications of potential for moderate-to-large earthquakes.

STRESS STATE

The focus of this final section is a summary of results presented by Arabasz (1984) from a case study of "Swarm seismicity and deep hydraulic fracturing within 10 km of the southern Wasatch fault." The information allows inductive reasoning about the orientation and magnitude of principal stresses in the vicinity of the Wasatch fault--directly relevant to understanding its mechanical behavior.

In June-July 1982 during the course of a 7-week microearthquake field experiment in the vicinity of the southern Wasatch fault, two earthquake swarms ($M_L \leq 2.1$) were recorded originating within a few kilometers of a deep exploration well (Chevron U.S.A. #1 Chriss Canyon, TD 5,344 m), coincidentally located within a temporary 10-station network. The well penetrates a section of Jurassic and younger sedimentary rocks (Standlee, 1983). On April 16,

1982, an "acid-breakdown hydrofrac" had been made in the wellbore at a depth of 5,070 m. A causal connection between the observed swarm seismicity and pore-pressure changes due to the deep fluid injection 2 to 3 months earlier is suggested by: (1) hypocentral clustering in the vicinity of the wellbore, (2) distance-delay times consistent with fluid diffusion, (3) significant timing of the swarm seismicity compared to the record of continuous monitoring by the University of Utah's permanent seismic network (3 stations within 25 km), and (4) near-critical stress differences for frictional sliding inferred from the hydrofrac results.

On the basis of the instantaneous shut-in pressure measured for the hydrofrac and corrected for depth, an in situ minimum horizontal compressive stress S_h of approximately 750 bars (75 MPa) is estimated at the hydrofrac depth of 5,070 m. Figure 9a shows the value of S_h in stress-depth space together with the lithostat (assumed to correspond to the maximum vertical stress S_v), the hydrostat, and the domain of S_h associated with a critical maximum stress difference appropriate for incipient frictional sliding on a pre-existing fault (e.g., Zoback and others, 1978). Also shown in Figure 9a are a range of values for S_h determined by Zoback (1981) from hydrofrac tests in a shallow well about 90 km to the north, and the average gradient for S_h determined by McGarr and Gay (1978) for sedimentary basins in the U.S. The maximum horizontal compressive stress S_H is inferred to lie midway or more between the values of S_h and S_v (discussed below).

Figure 9b shows a Mohr-circle stress plane in which S_v and S_h from the deep hydrofrac are assumed to represent extremal principal stresses--following the usual assumption that one of the principal stresses is vertical (e.g.,

Zoback and Zoback, 1980, p. 6113) and given normal-faulting mechanisms for nearby seismicity. Accounting for hydrostatic pore pressure, maximum deviatoric stress is 213 bars. Options for failure to "drive" the Mohr circle into a failure envelope for frictional sliding on a pre-existing fault (following Byerlee's law) include: (1) decreasing the mean stress (i.e., increasing pore pressure) by about 70 bars, (2) decreasing S_h by about 50 bars, or (3) decreasing the coefficient of static friction to about 0.5. There are obvious uncertainties in the various parameters, but if the observed earthquake activity was indeed causally related to the fluid injection, then the maximum and minimum principal stresses have probably been reasonably estimated to within tens of bars.

Figure 9c illustrates additional information on stress state near the southern Wasatch fault that can be inferred from the observed swarm earthquakes. Corresponding focal mechanisms based on both P-wave polarities and SV/P amplitude inversion indicate: normal faulting, a consistent northerly-trending nodal plane dipping steeply (72° - 86°)E, and near-horizontal T-axes trending WNW-ESE. Assuming that one of the principal stresses is vertical, S_v then corresponds to S_1 , the maximum principal stress, and the direction of S_3 the minimum principal stress will be in the horizontal plane and its azimuth should be estimated by the average direction of T-axes from the focal mechanisms. The intermediate principal stress S_2 will also be horizontal and orthogonal to S_3 .

Angelier (1979) describes constraints on the geometric range of allowable slip on a pre-existing fault if the orientation of principal stresses is known. Further, the slip direction on a pre-existing fault is uniquely deter-

mined if the relative magnitude of the principal stresses is also prescribed. Information in the lower-right part of Figure 9c illustrates the range of allowable slip on the fault plane plotted as a continuous line. Further, whether one selects the northerly nodal plane or its auxiliary plane, the focal mechanisms imply a value of 0.5 to 1.0 for the parameter ϕ , defined in Figure 9c, for the specified stress orientation. Note that the parameter ϕ describes on a scale of 0 to 1 where S_2 lies between S_3 and S_1 and defines the shape of the stress ellipsoid. The southern Wasatch fault lies within the Basin and Range-Colorado Plateau transition where eastward interchange of S_H with S_V is demonstrated by abundant strike-slip focal mechanisms in the Sevier Valley area (Arabasz, 1983; Julander, 1983).

A final point illustrated in the upper-left part of Figure 9c is that the specified stress orientation prescribes the range of allowable slip directions on the southern Wasatch fault. For the three planes aligned with the strike direction of the Wasatch fault west of the Chriss Canyon well and with arbitrary dips of 60° , 30° , and 10° , allowable slip is constrained to be nearly purely dip slip. Given the specified stress state, faults oriented NNE perpendicular to S_3 and with 60° dip should have optimal susceptibility to slip. Fault slip triggered by the pore-fluid diffusion did not occur on optimally oriented faults within the southern Wasatch fault stress field. There would appear to be variations in strength and/or pore pressure of the order of tens of bars between, say, the optimally oriented upper part of the Wasatch fault and less favorably oriented block-interior faults that accommodated the swarm seismicity.

REFERENCES

- Allmendinger, R.W., Sharp, J. W., Von Tish, D., Serpa, L., Brown, L., Kaufman, S., Oliver, J., and Smith, R.B., 1983, Cenozoic and Mesozoic structure of the eastern Basin and Range from COCORP seismic reflection data: *Geology*, v. 11, p. 532-536.
- Angelier, J., 1979, Determination of the mean principal direction of stresses for a given fault population: *Tectonophysics*, v. 56, p. T17-T26.
- Arabasz, W.J., 1983, Geometry of active faults and seismic deformation within the Basin and Range-Colorado Plateau transition, central and SW Utah (abs.): *Earthquake Notes*, v. 54, no. 1, p. 48.
- Arabasz, W. J., 1984, Swarm seismicity and deep hydraulic fracturing within 10 km of the southern Wasatch fault: *Earthquake Notes*, v. 55, no. 1, p. 30-31.
- Arabasz, W.J., Richins, W.D., and Langer, C.J., 1981, The Pocatello Valley (Idaho border) earthquake sequence of March to April 1975: *Bulletin of the Seismological Society of America*, v. 71, p. 803-826.
- Arabasz, W.J., and Smith, R.B., 1981, Earthquake prediction in the Intermountain seismic belt--an intraplate extensional regime: *in* *Earthquake Prediction--An International Review*, American Geophysical Union Maurice Ewing Series, v. 4, p. 248-258.
- Arabasz, W.J., Smith, R.B., and Richins, W.D. (editors), 1979, *Earthquake Studies in Utah, 1850 to 1978: Special Publication*, University of Utah, Salt Lake City, 552 p.
- Arabasz, W.J., Smith, R.B., and Richins, W.D., 1980, Earthquake studies along the Wasatch Front, Utah: Network monitoring, seismicity, and seismic hazards: *Bulletin of the Seismological Society of America*, v. 70, p. 1479-1499.
- Benjamin, J.R., and Cornell, C.A., 1970, *Probability, Statistics, and Decision for Civil Engineers*: McGraw-Hill, New York, 684 p.
- Bucknam, R.C., Algermissen, S.T., and Anderson, R.E., 1980, Patterns of late Quaternary faulting in western Utah and an application to earthquake hazard analysis: *in* *U.S. Geological Survey Open-File Report 80-801*, p.

299-314.

- Cape, C.D., McGeary, S., and Thompson, G.A., 1983, Cenozoic normal faulting and shallow structure of the Rio Grande rift near Socorro, New Mexico: Geological Society of America Bulletin, v. 94, p. 3-14.
- Das, S., and Scholz, C., 1983, Why large earthquakes do not nucleate at shallow depths: Nature, v. 305, p. 621-623.
- Dixon, J.S., 1982, Regional structural synthesis, Wyoming salient of western overthrust belt: American Association of Petroleum Geologists Bulletin, v. 66, p. 1560-1580.
- Ellsworth, W.L., Lindh, A.G., Prescott, W.H., and Herd, D.G., 1981, The 1906 San Francisco earthquake and the seismic cycle: in Earthquake Prediction--An International Review, American Geophysical Union Maurice Ewing Series, v. 4, p. 126-140.
- Griscom, M., 1980, Space-time seismicity patterns in the Utah region and an evaluation of local magnitude as the basis of a uniform earthquake catalog: M.S. thesis, University of Utah, Salt Lake City, 133 p.
- Habermann, R.E., 1981, Precursory seismicity patterns: Stalking the mature seismic gap: in Earthquake Prediction--An International Review, American Geophysical Union Maurice Ewing Series, v. 4, p. 29-42.
- Julander, D.R., 1983, Seismicity and correlation with fine structure in the Sevier Valley area of the Basin and Range--Colorado Plateau transition, south-central Utah: M.S. thesis, University of Utah, Salt Lake City, 143 p.
- Julander, D.R., and Arabasz, W.J., 1982, Seismicity and correlation with fine structure in the Sevier Valley area of the Basin and Range--Colorado Plateau transition (abs.): Eos, Transactions of the American Geophysical Union, v. 63, p. 1024.
- McGarr, A., and Gay, N.C., 1978, State of stress in the earth's crust: Annual Reviews of Earth and Planetary Sciences, v. 6, p. 405-436.
- McKee, M.E., and Arabasz, W.J., 1982, Microearthquake studies across the Basin and Range--Colorado Plateau transition in central Utah: in Utah Geological Association Publication 10, p. 137-149.

Richins, W.D., Arabasz, W.J., and Langer, C.J., 1983, Episodic earthquake swarms near Soda Springs, Idaho, 1981-82 (abs.): Earthquake Notes, v. 54, no. 1, p. 99.

Sanders, C.O., and Kanamori, H., 1984, A seismotectonic analysis of the Anza gap, San Jacinto fault zone, southern California: Journal of Geophysical Research (in press).

Schwartz, D.P., and Coppersmith, K.J., 1984, Fault behavior and characteristic earthquakes: Examples from the Wasatch and San Andreas faults: Journal of Geophysical Research (in press).

Sibson, R.H., 1982, Fault zone models, heat flow, and the depth distribution of earthquakes in the continental crust of the United States: Bulletin of the Seismological Society of America, v. 72, p. 151-163.

Smith, R.B., 1974, Seismicity and earthquake hazards of the Wasatch Front, Utah: Earthquake Information Bulletin, v. 6, p. 12-17.

Smith, R.B., 1978, Seismicity, crustal structure, and intraplate tectonics of the Western Cordillera: in Geological Society of America Memoir 152, 111-144.

Smith, R.B., and Bruhn, R.L., 1984, Intraplate extensional tectonics of the eastern Basin-Range: Inferences on structural style from seismic reflection data, regional tectonics and thermal-mechanical models of brittle/ductile deformation: Journal of Geophysical Research (in press).

Standlee, L.A., 1983, Structure and stratigraphy of Jurassic rocks in central Utah: Their influence on tectonic development of the Cordilleran foreland thrust belt: in Rocky Mountain Association of Geologists Guidebook--1982, p. 357-382.

Zoback, M.D., 1981, Hydraulic fracturing stress measurements and fracture studies in Hole DH-103, Fifth Water Power Plant Site, Central Utah Project: Report to U.S. Bureau of Reclamation, Contract No. 0-07-40-51580, 42 p.

Zoback, M.D., Healy, J.H., Roler, G.S., Gohn, G.S., and Higgins, B.B., 1978, Normal faulting and in situ stress in the South Carolina coastal plain near Charleston: Geology, v. 6, p. 147-152.

Zoback, M.L., 1983, Structure and Cenozoic tectonism along the Wasatch fault zone, Utah: in Geological Society of America Memoir 157, p. 3-27.

Zoback, M.L., and Zoback, M., 1980, State of stress in the conterminous United States: Journal of Geophysical Research, v. 85, p. 6113-6156.

FIGURE CAPTIONS

- Figure 1. Results from detailed studies near Richfield, Utah (Julander and Arabasz, 1982; Julander, 1983; Arabasz, 1983). Spatially discontinuous seismicity with depth appears to reflect local structural control by a low-angle detachment, rather than a brittle-ductile transition (see text for discussion). Local P-wave velocity structure determined from nearby quarry blasts as refraction sources and by analysis of local earthquake data for multilayering using both the minimum-apparent-velocity technique and a simultaneous velocity-hypocenter inversion technique.
- Figure 2. Epicenter map (upper left) and cross-sectional views of earthquake foci from special study of an earthquake swarm sequence ($M_L < 4.7$) near Soda Springs, Idaho, October 1982 (adapted from Richins and others, 1983). Apparent discontinuity in the frequency distribution of earthquakes with depth coincides with the pre-Neogene Meade thrust fault.
- Figure 3. Schematic geologic cross-section of the upper crust illustrating complex association of seismicity with geological structure in the Intermountain seismic belt. Starbursts indicate foci of moderate-to-large earthquakes; small circles, microseismicity; lines in subsurface, faults. Arrows indicate sense of slip on faults; two-directional arrows, extensional backsliding on pre-existing low-angle faults possibly formed as thrust faults. Letters identify examples referred to in text. Base of seismogenic layer is approximately at 10-15 km depth.
- Figure 4. Epicenter map of the Wasatch Front area for October 1974 through June 1978 based on seismic monitoring by the University of Utah (reproduced from Arabasz and others, 1980). Dashed elliptical areas outline seismicity gaps defined on basis of pre-1974 seismicity and discussed in text.
- Figure 5. Updated epicenter map of the Wasatch Front area for a 5.5-yr period subsequent to that in Figure 4. Dashed elliptical areas as in Figure 4 for comparison.
- Figure 6. Epicenter map (above) and space-time plot (below) of earthquake activity in the Utah region (reproduced from Arabasz and Smith, 1981). The hachured space-time

compartment in the lower figure indicates a seismicity gap identified by Arabasz and Smith (1981) and discussed in text here.

Figure 7. Epicenter maps of the Utah region, July 1978-December 1983, based on seismic monitoring by the University of Utah, for all shocks greater than or equal to (a) magnitude 2.5 and (b) magnitude 3.5. The dashed rectangles correspond to the spatial compartment of the seismicity gap defined in Figure 6. Sizes and dates of occurrence are specially indicated for the larger earthquakes in that compartment since July 1978.

Figure 8. (a) Cumulative seismicity, January 1950-December 1983, within the Wasatch Front spatial compartment outlined in Figures 6 and 7. I_0 and M_L specify, respectively, the sample thresholds of Modified Mercalli epicentral intensity for shocks prior to July 1962, and the local Richter magnitude for shocks after that date. Vertical arrows indicate changes in rate of occurrence. (b) Kolmogorov-Smirnov test of the cumulative distribution of interevent times associated with the sample for $I_0 > V$, $M_L > 4.3$, indicated in (a) above. The maximum absolute difference D between the observed distribution and the continuous distribution, $F(t)$, predicted for a Poisson process is less than the critical value required to reject, at the 95 percent confidence level, the hypothesis that the observed distribution is non-Poisson.

Figure 9. Results presented by Arabasz (1984) relating to inferences of stress state in the vicinity of the southern Wasatch fault. These include: (a) the location in stress-depth space of a value of minimum horizontal compressive stress S_h of 750 bars (75 MPa) determined at a depth of 5.1 km from an "acid-breakdown hydrofrac"; (b) a Mohr-circle diagram relating the estimated stress state at 5.1 km depth from (a) to criteria for frictional failure on a pre-existing plane of weakness; and (c) key observations, presented in stereographic projection, that allow inferences of the orientation and relative magnitude of principal stresses from small earthquakes inferred to have been induced by the deep hydrofrac. See text for complete explanation.

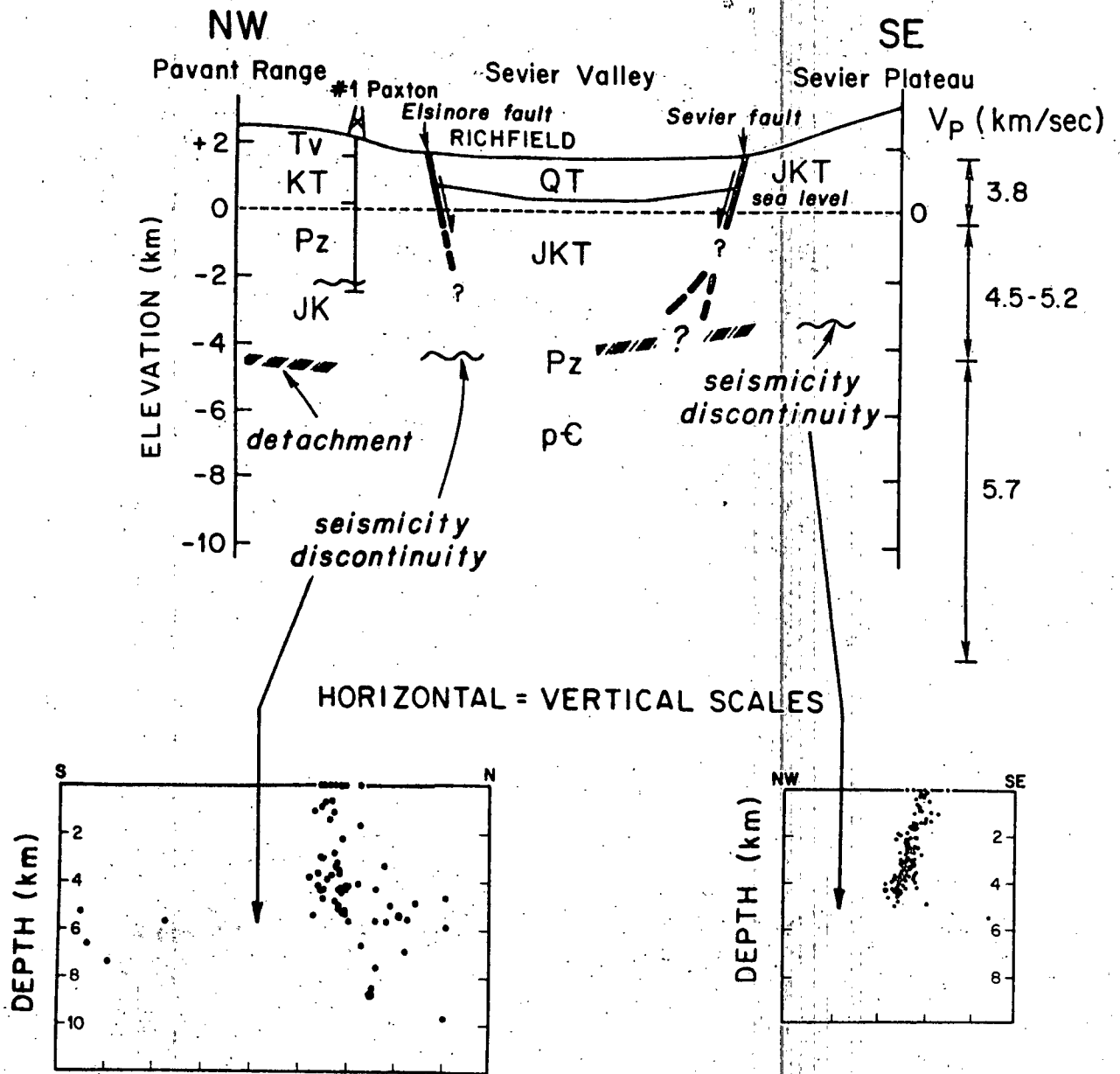


FIGURE 1.

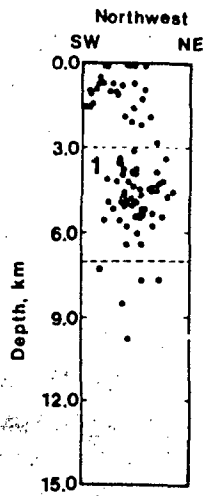
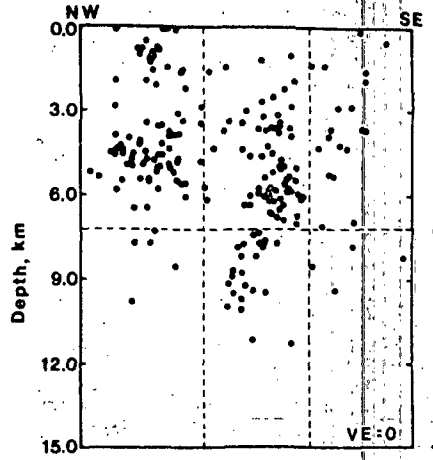
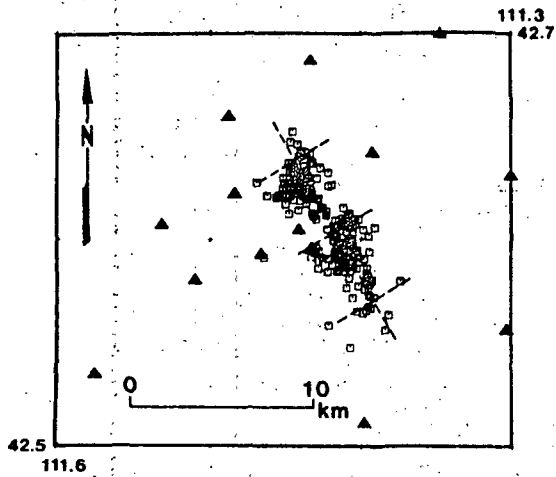


FIGURE 2.

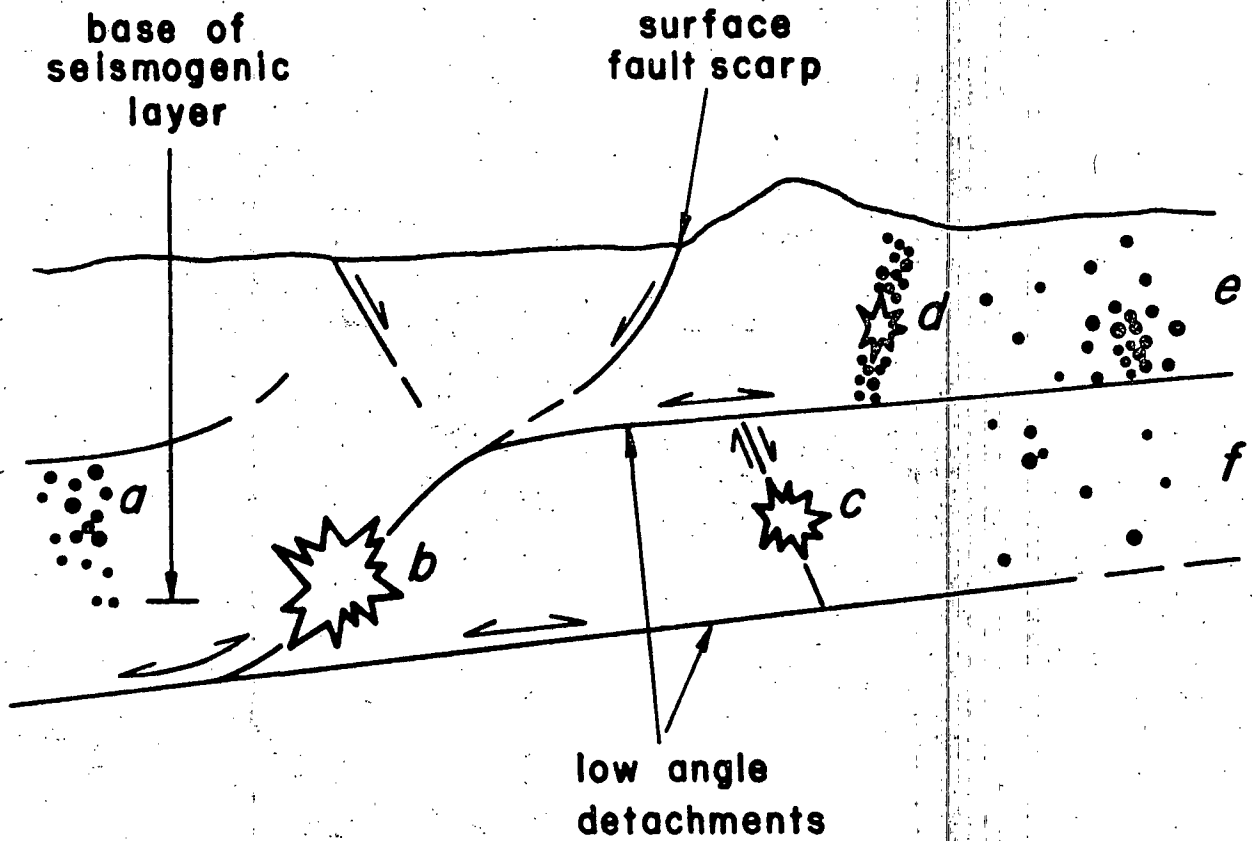
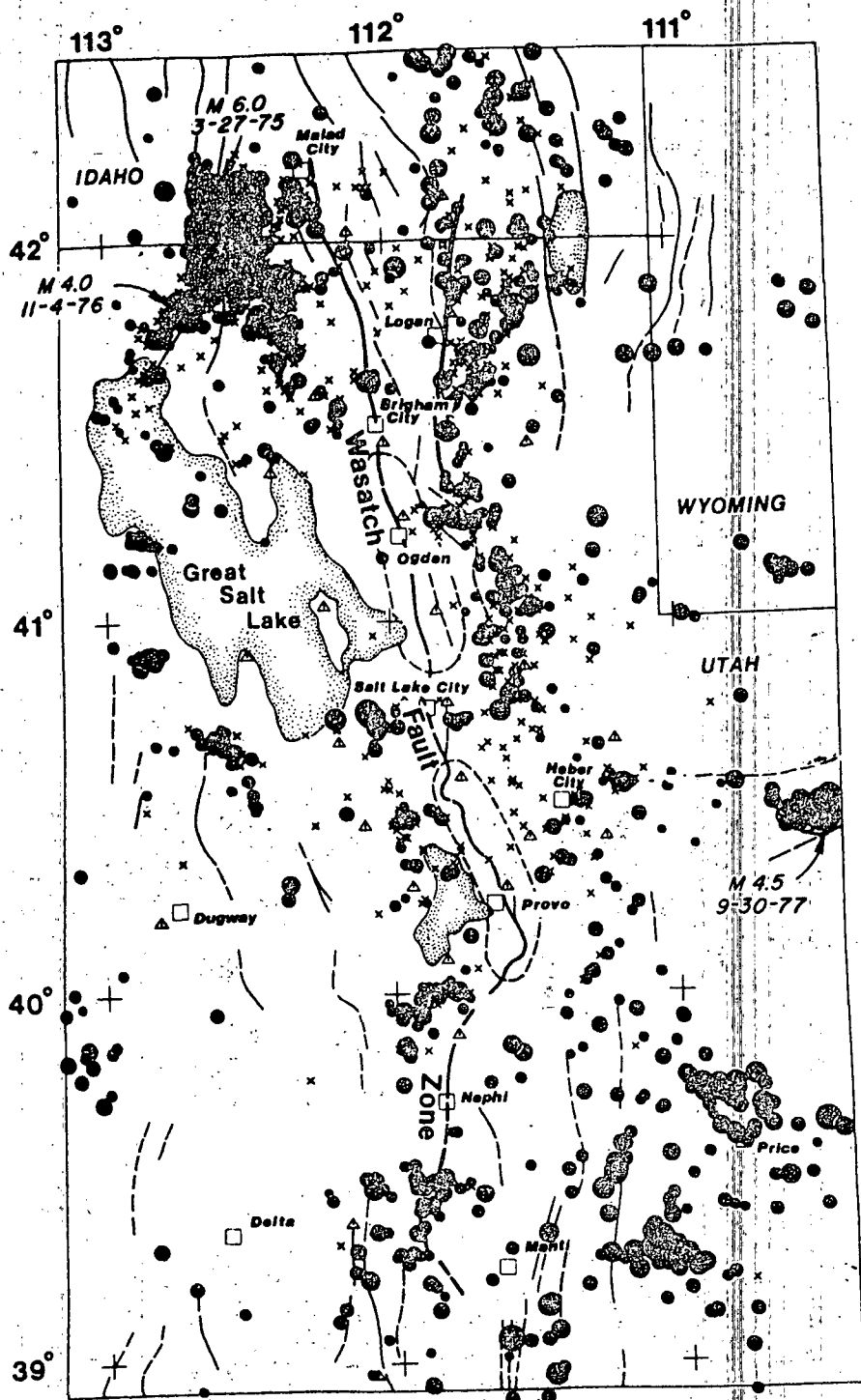
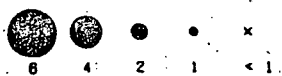


FIGURE 3.



WASATCH FRONT EQ'S: OCT 74 TO JUN 78

MAGNITUDE SCALE (ML)



SEISMOGRAPH STATION

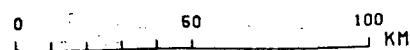
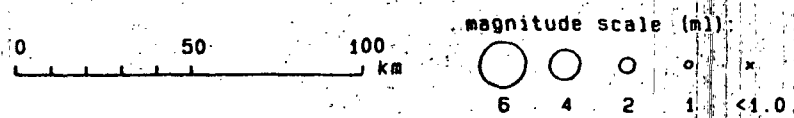
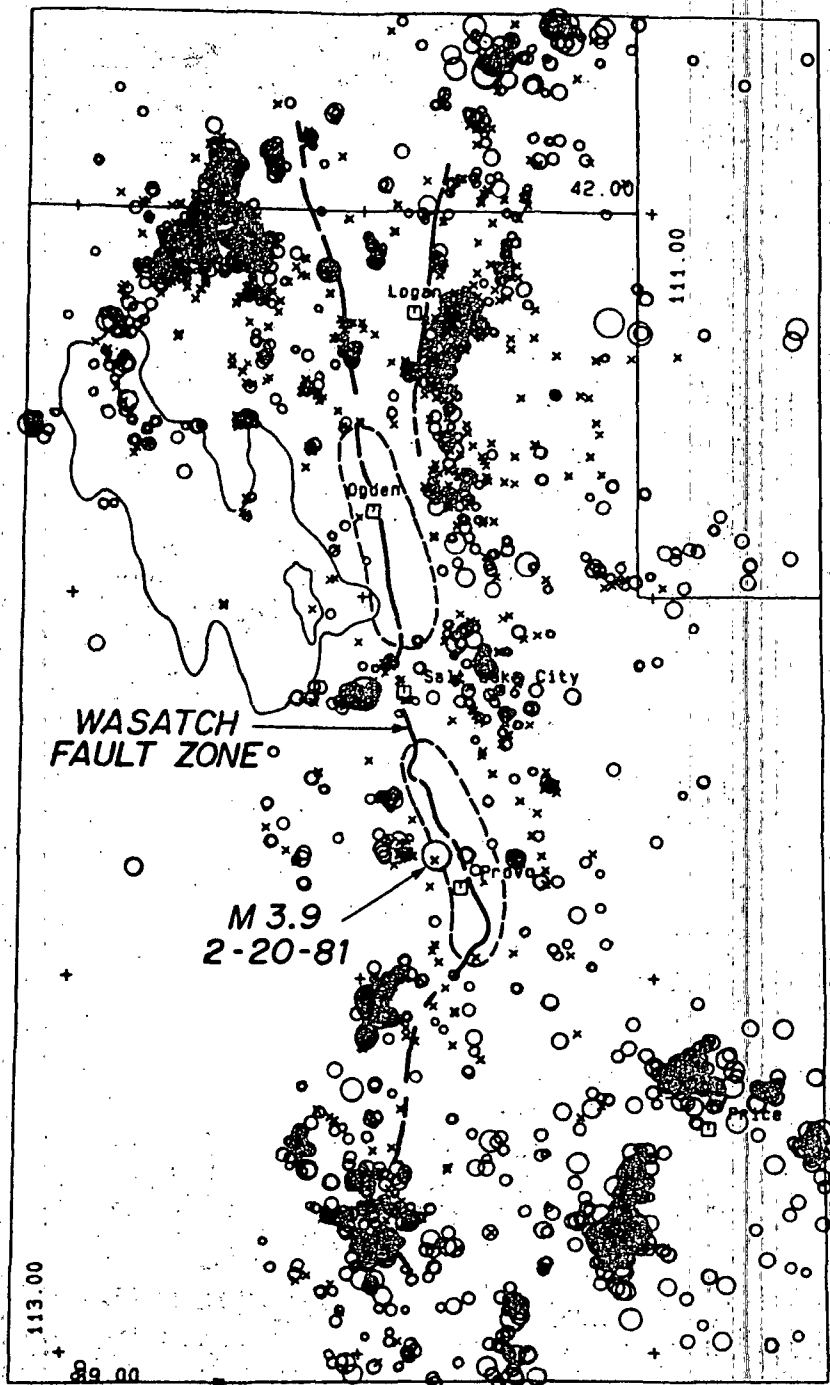
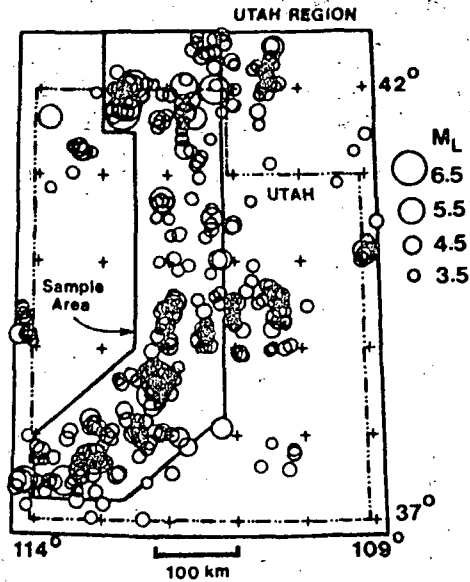


FIGURE 4.

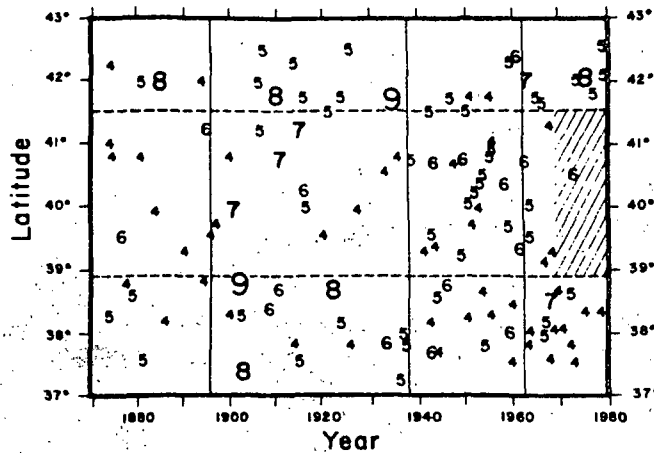


JULY 1, 1978 TO DECEMBER 31, 1983

FIGURE 5.



Earthquakes ($M_L \geq 3.5$) in the Utah region, 1850-1979. Pre-instrumental shocks have Modified Mercalli epicentral intensities of IV or greater.



Space-time plot of earthquakes, in terms of Modified Mercalli epicentral intensity ($I_0 \geq 4$), within the sample area of Figure 3 as a function of latitude. Vertical lines are time markers for sample completeness: $I_0 \geq 7$ since 1896 and $I_0 \geq 6$ since 1938; shocks of $I_0 \geq 5$ are complete since 1950, and those of $I_0 \geq 4$ or $M_L \geq 3.5$ since 1962 when instrumental monitoring began. Hatched area and dashed lines outline space-time compartments discussed in text.

FIGURE 6.

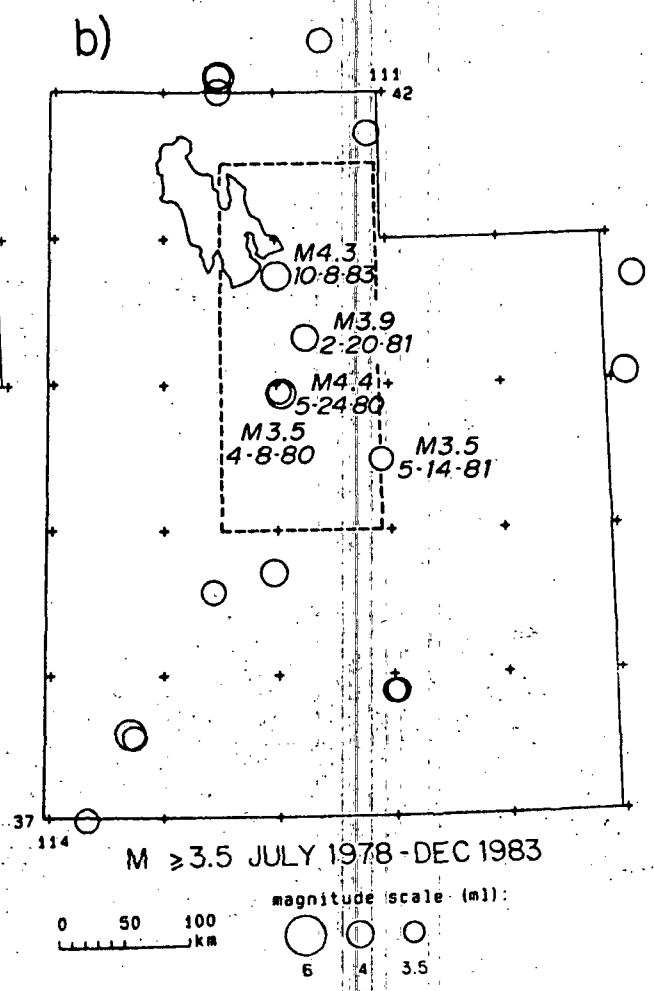
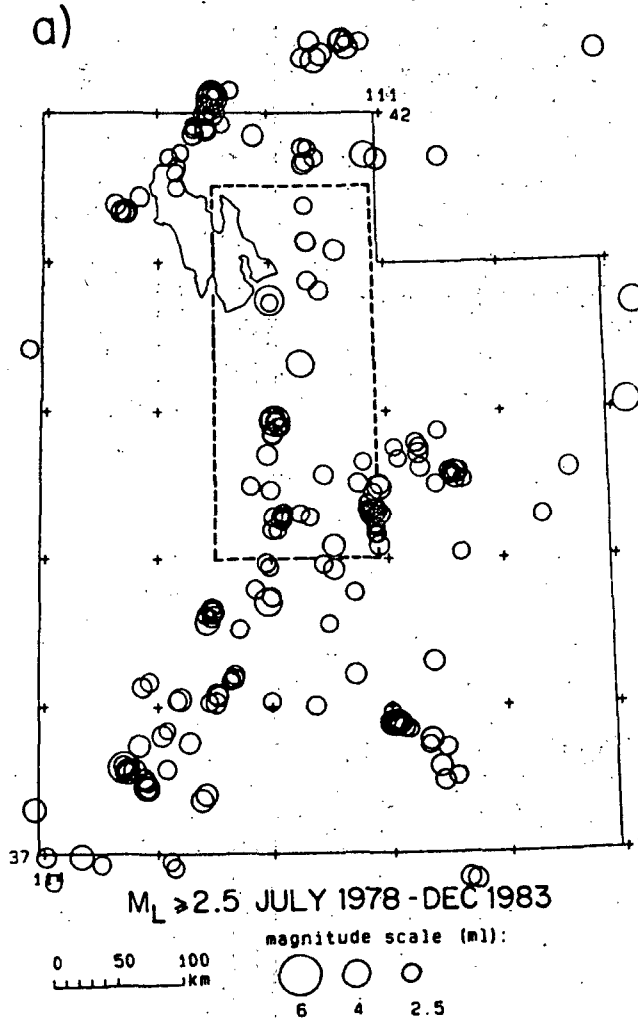


FIGURE 7.

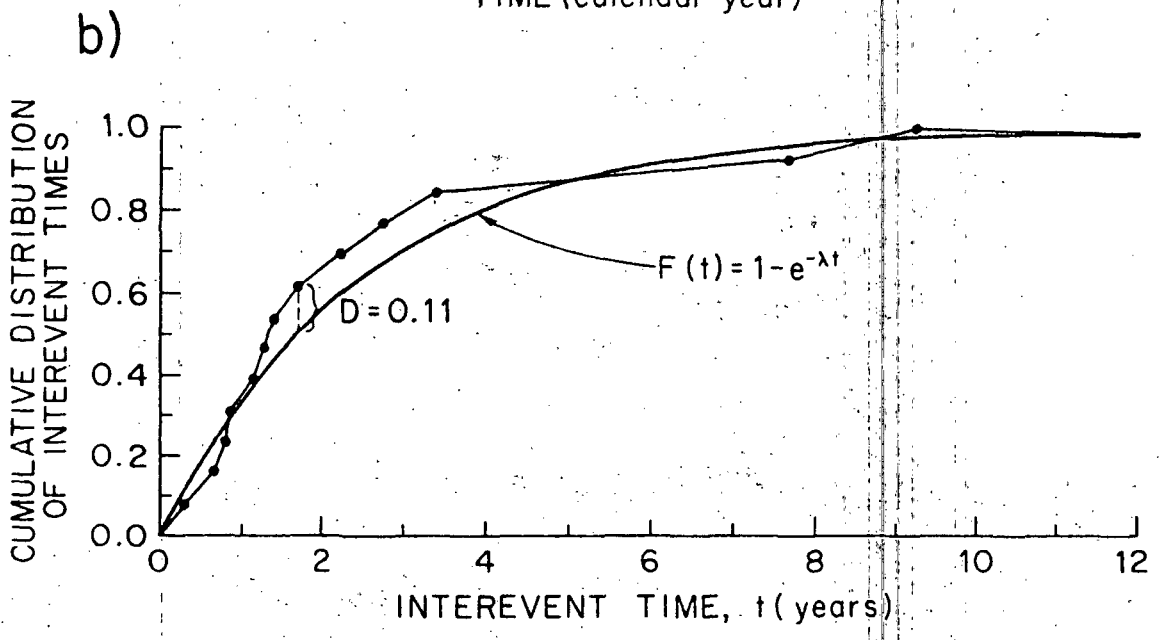
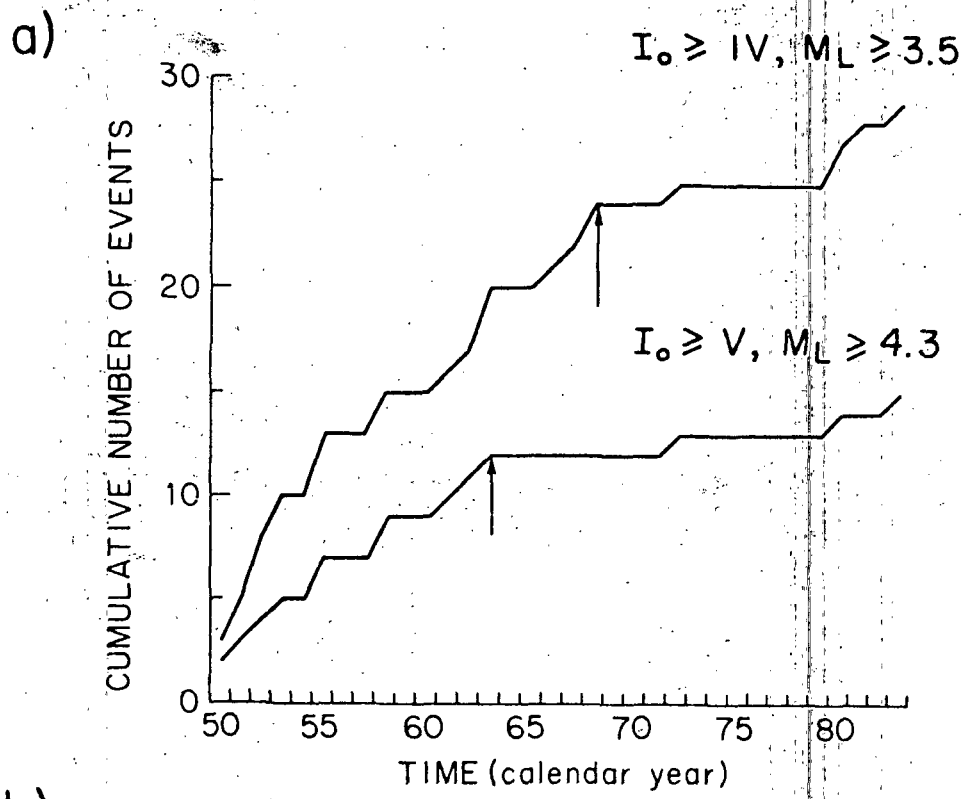


FIGURE 8.

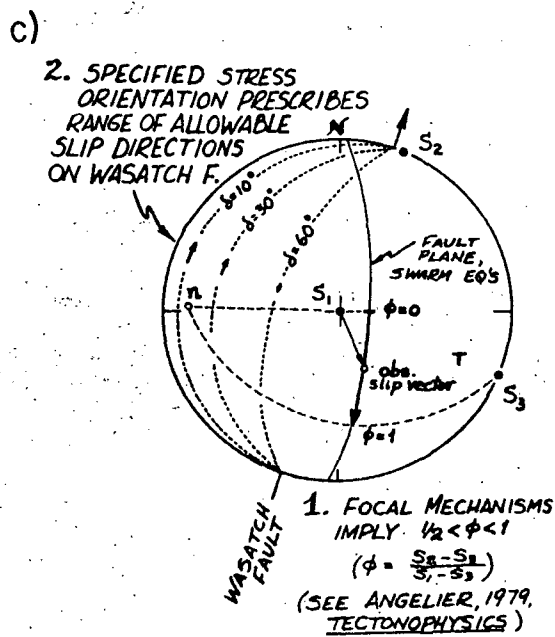
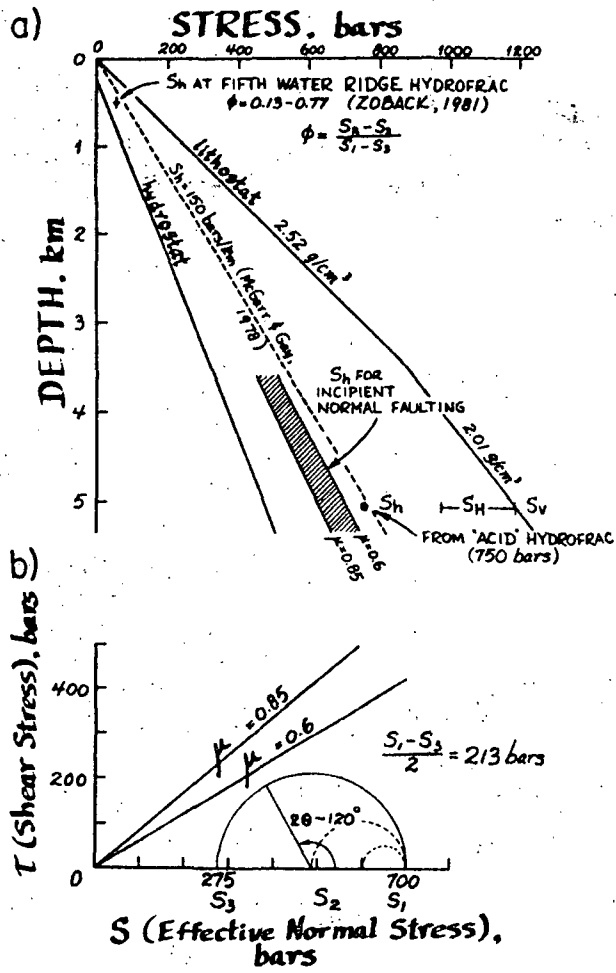


FIGURE 9.